THE ROLE OF MOBILE GENETIC ELEMENTS ON THE SURFACTANT ENHANCED BIOREMEDIATION OF PETROLEUM CONTAMINATED SOIL

by

Aslınur Çalışıyor

B.Sc. in Molecular Biology and Genetics, Istanbul Technical University, 2016

M.Sc. in Environmental Sciences, Boğaziçi University, 2018

Submitted to the Institute of Environmental Sciences in partial fulfillment of

the requirements for the degree of

Doctor of Philosophy

in

Environmental Sciences

Boğaziçi University

2025

THE ROLE OF MOBILE GENETIC ELEMENTS ON THE SURFACTANT ENHANCED BIOREMEDIATION OF PETROLEUM CONTAMINATED SOIL

APPROVED BY:

Assoc. Prof. Dr. Ulaş Tezel . . . . . .
Dissertation Advisor

Prof. Dr. Sevcan Aydın . . . . . .

Prof. Dr. Kozet Yapsaklı Bakırcı . . . . . .

Prof. Dr. Ferhan Çeçen . . . . . .

Assist. Prof. Dr. Berat Z. Haznedaroğlu . . . . . .

DATE OF APPROVAL: 12/06/2025

ACKNOWLEDGEMENTS

First and foremost, I would like to express my deepest gratitude to my thesis advisor, Assoc. Prof. Dr. Ulaş Tezel, for his invaluable support, insightful guidance, and constant encouragement throughout this journey. I feel truly fortunate to have conducted my thesis under his supervision, and I am especially grateful for the trust he placed in me from the very beginning. I am also sincerely thankful to my co-advisor, Prof. Dr. Bahar İnce, who has been a continuous source of support during my time at Boğaziçi University. Her confidence in my abilities and kind encouragement have always been deeply appreciated. I would like to extend my heartfelt thanks to the members of my dissertation committee; Prof. Dr. Ferhan Çeçen, Prof. Dr. Sevcan Aydın, Prof. Dr. Kozet Bakırcı, and Assist. Prof. Dr. Berat Z. Haznedaroğlu, for their valuable feedback and kind support.

This study was financially supported by Presidency of the Council of Higher Education (YÖK) and Istanbul Technical University, under the project titled “Development and Field Testing of a Bio-Ecological Remediation Model for Petroleum-Contaminated Soil” (Project Code: TGA-2024-45328), for which I am truly grateful.

My sincere thanks go to my dear colleagues and friends Aslıhan Başak Dağ and Firdevs Ceylan for their kind support, endless patience, and joyful spirit in the lab. I also thank Rüya Üçel, Recep Can Altınbağ and Berkay Becermen from the Institute of Environmental Sciences for their support and friendship.

To my beloved family, my mother Yasemin Dingersu, my father Özden Çalışıyor, and my sister Yaren Çalışıyor, thank you for your unconditional love and encouragement. To my partner, Yarkın Sözbir, your steady presence, encouragement, and belief in me carried me through the most challenging moments of this journey. I am truly grateful to have had his strength beside me every step of the way.

Lastly, I am grateful to my colleagues at Massive Bioinformatics; Naz Kanıt, Gamze Gürsoy, Seray Karaçay, Onur Yavuz, Erdi Kılıç, Bekir Berke Sincanlı, Zeynep Güngör, Ahmet Samet Gürkan, Nilsu Şimşek, and Tutku Çekigil for their generous support. I also extend my heartfelt thanks to Prof. Dr. Orhan İnce, Assoc. Prof. Dr. Gözde Özbayram, and Dr. İbrahim Halil Miraloğlu for their lifelong mentorship and unwavering belief in my potential. Their continued guidance has shaped both my academic and personal growth.

ABSTRACT

THE ROLE OF MOBILE GENETIC ELEMENTS ON THE SURFACTANT ENHANCED BIOREMEDIATION OF PETROLEUM CONTAMINATED SOIL

Bioremediation of petroleum hydrocarbons (PHCs) in contaminated soils remains a major challenge due to their persistence, low solubility, and limited microbial availability. This study evaluated the effects of non-ionic surfactants, Tween-20 and Triton X-100, on PHC degradation by a petroleum-enriched consortium (PEC). Experiments were designed to compare PEC activity across different combinations of crude oil and surfactants. Microbial growth, total petroleum hydrocarbon (TPH) removal, gene expression, and mobile genetic element (MGE) mobilization were assessed. In the PEC + Crude Oil + Tween-20 group, microbial counts reached 1.1×10^8 CFU/mL by Day 4, compared to 5.0×10^7 CFU/mL in PEC + Crude Oil and 4.7×10^7 CFU/mL in PEC + Tween-20. Residual TPH dropped to 0.59 ± 0.50 mg/g in the PEC + Tween-20 group, lower than 0.78 ± 0.11 mg/g in PEC alone and 3.66 ± 0.18 mg/g in the crude oil-only control. Transcriptomic data showed that Tween-20 induced hydrocarbon degradation and stress-related genes. ISPre2 transposon was frequently mobilized into the *sacB* region of the pMAT1 plasmid at 4664 bp (CTAA) and 4140 bp (TTAA), suggesting enhanced horizontal gene transfer. These insertions were associated with hydrocarbon catabolic gene clusters. In contrast, Triton X-100 supported moderate microbial growth and degradation (TPH: 2.52 ± 1.13 mg/g in PEC + TX) but showed limited transcriptional and genetic activation. Overall, Tween-20 demonstrated dual benefits by enhancing PHC bioavailability and promoting adaptive microbial responses. These findings support its use in surfactant-assisted bioremediation strategies for petroleum-contaminated soils.

ÖZET

PETROL İLE KİRLENMİŞ TOPRAKLARIN YÜZEY AKTİF MADDE DESTEKLİ BIYOREMEDİASYONUNDA MOBİL GENETİK ELEMANLARIN ROLÜ

PHC ile kontamine olmuş topraklarda biyoremediasyon süreci, söz konusu bileşiklerin düşük çözünürlükleri ve mikroorganizmalar tarafından zor erişilebilir olmaları nedeniyle verimlilik açısından ciddi kısıtlamalar içermektedir. Bu çalışmada, non-iyonik sürfaktanlar olan Tween-20 ve Triton X-100'ün, petrol ile zenginleştirilmiş mikrobiyal konsorsiyumun (PEC) PHC bozunumu üzerindeki etkileri değerlendirilmiştir. Deneyler, PEC'in ham petrol ve sürfaktanların farklı kombinasyonları altındaki performansını karşılaştırmalı olarak inceleyecek şekilde tasarlanmıştır. Mikrobiyal büyüme, toplam petrol hidrokarbonu (TPH) giderimi, gen ekspresyonu ve mobil genetik element (MGE) mobilizasyonu değerlendirilmiştir. PEC + Ham Petrol + Tween-20 grubunda, mikrobiyal sayım 4. gün sonunda 1.1×10^8 CFU/mL'ye ulaşırken; bu değer, sadece ham petrol içeren grupta 5.0×10^7 CFU/mL ve sadece Tween-20 içeren grupta 4.7×10^7 CFU/mL olarak ölçülmüştür. TPH seviyesi, PEC + Tween-20 grubunda 0.59 ± 0.50 mg/g'a kadar düşmüş; bu değer, PEC grubunda 0.78 ± 0.11 mg/g ve sadece ham petrol içeren kontrol grubunda 3.66 ± 0.18 mg/g olarak kaydedilmiştir. Transkriptom analizleri, Tween-20'nin hem hidrokarbon bozunumu hem de stres yanıtı ile ilişkili genleri indüklediğini göstermiştir. ISPre2 transpozonunun pMAT1 plazmidinin *sacB* bölgesine (4664 bp, CTAA ve 4140 bp, TTAA) sıkça entegre olduğu görülmüş ve bu bölgelerdeki yerleşimler, hidrokarbon katabolizmasında görevli gen kümeleri ile ilişkilendirilmiştir. Buna karşılık, Triton X-100 orta düzeyde mikrobiyal büyüme ve bozunum sağlamış (TPH: 2.52 ± 1.13 mg/g, PEC + TX) ancak transkripsiyonel ve genetik aktivasyon düzeyi sınırlı kalmıştır. Sonuçlar, Tween-20'nin PHC biyoyararlanımını artırarak ve mikrobiyal adaptif yanıtları destekleyerek biyoremediasyon verimliliğini anlamlı ölçüde iyileştirdiğini ortaya koymaktadır.

TABLE OF CONTENTS

ACKNOWLEDGEMENTS iii
ABSTRACT iv
ÖZET v
TABLE OF CONTENTS vi
LIST OF FIGURES ix
LIST OF TABLES xiii
LIST OF SYMBOLS/ABBREVIATIONS xiv
1. INTRODUCTION xiv
2. LITERATURE REVIEW 6
2.1. PHCs and Environmental Impacts 6
2.1.1. PHC Contamination Sources 6
2.1.2. Environmental and Health Impacts 7
2.2. Characteristics of PHCs Affecting Their Behavior and Transport in Soil 8
2.2.1. Chemical and Molecular Structure 8
2.2.2. Low Solubility and Hydrophobicity 10
2.2.3. Sorption/Desorption Dynamics with SOM 12
2.2.4. Bioavailability and Microbial Degradation 13
2.3. Challenges in Remediating Petroleum-Contaminated Soils 14
2.3.1. Limitations of Physical and Chemical Remediation Methods 14
2.3.2. Biological Constraints in PHC Remediation 15
2.4. Bioremediation as Preferred Approach for PHC Contamination 16
2.4.1. Overview of Bioremediation Techniques 16
2.4.2. Various Bioremediation Methods and Their Integration 19
2.5. A Synergistic Approach: Bioaugmentation and Surfactant-Assisted Biodegradation 23
2.5.1. Empowering Microbial Communities: The Role of Bioaugmentation 23
2.5.2. Accelerating the Bioremediation: The Power of Surfactants 24
2.5.3. Mechanisms of Synergy: Enhancing Bioavailability, Enabling Microorganisms to Drive Degradation 28
2.6. Genetic and Microbial Insights into Hydrocarbon Degradation Pathways 31
2.6.1. Hydrocarbon Degradation Mechanisms 31
2.6.2. Hydrocarbon-Degrading Microorganisms 35
2.6.3. The Role of Mobile Genetic Elements in Hydrocarbon Biodegradation 39
3. MATERIALS AND METHODS 42

3.1. Characterization of Petroleum Contaminated Soil 43
3.1.1. Sampling and TPH Analysis of Contaminated Soil 43
3.1.2. Microbial Community Analysis on Contaminated Soil 44
3.2. Enrichment of PHC Degrading Microbial Community 46
3.2.1. Reactor Setup and Serial Transfer Process 47
3.2.2. Monitoring Growth 49
3.2.3. 16S Amplicon Sequencing and Analysis 50
3.2.4. TPH Analysis 50
3.3. Isolation of Dominant PHC-Degrading Bacteria 51
3.3.1. Preparation of Soil Isolate Library 51
3.3.2. Isolate PCH Biodegradability Assay 52
3.3.3. Whole Genome Sequencing of Soil Isolates 52
3.4. Determination of MIC of Surfactants for PEC via Broth Macrodilution Assay 53
3.5. Evaluation of Surfactant-Enhanced Biodegradation of Crude Oil by PEC 57
3.6. Differential Gene Expression in Crude Oil Degrading Culture in the Presence of Surfactants 58
3.6.1. DNA Isolation and Shotgun Metagenomics 58
3.6.2. Inoculum Preparation and Experimental Setup 60
3.6.3. Monitoring Crude Oil Degradation and RNA Isolation for Gene Expression Analysis 61
3.7. Transformation of Hydrocarbon Degraders with a pMAT1 Trap Plasmid 64
3.8. Surfactant-Induced Gene Mobilization in PHC-Degrading Bacteria 66
3.8.1. Setup for Gene Mobilization Enrichment 66
3.8.2. Monitoring of Gene Mobilization 67
4. RESULTS AND DISCUSSION 71
4.1. Microbial Community Structure of Petroleum Contaminated Soil 71
4.2. Outcomes of Microbial Enrichment in PHC-Contaminated Soil: Growth, Community Shifts and Biodegradation 75
4.2.1. Microbial Growth Patterns During Enrichment 75
4.2.2. 16S rRNA Based Microbial Profiling of Microbial Communities During Enrichment 79
4.2.3. Petroleum Degradation Activity of the Starter Culture during Enrichment Process 83
4.2.4. Overall Results of Enrichment of PHC-Degrading Microbial Community 87
4.3. Identification of PHC Degraders and Evaluation of Their Genetics 87

4.3.1. 16S rRNA based Identification of Dominant Bacteria in PEC 87
4.3.2. Biodegradation of Crude Oil by Individual PEC Isolates 89
4.3.3. Whole Genome Sequencing Analysis 91
4.3.4. Subsystem-Based Functional Analysis of the Isolates' Complete Genomes 95
4.3.5. Evaluating Functional Genes Related to Hydrocarbon Degradation in PEC Isolates 102
4.4. Determination of Surfactant Tolerance Levels: MIC Analysis of Selected Strains 106
4.5. Petroleum Biodegradation in the Presence of Surfactants 109
4.5.1. Growth of PEC Cultures on Crude Oil in the Presence of Surfactants 109
4.5.2. Evaluation of TPH Degradation in the Presence of Surfactants 111
4.6. Comprehensive Analysis of Crude Oil Degradation: Microbial Growth, TPH Degradation, and Gene Expression Response to Surfactants 112
4.6.1. Effect of Surfactants on Microbial Growth on Crude Oil 112
3.6.2. Effect of TW and TX on TPH Degradation 114
3.6.3. Effect Gene Expression Profile in Crude Oil-Degrading Cultures 115
4.7. Identification of Mobile Gene Clusters in Crude Oil Degraders When Exposed to Surfactants 126
4.7.1. Microbial Proliferation Analysis 126
4.7.2. TPH Degradation During Biodegradation Assay 127
4.7.3. Determination of Transposition Rate 129
4.7.4. Monitoring of Gene Mobilization 130
5. CONCLUSIONS AND RECOMMENDATIONS 137
REFERENCES 141
APPENDIX A: 16S rRNA SEQUENCES OF ISOLATED PHC DEGRADERS 158

LIST OF FIGURES

Figure 1.1. Conceptual content of the research. 5

Figure 2.1. Aliphatic hydrocarbon degradation pathways. 31

Figure 2.2. Reactions for the degradation of alkanes through aerobic pathways. 33

Figure 2.3. Aromatic hydrocarbon degradation pathways. 33

Figure 2.4. Reactions for the degradation of aromatics through aerobic pathways. 35

Figure 3.1. Methodological framework. 43

Figure 3.2. Clean-contaminated soil and crude oil from petroleum refinery and homogenized soil sample. 44

Figure 3.3. PCR condition for 16S microbial community analysis. 45

Figure 3.4. The workflow of PHC degrading microbial community enrichment process and monitoring. 47

Figure 3.5. The workflow of isolation of dominant PHC-degrading bacteria. 51

Figure 3.6. The workflow conducted for the determination of MIC with different surfactants for existing PHC-degrading cultures. 53

Figure 3.7. The workflow for evaluation of surfactant-enhanced biodegradation of PHC. 57

Figure 3.8. The workflow of degradation test setup for gene expression profiling. 60

Figure 3.9. The workflow of post analysis for gene expression profiling analysis. 62

Figure 3.10. The workflow of transformation of hydrocarbon degraders with trap plasmid pMAT1. 64

Figure 3.11. The circular genome visualization of pMAT1 trap plasmid. 65

Figure 3.12. The workflow of degradation test setup for monitoring the gene mobilization. 66

Figure 3.13. The workflow of post analysis for monitoring the gene mobilization. 67

Figure 4.1. The relative abundance of microbial communities at the phylum level in clean and polluted soils. 72

Figure 4.2. The relative abundance of microbial communities at the species level in clean and polluted soils. 74

Figure 4.3. Visible colonies on and around the crude oil droplets. 75

Figure 4.4. Visual comparison of microbial growth: turbidity in experimental flask vs. clarity in negative control flask. 76

Figure 4.5. Microbial growth curve in 4^{th} and 5^{th} incubation period. 78

Figure 4.6. Relative abundances of dominant bacterial taxa throughout successive enrichment transfers (Incubation Period 1 – 4).. 81

Figure 4.7. Heat map showing the relative abundance (% of total 16S-rRNA reads) of the 30 most dominant bacterial taxa in the control inoculum and after four consecutive enrichment transfers (Incubation Periods 1–4). 82

Figure 4.8. Statistical comparison of residual TPH at the end of each successive incubation periods with the control missing the PEC. 84

Figure 4.9. Comparison of TPH chain-length distribution (C_8-C_{40}) across eight enrichment cycles. 86

Figure 4.10. Maximum-Likelihood phylogenetic tree of soil isolates based on 16S rRNA sequences showing bootstrap-supported clades and subclusters. 89

Figure 4.11. CFU counts demonstrating growth of OTU001 and OTU002 in petroleum-containing medium. 90

Figure 4.12. CFU counts demonstrating growth of OTU003 and OTU004 in petroleum-containing medium. 91

Figure 4.13. Total base counts per OTU derived from WGS analysis.....92

Figure 4.14. Unaligned contig of 349,094 bp identified in OTU001 whole genome sequence.....94

Figure 4.15. Unaligned contig of 68,773 bp identified in OTU003 whole genome sequence.....95

Figure 4.16. Circular SEED map of the OTU001 genome highlighting hydrocarbon degradation gene clusters and HGT elements. 97

Figure 4.17. Circular SEED map of the OTU002 genome highlighting hydrocarbon degradation gene clusters and HGT elements. 98

Figure 4.18. Circular SEED map of the OTU003 genome highlighting hydrocarbon degradation gene clusters and HGT elements. 100

Figure 4.19. Circular SEED map of the OTU004 genome highlighting hydrocarbon degradation gene clusters and HGT elements. 102

Figure 4.20. Heatmap of alkane and aromatic hydrocarbon degradation operons across OTU001–OTU004 genomes, annotated using the HADEG database.....103

Figure 4.21. Growth-inhibition profiles of six surfactants (CTAB, DDAC, BDAC, SDS, Tween-20, and Triton X-100) on PEC culture. 107

Figure 4.22. CFU counts demonstrating microbial growth in the presence of Tween-20 and TritonX-100 respectively.....110

Figure 4.23. TPH biodegradation efficiency for Tween-20 and Triton X-100 amended PEC.....111

Figure 4.24. Impact of surfactants on microbial growth on crude oil. 114

Figure 4.25. Residual TPH concentrations (mg/g) in soil samples after 5-day incubation.....115

Figure 4.26. Comparison of gene expression profiles in SET-1 and SET-2 at the second day of incubation. 117

Figure 4.27. Comparison of gene expression profiles in SET-1 and SET-2 at the fourth day of incubation. 118

Figure 4.28. Comparison of gene expression profiles in SET-2 and SET-3 at the second day of incubation 120

Figure 4.29. Comparison of gene expression profiles in SET-2 and SET-3 at the fourth day of incubation. 121

Figure 4.30. Comparison of gene expression profiles in SET-2 and SET-4 at the second day of incubation. 123

Figure 4.31. Heatmap of Gene Expression Profiles in SET-2 and SET-4 at the fourth day of incubation. 124

Figure 4.32. Microbial growth of different experimental sets with isolates with pMAT1 plasmid. 127

Figure 4.33. TPH Degradation Efficiency 128

Figure 4.34. Transposition rate in gene mobilization assay. 130

Figure 4.35. Comparative analysis of IS elements and transposase abundance across genomes of four distinct OTUs. 131

Figure 4.36. Distribution of transposon genes and IS Elements within Contig001. 132

Figure 4.37. Position of the XBaI as restriction enzyme for pMAT1 plasmid. 133

Figure 4.38. Distribution of high and low frequency transposons. 134

Figure 4.39. ISPre2 transposase in *Pseudomonas frederiksbergensis* genome.....134

Figure 4.40. The regions preferred by the ISPre2 transposon on the plasmid, the number of transpositions it perform in those regions, and the repeat sequences.....135

Figure 4.41. ISPre1 and ISPre2 transposons on pCAR1 plasmid. 136

LIST OF TABLES

Table 3.1. The composition of M9 Mineral Medium. 48

Table 3.2. Flask contents for enrichment test setup. 49

Table 3.3. Contents of M63B1 medium. 50

Table 3.4. The surfactants and their molecular characteristics. 54

Table 3.5. Preparation of surfactant stock solutions. 55

Table 3.6. Setup details of surfactant biodegradation assay. 58

Table 3.7. Setup for degradation experiment during gene expression profiling. 61

Table 3.8. Experimantal setup details for monitoring the gene mobilization. 67

Table 4.1. Taxonomic classification and distribution of OTUs derived from 16S rRNA sequencing of soil-isolate library colonies 88

Table 4.2. Phylogenetic similarity and genetic potential for hydrocarbon degradation of OTUs based on WGS analysis. 92

Table 4.3. MICs and CMCs of six surfactants tested against PEC culture 109

LIST OF SYMBOLS/ABBREVIATIONS

Symbol	**Explanation**
µl	Microliter
π	Nucleotide Diversity

Abbreviation	**Explanation**
ABC	ATP-Binding Cassette
BDAC	Tetredecylbenzyldimethyl Ammonium Chloride
CMC	Critical Micelle Concentration
CTAB	Cetyltrimethylammonium Bromide
DDAC	Didecyldimethyl Ammonium
DNA	Deoxyribonucleic Acid
GMO	Genetically Modified Organisms
HGT	Horizontal Gene Transfer
ICE	Integrative and Conjugative Element
km	Kanamycin
kmR	Kanamycin Resistance Gene
MGE	Mobile Genetic Element
MIC	Minimum Inhibitory Concentration
NAPL	Non-Aqueous Phase Liquid
OD	Optical Density
PEC	Petroleum Enriched Culture
PAH	Polycyclic Hydrocarbon
PCR	Polymerase Chain Reaction
PHC	Petroleum Hydrocarbon
Sd	Standard Deviation
SDS	Sodium Dodecyl Sulfate
SOM	Soil Organic Matter
TPH	Total Petroleum Hydrocarbon
TX	TritonX-100
TW	Tween-20
WGS	Whole Genome Sequencing

1. INTRODUCTION

Petroleum pollution is a major global issue because it harms ecosystems, human health and global economy. The main sources for petroleum pollution include leaks and spills that occur during storage, transport and disposal of petroleum products. Recent studies show that such pollution contaminates soil and groundwater, damages marine ecosystems, and disturbs soil environment (Falih et al., 2024). Contaminated soil is especially critical: petroleum hydrocarbons (PHCs) seep into the ground, lower soil fertility and disturb terrestrial ecosystems. Because PHCs persist for long periods, they can build up in plants and move through the food chain, threatening biodiversity and human health (Mekonnen et al., 2024). When contaminated food and water are consumed, this can lead to a number of health concerns, such as skin disorders, respiratory disorders, and chronic illnesses like cancer (Babuji et al., 2023). Soil pollution also cuts crop yields, impacting food security and local incomes. The high cost of cleanup, restoring farmland, and lost agricultural revenue places a heavy economic burden on farming communities (UNEP, 2023). Bioremediation technology has advanced, and stringent land-use laws have been implemented to stop additional contamination in an effort to minimize petroleum pollution in soil. However, to properly manage and rehabilitate petroleum-contaminated lands, greater international cooperation and ongoing study are required, as evidenced by the persistence of soil pollution incidents. Maintaining agricultural output and safeguarding public health require addressing the long-term effects of soil contamination (World Bank, 2023).

Among the different strategies used for cleaning contaminated soils, bioremediation stands out as both practical and eco-friendly due to its low cost and small environmental footprint. Bioremediation uses the natural metabolic processes of microorganisms to break down and detoxify toxic chemical substances in place, in contrast to physical and chemical remediation approaches, which frequently require the isolation of contaminated soil and treatment *ex-situ*. Because it works *in-situ*, this approach avoids the large volumes of secondary waste typically produced by conventional techniques and causes far less site disturbance (Varjani, 2017).

Although chemical remediation techniques like chemical oxidation and soil washing can be successful in eliminating pollutants, they frequently include the use of dangerous chemicals that might deteriorate the environment. In contrast, physical techniques like landfilling and soil excavation are expensive and may result in the irreversible loss of valuable land. As an alternative, bioremediation uses native or supplemented microorganisms, mainly bacteria and fungi, to convert complex PHCs into nontoxic byproducts like water and carbon dioxide (Das and Chandran, 2011).

By working with the soil's own biology rather than against it, this strategy not only restores fertility but also support long-term ecosystem stability.

The effectiveness of bioremediation in treating soils polluted with petroleum has been shown in recent studies. In a field study, Ling et al. (2023) used surfactant-enhanced bioremediation (SEBR). Alpha olefin sulfonate was applied together with oil-degrading strain *Pseudomonas sp.* SB. After 98 days, total petroleum hydrocarbons (TPH) dropped by 57.4%. This method also enhanced the removal of long-chain hydrocarbons (C_{21}–C_{40}) by 55.9%, highlighting the efficacy of combining surfactants with microbial strategies for tackling complex contamination. The study further revealed that the inclusion of surfactants not only increased the bioavailability of hydrocarbons but also stimulated the growth of hydrocarbon-degrading bacterial genera such as *Alcanivorax* and *Pseudomonas*. These results show that SEBR is a promising option for large-scale environmental remediation projects.

Fungi can also play an important role. Harms et al. (2011) reported that strains of *Aspergillus* and *Penicillium* could efficiently degrade polycyclic aromatic hydrocarbons (PAHs), which are among the most harmful substances found in petroleum. These fungi utilize ligninolytic enzymes, such as laccases and peroxidases, to break down PAHs into less toxic compounds. The study reported that fungal-mediated degradation could reduce PAH concentrations by up to 70% under optimized conditions, with the added benefit of enhancing soil quality and microbial diversity.

Bioremediation uses native or added microorganisms to break down PHCs, but its success depends on hydrocarbon bioavailability, soil conditions, microbial community structure, and the supply of nutrients (Das and Chandran, 2011). Highly hydrophobic and poorly soluble PHCs strongly bind to soil organic matter (SOM), hence limiting their bioavailability and prolonging contamination (Harmsen and Naidu, 2013). Soil heterogeneity add an additional layer of complexity: variations in porosity and particle size create patchy contaminant zones and uneven treatment efficiency (Urum & pekdemir, 2004; Semple et al., 2004). Although bioremediation is an attractive green option, we still need integrated strategies to overcome mass transfer limitations, address recalcitrant hydrocarbon fractions, and optimize the interplay among soil, pollutants and microbial populations.

Conventional bioremediation methods for petroleum-contaminated soils usually confront significant cost, scale, and efficiency constraints, resulting in partial or inefficient pollutant degradation (Varjani, 2017; Al-Hawash et al., 2018). These constraints show the need for more comprehensive and innovative strategies that can effectively manage the persistence and complexity of PHCs in the environment. Recent progress relies on mixed microbial communities whose diverse

metabolic routes break down both aliphatic and aromatic hydrocarbons. Das and Chandran (2011) demonstrated that carefully selecting and optimizing bacterial-fungal consortia can target a wider range of hydrocarbon structures while keeping harmful by-products to minimum.

The application of chemical surfactants to contaminated soils presents a promising approach to enhance bioavailability. Surfactants decrease the interfacial tension between hydrocarbons and soil particles, thereby improving the solubility and dispersion of hydrophobic compounds (Mao et al., 2015). Surfactants boost the interaction between hydrocarbons and microbial enzymes by mobilizing bound contaminants. Still, some synthetic surfactants can be toxic, long-lasting or costly. To limit such drawbacks, it is essential to pick surfactants that minimize secondary pollution, apply them at doses that do not disturb soil structure, and match them to local site conditions. Careful selection and controlled use can therefore boost biodegradation while keeping environmental risk low.

Maintaining suitable soil conditions is just as important as adding surfactants to facilitate microbial metabolism of hydrocarbons. Supplying key nutrients such as nitrogen and phosphorus keeps hydrocarbon degrading microbes active (Das & Chandran, 2011). Monitoring and adjusting parameters such as pH, temperature, and moisture content can further optimize biodegradation processes, allowing the system to adapt to site-specific variations. In this context, surfactant-enhanced bioremediation offers a compelling solution because it simultaneously tackles the mass-transfer limitations while leveraging the innate resilience and adaptability of microbial consortia (Mao et al., 2015; Varjani, 2017).

Bioremediation is important not just for cleaning up contaminated soils, but also for supporting sustainable land use. According to Oro and colleagues (2024), bioremediation improves yields from agriculture by restoring soil health and lowers the possibility of pollutants making their way into the food chain. Bioremediation offers a more economical and environmentally friendly alternative to traditional remediation techniques, which can be costly and harmful to the environment, especially when encountering large-scale contamination. Applying it *in-situ* reduces the requirement for large-scale infrastructure or for transporting contaminated soil (Perez-Vazquez et al., 2024). Because of its advantages over physical and chemical procedures along with its positive effects on the environment, it is a key component of sustainable remediation solutions (Mishra et al., 2023). The identification of novel microbial strains and the optimization of bioremediation procedures may significantly improve the technique's efficacy in dealing with global concerns related to soil contamination as research progresses (Alidoosti et al., 2024).

Mobile genetic elements (MGEs)—plasmids, transposons, integrative-conjugative elements and class 1 integrons—play a pivotal role in microbial adaptation to hydrocarbon stress by shuttling catabolic genes such as *alkB, xyl* and *nah* among bacteria inhabiting oil-impacted soils. These elements not only provide ready-made enzymatic cassettes for the initial oxidation of aliphatic and aromatic fractions but also carry accessory functions that improve surfactant tolerance and heavy-metal resistance, traits often co-selected in contaminated sites (Top & Springael, 2003; Dennis & Zylstra, 2004). Laboratory and field studies have shown that exposure to non-ionic surfactants or sub-inhibitory levels of petroleum fuels triggers SOS responses and conjugative transfer, markedly increasing the copy number of degradative plasmids within days (Ma et al., 2020). Consequently, horizontal gene transfer (HGT) accelerates both the emergence of specialist degraders and the functional redundancy needed for robust, community-wide mineralization of TPHs. Understanding how environmental cues modulate MGE mobilization is therefore essential for designing bioaugmentation strategies that couple surfactant-enhanced bioavailability with rapid genetic dissemination of hydrocarbon-degradation pathways.

The primary objective of this thesis is to investigate the mobilization and transfer dynamics of MGEs during the biodegradation of TPHs in the presence of surfactants (Figure 1.1). This study aims to monitor the horizontal transfer of MGEs within microbial communities under varying environmental conditions and to explore the relationship between MGE mobilization and TPH degradation efficiency. By incorporating surfactants, the bioavailability of hydrocarbons will be enhanced, enabling more effective microbial activity and facilitating the distribution of functional genetic elements across microbial populations. This research will also assess how surfactants influence the microbial community structure and their genetic potential for hydrocarbon degradation. The outcomes are expected to provide valuable insights into the role of MGEs in enhancing microbial biodegradation processes, contributing to the development of sustainable and environmentally friendly bioaugmentation strategies.

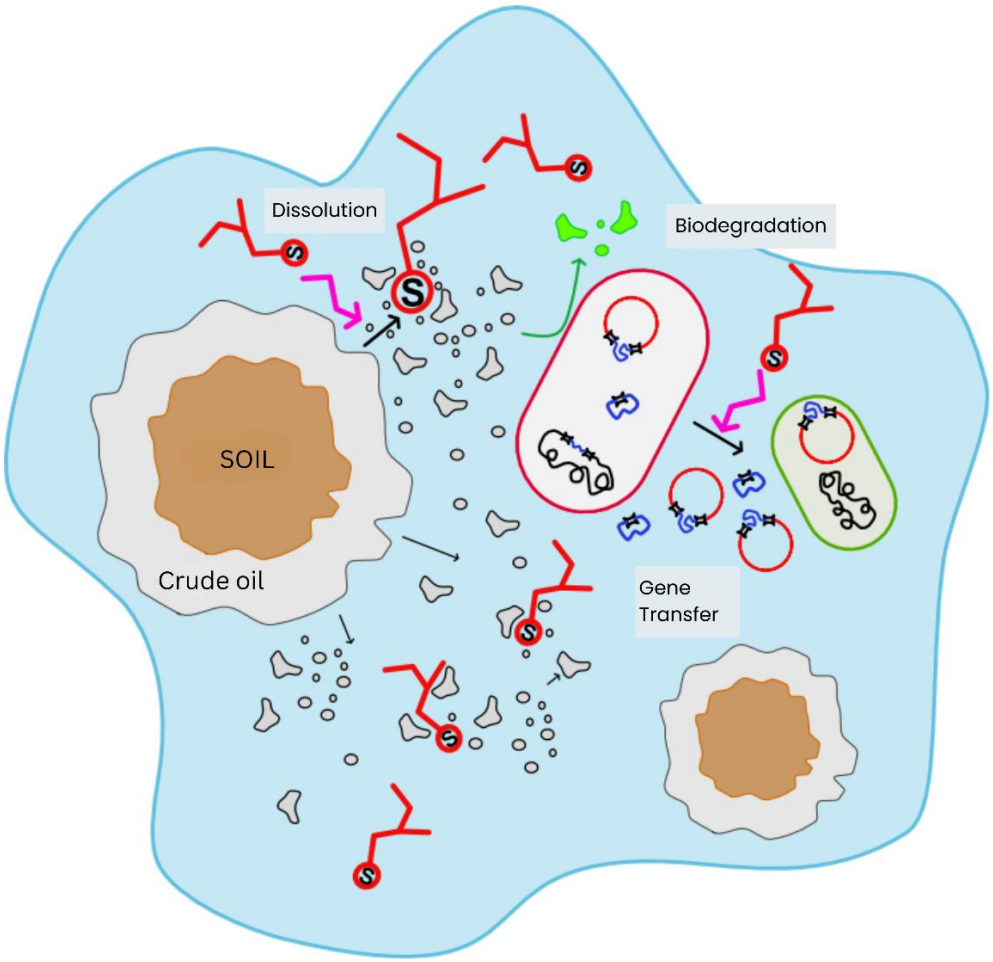


Figure 1.1. Conceptual content of the research.

2. LITERATURE REVIEW

2.1. PHCs and Environmental Impacts

PHCs, which are widespread pollutants primarily resulting from industrial activities and the combustion of fossil fuels, represent a significant and persistent environmental challenge. These compounds contaminate soil and water systems through various pathways, including crude oil spills, industrial effluents, and urban runoff. Due to their complex chemical structures, PHCs exhibit strong resistance to natural degradation processes, leading to their prolonged persistence in the environment. This persistence facilitates bioaccumulation, thereby increasing toxicity risks for ecosystems and human health alike. Additionally, PHCs adversely affect biodiversity by disrupting soil microbial communities that are crucial for maintaining soil fertility and overall ecosystem functioning. Given their documented health hazards and ecological impacts, it is crucial to deepen our understanding of the effects of PHCs on soil and water quality in order to promote both environmental sustainability and public health protection.

2.1.1. PHC Contamination Sources

The primary sources of PHC contamination include oil spills during transportation, accidental leaks from pipelines, operational discharges from offshore platforms, and leaks from storage facilities. Additionally, urban runoff carrying automotive oils, discharges from refineries, and residues from incomplete fossil fuel combustion further contribute to PHC pollution. These contaminants infiltrate soil, water, and sediment, where they can persist for extended periods and pose significant environmental and public health risks (Falih et al., 2024).

Over the past five years, increasing attention has been given to the scale and impacts of oil spills globally. Data from the International Tanker Owners Pollution Federation (ITOPF) show that, although oil spills from tankers have declined in recent decades due to improved safety measures, they continue to pose a significant threat, with 6.3 million liters of oil released in 2020 alone (ITOPF, 2022). The United Nations Environment Programme (UNEP) has reported that oil spill incidents consistently cause extensive contamination of marine and coastal ecosystems, leading to considerable soil pollution in coastal and offshore areas. Moreover, onshore activities such as oil exploration and extraction have caused severe soil contamination, particularly in regions like the Niger Delta.

Research indicates that hydrocarbon concentrations in these areas exceed safe environmental thresholds (UNEP, 2011).

Recent estimates by the World Bank (2022) suggest that approximately 1.3 billion tons of oil-contaminated soil exist worldwide, with a significant portion attributed to oil spills. This environmental burden is particularly pronounced in regions with intensive oil extraction and transportation activities. A study conducted in the Northern Peruvian Amazon demonstrated that PHC concentrations in soils near oil extraction sites were substantially elevated compared to background levels. TPH in contaminated soils ranged from 1,700 mg/kg to 65,000 mg/kg, far exceeding the typical threshold of 50 mg/kg. This represents an increase of over 1,000%, highlighting the long-term environmental impact of oil extraction operations in the region (Rosell-Melé et al., 2018). Due to the persistent nature of PHCs and inadequate remediation efforts, this contamination is expected to endure for decades. These findings emphasize the urgent need for improved remediation strategies to effectively address soil pollution associated with oil extraction.

2.1.2. Environmental and Health Impacts

The persistence and bioaccumulation of PHCs, particularly PAHs, in terrestrial and aquatic environments pose significant environmental and public health challenges. Due to their hydrophobic nature, PHCs strongly adsorb to soil particles, which hinders microbial degradation and leads to their prolonged persistence in the environment. PAHs, a subclass of polycyclic hydrocarbons, are especially stable and toxic because of their complex molecular structures. This stability enables them to remain in ecosystems for decades, continuously threatening both human health and ecological integrity.

A research study by Hylland (2006) offers a comprehensive analysis of PAH ecotoxicology in marine habitats, emphasizing their persistence and the threats they present to aquatic organisms. The study highlights that PAHs can accumulate in marine species' tissues, resulting in hazardous consequences that can transfer via the food chain and ultimately affect human health. This highlights the necessity for efficient monitoring and remediation solutions for addressing PHC contamination in diverse environments.

Numerous health risks have been linked to exposure to PHCs in contaminated soil and water. The IARC (2022) classifies certain PAHs, such as benzo[a]pyrene, as carcinogenic, indicating that prolonged exposure increases the risk of cancer, especially among populations living near oil spill

sites or industrial areas. Additionally, ingestion of PHCs through drinking water or direct contact with polluted soils can cause immune suppression, liver toxicity, and reproductive effects. These compounds can also bioaccumulate through the food chain, increasing toxicity risks at higher trophic levels (Agency for Toxic Substances and Disease Registry (ATSDR), 1999).

PHCs significantly affect ecosystem biodiversity and soil health, in addition to their direct health hazards. The toxicity of PHCs disrupts microbial communities essential for nutrient cycling, which in turn inhibits crop productivity and diminishes soil fertility. These microbial disturbances adversely impact soil structure, carbon cycling, and nitrogen availability—processes vital for ecosystem stability (Yu et al., 2024). Biodiversity declines in contaminated environments due to the suppression of sensitive species, initiating a cascade of effects that destabilize ecological balance. The ecological damage caused by PHCs underscores the urgent need for effective remediation and prevention strategies to mitigate their long-term environmental impact.

2.2. Characteristics of PHCs Affecting Their Behavior and Transport in Soil

Environmental pollution caused by PHCs is complex and influenced by various factors, including bioavailability, microbial degradation, and sorption/desorption processes. The poor solubility and hydrophobic nature of PHCs lead to strong binding with soil SOM, which restricts microbial communities' ability to degrade these compounds. Understanding the interactions among these factors is essential for developing targeted remediation strategies that can effectively reduce PHC pollution and mitigate associated environmental impacts.

2.2.1. Chemical and Molecular Structure

PHCs comprise a variety of organic compounds primarily made up of hydrogen and carbon. The structural differences among these compounds play a crucial role in their environmental persistence, chemical properties, and potential toxicity. Aliphatic and aromatic hydrocarbons are the two main classes of PHCs, each exhibiting distinct molecular characteristics that influence their environmental behavior and resistance to degradation. Their persistence in natural environments is largely determined by structural features such as the degree of branching, ring structures, and aromaticity (Nzila, 2018).

Aliphatic hydrocarbons are classified based on the type of carbon-carbon bonds they contain: alkanes, alkenes, alkynes. Alkanes, also known as saturated hydrocarbons, are highly stable and less

reactive due to the absence of functional groups, containing only alkanes. Their chemical stability makes them particularly resistant to microbial degradation, with resistance increasing as branching and structural complexity rise (Singh et al., 2012). Additionally, alkanes are highly hydrophobic and exhibit low solubility in water, which contributes to their accumulation in soil and sediment matrices where they can persist for extended periods. Their ability to resist natural degradation processes poses a long-term pollution risk to both aquatic and terrestrial ecosystems (Alexander, 1999).

Alkenes and alkynes, characterized by double and triple bonds respectively, are more reactive than alkanes due to their unsaturated structures. The presence of double or triple bonds increases their susceptibility to oxidative degradation pathways, promoting microbial or chemical breakdown. However, certain environmental conditions can slow these degradation processes, leading to prolonged accumulation of these compounds in ecosystems heavily contaminated with PHCs.

Aromatic hydrocarbons contain at least one benzene ring, which contributes significantly to their remarkable chemical stability due to the delocalized π-electron system within the ring structure. Aromatic compounds such as benzene, toluene, and ethylbenzene are highly resistant to environmental degradation because of this stability (Haritash & Kaushik, 2009). When multiple benzene rings are fused together, they form PAHs, which exhibit even greater environmental persistence and bioaccumulation potential. As the molecular weight of PAHs increases, their molecular stability improves. Higher molecular weight PAHs tend to be less soluble in water and more strongly adsorbed to soil and sediment particles, reducing their bioavailability but increasing their environmental persistence. Consequently, PAHs are recognized as significant pollutants, with many compounds classified as carcinogenic or mutagenic due to their interactions with biological molecules such as DNA and cellular membranes, leading to toxicity and adverse health effects in exposed organisms (Rabani et al., 2020).

The structural complexity and multi-ring configuration of PAHs render them resistant to both biotic and abiotic degradation, intensifying the environmental risks they pose. Although high molecular weight PAHs exhibit low water solubility, they readily sorb onto particles, leading to gradual accumulation in organic-rich soils and sediments. Beyond their their potential to damage genetic material, PAHs can undergo photochemical reactions under sunlight, producing more toxic intermediates such as hydroxylated derivatives and quinones. These byproducts bioaccumulate and present increased risks to both aquatic and terrestrial organisms (Hylland, 2006). The formation of reactive intermediates further complicates remediation efforts, as these transformation products often pose greater threats to human health and the environment than the parent compounds.

In conclusion, the mobility, environmental toxicity, and chemical composition of PHCs, particularly the differences between aliphatic and aromatic hydrocarbons, play a major role in their environmental behavior. Branched alkanes, cycloalkanes, and aromatic hydrocarbons, especially PAHs, are highly resistant to natural degradation processes. This underscores the need for tailored remediation approaches, unlike simpler alkanes that may degrade under favorable conditions over time. Understanding the structural diversity of these hydrocarbons is essential for managing and reducing their long-term environmental impacts (Das and Chandran, 2011).

2.2.2. Low Solubility and Hydrophobicity

Non-aqueous phase liquids (NAPLs) play a significant role in the environmental behavior of PHCs. Due to their high hydrophobicity and low solubility, PHCs tend to aggregate in aqueous environments, forming NAPLs that restrict their mobility and reduce their interaction with water. This behavior arises from the nonpolar molecular structure of PHCs, which mainly consist of hydrocarbon chains or aromatic rings; consequently, PHCs preferentially partition into nonpolar phases rather than dissolving in water (Mackay & Callcott, 1998). This partitioning diminishes their mobility and bioavailability for biodegradation, substantially influencing their interactions within aquatic environments.

Aromatic hydrocarbons and PAHs, due to their higher molecular weight and structural complexity, exemplify the low solubility characteristic of PHCs. Specifically, PAHs strongly sorb to organic-rich sediments, contributing to their prolonged environmental persistence. Studies have shown that the water solubility of PAHs decreases exponentially with increasing molecular weight, rendering them less accessible to microbial degraders (Alexander, 2000). The long-term persistence of PHCs in contaminated soils and sediments is primarily attributed to their reduced bioavailability, which intensifies their ecological impact and slows microbial degradation rates.

Partitioning into NAPLs and a strong affinity for soil and sediment matrices are additional factors that contribute to the resistance of PHCs to natural attenuation. Consequently, advanced remediation techniques that enhance the bioavailability of these compounds are necessary. For instance, the use of surfactants or co-solvents has been explored to increase the water solubility of PHCs and improve their accessibility to degrading microbial communities (Semple et al., 2001). Effective bioremediation strategies addressing the ecological and environmental challenges posed by PHC pollution must be grounded in a comprehensive understanding of these interactions.

Hydrophobicity drives the concentration of PHCs in nonpolar environments, reflecting their low solubility. These compounds preferentially partition into organic-rich soil matrices or sediment particles. Such partitioning reduces their availability to water-soluble reactive species, thereby slowing chemical and biological degradation processes. Additionally, studies have demonstrated that highly hydrophobic PHCs accumulate in the lipid membranes of organisms, leading to bioaccumulation across different trophic levels. This poses long-term risks to biota (Karapanagioti et al., 1999).

Discharge of PHCs in concentrated or large quantities can lead to the formation of NAPLs, which exist as a separate liquid phase that does not readily dissolve or mix with water. Based on their density, NAPLs are classified into two types: light NAPLs (LNAPLs), which are less dense than water and tend to float on the water surface, and dense NAPLs (DNAPLs), which are denser than water and sink, accumulating at the bottom of aquatic environments or penetrating deeper into soil layers (Pankow and Cherry, 1996). DNAPLs typically contain heavier hydrocarbons, more chlorinated compounds, or high-molecular-weight PAHs, while LNAPLs generally consist of lighter hydrocarbons such as diesel and gasoline (MacKay et al., 1994).

Viscosity, density, and molecular interactions between PHCs and the surrounding soil or water significantly influence the complex behavior of NAPLs in the environment. During phase separation, LNAPLs form persistent contaminant layers that float on the water surface, posing serious threats to aquatic ecosystems and surface water quality (Pankow & Cherry, 1996). Conversely, DNAPLs can penetrate deeply into groundwater aquifers, creating long-term pollution sources that are difficult to remediate due to their resistance to dissolution and the challenges associated with accessing deeper geological formations (Rivett and Allen King, 2003).

The formation of NAPLs significantly hinders the remediation of PHC-contaminated environments. Due to their low solubility, PHCs are released slowly through dissolution, making both LNAPLs and DNAPLs persistent long-term contaminants. This gradual release in soil and groundwater can extend contamination timelines and increase the environmental persistence of PHCs (Kueper et al., 2014). Moreover, NAPLs exhibit resistance to conventional remediation techniques such as bioremediation and chemical oxidation, owing to their immiscibility with water and strong affinity for organic materials. As a result, these methods are often less effective against hydrophobic, phase-separated contaminants.

NAPLs exhibit limited responsiveness to dilution, meaning that even small amounts can maintain high local concentrations of PHCs, potentially leading to acute toxicity in affected environments. The persistence of NAPLs, along with their capacity to generate toxic intermediates through extended degradation processes, underscores the need for targeted remediation strategies that specifically address their unique chemical properties and phase behavior (Leharne, 2021).

The limited solubility and hydrophobic nature of PHCs are key factors contributing to their environmental persistence, influencing their behavior in soil, water, and sediment ecosystems. These unique properties enable NAPLs to separate from water and persist as long-term contaminant sources. Given the challenges posed by NAPL behavior, the development of innovative remediation strategies is essential to effectively mitigate the long-term ecological and health risks associated with PHC contamination.

2.2.3. Sorption/Desorption Dynamics with SOM

The process of sorption involves the adhesion of PHCs to soil particles or organic matter, whereas desorption refers to their release back into the soil solution. Understanding the dynamics of these processes is essential for predicting the fate of PHCs in contaminated soils. Environmental factors such as pH and temperature, alongside the chemical structures of hydrocarbons and the properties of SOM, significantly affect sorption and desorption behaviors. Kupryianchyk et al. (2012) demonstrated that the addition of activated carbon can enhance the sorption of hydrophobic organic compounds in sediments, substantially reducing their bioavailability and mobility. Their study reported that activated carbon amendments decreased PAH concentrations in pore water by up to 90%, underscoring the importance of sorption enhancement in remediation strategies.

For nonpolar PHCs, hydrophobic interactions serve as the primary sorption mechanism driving strong binding to SOM. As PHCs sorb onto organic matter, their concentrations in the aqueous phase decrease, limiting their bioavailability for microbial degradation. This effect is especially pronounced for higher molecular weight compounds and PAHs, which exhibit stronger sorption affinity to soil matrices (Kueper et al., 2014). Consequently, these compounds can persist in soils for extended periods, potentially leading to long-term ecological risks.

Desorption dynamics play a crucial role in determining the availability of previously adsorbed PHCs. Factors such as temperature fluctuations, microbial activity, and changes in moisture content can trigger desorption, increasing PHC concentrations in the soil solution and making them accessible

for microbial degradation (Wang et al., 2021). However, desorption rates can be slow, particularly for contaminants strongly bound to soil particles, resulting in prolonged periods during which PHCs remain unavailable for biodegradation.

The interaction between sorption and desorption critically influences the rate of PHC biodegradation. Increased sorption reduces the bioavailability of PHCs, thereby slowing microbial degradation. Conversely, efficient desorption enhances microbial activity by increasing bioavailability, which accelerates degradation rates. Achieving an appropriate balance between these processes is essential in contaminated environments, where microbial communities often adapt to fluctuations in contaminant availability (Leharne, 2021).

2.2.4. Bioavailability and Microbial Degradation

The bioavailability of PHCs plays a critical role in their biodegradation by microbial communities in contaminated environments. Understanding the dynamics of sorption and desorption between PHCs and SOM provides valuable insights into biodegradation processes, particularly regarding how these interactions influence the accessibility of PHCs for microbial degradation.

Bioavailability refers to the rate and extent at which PHCs are accessible to microbial organisms for degradation. This accessibility is influenced by various factors, including the chemical composition and physical state of PHCs, as well as their interactions with soil matrices. Due to their low water solubility, bacteria have limited access to hydrophobic compounds such as aliphatic hydrocarbons and PAHs. Their hydrophobic nature leads these substances to partition into the soil's organic phase, where they bind strongly to organic matter and soil particles (Harms and Bosma, 1997).

SOM significantly influences the bioavailability of PHCs. As a key soil component formed through the decomposition of plant and animal residues, SOM contributes to maintaining soil structure and properties. Its complex composition provides a high sorption capacity, allowing interactions with various hydrophobic organic pollutants. PHCs that sorb to SOM exhibit reduced diffusion into the aqueous phase, leading to decreased bioavailability. This reduction in bioavailability can slow microbial degradation rates, thereby prolonging the persistence of PHCs in contaminated environments (Chen et al., 2019).

The microbial degradation of PHCs primarily involves the metabolic activity of microorganisms that utilize these compounds as sources of carbon and energy. The concentration and availability of contaminants in the environment play a critical role in determining the efficiency of these processes. In response to the stress imposed by PHCs, microbial communities adapt, with certain populations becoming specialized in degrading specific hydrocarbons. Additionally, microbial activity and the degradation rates of adsorbed PHCs are influenced by environmental factors such as nutrient availability, temperature, and moisture content (Deborah Gnana Selvam and Thatheyus, 2018).

2.3. Challenges in Remediating Petroleum-Contaminated Soils

Remediation of petroleum-contaminated soils is inherently challenging due to the complexity of both PHCs and soil properties. PHCs are characterized by strong hydrophobicity and low water solubility, which lead to their preferential partitioning into SOM and sorption within soil matrices (Harmsen and Naidu, 2013). These properties limit their solubility in soil, making degradation and cleanup difficult. Furthermore, the presence of diverse organic and mineral components in soils complicates the consistent application of remediation treatments, thereby prolonging contaminant retention in subsurface environments (Urum & Pekdemir, 2004; Semple et al., 2004). Given the persistent threat that PHCs in soil pose to ecosystems and human health, the development of effective remediation strategies that address both biological and physical barriers to contaminant degradation is essential.

These challenges have led to the development of a wide array of remediation techniques; however, each method faces specific limitations when applied to petroleum-contaminated soils. Understanding these constraints is essential for designing treatment approaches that are both cost-effective and environmentally sustainable.

2.3.1. Limitations of Physical and Chemical Remediation Methods

Common physical and chemical remediation techniques for PHC-contaminated soils include chemical oxidation, air sparging, and thermal desorption. However, these methods have notable limitations. The complex soil matrix, which is characterized by variable porosity, particle size distribution, and mineral composition, can generate matrix effects that impede the uniform distribution of heat, chemicals, or other treatment agents. For example, limited porosity in dense or clay-rich soils often reduces the efficiency of thermal desorption, which relies on heating the soil to

volatilize PHCs. This limitation can diminish heat transfer and result in incomplete contaminant removal (Bykova et al., 2021).

The strong sorption of PHCs to SOM, which limits their mobility within the soil matrix, also leads to mass transfer limitations. Adsorption onto soil particles or entrapment within micropores makes PHCs inaccessible to remediation techniques (Semple et al., 2004). For example, in chemical oxidation processes, oxidizing agents may fail to reach pollutants confined within soil micropores, resulting in partial oxidation and residual PHCs (Li et al., 2014). Because PHCs desorb slowly over time, this residual contamination poses long-term risks, including the potential for recontamination of soil and groundwater resources (Reddy & Adams, 2001).

Furthermore, prolonged retention of contaminants within soil matrices is a well-documented phenomenon in remediation science. Studies have shown that contaminants such as PAHs can become sequestered in soil micro pores or aged organic matter over time, making them resistant to extraction and degradation (Alexander, 2000). Both *ex-situ* and *in-situ* physical remediation techniques face challenges due to this sequestration effect, as contaminants may reemerge years after initial treatment, necessitating ongoing efforts and continuous monitoring (Urum & Pekdemir, 2004).

2.3.2. Biological Constraints in PHC Remediation

Bioremediation, which employs microbial communities to degrade PHCs, has emerged as a sustainable alternative to traditional physical and chemical remediation methods. However, biological approaches face inherent limitations, particularly in soils where contaminant bioavailability is low. The low water solubility of PHCs restricts their accessibility to native microbial populations that rely on aqueous-phase diffusion for uptake. Consequently, the effectiveness of microbial degradation is reduced, as only the fraction of PHCs dissolved in soil water is bioavailable (Semple et al., 2003).

Furthermore, many indigenous microbial communities lack the necessary catabolic enzymes to degrade complex hydrocarbon structures. Although some microbes possess metabolic pathways capable of breaking down PHCs, studies have shown that their abundance and activity levels are often insufficient for effective remediation. This limitation is particularly pronounced in soils with low microbial diversity or in areas without prior hydrocarbon exposure (Margesin & Schinner, 2001; Bento et al., 2005). Tyagi et al. (2011) reported that microbial communities in pristine soils had a limited capacity to degrade PHCs compared to those in chronically contaminated sites. To address

this limitation and enhance remediation efficiency, techniques such as bioaugmentation, biostimulation, or the introduction of specific microbial strains are frequently employed.

Environmental factors such as soil pH, oxygen concentration, and nutrient availability play critical roles in influencing microbial activity and survival, thereby directly affecting the rate of PHC degradation in contaminated soils. Aerobic hydrocarbon-degrading bacteria exhibit reduced activity in subsurface environments with low oxygen levels, necessitating the development of novel *in-situ* bioremediation approaches to address these challenges. Additionally, limited pollutant bioavailability and metabolic constraints of native microbial communities further impact the effectiveness of conventional biological remediation techniques. Integrated remediation strategies that combine physical, chemical, and biological methods offer promising solutions to overcome these barriers. Varjani (2017) emphasizes the importance of such integrated approaches, noting that overcoming microbial and environmental limitations through combined treatments can enhance degradation efficiency. Wu et al. (2021) explored interfacial solar evaporation as an innovative technique to mitigate heavy metal contamination in moist soils, illustrating how advanced physical and chemical technologies can complement biological remediation efforts. These findings highlight the value of multidisciplinary approaches for the effective management of petroleum-contaminated soils.

2.4. Bioremediation as Preferred Approach for PHC Contamination

2.4.1. Overview of Bioremediation Techniques

Bioremediation is a widely applied, cost-effective, and environmentally friendly approach that uses microorganisms to degrade or remove pollutants from contaminated environments, including PHCs. This strategy harnesses the metabolic capabilities of microbial communities to transform pollutants into less harmful substances, thereby restoring the ecological balance of affected sites. Due to its adaptability and lower environmental impact compared to more aggressive chemical or physical remediation methods, bioremediation is regarded as a "green" solution in environmental management, particularly for soils and waters contaminated with organic pollutants (Vidali, 2001).

The appeal of bioremediation lies primarily in its cost-effectiveness and reduced environmental impact. Compared to traditional methods such as chemical oxidation or thermal desorption, bioremediation offers advantages including lower resource consumption, reduced waste generation, and preservation of the physical and chemical properties of the treated environment (Pande et al., 2020). Additionally, bioremediation can be tailored to target specific types of contamination and

environmental conditions, providing a flexible solution for diverse remediation needs. However, it is essential to carefully evaluate the advantages and limitations of each method, as the efficiency of bioremediation is highly influenced by environmental factors and the bioavailability of pollutants (Alori et al., 2022).

Bioremediation methods are generally classified into two main strategies: *ex-situ* and *in-situ* bioremediation. Both rely on microbial degradation but differ in their application and scale, each presenting unique advantages and challenges. *Ex-situ* bioremediation involves the physical removal of contaminated soil or water from the site, which is then treated under controlled conditions in environments such as bioreactors or composting systems to optimize microbial activity. In contrast, *in-situ* bioremediation treats contaminants directly at their original location without excavation or transport (Boopathy, 2000). Selecting between *ex-situ* and *in-situ* approaches involves trade-offs related to environmental disturbance, cost, and control. Although *ex-situ* methods may entail higher logistical costs and potential environmental impacts, they provide a highly controlled setting that can accelerate degradation rates. *In-situ* methods, meanwhile, are less invasive and better suited for large-scale applications but require careful consideration of site-specific conditions and longer timeframes to achieve effective remediation. Balancing contamination scenarios, environmental context, and remediation goals is essential when choosing the most appropriate bioremediation strategy (Vidali, 2001; Perez-Vazquez et al., 2024).

Ex-situ bioremediation involves the physical removal of contaminated soil or water from the affected site, allowing treatment in a controlled environment. Techniques such as composting piles, bioreactors, and bio-slurry systems enable precise regulation of factors including temperature, pH, oxygen levels, and nutrient supply, all of which are critical for maximizing microbial activity and degradation rates (Koul and Taak, 2018). *Ex-situ* approaches often offer improved remediation outcomes due to the ability to closely monitor and adjust limiting factors such as nutrient availability and moisture content that affect microbial degradation (Chaineau et al., 2005). Common *ex-situ* methods include composting, landfarming, biopiles, and slurry-phase bioreactors. In biopiles, contaminated soil is excavated, heaped, aerated, and often supplemented with nutrients and moisture to facilitate aerobic microbial degradation. Landfarming involves spreading contaminated soil over a large area and periodically tilling it to enhance microbial breakdown. Composting utilizes organic waste to stimulate microbial communities, accelerating biodegradation under thermophilic conditions, which is especially effective for certain organic pollutants. Slurry-phase bioreactors mix contaminated soil or sediment with water to create a slurry treated under highly controlled conditions to achieve elevated degradation rates (Boopathy, 2000; Vidali, 2001).

However, *ex-situ* methods are associated with significant environmental and logistical costs. Compared to *in-situ* techniques, excavation, transportation, and disposal of contaminated material require substantial resources and often heavy machinery, leading to a higher carbon footprint. Additionally, secondary contamination risks exist during soil handling and transport. *Ex-situ* remediation can also disrupt soil structure and ecosystem functions, potentially causing long-term adverse effects on soil health and fertility (Jørgensen et al., 2000). Therefore, *ex-situ* approaches are generally preferred for smaller, heavily contaminated sites or cases where *in-situ* remediation is impractical.

In-situ bioremediation targets contaminants directly within their natural environment, typically in soil or water. This approach is particularly advantageous for large-scale contamination sites or locations with limited accessibility, such as aquifers or densely vegetated areas, as it avoids excavation and transportation. This results in reduced operational costs, minimized environmental disturbance, and preservation of the natural structure and composition of the contaminated site (Alvarez & Illman, 2006). Common *in-situ* techniques include bioventing, biosparging, bioaugmentation, and natural attenuation. Bioventing enhances aerobic degradation by supplying oxygen or air to the unsaturated soil zone, facilitating microbial oxidation of contaminants. Biosparging is applied to groundwater contamination by injecting air below the water table, promoting upward migration of pollutants toward aerobic degradation zones. Natural attenuation relies on indigenous microbial communities to degrade contaminants without external inputs, although monitoring is essential to ensure effectiveness and progress (Abed et al., 2014). Bioaugmentation involves introducing specific microorganisms capable of degrading pollutants more efficiently than native populations, particularly when indigenous microbes lack the necessary enzymatic pathways. This method shows promise for persistent contaminants but depends on the introduced microbes' ability to compete and survive within the native microbial community (Chettri et al., 2023).

In-situ bioremediation offers benefits such as reduced environmental impact and suitability for extensive contaminated areas; however, it is limited by site-specific physical and chemical factors. Soil porosity, contaminant distribution, and oxygen availability critically affect treatment efficacy. Uneven distribution of nutrients and oxygen may lead to inconsistent or inadequate degradation (Jørgensen et al., 2000). Additionally, the longer timeframe required for *in-situ* remediation makes it less appropriate when rapid decontamination is necessary.

2.4.2. Various Bioremediation Methods and Their Integration

Natural attenuation is the most commonly used bioremediation method, relying on the inherent capacity of native microbial communities to degrade pollutants over time without external intervention. Although economical and minimally disruptive, the effectiveness of this approach depends on site-specific factors such as pollutant concentration, soil characteristics, and environmental conditions. Due to the longer time required to observe significant results, natural attenuation may be less suitable for situations demanding rapid decontamination (Rabus et al., 2016).

A study by Röling et al. (2002) investigated natural attenuation of PHCs in marine environments following an oil spill. Over several weeks, a marked reduction in hydrocarbon concentrations, including TPHs, was observed. Key microbial taxa such as *Alcanivorax* and *Cycloclasticus*, known for their hydrocarbon-degrading abilities, were identified, highlighting the efficiency of indigenous microbial communities in adapting to environmental changes and degrading hydrocarbons in marine settings.

Another recent study by Song et al. (2023) examined Collaborative Monitored Natural Attenuation (CMNA), an enhanced remediation strategy that combines natural attenuation processes with active monitoring and interventions, for remediating PHC (C_{10}-C_{40}) and 1,2-dichloroethane (1,2-DCA) contamination at a petrochemical site in Northeast China. Over four years, significant reductions in pollutants were achieved. PHCs in soil were reduced with a half-life of 693 days, whereas 1,2-DCA in groundwater degraded more slowly, with a half-life of 1,733 days, suggesting the necessity of enhancement measures such as nutrient supplementation. Microbial analyses during monitoring showed an increase in petroleum-degrading bacteria, particularly *Actinobacteria* and *Proteobacteria,* which played a crucial role in facilitating pollutant degradation. These findings demonstrate CMNA as a sustainable and effective soil remediation strategy, although groundwater treatment may require additional interventions.

Biostimulation enhances natural attenuation by supplying nutrients, electron donors, or other growth-promoting substances to contaminated environments, thereby accelerating microbial activity and contaminant degradation. However, the effectiveness of biostimulation can be limited by the availability of appropriate nutrients and the need for careful environmental control to prevent the proliferation of non-degrading microbial populations (Das and Chandran, 2011).

Several studies have demonstrated the efficacy of biostimulation in remediating PHC-contaminated soils. For example, Hamoud et al. (2018) reported a decrease in total TPH levels from 38% to 1.4% over 90 days in oil-polluted soil treated with carrot peel waste. This significant reduction underscores the importance of nutrient-rich amendments in stimulating hydrocarbon-degrading microbial communities. The study emphasized that optimizing nutrient concentrations and ensuring adequate soil aeration are critical factors for enhancing microbial activity and accelerating hydrocarbon breakdown.

Similarly, Nong et al. (2023) demonstrated the effectiveness of biostimulation in degrading TPHs in contaminated soils by applying a combination of nitrogen and phosphorus nutrients to stimulate indigenous microbial populations. Over a 300-day period, biostimulation achieved TPH degradation rates of 99.75% in surface soils, 95.73% in middle layers, and 99.84% in deeper soils. These results significantly outperformed natural attenuation, which showed minimal degradation across the same soil depths. Nutrient addition enhanced microbial activity and diversity, particularly favoring hydrocarbon-degrading genera such as *Pseudomonas* and *Bacillus*. These findings highlight biostimulation as a promising strategy for accelerating PHC biodegradation in complex soil environments while maintaining ecosystem health.

Genetically modified organisms (GMOs) offer a novel approach to bioremediation by enhancing the breakdown of complex pollutants through engineered metabolic pathways. Van Beilen and Funhoff (2007) demonstrated the effectiveness of genetically modified *Pseudomonas putida* strains in degrading hydrocarbons, particularly highlighting the role of alkane hydroxylases in the degradation of long-chain alkanes. Their research showed that engineered strains could degrade up to 85% of specific hydrocarbons in laboratory conditions within 30 days, significantly outperforming native, unmodified strains. Cases and De Lorenzo (2005) reported successful applications of GMO strains in environmental remediation, with genetically engineered microbial consortia achieving more than 90% reduction in TPHs in pilot-scale bioreactors. These findings underscore the potential of GMOs to address contaminants that native microbial populations cannot effectively degrade. However, field application of these technologies requires strict compliance with regulatory frameworks and comprehensive environmental safety assessments due to potential ecological risks, such as HGT to non-target organisms.

Phytoremediation is a bioremediation technique that utilizes plants to stabilize, remove, or degrade pollutants in soil. While primarily applied to heavy metals, several plant species have been shown to support microbial degradation of PHCs through interactions within the rhizosphere. As a

green and sustainable approach, phytoremediation is most effective when integrated with other bioremediation methods, although it generally requires longer timeframes to achieve significant results (Gerhardt et al., 2009).

A recent study by Sharuddin et al. (2024) explored rhizobacterial-assisted phytoremediation using S*cirpus grossus* for the treatment of crude oil sludge with high TPH concentrations. Conducted in a controlled greenhouse environment over 28 days, the batch phytoremediation system reduced the initial TPH concentration of 37,554 mg/kg by 75%. Significant accumulation of TPHs was detected in the plant roots and stems, measuring 15,319 mg/kg and approximately 8,000 mg/kg, respectively. The presence of rhizobacteria in the rhizosphere enhanced degradation by creating a nutrient-rich microenvironment, thereby stimulating microbial activity. These results highlight *S. grossus* as a promising, sustainable, and cost-effective strategy for mitigating TPH contamination in crude oil sludge.

Rather than relying on a single technique, bioremediation experts recognize that combining multiple methods often yields superior results by enhancing the overall remediation process. Techniques such as natural attenuation, biostimulation, bioaugmentation (with native or GMOs), surfactant-assisted degradation, and phytoremediation are frequently integrated to maximize hydrocarbon degradation. When applied together, these methods can overcome limitations inherent in each approach when used alone.

Natural attenuation, which depends on the intrinsic ability of microbial communities to degrade hydrocarbons over time, often serves as the baseline for many bioremediation projects. However, its effectiveness can be limited and slow in heavily contaminated soils. Biostimulation, involving the addition of nutrients or growth enhancers like nitrogen and phosphorus, which are typically deficient in contaminated environments, can significantly boost microbial activity. Andreolli et al. (2015) reported that biostimulation achieved a 70% reduction in high molecular weight hydrocarbons within 60 days, outperforming bioaugmentation (55% reduction) and natural attenuation (45% reduction). These results emphasize potential of biostimulation to accelerate biodegradation in hydrocarbon-impacted soils.

Agnello et al. (2016) evaluated four bioremediation strategies for soils co-contaminated with heavy metals and PHCs: natural attenuation, phytoremediation, bioaugmentation, and bioaugmentation-assisted phytoremediation. The combined bioaugmentation and phytoremediation approach demonstrated the highest efficiency, reducing TPHs by 68% over 90 days—surpassing

bioaugmentation alone (59%), phytoremediation alone (47%), and natural attenuation (37%). Natural attenuation relies on inherent soil processes, while phytoremediation utilizes *Medicago sativa* (alfalfa) to enhance degradation. The alfalfa root system stimulated microbial activity and stabilized metals in the rhizosphere. Bioaugmentation with *Pseudomonas aeruginosa* enhanced microbial community efficiency through mechanisms such as biosurfactant production, thereby improving hydrocarbon degradation rates. This integrative strategy effectively combined plant and microbial systems, yielding optimal remediation outcomes. The study highlights the promise of combined bioaugmentation-assisted phytoremediation, especially in co-contaminated sites.

A recent study by Zhen et al. (2021) investigated the synergistic effects of biochar and rhamnolipid biosurfactants on PHC bioremediation in soils. Modified biochars, particularly sludge biochar treated with rhamnolipids, significantly enhanced TPH removal, achieving a 32.9% reduction over 90 days. Short-chain alkanes (C_8–C_{12}) showed the highest degradation rates, exceeding 70%, while long-chain hydrocarbons and PAHs were less effectively degraded. The rhamnolipid-modified biochars also increased microbial diversity and abundance, particularly enriching hydrocarbon-degrading genera such as *Muricauda*. Although microbial activity led to increased CO_2 and CH_4 emissions, N_2O emissions decreased, indicating a complex environmental impact. This integrative approach underscores the potential of combining biosurfactants with biochar to improve PHC bioavailability and degradation efficiency, offering a promising strategy for soil remediation.

Overall, integrating multiple bioremediation methods represents the most effective strategy for treating petroleum-contaminated soils. Each technique offers distinct advantages that, when combined, compensate for the limitations associated with individual methods. Research has shown that combining surfactant-assisted biodegradation with autochthonous bioaugmentation significantly enhances hydrocarbon degradation rates. This synergistic approach accelerates the breakdown of even the most recalcitrant pollutants by increasing contaminant bioavailability through surfactants and leveraging the adaptability of native microbial communities. These findings underscore the potential of integrated bioremediation techniques to deliver both economic and environmental benefits in large-scale soil remediation projects. Future research aimed at refining these technologies while addressing ecological concerns could establish integrated approaches as the standard for responsible and effective remediation of petroleum-impacted sites.

2.5. A Synergistic Approach: Bioaugmentation and Surfactant-Assisted Biodegradation

2.5.1. Empowering Microbial Communities: The Role of Bioaugmentation

Bioaugmentation is a widely used bioremediation method involving the introduction of specific microbial strains known for their hydrocarbon-degrading capabilities into contaminated sites. This approach can significantly accelerate degradation rates, particularly in environments where native microbial populations are limited or slow to respond. While the compatibility of introduced microbes with the existing ecosystem must be carefully considered, bioaugmentation has demonstrated considerable potential, especially when integrated with other remediation techniques (Chettri et al., 2023).

Allochthonous bioaugmentation refers to the introduction of non-native microbial strains to contaminated sites to enhance pollutant degradation. This strategy is particularly advantageous when indigenous microbial communities are absent or ineffective in degrading the target contaminants. However, a key challenge of allochthonous bioaugmentation lies in the ability of the introduced microorganisms to survive and remain active under prevailing environmental conditions and within the existing microbial community (Mrozik & Piotrowska-Seget, 2010).

Studies such as those by Tyagi et al. (2011) demonstrate that despite inherent challenges, bioaugmentation can accelerate the degradation of complex contaminants like PHCs by introducing specialized degraders that complement native microbial communities. Autochthonous bioaugmentation, which involves stimulating the growth of indigenous microbial populations already present in the soil, enhances natural biodegradation processes in contaminated environments. These native microbes are particularly effective at degrading specific pollutants due to their adaptation to the prevailing contaminants, such as PHCs. This approach minimizes ecological disturbance by supporting native bacteria and allowing them to adjust to local environmental conditions and contaminants, thereby enhancing natural attenuation without significantly altering the existing microbial community structure. Several studies have confirmed the efficacy of autochthonous bioaugmentation in reducing PHC concentrations in contaminated soils.

In a recent study, Behera et al. (2021) evaluated the efficacy of a two-step bioaugmentation strategy (TSBS) for the bioremediation of PHC-contaminated refinery sludge. The study utilized an indigenous bacterial consortium consisting of *Dietzia lutea*, *Staphylococcus warneri*, and *Stenotrophomonas pavanii* strains. Under optimized conditions (pH 7, temperature 34°C, and sludge

concentration of 2% (w/v)) TSBS achieved an impressive 91.5% reduction in TPHs within 15 days. This performance surpassed the 77.3% degradation observed with a single-step bioaugmentation, highlighting the advantages of repeated microbial inoculation in sustaining metabolic activity and accelerating pollutant degradation. These findings underscore the potential of TSBS for scaling up eco-friendly and efficient bioremediation in industrial settings.

Another study by Al-Kindi and Abed (2016) applied bioremediation techniques to oil-contaminated desert soils. By maintaining moisture and supplementing nutrients through the addition of organic wastes such as spent mushroom compost and poultry manure, they achieved significant TPH reductions over 90 days.

A study conducted in Japan investigated autochthonous bioaugmentation in cold coastal regions, particularly along the shores of Hokkaido. Utilizing indigenous microbial consortia enriched from local sea sands, researchers enhanced crude oil degradation in microcosm experiments. The inoculated consortia degraded approximately 50% of crude oil within two weeks under controlled conditions. This study demonstrated that autochthonous bioaugmentation not only improved hydrocarbon degradation rates but also preserved ecological balance by employing site-specific microbial populations, offering a sustainable remediation strategy for oil-contaminated sites (Hosokawa et al., 2009).

2.5.2. Accelerating the Bioremediation: The Power of Surfactants

The use of chemical surfactants in environmental remediation has gained significant attention due to their ability to enhance the solubility and bioavailability of PHCs in contaminated sites. Surfactants act as emulsifying agents by dispersing hydrophobic pollutants into micelles, thereby improving their distribution in aqueous environments and facilitating microbial degradation. Based on their ionic charge, surfactants are classified as non-ionic, anionic, or cationic, each exhibiting distinct interactions with PHCs and soil particles. Non-ionic surfactants demonstrate stability under varying environmental conditions, while anionic surfactants effectively reduce adsorption losses. Cationic surfactants can increase bioavailability; however, careful optimization is required to prevent potential microbial toxicity at high concentrations. The interactions between different surfactant types, PHCs, and environmental matrices underscore the importance of selecting appropriate surfactants tailored to specific remediation contexts to maximize treatment efficacy (Liu et al., 2021).

Non-ionic surfactants, such as Triton X-100 and Tween-20, enhance the solubility and bioavailability of PHCs by reducing surface and interfacial tension, which promotes the dispersion of hydrophobic contaminants in aqueous environments. Their uncharged nature renders them more resistant to environmental factors like pH and ionic strength, thereby minimizing interactions with soil particles. Structurally, these surfactants consist of hydrophilic polyoxyethylene chains and hydrophobic aliphatic or aromatic moieties, enabling micelle formation that encapsulates hydrophobic polycyclic hydrocarbons, enhancing their solubility and bioavailability to degrading microorganisms (Kumar et al., 2024).

Tween-20, a non-ionic ethoxylated sorbitan monolaurate, has been shown to effectively mobilize hydrophobic compounds in petroleum-contaminated soils and is relatively unaffected by environmental pH fluctuations. By forming micelles around hydrocarbon molecules, Tween-20 increases PHC bioavailability and facilitates microbial degradation (Shen et al., 2022). Triton X-100 comprises a hydrophobic alkyl tail and a hydrophilic ethoxylated phenol head, enabling it to substantially reduce water surface tension and improve PHC dispersion. Cameotra and Makkar (2004) demonstrated that Triton X-100 maintains stability and efficacy across a wide range of temperatures and salinity conditions.

The effectiveness of these surfactants can vary depending on soil properties and environmental factors such as temperature, organic matter content, and salinity. Although Triton X-100 and Tween-20 generally enhance PHC solubility, their bioavailability improvement may be limited by interactions with SOM or adsorption onto soil particles, which can reduce micelle formation capacity. Nevertheless, their non-ionic nature generally offers greater adaptability than ionic surfactants, allowing them to facilitate PHC degradation effectively across diverse bioremediation settings.

Anionic surfactants primarily interact with PHC components through their negatively charged head groups, which facilitate the dispersion of hydrophobic substances and enhance microbial uptake. By lowering surface and interfacial tension between hydrophobic PHC molecules and the aqueous phase, these surfactants increase hydrocarbon bioavailability for microbial degradation. Two commonly used anionic surfactants in bioremediation are sodium dodecyl sulfate (SDS) and dioctyl sulfosuccinate (DOSS). SDS, with its hydrophobic dodecyl tail and negatively charged sulfate head, solubilizes hydrocarbons by forming micelles that encapsulate PHC molecules, thereby increasing the surface area accessible to microbial enzymes and promoting microbial degradation (Mukherjee et al., 2017).

DOSS, characterized by a sulfosuccinate head and two long alkyl chains, facilitates both hydrophilic and hydrophobic interactions that enhance PHC dispersion in the environment. It significantly improves the bioavailability of high-molecular-weight hydrocarbons by forming persistent micelles capable of capturing larger PHC molecules, making them more accessible to microorganisms in hydrophobic environments (Ghazali et al., 2004). Additionally, the strong negative charge of DOSS repels other anionic soil components, reducing adsorption onto soil particles and allowing a greater proportion of the surfactant to remain active in the aqueous phase. This property enables DOSS to function effectively in a wide range of environmental conditions, including soils with high organic content.

Both SDS and DOSS enhance PHC solubility and reduce soil adsorption, facilitating microbial uptake. Their anionic nature minimizes surfactant losses due to soil adsorption—a common limitation of non-ionic surfactants—thereby promoting efficient biodegradation of PHCs in contaminated environments.

Cationic surfactants, characterized by positively charged head groups, significantly enhance the solubility and bioavailability of PHCs in contaminated environments. Their hydrophobic tails bind to the nonpolar regions of PHCs, emulsifying hydrocarbons and facilitating their dispersion in aqueous media. Cationic surfactants such as cetyltrimethylammonium bromide (CTAB) exhibit strong affinity for negatively charged surfaces, including soil particles and microbial cell membranes, due to their positive charge. This interaction promotes the adhesion of hydrocarbons to microbial cells, thereby enhancing microbial uptake and biodegradation rates (Karthick et al., 2019).

CTAB, a quaternary ammonium compound, is widely used in bioremediation owing to its amphiphilic nature, which increases the solubility of nonpolar compounds. It interacts with hydrocarbon chains via its hydrophobic tail, while the charged ammonium head stabilizes emulsified droplets, improving hydrocarbon bioavailability to microorganisms (Liu et al., 2021). However, CTAB and similar cationic surfactants can exhibit toxicity toward certain microbial communities, potentially inhibiting biodegradation if applied at high concentrations. The positively charged head groups bind strongly to negatively charged phospholipids in microbial membranes, disrupting membrane integrity and causing cell lysis (Halder et al., 2015).

Kumari et al. (2019) studied the synergistic effects of SDS and CTAB mixtures on crude oil-water interfacial tension and oil recovery. The mixture, especially SDS : CTAB at 0.7 : 0.3 ratio, achieved the lowest interfacial tension and the highest oil recovery efficiency of 90.09%. This

highlights the effectiveness of mixed surfactant systems in enhancing oil recovery and potentially increasing hydrocarbon bioavailability for environmental remediation. Nevertheless, the toxicity risk, particularly at higher doses, may limit cationic surfactant applications. Therefore, precise optimization is crucial in environmental contexts to avoid adverse effects on essential microbial populations responsible for biodegradation, balancing increased bioavailability against potential toxicity.

Surfactant-assisted biodegradation of PHCs is an effective strategy for remediating contamination in soil and aquatic ecosystems. Due to their amphiphilic nature, surfactants reduce surface and interfacial tension, enhancing the solubility and bioavailability of hydrophobic pollutants. This promotes the breakdown of PHCs into smaller particles, facilitating microbial uptake and accelerating metabolic degradation processes (Wang et al., 2019).

Xu et al. (2018) investigated the effects of surfactants such as Tween-80 on crude oil-contaminated soils. Over an 80-day remediation period, Tween-80 enhanced the emulsification of hydrophobic hydrocarbons, resulting in a 77% degradation efficiency for TPHs. The increased solubilization of complex hydrocarbons enabled native microbial populations to more efficiently metabolize long-chain and aromatic hydrocarbons, highlighting the role of surfactants in stimulating microbial activity in soils with limited pollutant bioavailability.

Cui et al. (2021) examined the impact of surfactants Tween-80 and rhamnolipid on PHC biodegradation by mixed bacterial consortia. Surfactant addition significantly improved degradation rates, achieving 81.58% with Tween-80 and 88.35% with rhamnolipid over 10 days at a PHC concentration of 10 g/L. The study demonstrated that surfactants enhanced PHC bioavailability and stimulated key metabolic pathways by upregulating degradation-related genes such as *alkB* and *nah*, thereby increasing microbial activity.

Cecotti et al. (2018) evaluated the efficacy of Triton X-100 in degrading PAHs in aged contaminated soils. Sub-critical micelle concentration doses of Triton X-100 were more effective than doses at or above the critical micelle concentration (CMC). Over 63 days, PAH concentrations decreased from 266 mg/kg to 135 mg/kg under sub-CMC treatment. Enhanced degradation of typically recalcitrant high-molecular-weight PAHs was attributed to improved hydrocarbon solubilization and reduced surfactant toxicity, which fostered the proliferation of PAH-degrading taxa including *Sphingomonadales* and *Acidobacteriales*.

Yan et al. (2016) studied the synergistic effects of surfactant flushing combined with bioremediation for PHC removal from contaminated soil. Using Tween-80 to enhance hydrocarbon solubilization, followed by bioremediation with indigenous microbes, the integrated approach achieved a 60% reduction in TPHs within 45 days.

This synergistic approach improved hydrocarbon removal efficiency and promoted the proliferation of hydrocarbon-degrading microbial communities. The research underscores the importance of combining surfactant-assisted techniques with biological processes to achieve optimal remediation outcomes. Collectively, these studies demonstrate that surfactants play a crucial role in enhancing bioremediation efficiency by increasing hydrocarbon bioavailability and stimulating microbial activity. Selecting appropriate surfactant types and concentrations is vital for maximizing degradation rates while minimizing potential ecological risks. These findings highlight the effectiveness of integrating physical and biological remediation methods to tackle complex hydrocarbon contamination challenges.

2.5.3. Mechanisms of Synergy: Enhancing Bioavailability, Enabling Microorganisms to Drive Degradation

Surfactants play a crucial role in modern bioremediation strategies by effectively addressing challenges associated with hydrophobic contaminants such as PHCs. By reducing surface and interfacial tension, surfactants increase the bioavailability of hydrophobic pollutants, enhancing their dispersion and solubilization for microbial degradation. Their unique amphiphilic structures enable the encapsulation of PHCs within micelles, facilitating pollutant uptake and transport in aqueous environments. This mechanism significantly improves the efficiency of bioremediation, particularly for complex hydrocarbons in contaminated soils and water systems, while addressing critical limitations of traditional approaches.

Surfactants, also known as surface-active agents, enhance the bioavailability of hydrophobic contaminants such as PHCs by reducing surface and interfacial tension and promoting micelle formation. These mechanisms are fundamental to how surfactants facilitate contaminant degradation and removal during bioremediation. Surface tension arises from cohesive forces at the interface between a liquid and its surrounding environment, caused by unequal molecular interactions at the surface. Interfacial tension refers to the analogous force present at the boundary between two immiscible phases, such as oil and water. Due to their hydrophobic and hydrophilic properties, PHCs in water tend to form distinct boundaries, limiting their dispersion and accessibility to microbes.

Surfactants reduce surface and interfacial tension, promoting the dispersion and distribution of hydrophobic substances in water and thereby enhancing conditions for biodegradation (Rosen and Kunjappu, 2012).

Surfactants position themselves at the interface between two phases, with hydrophilic heads in the aqueous phase and hydrophobic tails in the nonpolar phase (e.g., oil). This unique orientation disrupts cohesive forces at the interface, effectively lowering surface and interfacial tension. By reducing the energy required to overcome the water-oil barrier, surfactants facilitate the dispersion of hydrophobic molecules into the aqueous phase (Holmberg et al., 2002). Minimizing surface and interfacial tension is crucial in environmental bioremediation, as it increases the contact area between water and contaminants, promoting emulsification and solubilization of hydrophobic pollutants and improving their accessibility to microorganisms.

Biosurfactants, such as rhamnolipids produced by Pseudomonas aeruginosa, play a significant role by reducing surface tension, aiding emulsification, and enhancing the bioavailability of hydrophobic compounds, thereby facilitating microbial degradation (Pacwa-Płociniczak et al., 2011). When surfactant concentrations exceed the CMC, they self-assemble into micelles—spherical structures with hydrophobic tails inward and hydrophilic heads outward—creating a hydrophilic exterior and hydrophobic core. These micelles encapsulate hydrophobic PHC molecules within their core, solubilizing them in aqueous solutions and markedly increasing their solubility and bioavailability for microbial degradation. This micellization process is essential for improving the transport and degradation of hydrophobic pollutants in soil and groundwater bioremediation (Rosen & Kunjappu, 2012).

Surfactants' ability to reduce surface and interfacial tension and form micelles has important implications for mass transfer and contaminant accessibility. By altering the physical properties at the contaminant-water interface, surfactants overcome mass transfer limitations commonly associated with hydrophobic pollutants in aquatic environments. This enhancement accelerates contaminant diffusion to microbial cells, a critical step in bioremediation. Furthermore, micelles facilitate the transport of insoluble contaminants across biological membranes, promoting microbial degradation (Holmberg et al., 2002).

In summary, surfactants solubilize PHCs and reduce interfacial tension, thereby increasing their bioavailability and microbial uptake, which enhances remediation efficiency in contaminated environments.

The interaction between surfactants and microbial communities underscores their importance in environmental remediation. Micelles increase the accessibility of PHCs to indigenous microbial populations, which have evolved specialized metabolic pathways for pollutant degradation. Native microbes, adapted to local environmental conditions, demonstrate greater resilience and higher hydrocarbon degradation efficiency compared to non-native species. Combining surfactant-assisted enhancement of bioavailability with the metabolic capabilities of indigenous microbial communities offers a powerful bioremediation strategy. This synergy minimizes ecological disturbance while maximizing contaminant removal, with surfactants acting as facilitators and microbes as active degraders.

The utilization of native microorganisms, or autochthonous microbial communities, in bioaugmentation offers considerable advantages, particularly for the bioremediation of petroleum-contaminated soils. Due to their inherent adaptation to specific environments, these organisms possess the metabolic capacity and resilience necessary for effective pollutant degradation. Their integration within the existing microbial ecology enhances their survival and proliferation, making them well-suited for long-term remediation efforts.

A key benefit of employing native microbes in bioaugmentation is their environmental adaptability. This trait is especially valuable when addressing complex hydrocarbons present in petroleum, as these microbes have evolved in contaminated areas and developed specialized metabolic pathways for hydrocarbon degradation (Head et al., 2006). Indigenous microbial communities exhibit superior pollutant degradation efficiency compared to non-native species, which often require extended adaptation periods. Their capacity to tolerate environmental fluctuations—including changes in pH, temperature, moisture, and nutrient availability—ensures consistent bioremediation performance under variable conditions (Ayilara and Babalola, 2023).

Gentry et al. (2004) demonstrated that native microbial populations in contaminated soils show greater tolerance to fluctuating nutrient and oxygen levels than introduced microbes, suggesting that autochthonous communities contribute to more stable and effective bioremediation outcomes. Moreover, employing local microbial communities minimizes the ecological risks associated with introducing foreign microorganisms, which can disrupt indigenous microbial balance through competition, displacement, or unforeseen ecological effects. In contrast, native microbes are integral to the local ecosystem, having established interactions with other organisms, thus preserving ecological equilibrium during bioaugmentation (Davis & Madsen, 1996).

In summary, native microbial communities offer significant benefits for bioaugmentation due to their ecological stability, localized pollutant responsiveness, and resilience to environmental changes. These advantages make them ideal candidates for sustainable and effective bioremediation, facilitating higher degradation rates while minimizing ecological risks.

The integration of surfactants with autochthonous bioaugmentation highlights the potential of combining physical-chemical and biological approaches to improve remediation outcomes. While native microbial communities enhance long-term stability and efficiency in degradation processes, surfactants alleviate mass transfer limitations. Together, these methods offer a sustainable and effective strategy for addressing the challenges of hydrocarbon contamination. Ongoing research suggests that optimizing surfactant formulations and tailoring microbial applications will further advance environmental remediation technologies.

2.6. Genetic and Microbial Insights into Hydrocarbon Degradation Pathways

2.6.1. Hydrocarbon Degradation Mechanisms

The degradation of aliphatic hydrocarbons in contaminated environments involves well-defined metabolic pathways mediated by specific microbial communities. These pathways are categorized into aerobic and anaerobic mechanisms, each employing distinct enzymatic processes and genetic regulation. Understanding these pathways is crucial for designing effective bioremediation strategies, particularly in petroleum-contaminated soils and aquatic systems containing hydrocarbons (Meckenstock et al., 2016). Under aerobic conditions, alkane degradation is initiated by oxidation at either the terminal or sub-terminal position of the hydrocarbon chain (Figure 2.1).

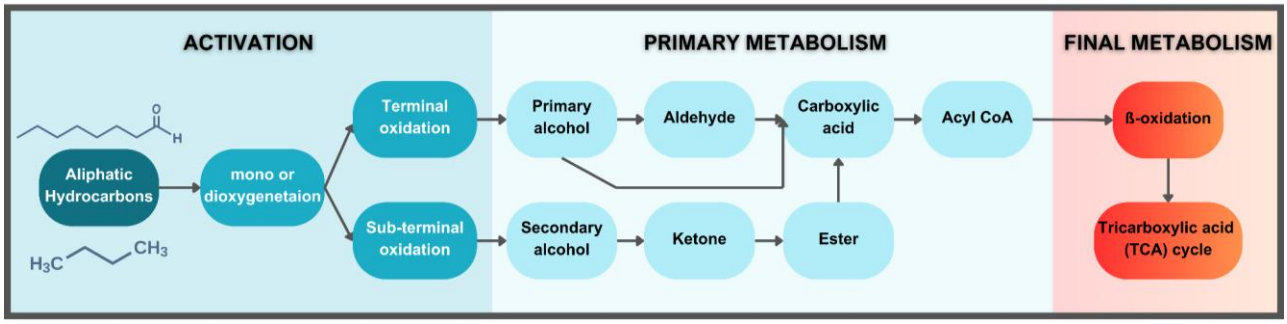


Figure 2.1. Aliphatic hydrocarbon degradation pathways (Sierra-Garcia et al., 2020).

The *alkB* gene encodes alkane hydroxylase, a key enzyme that catalyzes the incorporation of an oxygen atom into the alkane molecule, producing an alcohol. This alcohol is subsequently converted

to an aldehyde and then to a fatty acid through the action of alcohol dehydrogenases (*adh*) and aldehyde dehydrogenases (*aldH*). The resulting fatty acids undergo β-oxidation, yielding acetyl-CoA units for energy production (Ji et al., 2013). The *cyp153* gene, which encodes cytochrome P450 monooxygenase, offers an alternative alkane activation pathway, particularly in Gram-negative bacteria such as *Marinobacter* (Meckenstock et al., 2016). In *Geobacillus thermodenitrificans*, the *ladA* gene encodes a flavin-dependent alkane monooxygenase responsible for degrading long-chain alkanes (C_{15}–C_{36}) (Abbasian et al., 2015). These findings highlight the diversity of aerobic degradation pathways and the metabolic versatility of hydrocarbon-degrading microorganisms.

Under anaerobic conditions, alkanes are activated via fumarate addition, a mechanism distinct from oxygen-dependent pathways. The *assA* and *assB* genes encode alkylsuccinate synthase, which catalyzes the addition of fumarate to alkanes, forming alkylsuccinate intermediates. These intermediates undergo further enzymatic degradation into fatty acids that enter energy-generating metabolic routes (Meckenstock et al., 2016; Rabus et al., 2016). In sulfate-reducing bacteria like *Desulfatibacillum aliphaticivorans*, these genes facilitate the degradation of medium- to long-chain hydrocarbons in anoxic environments (Brzeszcz and Kaszycki, 2018).

Efficient transport and uptake mechanisms are crucial for hydrocarbon degradation. The *fadL* gene encodes fatty acid transport proteins that mediate the uptake of hydrophobic compounds into microbial cells (Ji et al., 2013). Outer membrane proteins such as *ompT* assist in hydrocarbon transport across membranes, enhancing bioavailability (Rabus et al., 2016). Additionally, ATP-binding cassette (ABC) transporters are essential for the uptake of long-chain alkanes (Abbasian et al., 2015).

Micelle-mediated solubilization, often facilitated by surfactants or biosurfactants, further enhances hydrocarbon degradation rates. Cationic surfactants like CTAB reduce surface tension and improve hydrocarbon emulsification, facilitating microbial absorption. Synthetic surfactants such as SDS have been shown to synergistically increase the bioavailability and degradation of hydrophobic hydrocarbons when combined with microbial pathways (Yan et al., 2016).

Genetic regulation and HGT are pivotal in hydrocarbon degradation. The *rubA* and *rubB* genes encode subunits of Rieske non-heme iron oxygenase, vital for hydrocarbon oxidation in both aerobic and anaerobic conditions (Ji et al., 2013). Genes such as *xylM* and *xylE* participate in the meta-cleavage pathway, enabling the breakdown of intermediates like catechol, which ensures complete mineralization of hydrocarbons (Meckenstock et al., 2016).

Indigenous microbial communities enriched with genes such as *cyp153* and *alkB* exhibit enhanced degradation capabilities due to their specialized metabolic pathways and adaptation to specific contaminants (Head et al., 2006). These microbes commonly dominate historically contaminated sites, playing a key role in natural attenuation processes (Ayilara and Babalola, 2023) (Figure 2.2).

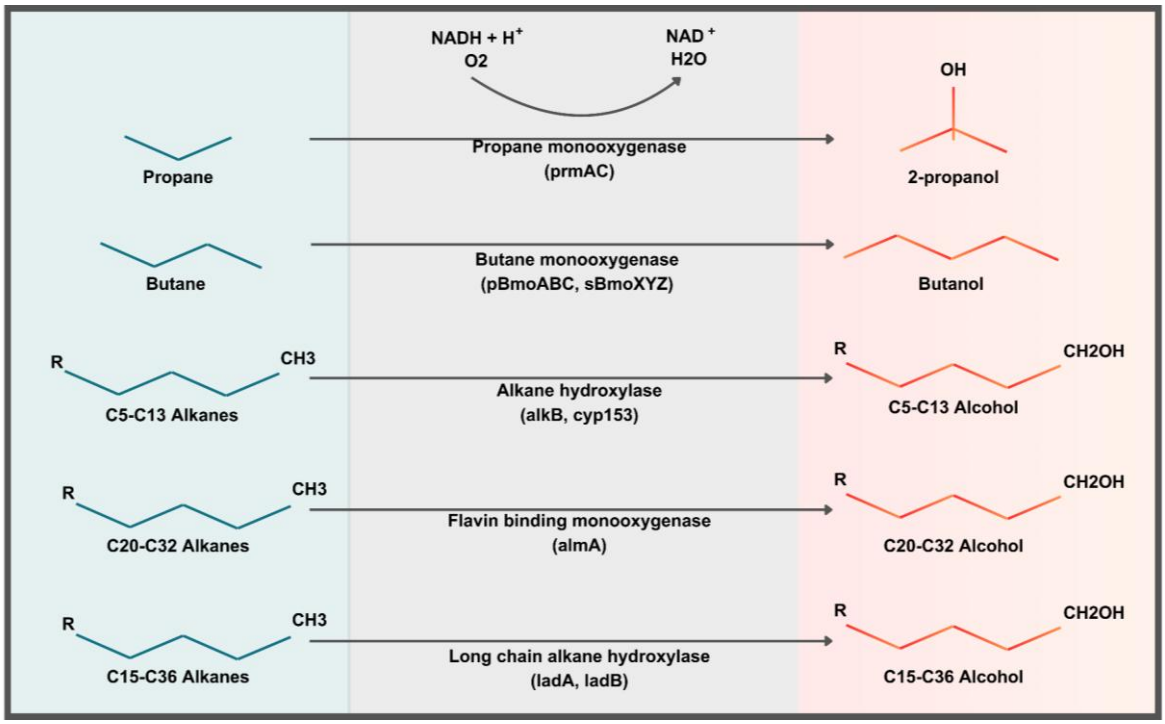


Figure 2.2. Reactions for the degradation of alkanes through aerobic pathways (Khot et al., 2022).

The degradation of aromatic hydrocarbons in contaminated environments involves complex biochemical pathways mediated by specialized microbial communities. These pathways are categorized into aerobic and anaerobic mechanisms, each utilizing distinct enzymes and genetic systems for hydrocarbon breakdown. A comprehensive understanding of these processes is essential for developing effective bioremediation strategies, particularly in environments impacted by PHCs (Meckenstock et al., 2016; Rabus et al., 2016) (Figure 2.3).

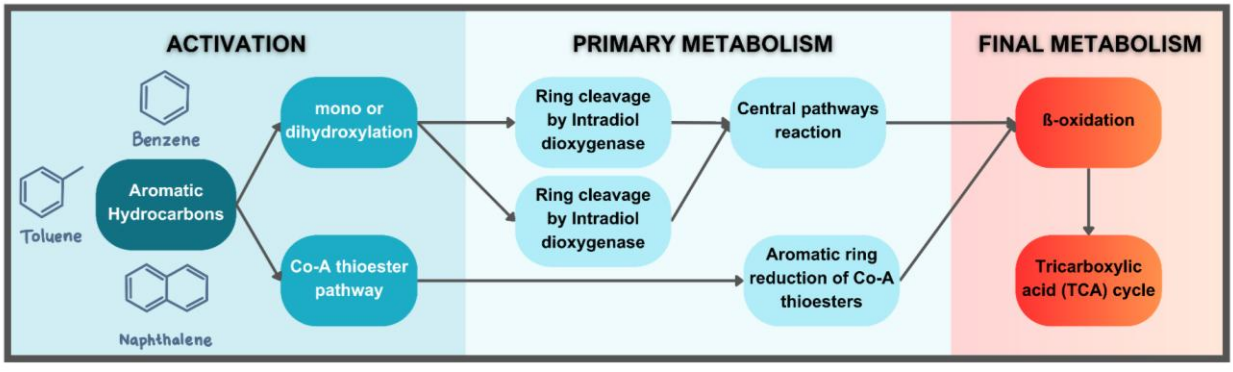


Figure 2.3. Aromatic hydrocarbon degradation pathways (Sierra-Garcia et al., 2020).

Dioxygenase-mediated activation is typically the initial step in the aerobic degradation of aromatic hydrocarbons. Key enzymes such as toluene dioxygenase (encoded by the *tod* gene) and naphthalene dioxygenase (encoded by the *nah* gene) introduce oxygen into the aromatic ring, forming cis-dihydrodiols. These intermediates are further oxidized to catechols, which undergo ring cleavage via either the ortho- or meta-cleavage pathways. Catechol 1,2-dioxygenase (encoded by *cat* gene) catalyzes the ortho-cleavage pathway, producing intermediates like β-ketoadipate that enter the Krebs cycle for complete mineralization. Conversely, in organisms such as Pseudomonas putida, the meta-cleavage pathway, facilitated by catechol 2,3-dioxygenase (encoded by *xyl* gene), generates semi-aldehydes that are subsequently converted into Krebs cycle intermediates (Rabus et al., 2016; Fuentes et al., 2014).

Under anaerobic conditions, aromatic hydrocarbons are activated via alternative mechanisms such as fumarate addition. The enzyme benzylsuccinate synthase, encoded by *bssA*, catalyzes the addition of fumarate to aromatic hydrocarbons, forming benzylsuccinate intermediates. These intermediates are further degraded to benzoyl-CoA, a key compound in anaerobic pathways, through reactions analogous to β-oxidation. The reductive de-aromatization of benzoyl-CoA is catalyzed by benzoyl-CoA reductase, encoded by genes including *bcrA*, *bamA*, and *bamB*, yielding simpler metabolites that are metabolized for energy production. These pathways are especially important in oxygen-limited environments such as groundwater and deep subsurface sediments (Haritash and Kaushik, 2020; Meckenstock et al., 2016).

The genetic and enzymatic diversity within microbial communities is critical for efficient aromatic hydrocarbon degradation. Genes like *nidA* and *nidA3B3*, encoding dioxygenases, are vital for the breakdown of high-molecular-weight PAHs such as pyrene. These enzymes are often regulated by operons responsive to specific hydrocarbons, enabling microbial adaptation to diverse contamination profiles. Transport proteins encoded by genes such as *fadL* and *ompT* further enhance degradation efficiency by facilitating the uptake and bioavailability of hydrophobic compounds (Varjani, 2017; Rabus et al., 2016) (Figure 2.4).

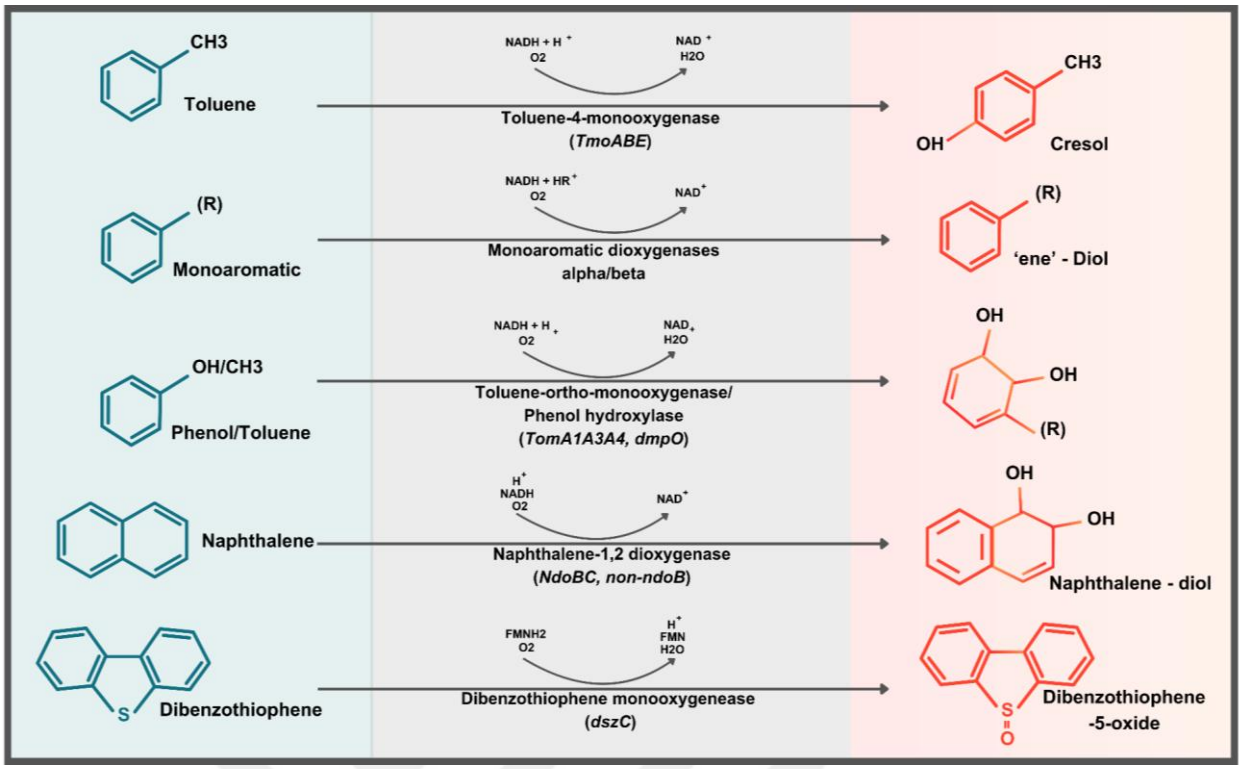


Figure 2.4. Reactions for the degradation of aromatics through aerobic pathways (Khot et al., 2022).

2.6.2. Hydrocarbon-Degrading Microorganisms

Hydrocarbon-degrading microorganisms play a crucial role in mitigating the impacts of petroleum contamination. These microbes utilize hydrocarbons as carbon and energy sources, contributing to the detoxification of polluted environments. Extensive research has focused on the hydrocarbonoclastic capabilities of genera such as *Pseudomonas*, *Achromobacter*, *Rhodococcus*, and *Alcanivorax*. Their metabolic flexibility allows them to degrade a broad spectrum of hydrocarbons, including both aliphatic and aromatic compounds, through intricate enzymatic pathways. This versatility reflects their evolutionary adaptation to diverse hydrocarbon substrates and environmental conditions, enabling efficient degradation of various pollutants.

Hydrocarbon degradation encompasses a diverse range of metabolic pathways evolved to address the inherent complexity of these compounds. This complexity is matched by a variety of enzymatic processes, each finely tuned to specific hydrocarbon structures and environmental conditions. Key enzymes, such as monooxygenases encoded by the *alkB* gene cluster, catalyze terminal or sub-terminal oxidation, commonly involved in the metabolism of aliphatic hydrocarbons like linear alkanes. In contrast, aromatic hydrocarbons, including PAHs, require more intricate mechanisms. Enzymes such as naphthalene dioxygenases facilitate the initial cleavage of aromatic rings, generating intermediates like catechol that enter central metabolic pathways. Numerous

bacterial species harbor these pathways; for example, *Achromobacter xylosoxidans* degrades complex PAHs through catechol 2,3-dioxygenase activity, while *Pseudomonas sp.* AS1, isolated from an arsenic-contaminated site, efficiently degrades naphthalene via a classical pathway involving the *nahA* gene.

Collaboration among microbial consortia significantly enhances hydrocarbon degradation by leveraging complementary metabolic pathways of different strains, creating a synergistic system for efficient breakdown. In bioaugmentation studies, consortia of biosurfactant-producing bacteria such as *Pseudomonas aeruginosa* and *Achromobacter xylosoxidans* have demonstrated marked improvements in the degradation rates of PAHs and TPHs. Villaverde et al. (2019) reported that co-culturing *A. xylosoxidans* with surfactant-producing bacteria resulted in a 57.5% increase in pyrene mineralization. Similarly, Wang et al. (2020) observed a 60% reduction in TPH levels after seven days of treatment with *Pseudomonas putida*. These findings underscore the critical role of substrate bioavailability and microbial cooperation in enhancing bioremediation efficiency. Through the exchange of metabolites and biosurfactants, such cooperative interactions enable microorganisms with limited access to hydrophobic hydrocarbons to participate effectively in the degradation process.

The genus *Rhodococcus*, recognized for its large genome and diverse catabolic capabilities, plays a vital role in hydrocarbon degradation, particularly of recalcitrant aromatic compounds. *Rhodococcus erythropolis* exhibits exceptional resilience and adaptability, thriving in environments with high hydrocarbon concentrations. A notable study demonstrated that *R. erythropolis* could tolerate benzene concentrations as high as 2% (v/v) in continuous culture, maintaining activity for over 30 days and achieving an impressive 89% benzene degradation (Martínková et al., 2009). This ability to produce surfactants, including trehalose-containing glycolipids, enhances the uptake and breakdown of hydrophobic hydrocarbons, making it effective for mitigating oil spills and industrial pollution. Furthermore, *Rhodococcus* strains display tolerance to elevated concentrations of toxic hydrocarbons, underscoring their utility in bioremediation under challenging environmental conditions.

Alcanivorax and *Burkholderia*, both members of the phylum *Proteobacteria*, play vital roles in hydrocarbon degradation in marine and terrestrial ecosystems. *Alcanivorax borkumensis*, a specialized hydrocarbonoclastic bacterium, thrives in oil-contaminated coastal environments. Hazen et al. (2010) reported a rapid increase in *A. borkumensis* populations following the Deepwater Horizon oil spill in the Gulf of Mexico, facilitating the degradation of aliphatic hydrocarbons through alkane monooxygenase pathways. In contrast, members of the order *Burkholderiales* possess a

broader substrate range, capable of degrading both aromatic and aliphatic hydrocarbons. A consortium comprising *Burkholderia*, *Pseudomonas*, and *Rhodococcus* demonstrated a 99% degradation efficiency of pyrene and other high-molecular-weight PAHs in simulated microcosms (Vaidya et al., 2017). These findings emphasize the synergistic potential of microbial consortia in enhancing hydrocarbon bioavailability and degradation, particularly in complex contaminated environments.

Pseudomonas frederiksbergensis is a highly adaptable and ecologically significant hydrocarbon-degrading bacterium, known for its exceptional metabolic versatility, resilience, and cooperative interactions within microbial communities. It demonstrates a remarkable ability to degrade a wide range of hydrocarbons, including alkanes, aromatic compounds, and jet fuels. In studies involving hydrocarbon-enriched desert soils, *P. frederiksbergensis* isolates exhibited substantial growth and degradation of compounds such as toluene, ethylbenzene, and n-propylbenzene, achieving degradation efficiencies exceeding 78% within 20 days under controlled laboratory conditions (Ruiz et al., 2021). Genomic analyses have revealed a comprehensive set of hydrocarbon degradation genes, including the *alkB* gene cluster for aliphatic hydrocarbons and dioxygenase enzymes responsible for the initial activation of aromatic hydrocarbons (Kim and Park, 2018). The genome also harbors genes associated with stress resistance, enabling adaptation to extreme environments characterized by fluctuations in pH, salinity, and heavy metal concentrations. Due to its metabolic flexibility and resilience, *P. frederiksbergensis* is particularly well-suited for bioremediation applications in sites contaminated with mixed pollutants.

Beyond hydrocarbon degradation, *P. frederiksbergensis* engages in synergistic interactions with other microorganisms. Co-cultivation with biosurfactant-producing bacteria enhances the availability and metabolism of hydrophobic substrates. Such microbial cooperation, observed in both natural and engineered systems, is vital for the complete mineralization of hydrocarbons by multispecies consortia (Ruiz et al., 2021). Korshunova et al. (2024) further highlighted the ecological importance of this strain, reporting up to 85% crude oil degradation in contaminated soils within 30 days, alongside the promotion of crop growth, including barley and clover.

While *Pseudomonas frederiksbergensis* exhibits broad metabolic capabilities, *Achromobacter spanius* specializes in aromatic hydrocarbon degradation, illustrating the diversity of hydrocarbonoclastic abilities among microbial species.

In contrast, *Achromobacter spanius* exhibits notable proficiency in degrading aromatic hydrocarbons such as toluene and benzene, utilizing genes encoding aromatic ring-hydroxylating dioxygenases and components of the protocatechuate catabolic pathway. Ruiz et al. (2021) reported that *A. spanius* thrives in consortia and, when co-cultured with biosurfactant-producing bacteria, achieved degradation efficiencies exceeding 70% for benzene and 62% for toluene within 14 days. The biosurfactants produced by consortium members significantly enhanced the bioavailability of hydrophobic hydrocarbons, facilitating these results. However, genomic analyses confirmed the absence of the *alkB* gene and other related genes necessary for alkane degradation in *A. spanius*, highlighting its specialization in aromatic hydrocarbons and its reliance on interactions with other microbial species within a consortium to access and degrade hydrophobic substrates.

Conversely, *Pseudomonas frederiksbergensis* displays greater metabolic versatility, capable of degrading both aromatic and aliphatic hydrocarbons. Its ability to metabolize medium- and short-chain alkanes is attributed to the presence of the *alkB* gene cluster, which is absent in *A. spanius*. Studies have shown that co-culturing *P. frederiksbergensis* with *A. spanius* expands the range of hydrocarbons degraded, with *P. frederiksbergensis* targeting alkanes and *A. spanius* focusing on aromatic compounds. This synergistic interaction exemplifies the effectiveness of microbial consortia in bioremediation by leveraging the distinct metabolic capabilities of multiple strains for comprehensive hydrocarbon degradation. Additionally, *P. frederiksbergensis* contributes to biosurfactant production, further enhancing the bioavailability of hydrophobic hydrocarbons for consortium members.

The study by Li (2021) highlights the metabolic potential of *Achromobacter* species in hydrocarbon degradation, underscoring the genus's genetic diversity and broad applicability in hydrocarbon remediation. Comprehensive genomic analysis revealed the presence of alkane degradation genes, including *alkB*, across all twenty *Achromobacter* strains examined. Furthermore, secondary metabolite profiling identified seventy-three gene clusters involved in the biosynthesis of biosurfactants and other biochemicals that facilitate hydrocarbon degradation and enhance bioavailability. These clusters encompass pathways for tetrahydropyrimidine and aryl polyenes, compounds that aid in hydrocarbon emulsification and support the adaptability of *Achromobacter* strains in contaminated environments.

Strains such as *Achromobacter xylosoxidans* exhibit extensive alkane degradation capabilities, effectively metabolizing hydrocarbons ranging from C_{12} to C_{43} under both aerobic and microaerophilic conditions. Additionally, *Achromobacter kerstersii* has been shown to produce rhamnolipid biosurfactants with significant interfacial activity, thereby improving oil recovery and

degradation efficiency. Biosurfactants reduce surface tension between hydrocarbons and soil particles, enhancing microbial access to hydrophobic substrates. In oil-contaminated soils, bacteria like *Achromobacter sp.* FM8-1 demonstrate enzymatic versatility by degrading phenylalanine and aromatic hydrocarbons via the naphthalene pathway.

Reviewing the hydrocarbon-degrading capabilities of these microorganism highlights that the success of bioremediation relies on understanding and harnessing the metabolic diversity and cooperative interactions among bacterial phyla. The phyla *Proteobacteria* and *Actinobacteria* exemplify the exceptional metabolic and genetic flexibility required to degrade complex hydrocarbons. Within these groups, genera such as *Achromobacter* and *Pseudomonas* illustrate how specific adaptations enable hydrocarbonoclastic activity under diverse and challenging environmental conditions. These findings emphasize the ecological importance of hydrocarbon-degrading bacteria at a broader taxonomic level and lay the groundwork for innovative biotechnological applications in pollution remediation, from oil spill cleanup to integrated soil and water treatment systems. Continued research into the genetic and functional diversity of key bacterial phyla will enhance their utility in addressing the escalating environmental challenges posed by hydrocarbon contamination.

2.6.3. The Role of Mobile Genetic Elements in Hydrocarbon Biodegradation

MGEs, such as plasmids, transposons, and integrative conjugative elements (ICEs), play a vital role in hydrocarbon degradation by facilitating HGT within microbial communities. These elements serve as vectors for the dissemination of catabolic genes responsible for the breakdown of aliphatic and aromatic hydrocarbons. Key hydrocarbon degradation genes, including *alkB* and *nah*, are frequently located on plasmids, promoting their transfer among bacterial populations (Shintani and Nojiri, 2013). The widespread presence of MGEs in contaminated environments underscores their critical role in bacterial adaptation, enabling the acquisition and evolution of hydrocarbonoclastic capabilities under selective pressure (Zhao et al., 2017).

Catabolic plasmids represent a particularly important class of MGEs due to their ability to carry complete metabolic pathways for hydrocarbon degradation. Boronin (2014) emphasized the critical role of conjugative plasmids, especially those belonging to the IncP-9 and IncP-7 groups, in the biodegradation of complex hydrocarbons, including PAHs. These plasmids not only facilitate pollutant breakdown but also promote the dissemination of catabolic genes to native microbial populations, thereby enhancing bioremediation efficiency. Additionally, ICEs and transposons identified in *Sphingomonas* and *Sphingobium* strains harbor genes encoding enzymes such as

biphenyl dioxygenase, which participate in PAH degradation and are flanked by insertion sequences (IS). This underscores the crucial role of MGEs in the integration and mobilization of catabolic pathways (Zhao et al., 2017).

Beyond facilitating genetic transfer, MGEs also contribute to structuring microbial consortia in contaminated environments. French et al. (2020) demonstrated that engineered vectors carrying catabolic genes can integrate into native bacterial communities, enhancing their ability to degrade PHCs. In a simulated oil spill experiment, conjugative plasmids encoding enzymes such as cytochrome P450 promoted crude oil degradation, resulting in a 46% reduction in total PHCs over 60 days. These findings highlight the potential of MGEs to augment the metabolic capacity of microbial consortia, particularly in situations where native degradation processes are insufficient.

HGT is fundamental for the adaptation and enhancement of microbial communities in hydrocarbon-contaminated environments. Shahi et al. (2017) demonstrated that the transfer of catabolic genes such as *alkB*, *nah*, and *phnAc* among bacterial species significantly improves their hydrocarbon-degrading capabilities. Using labeled conjugative plasmids, experiments showed the transfer of naphthalene biodegradation genes between soil bacteria, leading to the emergence of more efficient degrader strains. The study also found that nutrient-rich conditions, characterized by high carbon-to-nitrogen ratios, positively correlated with increased HGT rates, thereby promoting the dissemination of essential catabolic genes and enhancing bioremediation efficiency. These findings emphasize the importance of identifying key degrading genes and optimizing environmental parameters to facilitate gene transfer and boost the metabolic potential of microbial consortia.

Although most research has focused on hydrocarbon biodegradation, insights into the role of MGEs can be gained by examining their functions in other environmental systems. Miguel et al. (2020) reported that MGEs in wastewater treatment plants (WWTPs) harbor genes responsible for the degradation of organic micro pollutants, facilitating microbial adaptation to novel compounds. These findings suggest that WWTP systems could be leveraged to develop targeted bioaugmentation strategies for hydrocarbon-contaminated environments, thereby improving bioremediation outcomes. MGEs serve as stable genetic platforms that enable the integration of new catabolic genes. Applying appropriate selective pressures accelerates the evolution of metabolic pathways and promotes their dissemination within microbial communities.

Additional studies have demonstrated that MGEs promote the formation of synergistic microbial consortia, which collectively enhance hydrocarbon degradation rates. Boronin (2014) emphasized

that plasmid-mediated HGT among genera such as *Pseudomonas* and *Rhodococcus* supports the development of functionally integrated microbial communities capable of degrading a broad spectrum of hydrocarbons. Similarly, Zhao et al. (2017) reported that transposons and plasmids facilitate the horizontal transfer of aromatic hydrocarbon degradation pathways, highlighting the ecological importance of MGEs in microbial adaptation and pollutant breakdown.

In summary, MGEs are essential for microbial adaptation and cooperation in hydrocarbon-contaminated environments. They accelerate the spread of catabolic genes and foster the evolution of microbial consortia capable of addressing complex environmental challenges. Understanding and harnessing the potential of MGEs can facilitate the development of advanced bioremediation technologies, thereby improving the management of petroleum contamination.

3. MATERIALS AND METHODS

The study initiated with collection of soil sample from waste area of petroleum refinery for isolation of indigenous hydrocarbon-degrading microbial communities that is crucial in each step of the research. The samples underwent chemical and molecular characterization including TPH analysis and microbial community in respectively. Following characterization of petroleum contaminated soil, the samples were subjected to a pre-enrichment step using crude oil as main substrate due to the selective proliferation of microorganisms that play a vital role for PHC degradation pathways. The enrichment process was monitored by cell counting and TPH analysis, ended with 16S metagenomics analysis for determining the unique microbes consuming PHCs. Based on the results, soil isolate library was created with Petroleum Enriched Culture (PEC) for chosen the most potential strains that were utilized as inoculum in further studies.

Selected strains were subjected to Whole Genome Sequencing (WGS) for determination of the genes involved in PHC degradation pathways. Minimum inhibitory concentration (MIC) analysis was carried out for the selection of surfactant which may increase the bioavailability of PHCs, while not inhibit the microbial activity. Surfactant biodegradation assay was carried out with selected surfactants with determined concentrations for ensuring that combination of PEC and surfactant maximize the PHC degradation. After that, gene expression profiling was analyzed by RNA-Sequencing in time-course during the degradation test period. Gene mobilization was observed by trap plasmid transformation to selective bacterial strains. Then, plasmid was isolated and sequenced for monitoring the mobile genes within the trap plasmid.

This methodological framework (Figure 3.1) was designed to determination of the effectiveness of surfactants on PHC degradation by increasing bioavailability and then gene mobilization. Mainly, it was aimed to achieve the appropriate PHC degrading microbial community combining with the most potential surfactant for providing an environmental friendly, economical and quick bioremediation technique.

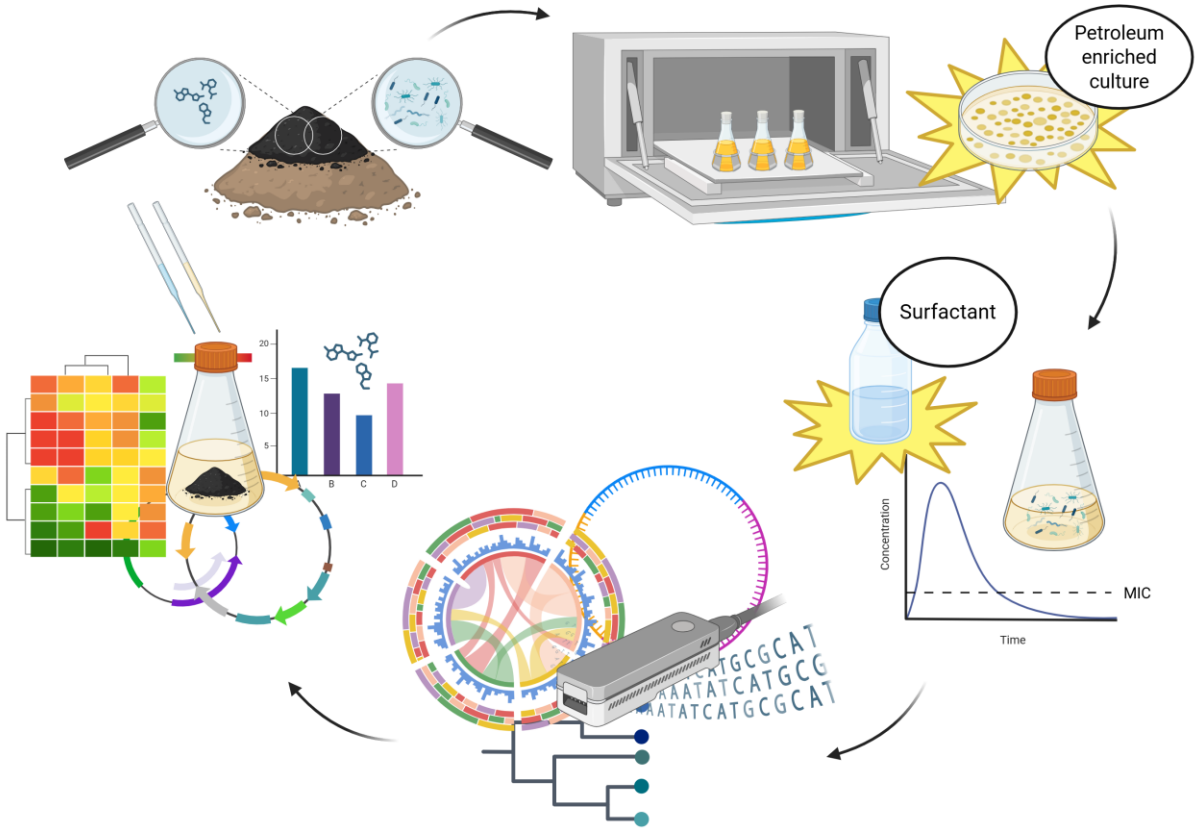


Figure 3.1. Methodological framework.

3.1. Characterization of Petroleum Contaminated Soil

3.1.1. Sampling and TPH Analysis of Contaminated Soil

Soil contaminated with crude oil and its derivatives was obtained from a petroleum refinery in the Western Raman region of Batman, Turkey, operated by the Turkish Petroleum Corporation. Soil samples were collected from three distinct regions categorized as uncontaminated, mildly contaminated, and highly contaminated, based on the level of contamination. Mildly and high contaminated soil were homogenized by kneading with mortar and pestle (Figure 3.2). The soil samples were maintained at +4 °C prior to analysis. Crude oil was also obtained from the same refinery for use in enrichment processes. The uncontaminated soil sample was used as a reference for comparison with the contaminated soil sample in molecular characterization.



Figure 3.2. Clean-contaminated soil and crude oil from petroleum refinery and homogenized soil sample.

3.1.2. Microbial Community Analysis on Contaminated Soil

DNA isolation from petroleum-contaminated soil and clean soil samples was performed using the Quick-DNA Fecal/Soil Microbe DNA Miniprep Kit (D6010, Zymo Research, USA). A total of 250 mg of each soil sample was added to ZR BashingBead™ Lysis Tubes (0.1 & 0.5 mm), followed by the addition of 750 µl BashingBead™ Buffer. The tubes were vortexed for 40 minutes at room temperature. Subsequently, the tubes were centrifuged at 10,000 × g for 1 minute, and 40 µl of the supernatant was transferred to Zymo-Spin™ III-F Filters placed in a collection tube. The filters were centrifuged at 8,000 × g for 1 minute. Next, 1,200 µl of Genomic Lysis Buffer was added to the filter, and the mixture was mixed thoroughly using pipetting. From this mixture, 800 µl was transferred onto Zymo-Spin™ IICR Columns and centrifuged at 10,000 × g for 1 minute. The liquid in the collection tube was discarded, and 200 µl of DNA Pre-Wash Buffer was added to initiate the washing step. The filter was centrifuged at 10,000 × g for 1 minute, followed by the addition of 500 µl of gDNA Wash Buffer, and centrifugation was repeated. The Zymo-Spin™ IICR Column was then placed into a clean 1.5 mL microcentrifuge tube, and 100 µl of DNA Elution Buffer was added to the filter. The tube was centrifuged at 10,000 × g for 30 seconds to elute the DNA. For further purification, the Zymo-Spin™ III-HRC Filter was placed into a clean collection tube, and 600 µl of Prep Solution was added onto the filter. The tube was centrifuged at 8,000 × g for 3 minutes. The eluted DNA was then transferred onto the prepared Zymo-Spin™ III-HRC Filter and centrifuged at 16,000 × g for 3 minutes. This process resulted in high-quality DNA suitable for molecular analyses. The concentration of DNA is measured by Qubit 4 Fluorometer (Q33226, Thermo Fisher, USA) with Qubit™ dsDNA HS Assay Kit (Q32851, Thermo Fisher, USA).

For 16S amplicon sequencing, PCR was first performed upon amplification of 16S rRNA regions. PCR Reaction contains 20 ng DNA, 1 µl 10 µM Forward primer (16S-27F; AGAGTTTGATCMTGGCTCAG), 1 µl 10 µM Reverse Primer (16S-1492R; CGGTTACCTTGTTACGACTT), 10 µl 2× HiFi Taq Master Mix, (HF101, MobiomX, Türkiye). PCR conditions are given in the Figure 3.3 included an initial denaturation at 95 °C for 3 minutes, followed by 30 cycles of denaturation at 95 °C for 15 seconds, annealing at 58 °C for 15 seconds, extension at 72 °C for 45 seconds, and a final extension at 72 °C for 5 minutes.

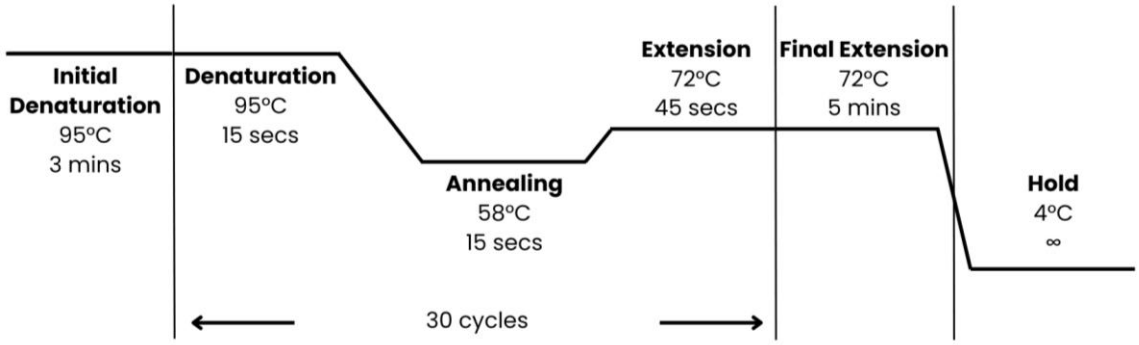


Figure 3.3. PCR condition for 16S microbial community analysis.

Amplification was confirmed by agarose gel electrophoresis before sequencing method. For agarose gel preparation, Agarose tablet (0.5 g) (AGAROSE-10, Bento Bioworks, UK) and 10X TBE Electrophoresis Buffer (TBE-50, Bento Bioworks, UK) were used in a 50 mL final volume. GelGreen DNA Stain (GG-100, Bento Bioworks, UK) was added to the gel solution before pouring the gel. For loading the samples, PCR product was mixed with Gel Loading Dye, Blue (6X) (LD-BL-1, Bento Bioworks, UK) and loaded into the gel. Electrophoresis was applied for 30 minutes at 120 V using Bento Lab Pro (BL1M1P, Bento Bioworks, UK). Band for each samples at approximately 1500 bp was observed, PCR products were confirmed for sequencing.

Library preparation followed the Native Barcoding 96 V14 kit (SQK-NBD114.96; Oxford Nanopore Technologies) ligation workflow. PCR products were end-repaired and A-tailed with NEBNext® Ultra™ II End Repair/dA-Tailing Module (E7546, NEB, UK), after which Blunt TA Ligase Master Mix (M0367, NEB, UK) was used to ligate unique barcodes. Reactions were quenched with 1 µl 0.5M EDTA, the barcoded samples were pooled, and the pool was cleaned with MagBead DNA (MBD01, Mobiomx, Türkiye). Sequencing adapters were attached using Rapid T4 DNA Ligase (RL00, Mobiomx, Türkiye) and the library was bead-purified once more. Quantification by Qubit 4 Fluorometer (Q33238, Thermo Fisher, USA) confirmed ≥75 fmol of library, which was loaded onto a primed SpotON Flow Cell 10.4.1 (FLO-MIN114, Oxford Nanopore Technologies, UK).

Sequencing was performed on a Mk1B™ (MIN-101B, Oxford Nanopore Technologies, UK) with the latest MinKNOW™ software and was allowed to proceed until each barcode accumulated at least 10,000 reads.

After sequencing, the raw FAST5 files were base-called and demultiplexed with the latest Guppy release, producing FASTQ reads. We checked read quality in FastQC (Andrews et al., 2010) to spot low-quality bases and adapter contamination. Next, Trimmomatic (Bolger et al., 2014) was used to trim the first 15 bp from each read and cap read length at 2 kb; reads with an average Phred score below 15 or a final length under 1 kb were discarded. High-quality reads were aligned to the NCBI nt database with BLAST (Johnson et al., 2008) for taxonomic assignment. Operational taxonomic units (OTUs) were clustered in Mothur (Schloss et al., 2009) at 99 % similarity, and OTUs contributing less than 0.1 % of total reads were removed before downstream analyses.

3.2. Enrichment of PHC Degrading Microbial Community

Overall, Figure 3.4 outlines the enrichment workflow used to select petroleum-hydrocarbon degraders. At each scheduled time-point, aliquots were withdrawn and subjected to parallel analyses: molecular assays (DNA extraction, 16S rRNA amplicon sequencing, and *alkB*-targeted qPCR) to track community shifts, and chemical measurements (TPH, n-alkane profile, and residual surfactant concentrations) to quantify degradation progress.

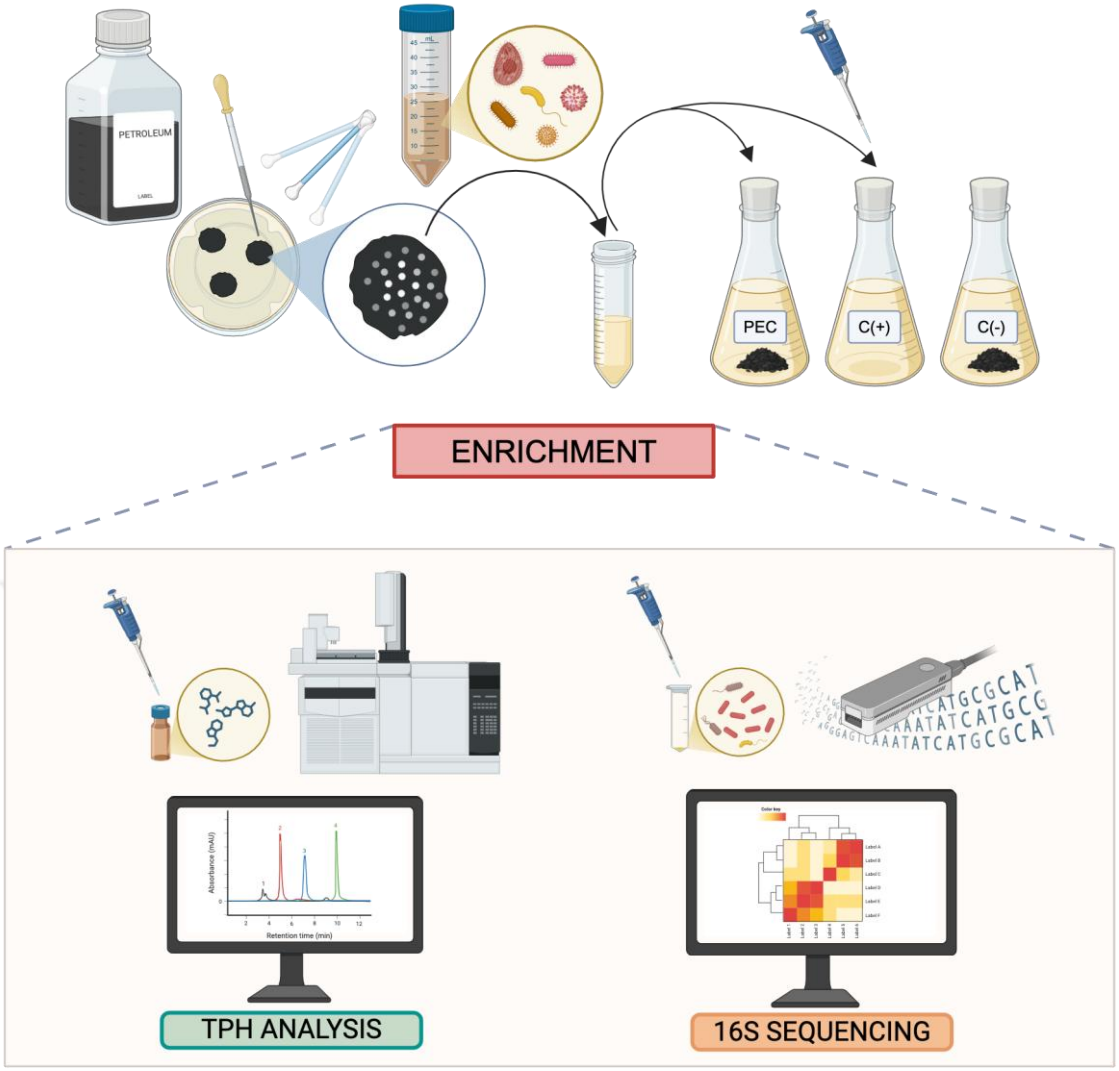


Figure 3.4. The workflow of PHC degrading microbial community enrichment process and monitoring.

3.2.1. Reactor Setup and Serial Transfer Process

Ten grams of petroleum-contaminated soil were suspended in 50 mL of isotonic saline (0.85 % NaCl) and shaken overnight at room temperature in triplicate for reproducibility. The suspension was then centrifuged at 7 500 rpm for 10 min. Supernatants were spread onto Bushnell-Haas agar plates (B4926, Sigma-Aldrich) prepared according to the manufacturer's protocol, and a single drop of crude oil was placed at multiple points on each plate as the sole carbon source. Plates were incubated at 25 °C until distinct growth on and around the oil drops was observed. After around ten days, oil drops were collected and transferred into LB broth (L3522, Sigma-Aldrich). The resulting petroleum-degrading "starter culture" was stored at 4 °C.

A carbon-free version of M9 mineral medium was preferred for the development of PEC. The M9 salt solution was prepared at a 10X concentration, including 75.2 g/L Na_2HPO_4-$2H_2O$, 30 g/L KH_2PO_4, 5 g/L NaCl, and 5 g/L NH_4Cl. Following the addition of 800 mL of distilled water, the pH was adjusted to 7.2 with NaOH, and distilled water was added to a final volume of 1 L. Stock solutions of 1 M $MgSO_4$ and 1 M $CaCl_2$ were also prepared. These stock solutions were sterilized by autoclaving at 121°C for 15 minutes. Stock solutions of 1 mg/mL biotin, 1 mg/mL thiamine, and a 100X trace element solution were made separately. The trace element solution comprised 5 g/L EDTA, 0.83 g/L FeCl-$6H_2O$, 84 mg/L $ZnCl_2$, 13 mg/L $CuCl_2$-$2H_2O$, 14.4 mg/L $CoCl_2$-$6H_2O$, 10 mg/L H_3BO_3, and 1.6 mg/L $MnCl_2$-$4H_2O$. At first, EDTA was included into the trace element solution, followed by the adjustment of pH to 7.5 with NaOH. The remaining components were subsequently added. The stock solutions were sterilized with a 0.22 µm filter. After the sterilization processes were completed, the M9 mineral medium was prepared under sterile conditions, ensuring a sterile environment near a Bunsen burner, using the amounts specified in Table 3.1 below.

Table 3.1. The composition of M9 mineral medium.

Volume	**Stock Solution**	**Concentration**
100 mL	M9 salt solution (10X)	1X
1 mL	1 M $MgSO_4$	1 mM
0.3 mL	1 M $CaCl_2$	0.3 mM
1 mL	Biotin (1 mg/mL)	1 µg
1 mL	Thiamine (1 mg/mL)	1 µg
10 mL	Trace elements solution (100X)	1X
up to 1 L	Distilled water	-

To initiate the enrichment, 900 µL aliquot of the PEC stored at 4 °C was centrifuged at 4 500 × g for 10 min, the supernatant was discarded, and the pellet was resuspended in 1 200 µL carbon-free M9 mineral medium. After a second centrifugation under the same conditions, the washed pellet was used for inoculation. For each replicate, a sterile 250 mL Erlenmeyer flask was set up with 100 mL carbon-free M9 mineral medium and 3.1 g of an autoclaved quartz river-sand/crude-oil mixture prepared at a 30 : 1 (w/w) sand-to-oil ratio (≈ 2 mm grain size). The washed starter culture was then inoculated into the flask. All procedures—including preparation of the sand–oil carrier and inoculation—were performed aseptically beside a Bunsen burner. Positive controls containing no oily-sand and negative controls without starter culture were also prepared and followed as the enrichment culture flasks.

Table 3.2. Flask contents for enrichment test setup.

Flask Name	Culture Volume (µl)	Crude oil-Sand (g)	M9 Mineral Medium (mL)
PEC-1	300	3.1	100
PEC-2	300	3.1	100
PEC-3	300	3.1	100
C(+)-1	300	-	100
C(+)-2	300	-	100
C(+)-3	300	-	100
C(-)	-	3.1	100

At each passage, 10 mL of well-mixed culture was aseptically withdrawn from the preceding flask and introduced into a fresh 250 mL Erlenmeyer containing 90 mL carbon-free M9 medium and 3.1 g of the sterile sand–crude-oil mix. Flasks were plugged with cellulose stoppers (Isolab 051.24.002) to avoid external contamination. This serial transfer was repeated five times; before every transfer, samples were taken from the spent culture for microbial profiling and TPH analysis.

3.2.2. Monitoring Growth

To track culture growth and decide when to transfer, we performed serial dilution and spot plating at set intervals. One millilitre of well-mixed culture was taken from each flask and diluted six times (10^{-1}–10^{-6}) in freshly prepared, autoclaved M63B1 medium (see Table 3.3 for composition). Ten microlitres of every dilution, plus the undiluted sample, were spotted in triplicate onto LB agar and incubated for 24 h. Colony counts were then used to calculate cell densities (CFU mL^{-1}), in order to verify the active growth of culture on crude oil as well as scheduling the next transfer.

Table 3.3. Contents of M63B1 medium.

Chemical Name	Chemical Formula	Amount
Dipotassium hydrogen phosphate	K_2HPO_4	7.40 g
Potassium dihydrogen phosphate	KH_2PO_4	3.00 g
Ammonium sulfate (20%)	$(NH_4)2SO_4$	10 mL
Magnesium sulfate (10%)	$MgSO_4 \cdot 7H_2O$	1 mL
Iron sulfate (1‰)	$FeSO_4 \cdot 7H_2O$	0.5 mL
Thiamine (0.5‰)	$C_{12}H_{17}CIN_4OS \cdot HCl \cdot H_2O$	2 mL
Ultra-pure water	H_2O	up to 1 L

3.2.3. 16S Amplicon Sequencing and Analysis

Genomic DNA was extracted from the initial enrichment culture and from three biological replicates at each of the four transfer points (five samples in total) using the DNeasy Blood & Tissue Kit (69504, Qiagen). For each replicate, 500 µL of culture was pelleted at 7 500 rpm for 10 min, the supernatant was discarded, and the pellet was resuspended in 180 µL ATL buffer. After a 30 min incubation at 37 °C, 20 µL proteinase K was added and the tubes were held at 56 °C until the lysate lost its gelatinous appearance. The mixture was vortexed, combined with 200 µL Buffer AL, vortexed again, and mixed with 200 µL 96–100 % ethanol. The entire volume was loaded onto a DNeasy Mini spin column, washed with 500 µL Buffer AW1 (11 000 rpm, 2 min) and 500 µL Buffer AW2 (14 000 rpm, 3 min), and DNA was eluted in 200 µL Buffer AE (1 min at room temperature, 11 000 rpm, 2 min). DNA concentrations were determined fluorometrically, and the three replicate eluates from each transfer were pooled. The five pooled DNA samples were then processed for 16S rRNA gene amplicon sequencing as outlined in Section 3.1.2.

3.2.4. TPH Analysis

At the end of each incubation period the residual sand was poured into 50 mL Falcon tubes, dried at 50 °C for 24 h, and then extracted as follows. Ten millilitres of hexane were added to each tube, the tubes were shaken at 2 000 rpm for 30 min, and centrifuged at 7 500 rpm for 5 min. A 1.5 mL aliquot of the hexane phase was transferred to a GC vial and stored at 4 °C until analysis.

TPH (C_{10}–C_{40}) were quantified by an accredited laboratory using the TS EN 14039 protocol. Briefly, 2 mL of the stored extract were mixed with 1 mL fresh hexane in a 50 mL Falcon, shaken 1 h, centrifuged at 3 500 rpm for 10 min, filtered through a PTFE membrane, and injected into an

Agilent 8890–5977B GC–MS operated under the GC-FID conditions specified by the standard. Calibration was performed with a certified TPH Mix (UST127, Sigma-Aldrich) prepared in hexane over 0.2–20 mg L^{-1}; retention times and characteristic ions for each n-alkane (C_{10}–C_{40}) were used for quantification.

3.3. Isolation of Dominant PHC-Degrading Bacteria

The workflow conducted for the isolation of dominant PHC-degrading bacteria is presented in Figure 3.5. The workflow is followed by activity tests, 16S sequencing, and whole-genome sequencing of novel PHC-degrading microorganisms.

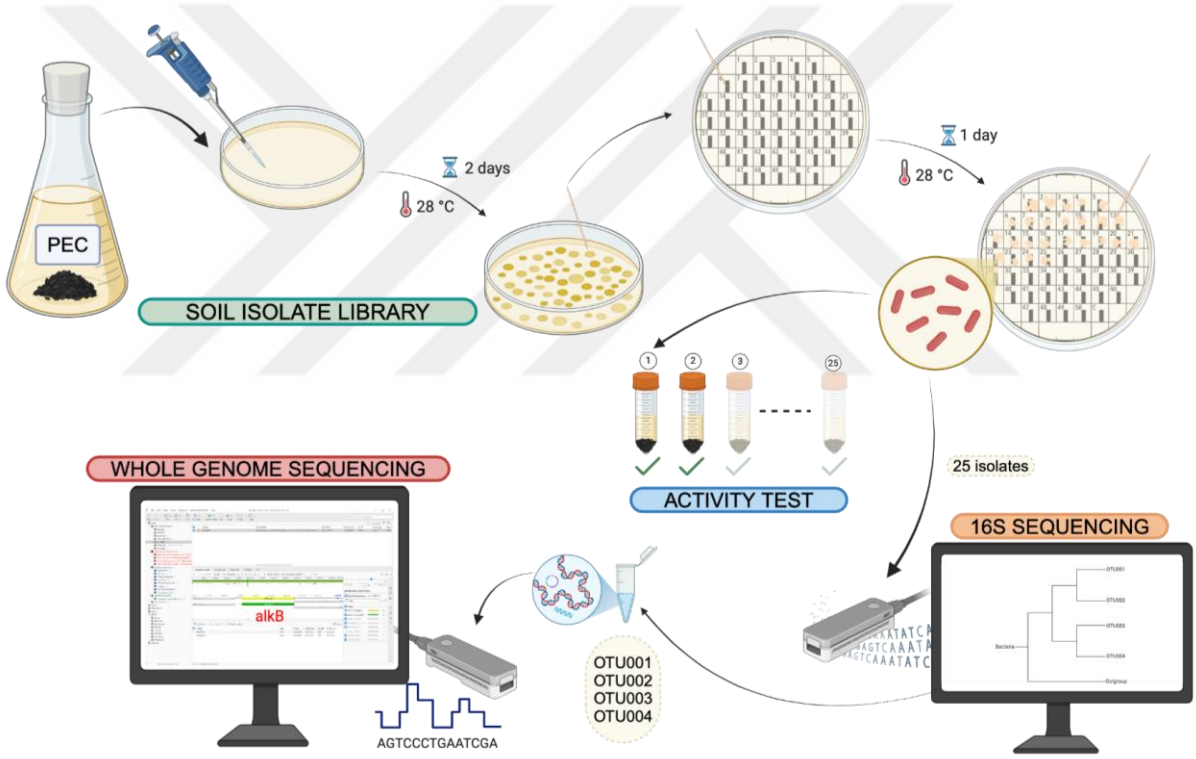


Figure 3.5. The workflow of isolation of dominant PHC-degrading bacteria.

3.3.1. Preparation of Soil Isolate Library

After the fifth serial transfer, sixth-generation enrichment cultures (PEC-1, PEC-2, and PEC-3) were serially diluted and spread on LB agar (28 °C, 24 h). Plates displaying ~100 colonies served as the source for random isolate selection: fifty colonies were picked from each plate and replica-patched onto four LB agar formulations—(i) antibiotic-free LB (control), (ii) LB + kanamycin (25 µg mL^{-1}), (iii) LB + tetracycline (12 µg mL^{-1}), and (iv) LB + ampicillin (100 µg mL^{-1}). Patches were incubated

at 28 °C for up to 72 h, and growth was recorded to assess intrinsic antibiotic resistance. Colonies that grew on the control plate were subsequently inoculated into 10 mL LB broth, cultured for 24 h (28 °C, 150 rpm), pelleted at 4 500 × g for 10 min, and resuspended in 1.35 mL LB. Dimethyl-sulfoxide was added to a final concentration of 10 % (v/v), and the suspensions were gently mixed and stored at -20 ºC.

3.3.2. Isolate PCH Biodegradability Assay

Twenty-five of the fifty antibiotic-screened isolates were re-streaked on LB agar, and a single colony from each plate was inoculated into 50 mL Falcon tubes containing 20 mL carbon-free M9 mineral medium supplemented with 3.2 g of an autoclaved sand–crude-oil carrier (30 : 1, w/w). For every isolate, a matched control tube (20 mL M9 without oil) was prepared. Each tube was loosely capped, and incubated at ambient temperature on an orbital shaker (100 rpm) for 10 d.

At the end of the incubation, 1.0 mL was withdrawn from each tube (n = 50). Samples were serially diluted (10^{-1}–10^{-6}) in M63B1 diluent, and 10 µL of every dilution were spotted in duplicate onto LB agar. Plates were incubated for 24 h at 28 °C and imaged with a Gel Doc XL+ System (Bio-Rad 170-8280; Epi-white illumination, auto-exposure 0.075 s). Colony-forming units (CFU mL^{-1}) were calculated for the oil-amended and control cultures to quantify hydrocarbon-dependent growth. Those 25 isolates were also grown in 1 mL LB broth and process for DNA isolation and 16S rRNA sequencing following the methodology detailed in Section 3.1.2.

3.3.3. Whole Genome Sequencing of Soil Isolates

Based on the bacterial community profile, one representative isolate per species was chosen for WGS to locate genes involved in aerobic PHC degradation and determine their genomic context. High-molecular-weight DNA was converted into barcoded libraries with the Native Barcoding 96 v14 kit (SQK-NBD114.96, Oxford Nanopore Technologies, UK). DNA ends were polished and A-tailed with the NEBNext® Ultra™ II End Repair/dA-Tailing Module (E7546, NEB, UK), followed by barcode ligation using Blunt/TA Ligase Master Mix (M0367, NEB, UK); the reaction was quenched with 1 µL 0.5 M EDTA. Barcoded samples were pooled, bead-purified with MagBead DNA (MBD01, Mobiomx, Türkiye), and adapter-ligated with Rapid T4 DNA Ligase (RL00, Mobiomx, Türkiye). After a second bead-clean-up, the pool was quantified on a Qubit 4 Fluorometer and loaded onto a primed SpotON Flow Cell R10.4.1 (FLO-MIN114, ONT) mounted on a MinION Mk1B™ (MIN-101B, ONT). Sequencing ran for up to 72 h under the latest MinKNOW™ software.

Raw POD5 files were base-called and demultiplexed with Dorado v0.8.0 (high-accuracy model, ONT) to generate FASTQ reads. Read quality was assessed with FastQC, then low-quality sequences were trimmed in Trimmomatic v0.39 (15 bp removed from each end). Filtered reads were assembled de novo with Flye (Zhang et al., 2022). Long contigs were taxonomically classified via local BLAST v2.15.0+ against the NCBI nt database (Johnson et al., 2008) and further checked against reference genomes (NCBI, 2021). The genome-sized contig was annotated with PGAP, and predicted proteins were queried against HADEG, the curated Hydrocarbon Aerobic Degradation Enzymes and Genes database (Rojas-Vargas et al., 2023). Assembly statistics and circular-chromosome validation were performed in Geneious Prime v2025.0.3, with the circular map visualized in the same software.

3.4. Determination of MIC of Surfactants for PEC via Broth Macrodilution Assay

Inhibitory effects of six different surfactants were evaluated on the PEC culture using macro broth dilution method (Table 3.4. and Figure 3.6).

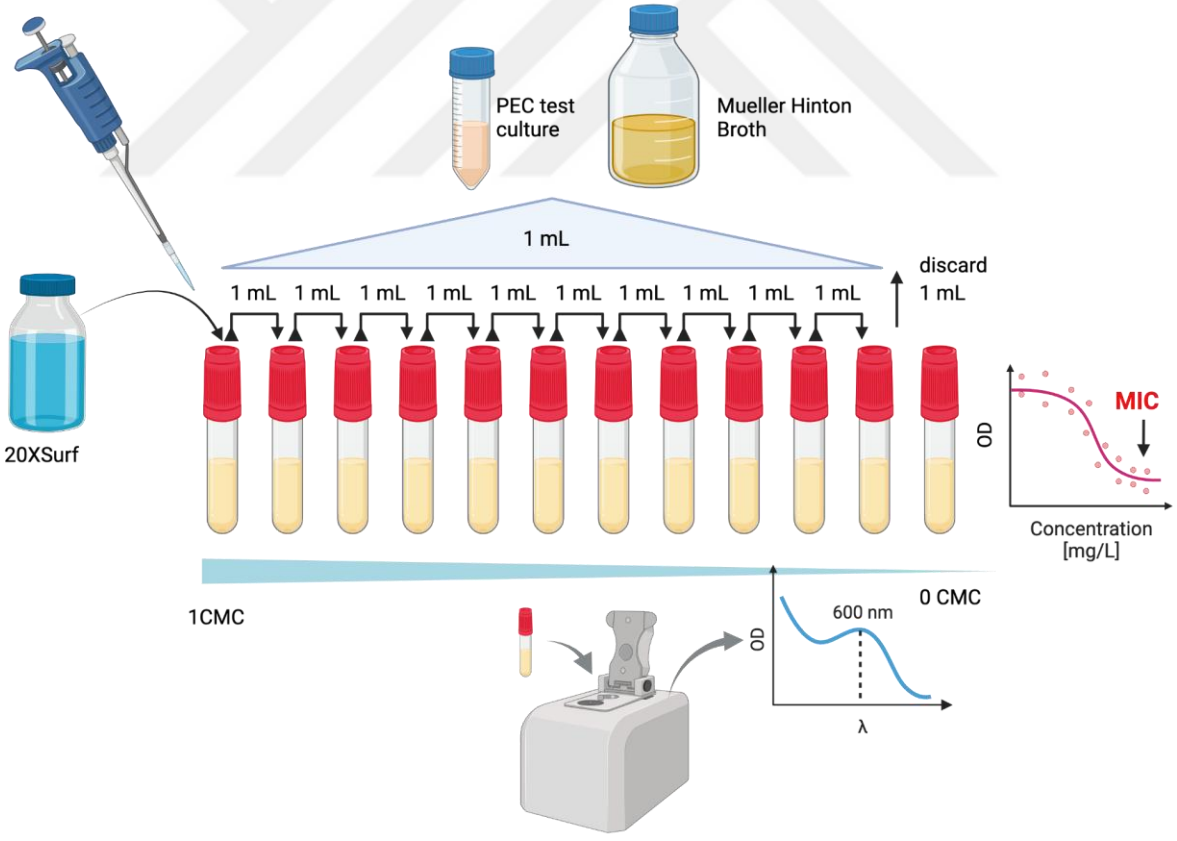
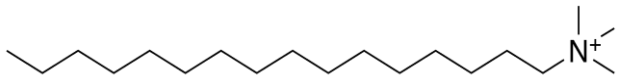
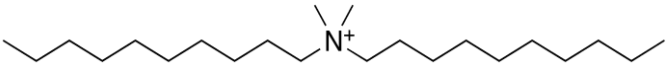
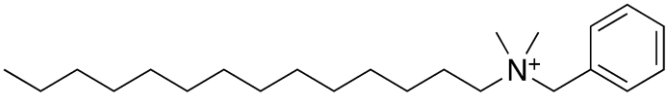
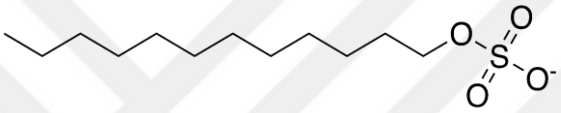
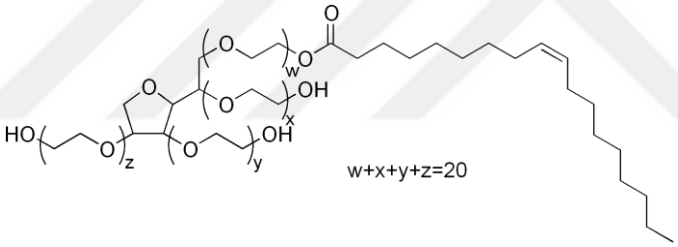
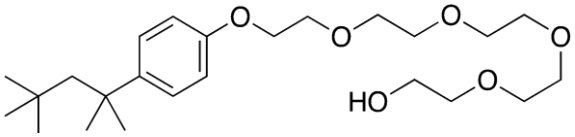


Figure 3.6. The workflow conducted for the determination of MIC with different surfactants for existing PHC-degrading cultures.

Table 3.4. The surfactants and their molecular characteristics.

Surfactant name	Molecular Structure	Surfactant Type	Reference
CTAB	 Cetyltrimethylammonium Bromide	Cationic	Goronja et al., 2016
DDAC	 Didecyldimethyl Ammonium	Cationic	Tezel, 2009
BDAC	 Tetredecylbenzyldimethyl Ammonium Chloride	Cationic	Tezel, 2009
SDS	 Sodium Dodecyl Sulfate	Anionic	Motin et al., 2015
TW	 Tween-20	Nonionic	Helenius et al., 1979
TX	 TritonX-100	Nonionic	Tiller et al., 1984

Eight 100 mL media bottles, each pre-loaded with a magnetic stir bar and 100 mL Milli-Q water, were autoclaved at 121 °C for 15 min. While the water remained hot (~60 °C), 20× CMC stock solutions of the surfactants were prepared by adding the exact masses listed in Table 3.5 directly to the sterile water and stirring until fully dissolved.

Table 3.5. Preparation of surfactant stock solutions.

Surfactant	MW (g/mol)	CMC (mM)	20X CMC (g/L)	g in 100 mL
CTAB	364.46	0.907	6.6	0.66
SDS	288.38	8.500	49.0	4.90
TritonX-100	625.00	0.240	3.0	0.30
DDAC	362.00	1.500	10.9	1.09
BDAC	339.97	1.720	11.7	1.17
Tween20	1228.00	0.049	1.2	0.12

Three sixth-generation enrichment cultures—PEC-1, PEC-2 and PEC-3—grown for about one month were evaluated by broth macrodilution. Two millilitres from each culture were transferred into 18 mL Mueller-Hinton Broth (MHB) in separate Falcon tubes, vortexed briefly and kept on ice until inoculation.

For every combination of PEC and surfactant, 24 glass tubes (13 × 100 mm) were prepared: 12 assay tubes (labelled 1–12) and 12 sterility controls (1C–12C). Tube 1 received 1.8 mL MHB plus 0.2 mL of a 20× CMC surfactant stock. Tubes 2–11 were filled with 1.0 mL MHB. A two-fold serial dilution was performed by transferring 1.0 mL from tube 1 to tube 2, mixing thoroughly, and repeating this step down to tube 11; 1.0 mL was discarded from tube 11 to equalise volumes. Tube 12, the zero-surfactant control, contained only 1.0 mL MHB.

After the dilution series was ready, 1.0 mL of the chilled PEC suspension was added to tubes 1–11. Tube 12 received an additional 1.0 mL MHB instead. The control set (1C–12C) was prepared in parallel with the same surfactant dilutions but without inoculum.

This protocol was repeated for all three PEC cultures against seven different surfactants. Tubes were incubated on an orbital shaker at 28 °C and 150 rpm for 24 hours. Post-incubation, optical density at 600 nm was measured for each assay tube using its sterility counterpart as blank. Absorbance data were processed in Berkeley Madonna with the equations at below to determine the MIC, defined as the lowest surfactant concentration that prevented detectable growth.

$$d/dt\ (OD)\ =\ -a \times (R - C) \tag{3.1}$$

$$a = IF\ C < Inh\ THEN\ 0\ ELSE\ b \tag{3.2}$$

$$R = IF\ C \geq MIC\ THEN\ C\ ELSE\ MIC \tag{3.3}$$

$$b = 0.000001 \tag{3.4}$$

$$Inh = 100 \tag{3.5}$$

$$MIC = 1500 \tag{3.6}$$

$$INIT\ OD = 1 \tag{3.7}$$

OD is the optical density, that is, an indicator of microbial growth, whereas MIC represents the lowest concentration at which the surfactant inhibits microbial growth. The C value also indicates the surfactant concentration. The "a" value in equation (b) gives the growth rate coefficient and depends on the surfactant concentration. The "Inh" value refers to the lower limit concentration at which growth inhibits. If "C < Inh", the growth rate coefficient is zero, otherwise the "b" value, that is, the minimum growth rate coefficient (main growth rate for the control group), is used. The "R" value in equation (c) is the concentration at which microbial growth is controlled. According to this equation, if the C value is greater than or equal to the MIC value, the "R" value is reached. "INIT OD" refers to the initial optical density. Berkeley Madonna software utilizes differential equations to calculate initial OD and surfactant concentrations by simulating how OD changes over time, allowing us to determine at what concentrations inhibition occurs. The stop time value for each surfactant should be changed to round up according to the highest concentration value.

3.5. Evaluation of Surfactant-Enhanced Biodegradation of Crude Oil by PEC

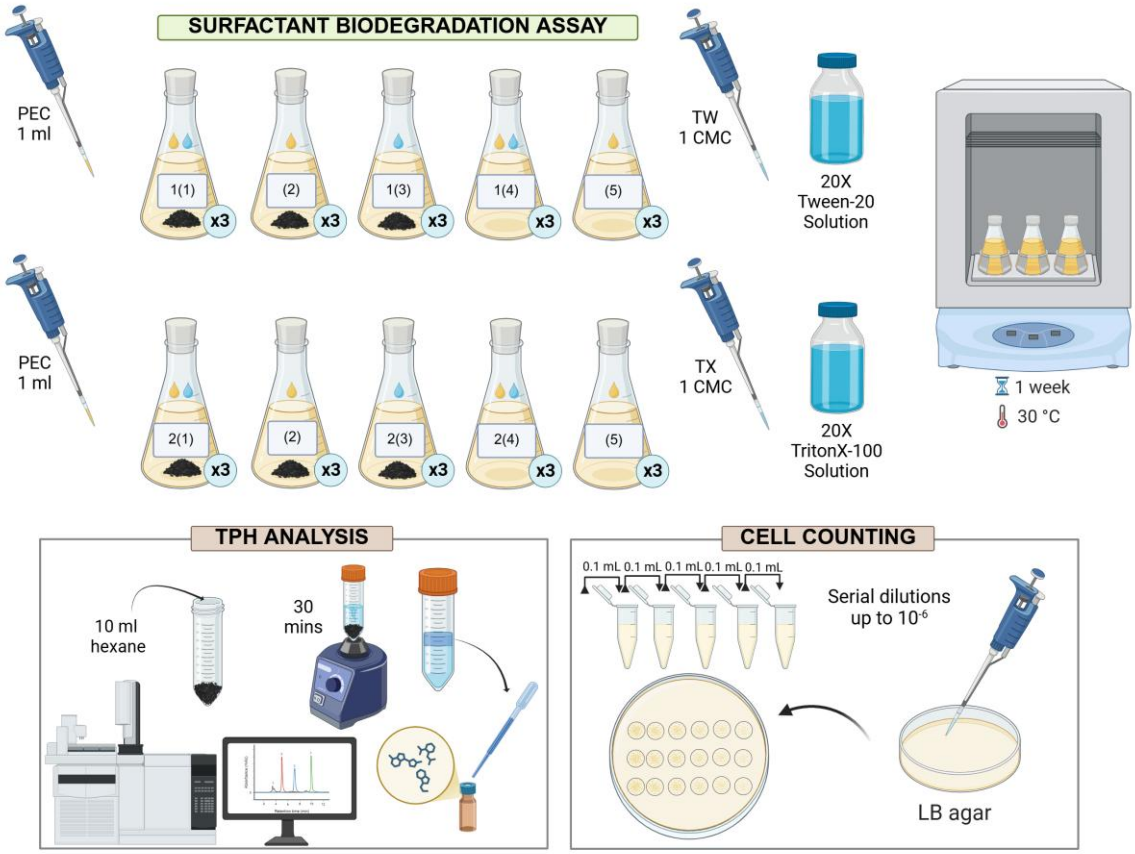


Figure 3.7. The workflow for evaluation of surfactant-enhanced biodegradation of PHC.

Biodegradation assays were conducted using triplicate PEC culture replicates (PEC-1, PEC-2, and PEC-3). Two separate tests were performed, each supplemented with two different surfactants as Tween-20 or TritonX-100, with a final concentration adjusted to 1 CMC. The detailed composition of each test bottle is provided in Table 3.6.

Table 3.6. Setup details of surfactant biodegradation assay.

No	Flask Name	20X TW solution (mL)	20X TX solution (mL)	Crude Oil-Sand (30:1 w/w) (g)	PEC Culture (mL)	M9 Mineral Medium (mL)
1(1)	PEC + Crude oil + TW	5	-	3.1	1	94
2(1)	PEC + Crude oil + TX	-	5	3.1	1	94
(2)	PEC + Crude oil	-	-	3.1	1	99
1(3)	Crude oil + TW	5	-	3.1	-	95
2(3)	Crude oil + TX	-	5	3.1	-	95
1(4)	PEC + TW	5	-	-	1	94
2(4)	PEC + TX	-	5	-	1	94
(5)	PEC only	-	-	-	1	99

All test flasks were incubated at 30 °C on an orbital shaker for 7 days. During the incubation period, daily spotting and colony counting were performed to monitor microbial growth as mentioned in Section 3.2.2. At the end of the incubation, solid samples were collected from each test flask containing the crude oil-sand mixture for TPH analysis. The collected solids were subjected to hexane extraction, and the TPH content was quantified according to Section 3.2.4.

3.6. Differential Gene Expression in Crude Oil Degrading Culture in the Presence of Surfactants

3.6.1. DNA Isolation and Shotgun Metagenomics

Before time-course gene expression analysis, we first sequenced the metagenome of the PEC at the end of 7-day incubation period. The DNA isolation was performed using the ZymoBIOMICS™ DNA Miniprep Kit (D4300, Zymo Research, USA). Initially, 25 mL of sample from each replicate was transferred into 50 mL Falcon tubes, followed by centrifugation at 7500 rpm for 5 minutes. The supernatant was discarded, and 750 µL of ZymoBIOMICS™ Lysis Solution was added to resuspend the pellet. The suspension was then transferred to ZR BashingBead™ Lysis Tubes (0.1 & 0.5 mm) and mixed on a horizontal vortex for 5 minutes. Following this, the mixture was centrifuged at 11,000 rpm for 1 minute, and 400 µL of the supernatant was transferred to a Collection Tube containing a Zymo-Spin™ III-F Filter. This was then centrifuged at 9200 rpm for 1 minute. The Zymo-Spin™ III-F Filter was discarded, and 1200 µL of ZymoBIOMICS™ DNA Binding Buffer was added to the

filtrate in the collection tube. The mixture was then transferred to a new Zymo-Spin™ IICR Column and centrifuged at 11,000 rpm for 1 minute. The liquid collected in the tube was discarded, and the remaining filtrate mixture was added to the column again and centrifuged at 11,000 rpm for another 1 minute. The collection tube was discarded, and 400 µL of ZymoBIOMICS™ DNA Wash Buffer 1 was added to the column, followed by centrifugation at 11,000 rpm for 1 minute into a new collection tube. The liquid was discarded, and 700 µL of ZymoBIOMICS™ DNA Wash Buffer 2 was added to the column. The column was centrifuged at 11,000 rpm for 1 minute, and the liquid was discarded. Another 200 µL of ZymoBIOMICS™ DNA Wash Buffer 2 was added, followed by centrifugation at 11,000 rpm for 1 minute. The Zymo-Spin™ IICR Column was then transferred to a sterile 1.5 mL Eppendorf tube, and 100 µL of ZymoBIOMICS™ DNase/RNase Free Water was added to the column matrix. The column was incubated at room temperature for 1 minute, followed by centrifugation at 11,000 rpm for 1 minute to elute the DNA. For further purification, a Zymo-Spin™ III-HRC Filter was placed into a new collection tube, and 600 µL of ZymoBIOMICS™ HRC Prep Solution was added to the column. The mixture was centrifuged at 9200 rpm for 3 minutes. The eluted DNA was then added to the Zymo-Spin™ III-HRC Filter placed in a sterile 1.5 mL microcentrifuge tube, and centrifuged at 13,000 rpm for 3 minutes. The resulting filtered DNA was ready for shotgun metagenomic analysis. This isolated DNA was then used for further shotgun metagenomics analysis to investigate the microbial community structure and functional genes involved in crude oil degradation in the presence of surfactants.

The library preparation and sequencing followed the protocol outlined in Section 3.3.4. Following the sequencing process, the data were recorded in POD5 format. These data were converted to FASTQ format using the high-accuracy model of Dorado (v0.8.0) software developed by Oxford Nanopore Technologies, UK. Barcodes in the FASTQ format underwent quality control assessments using fastQC software to evaluate the overall quality of the data. After quality control, low-quality reads were filtered using Trimmomatic (v0.39), and 15 bases were trimmed from both the beginning and the end of each sequence. Filtered reads in FASTQ format were then assembled into longer contigs using the Flye software with a de novo assembly approach. The long contigs obtained from de novo assembly were analyzed using Local BLAST (v2.15.0+) to identify the best species match. Quality control of the sequence data was achieved by comparison to reference genomes available in the National Center for Biotechnology Information database (NCBI, 2021). The full genome-sized contig was subjected to annotation using the PGAP tool. Statistical data related to the genome were obtained using the Geneious Prime (v2025.0.3) application.

3.6.2. Inoculum Preparation and Experimental Setup

Each enrichment culture - PEC-1, PEC-2 and PEC-3 - was regrown in five parallel Erlenmeyer flasks. To every flask we added 3.1 g of crude-oil-coated sand (30 : 1, w/w), 100 mL of M9 medium and 1 mL of the corresponding PEC inoculum. The flasks were incubated for seven days at 30 °C on an orbital shaker. After incubation, 40 mL from each flask was transferred to a 50 mL Falcon tube and centrifuged at 5000 rpm for 10 min. The supernatant was removed, and the pellet was gently resuspended in 1 mL of fresh M9 medium, yielding fifteen concentrated suspensions - five originating from each PEC culture (Figure 3.8).

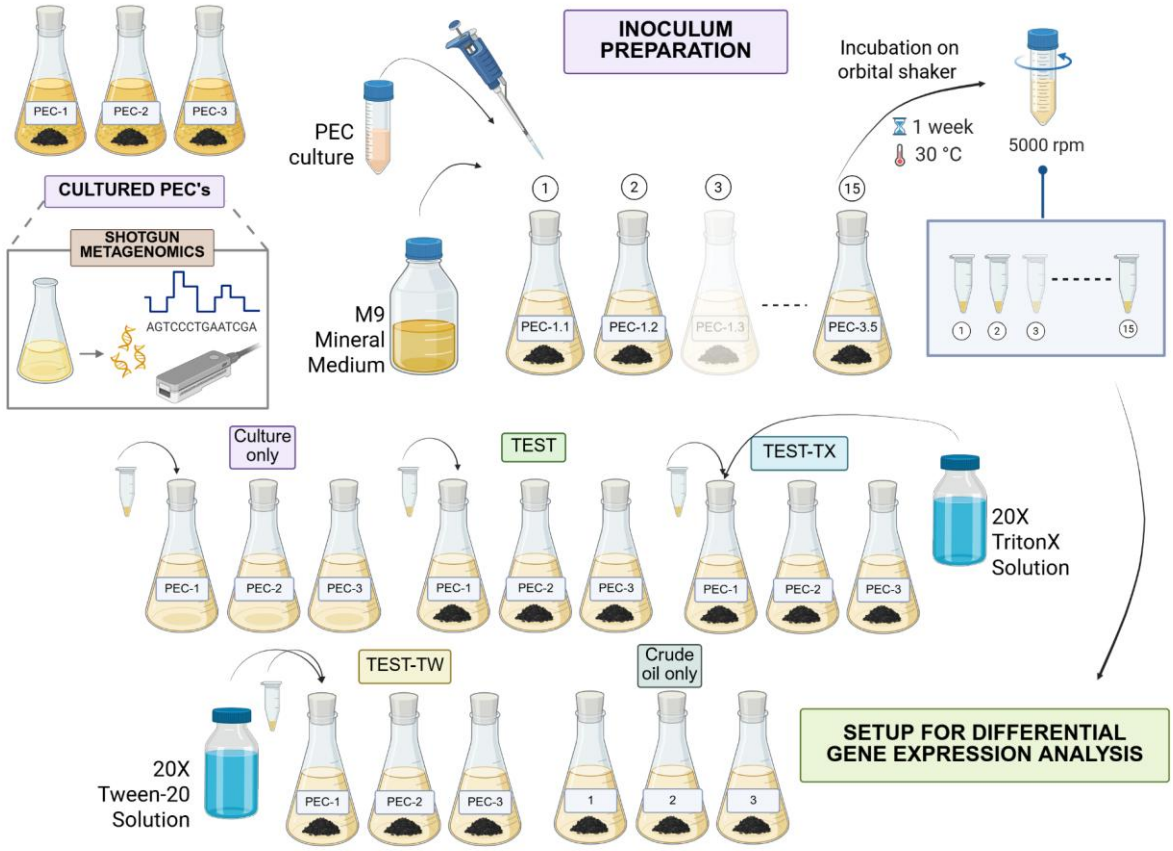


Figure 3.8. The workflow of degradation test setup for gene expression profiling.

After the inoculum was prepared, 15 autoclaved 250-mL Erlenmeyer flasks were utilized for the crude oil degradation experiment, organized into five sets with three flasks each. The composition of these five sets and their three replicates is given in Table 3.7 below. All sets were incubated at 30 °C under agitation for five days; during this period, TPH analysis for the liquid phase and cell counts were performed daily for each set. Moreover, daily samples were taken for RNA extraction to examine gene expression, with the exception of the negative control having no PEC.

Table 3.7. Setup for degradation experiment during gene expression profiling.

Flask Name	Culture only	TEST	TEST-TX	TEST-TW	Crude oil only
PEC	1 mL	1 mL	1 mL	1 mL	-
Crude oil-sand	-	3.1 g	3.1 g	3.1 g	3.1 g
M9 mineral medium	99 mL	99 mL	94 mL	94 mL	99 mL
TritonX-100 (TX)	-	-	5 mL	-	-
Tween-20 (TW)	-	-	-	5 mL	-

3.6.3. Monitoring Crude Oil Degradation and RNA Isolation for Gene Expression Analysis

In order to monitor TPH degradation, a liquid-liquid extraction was performed (Figure 3.9). Exactly, 1 mL of hexane and 1 mL of sample were added to 2 mL Eppendorf tubes, and then vortexed at high speed for 30 minutes. Afterwards, the upper hexane layer was then transferred to HPLC vials. Subsequently, TPH quantification was carried out according to the procedure described in Section 3.2.4.

Additionally, cell counts were determined by taking 1 mL samples from the flasks and performing serial dilutions up to a factor of 10^{-6} (Figure 3.9). The diluted samples were spotted on LB agar plates, which were incubated to observe colony formation as outlined in Section 3.2.2.

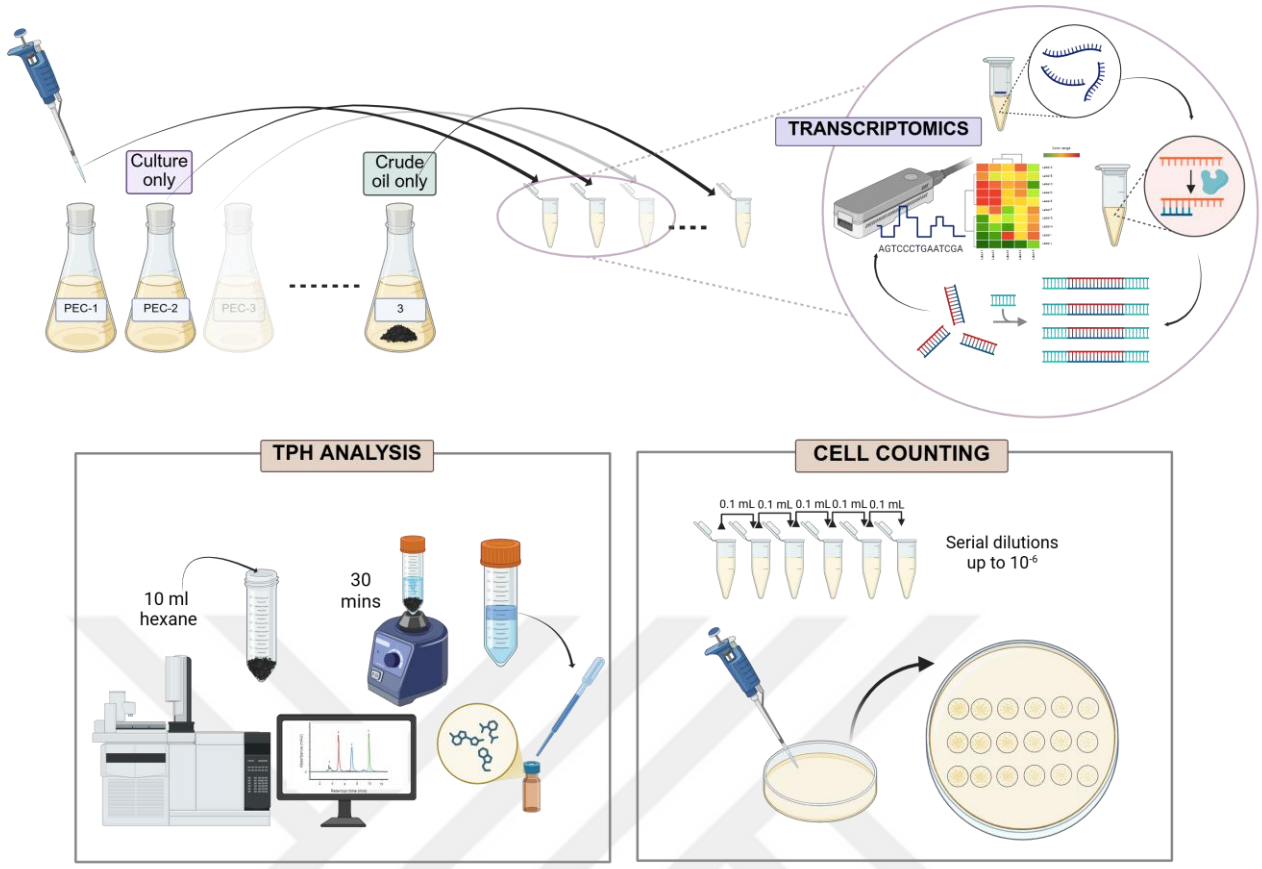


Figure 3.9. The workflow of post analysis for gene expression profiling analysis.

Prior to RNA isolation, a pretreatment was performed using TRIzol™ Reagent (15596026, Thermo Fisher, USA). A 20 mL sample was taken from each flask and centrifuged at 7500 rpm for 10 minutes. The supernatant was discarded, and 1 mL of TRIzol™ Reagent was added to the pellet. The pellet was resuspended in the reagent by pipetting, and the mixture was incubated at room temperature for 5 minutes. Following this, 0.2 mL of chloroform was added, and the tube was tightly sealed and vigorously shaken for at least 15 seconds. The tube was incubated at room temperature for 2–3 minutes and then centrifuged at 12,000 x g for 15 minutes at +4°C. This resulted in the formation of three phases: the upper aqueous phase containing RNA, the interphase, and the lower organic phase. The aqueous phase, containing RNA, was carefully pipetted into a new sterile 1.5 mL micro centrifuge tube, avoiding the interphase. For RNA purification, the Monarch Total RNA Miniprep Kit (T2010, NEB, UK) was used. All centrifugation steps were performed at 16,000 x g. To the TRIzol-extracted sample, an equal volume of ethanol (>95%) was added and mixed. The mixture was transferred to the RNA Purification Column placed in a collection tube, and centrifuged for 30 seconds. The collected liquid in the tube was discarded. Next, 500 µL of RNA Wash Buffer was added to the column, and centrifugation was performed for 30 seconds. The collected liquid was discarded, and 5 µL of DNase I and 75 µL of DNase I Reaction Buffer were mixed in a nuclease-free

micro centrifuge tube and transferred to the column to remove genomic DNA. The column was incubated at room temperature for 15 minutes. After incubation, 500 µL of RNA Priming Buffer was added to the column and centrifuged for 30 seconds. The collected liquid was discarded, and 500 µL of RNA Wash Buffer was added, followed by centrifugation for 30 seconds. Another 500 µL of RNA Wash Buffer was added and centrifuged for 2 minutes. The RNA Purification Column was then placed into a new sterile 1.5 mL nuclease-free micro centrifuge tube, and 30 µL of Nuclease-free Water was added to the column matrix. After incubating at room temperature for 1 minute, the tube was centrifuged at 16,000 x g for 30 seconds to elute the RNA. RNA concentration of samples was measured using the Qubit™ RNA HS Assay Kit (Q32852, Thermo Fisher, USA)

The eluted RNA was immediately subjected to reverse transcription to synthesize cDNA. For cDNA synthesis, LunaScript® RT SuperMix Kit (E3010, NEB, UK) was used. To the RNA sample (29 µL), 7.25 µL of LunaScript® RT SuperMix (M3010, NEB, UK) was added according to the provided protocol of the commercial kit. The cDNA synthesis was performed using the following program: 25 °C for 2 minutes, 55 °C for 60 minutes, and 95 °C for 1 minute. Finally, the cDNA concentration was measured using the Qubit™ dsDNA HS Quantification Assay Kit (Q32851, Thermo Fisher, USA).

The library preparation and sequencing was applied by following the protocol outlined in Section 3.3.4. The raw data were collected in POD5 format and processed using Dorado software for high accuracy. After processing, the resulting data were saved in unaligned BAM format (ubam files), then converted to FASTQ format using the FASTQ utility of Samtools software, crucial for maintaining data integrity (Li et al., 2009). The FASTQ files were aligned to the reference genomes from shotgun metagenomics using Minimap2 within the Geneious software framework, ensuring the accuracy and reliability of the sequence data and annotations (Heng Li, 2013). Quality control was initially carried out using FastQC and further analyzed using Qualimap bamqc software, which evaluated critical parameters such as coverage and mapping rates of the sequence data (García-Alcalde et al., 2012). These steps determined the reliability and usability of the sequence data. Gene counting and the identification of new transcripts were performed using the bambu version 3.2.4 R package, focusing on differences in gene expression and the presence of new genetic sequences. Annotations of genes were conducted using HADEG databases (Rojas-Vargas et al., 2023), crucial for understanding the functional roles of genes within cellular processes, particularly those involved in hydrocarbon degradation. Based on the annotation results, the sets were analyzed through pairwise comparisons, and these comparisons were visualized to create heatmaps.

3.7. Transformation of Hydrocarbon Degraders with a pMAT1 Trap Plasmid

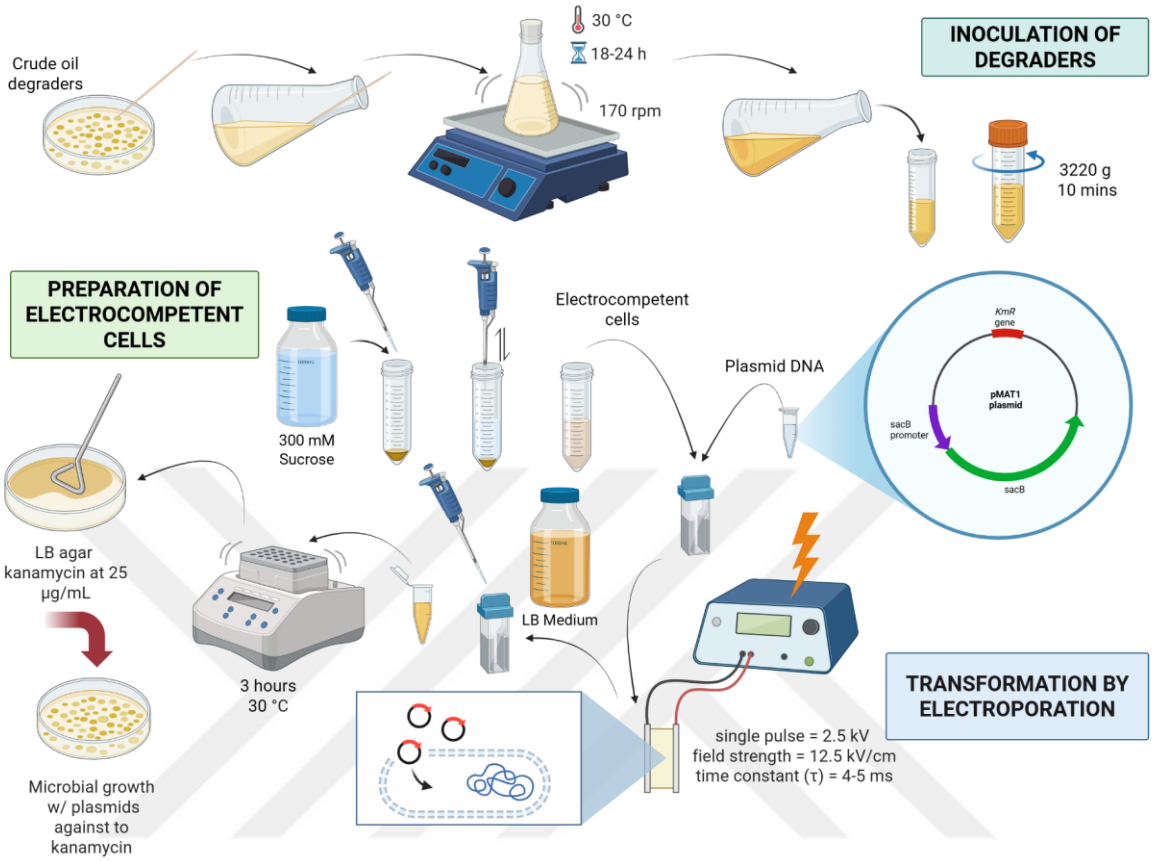


Figure 3.10. The workflow of transformation of hydrocarbon degraders with trap plasmid pMAT1.

The transformation of crude oil-degrading bacteria was carried out using the pMAT1 plasmid (Figure 3.11) which is an approximately 7 kb length of trap plasmid with kanamycin (*km*) resistance gene and Sucrose counter selection on *sacB* gene (Szuplewska et al., 2024). Trap plasmids pMAT1 was used for the identification of functional TEs of selected strains. The bacterial strains used for this transformation were selected from a soil isolate library. To prepare electro competent cells, a 100-mL Erlenmeyer flask containing 20 mL LB medium was inoculated with the selected bacterial strains, either from a fresh LB agar plate or a frozen stock. The cells were allowed to grow overnight (18–24 hours) at 30°C with shaking at 170 rpm. Once the culture reached saturation, it was transferred to a 50-mL Falcon tube and centrifuged at 3220 x g for 10 minutes. The supernatant was discarded, and the cell pellet was resuspended in 10 mL of 300 mM sucrose. The suspension was centrifuged again at 3220 x g for 10 minutes, and the supernatant was discarded. The pellet was resuspended in 1 mL of 300 mM sucrose and centrifuged at 7200 x g for 3 minutes at room temperature, followed by repeating this washing step twice. Finally, the pellet was resuspended in 500 µL of 300 mM sucrose to obtain a concentrated cell suspension with a density of approximately 5 x 10^{10} cells/mL. For

electroporation, 100 µL of the electro competent cell suspension was transferred to a sterile 1.5-mL Eppendorf tube, and approximately 500 ng of the plasmid DNA was added (in a total volume of <10 µL). The plasmid-DNA–cell mixture was pipetted into a 2-mm gap electroporation cuvette, ensuring no bubbles were formed to optimize the electroporation efficiency. The cuvette was then placed into an MicroPulser™ electroporator (Bio-Rad Laboratories; USA), with settings adjusted for E. coli (2.5 kV, field strength of 12.5 kV/cm, and a time constant (τ) between 4-5 ms), and a single pulse was applied. Immediately after the pulse, 900 µL of LB medium was added to the cuvette, and the cells were transferred to a sterile 1.5-mL Eppendorf tube and incubated aerobically at 30°C for 3 hours with gentle shaking. After the incubation, dilutions of the transformed cell suspension were spread onto LB agar plates containing 25 µg/mL of *km*. The plates were incubated at 30°C for 5–6 hours to allow colony formation, and the resulting colonies were subsequently used for further analysis related to crude oil degradation. This transformation procedure using the pMAT1 plasmid enabled the introduction of the plasmid into the crude oil-degrading bacterial strains from the soil isolate library for further studies on monitoring of gene mobilization during petroleum degradation with surfactants.

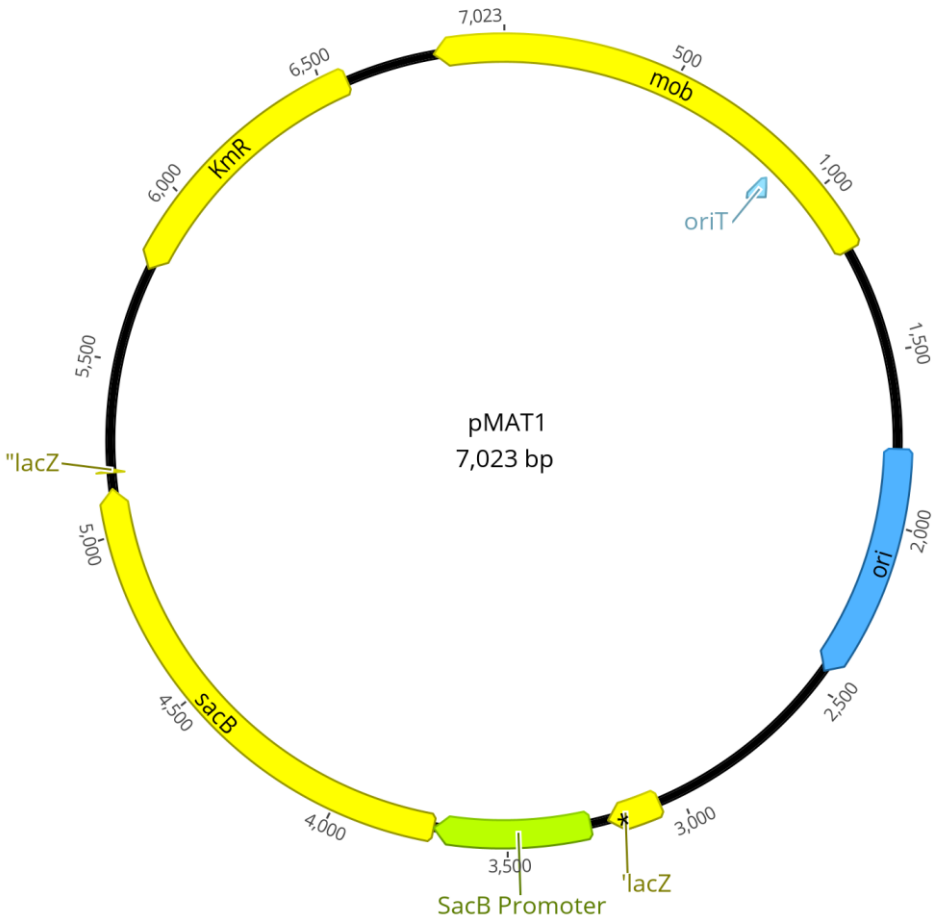


Figure 3.11. The circular genome visualization of pMAT1 trap plasmid.

3.8. Surfactant-Induced Gene Mobilization in PHC-Degrading Bacteria

3.8.1. Setup for Gene Mobilization Enrichment

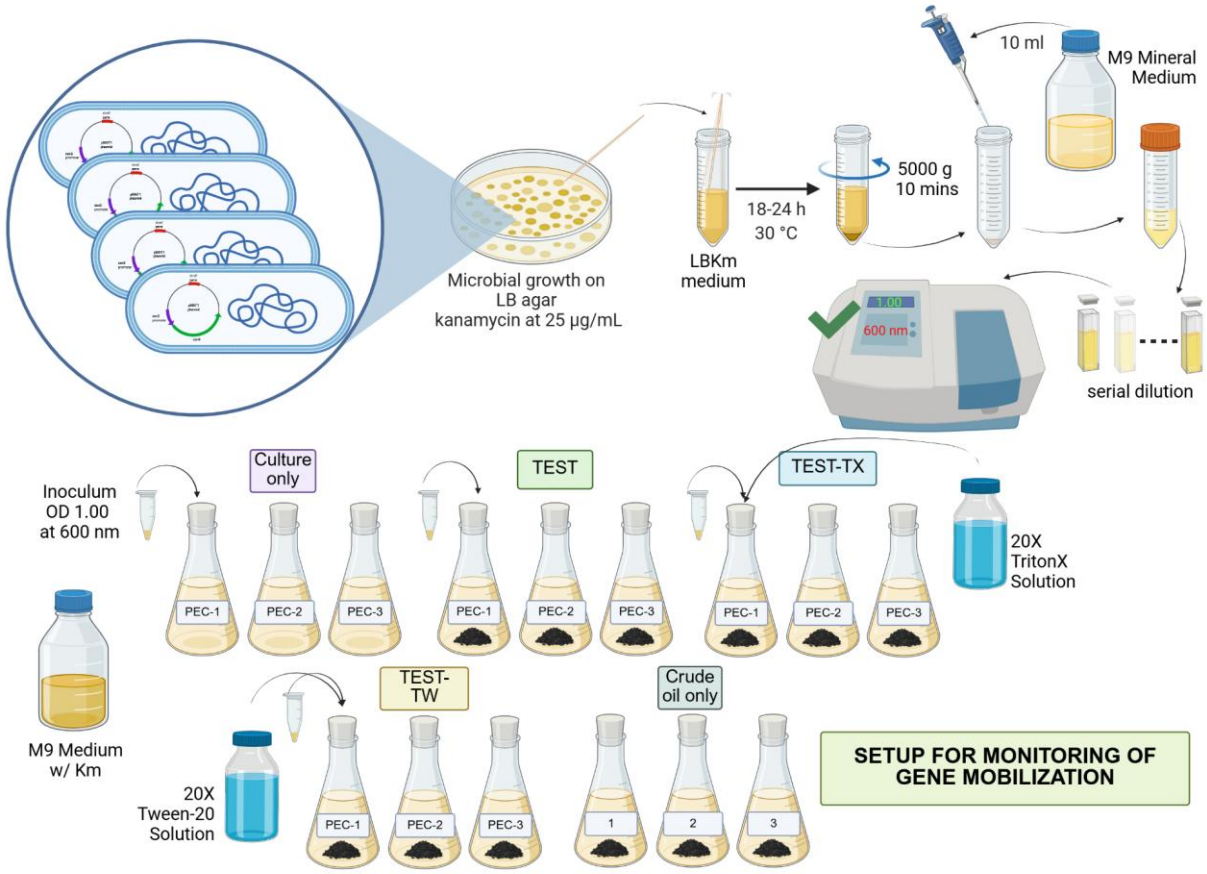


Figure 3.12. The workflow of degradation test setup for monitoring the gene mobilization.

The inoculum preparation involved growing the four transformed strains overnight in LB Broth medium with 0.25 µg/mL *km*, referred as LBKm, followed by centrifugation and resuspension in M9 medium. The cultures were diluted to an OD600 of 1.0 and then mixed to create a combined inoculum. For the gene mobilization assay, 15 autoclaved 250-mL Erlenmeyer flasks were prepared, grouped into five sets, each with three replicate flasks. The experimental setup was as follows in Table 3.8. The flasks were incubated at 30°C with shaking for five days, and daily monitoring was performed for TPH analysis and colony counting.

Table 3.8. Experimantal setup details for monitoring the gene mobilization.

Contents	Isolates w/ pMAT1	Isolates w/ pMAT1 + Crude oil	Isolates w/ pMAT1 + Crude oil + TX	Isolates w/ pMAT1 + Crude oil + TW	Crude oil only
Culture w/ pMAT1	1 mL	1 mL	1 mL	1 mL	-
Crude oil:sand	-	3.1 g	3.1 g	3.1 g	3.1 g
M9 Medium w/ Km	99 mL	99 mL	94 mL	94 mL	99 mL
TX	-	-	5 mL	-	-
TW	-	-	-	5 mL	-

3.8.2. Monitoring of Gene Mobilization

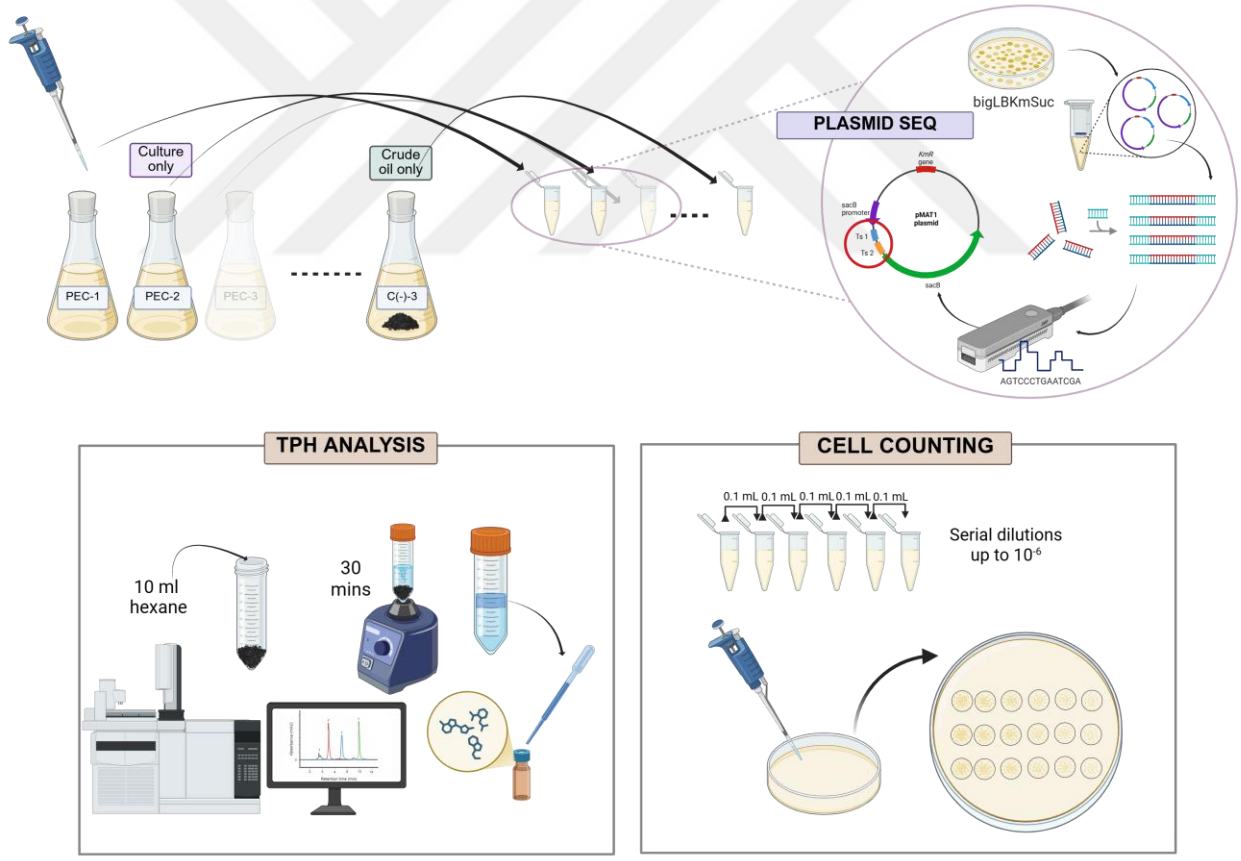


Figure 3.13. The workflow of post analysis for monitoring the gene mobilization.

During the five-day incubation, several analyses were conducted to monitor microbial activity and gene mobilization. For TPH analysis, a liquid-liquid extraction was performed by adding 1 mL of hexane to 1 mL of each sample, vortexing for 30 minutes, and transferring the upper hexane layer

to an HPLC vial. TPH measurement after pretreatment was carried out using the method specified in Section 3.2.4.

For microbial activity, the preparation of agar plates for the experiment involved three types of LB agar: labeled as LBKm, LBKmSuc, and bigLBKmSuc. For LBKm plates, 400 mL of LB agar was prepared and autoclaved. After autoclaving, the agar was cooled to approximately 60 °C, and 400 µL of a 1000X Kanamycin solution was added. The agar was mixed thoroughly and poured into 90mm petri dishes, allowing it to solidify. To prepare LBKmSuc plates, the same procedure was followed, with 400 mL of LB agar prepared and autoclaved. Once the agar reached 60 °C, 40 g of sucrose and 400 µL of 1000X Kanamycin solution were added. The mixture was well mixed and poured into 90mm petri dishes to solidify. For bigLBKmSuc plates, 400 mL of LB agar was prepared and autoclaved. After cooling to 60 °C, 40 g of sucrose and 400 µL of 1000X Kanamycin solution were added, mixed thoroughly, and poured into 120mm petri dishes to solidify. These plates were then used for the subsequent microbial growth and selection processes. Cell counting was performed by serially diluting 1 mL of the sample from each flask up to a factor of 10^{-6} and plating the dilutions onto LBKm and LBKmSuc agar plates. These plates were used to assess colony formation and track bacterial growth under selective pressure.

Plasmid extraction was conducted to determine gene mobilization utilizing samples collected at the end of the incubation period. 1 mL samples were centrifuged at 5000 x g for 10 minutes, and the pellet was resuspended in 100 µL of LB medium. The resuspended samples were plated onto bigLBKmSuc plates and incubated at 30 °C for 48 hours. After incubation, biofilm was scraped from the agar surface, transferred into cryotubes, and used for plasmid extraction using the GeneJet Miniprep Kit (K0502; Thermo Fisher, USA).

150 µL sample was centrifuged at 8000 rpm for 2 minutes at room temperature, and the supernatant was discarded. To the pellet, 250 µL of Resuspension Solution provided in the kit was added, and the mixture was vortexed to ensure complete homogenization. Next, 250 µL of Lysis Solution was added, and the tube was inverted 4-6 times to mix thoroughly, allowing the sample to become viscous and clear. Following this, 350 µL of Neutralization Solution was added, and the tube was again inverted 4-6 times to ensure thorough mixing. The mixture was then centrifuged for 5 minutes, during which cell debris and chromosomal DNA formed a pellet. The supernatant was transferred to a GeneJET spin column, and the column was centrifuged at 8000 rpm for 1 minute. The liquid in the collection tube was discarded, and 500 µL of Wash Solution was added to the column. After centrifuging for 60 seconds, the liquid was discarded, and the washing step was

repeated. The column was centrifuged once more for 1 minute to remove any residual wash solution. The column was transferred to a sterile 1.5 mL micro centrifuge tube, and 50 µL of Elution Buffer was added to the column matrix. The tube was incubated at room temperature for 2 minutes, followed by centrifugation for 2 minutes to elute the plasmid. Exonuclease V (RecBCD) (M0345 NEB, UK) was used to treat plasmid samples, followed by bead clean-up and concentration using CosMCPrep PUR4 beads (C42177, Beckman Coulter, USA). The final plasmid concentrations were measured using Qubit™ dsDNA HS Assay Kit (Q32851, Thermo Fisher, USA). Following this, plasmid sequencing and analysis were conducted. The Rapid Sequencing V14 kit (SQK-RAD114; Oxford Nanopore Technologies, UK) protocol was used for the library preparation of the sample. Subsequently, the samples were purified and measured using spectrofluorimetric method by Qubit 4 Fluorometer (Q33226, Thermo Fisher, USA) with Qubit™ dsDNA HS Assay Kit (Q32851, Thermo Fisher, USA). The total library was loaded onto a SpotON Flow Cell 10.4.1 (FLO-MIN114, Oxford Nanopore Technologies, UK) following priming, and the sequencing run initiated on a Mk1B™ device (MIN-101B, Oxford Nanopore Technologies, UK) utilizing the newest MinKNOW™ software. Following sequencing, the data in fast5 format were converted to fastq format by the newest version of guppy software for base-calling and de-multiplexing. Barcode and adapter sequences were removed using Guppy software, and universal primers and tags were eliminated by deleting 15 bases from both ends of the sequences. The raw data acquired from the sequencing process was assembled de novo utilizing Flye (v2.9.5). The assembly results were processed using the BLAST (v2.15) tool against the "nt_extracted" database, and the results were filtered to include only those with a similarity of 90% or higher (pident ≥ 90). A script was developed utilizing the BioPython library to acquire the reference genomes of the filtered organisms; consequently, the pertinent reference genomes were downloaded and consolidated using GenBank access numbers. The reads were aligned to the generated reference sequences utilizing the Geneious-Minimap2 tool, and the alignment results were obtained by examining them according to the "RefSeq" and "Mean Coverage" parameters. Subsequently, GenBank IDs and organism names were merged into a single dataset, followed by further filtering based on the threshold values of "RefSeq ≥ 80" and "Mean Coverage ≥ 30." Using the alignment files of the filtered organisms, variant analysis was conducted with the Geneious program, resulting in the generation of consensus sequences. Annotation was ultimately conducted using the PGAP tool alongside the acquired consensus sequences and the genus and species details of the organisms. The results were visualized utilizing the HADEG gene and sub pathways database, leading to the generation of heat map and bubble plot, respectively (Rojas-Vargas et al., 2023).

These steps ensured the isolation and identification of plasmids mobilized from crude oil-degrading bacteria exposed to surfactants, providing insights into the gene transfer and mobilization mechanisms in microbial populations.

4. RESULTS AND DISCUSSION

4.1. Microbial Community Structure of Petroleum Contaminated Soil

The 16S rRNA amplicon sequencing results for clean soil and petroleum-contaminated soil taken from the same area are presented in Figures 4.1 and 4.2, respectively, showing the heat map graphs between both soil types based on phylum and species level ($p<1$).

Significant variations in microbial community composition have been noted between clean and contaminated soils (Figure 4.1). In contaminated soil, there is a notable rise in specific phyla, including *Actinomycetota* (29.46%) and *Acidobacteriota* (7.24%), while groups associated with hydrocarbon degradation, such as *Bacillota* (28.55%) and *Pseudomonadota* (54.40%), predominate in uncontaminated soil. The *Pseudomonadota* phylum is extensive, with an observed rise in the amount of some species that breakdown PHCs in polluted soil, although a wider and more varied diversity of *Pseudomonadota* is present in uncontaminated soil. This finding aligns with the research conducted by Deng et al. (2025), which indicated that microbial activators enhance bioremediation by focusing on certain species within *Bacillota* and *Pseudomonadota* that are implicated in the breakdown of PHCs, especially in polluted soil respectively 4.63% and 40.39%. Furthermore, Mariano et al. (2024) reveal that hydrocarbon pollution results in diminished microbial diversity, whereas certain degradation-associated taxa, such as *Actinomycetota*, exhibit an increase. The research conducted by Singha et al. (2024) demonstrates that environmental factors, especially temperature, lead to major changes in microbial community composition and function, indicating that the current data necessitates enhancement through deeper investigations and the integration of environmental parameters.

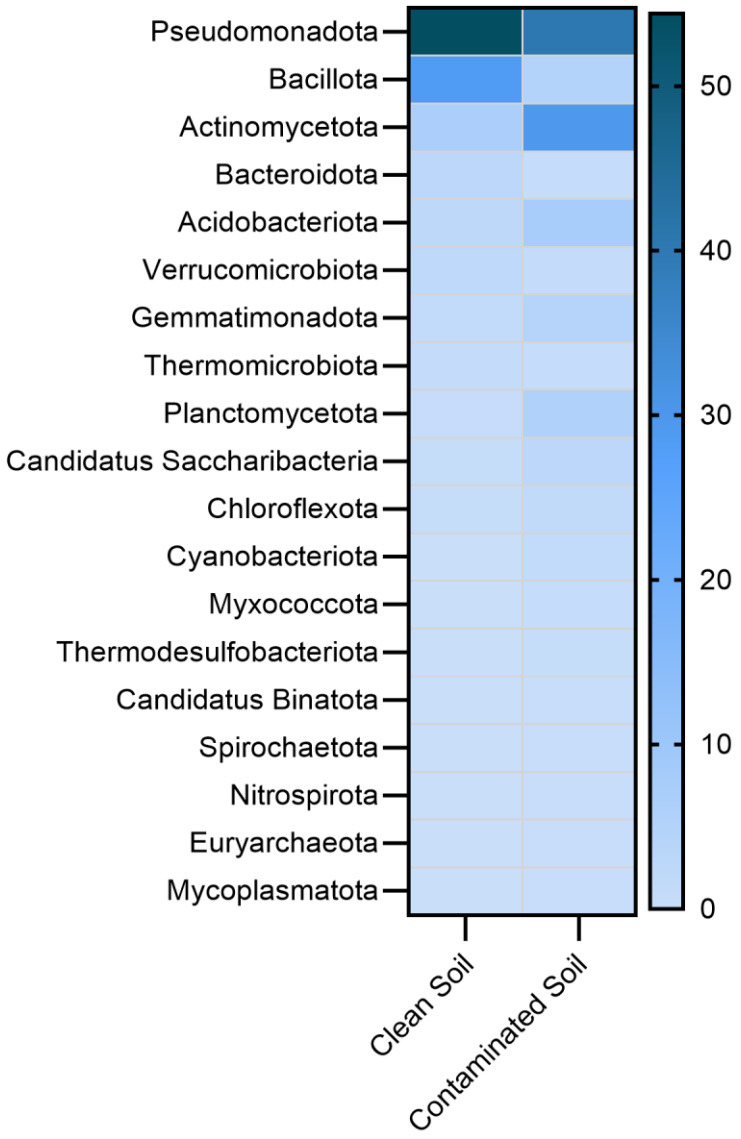


Figure 4.1. The relative abundance of microbial communities at the phylum level in clean and polluted soils.

Significant variations at the species level have been noted between contaminated and clean soils shown in Figure 4.2. In clean soil, bacteria such as *Brevundimonas subvibrioides* (10.62%), *Sphingosinicella flava* (5.33%), and various members of the *Sphingomonadaceae* family are prevalent, whereas in contaminated soil, more resilient microorganisms with a significant ability to degrade PAHs, including *Acinetobacter johnsonii* (4.59%), *Nocardioides* species, and *Acidobacteriota*, are prominent. This finding supports the results of Brzeszcz et al. (2024), which indicate that while bacterial species capable of degrading both n-alkanes and aromatic hydrocarbons are widespread in both contaminated and clean soils, their level of distribution is greater in contaminated soils. The genus *Nocardioides* has been shown to specialize in the biodegradation of

complex and hazardous organic contaminants, exhibiting significant tolerance to environmental stressors (Ma et al., 2023). It has been established that *Acinetobacter johnsonii* efficiently degrades diverse PHCs and improves bioremediation efficacy at optimal carbon-to-nitrogen ratios (Sui et al., 2023).

Conversely, while members of *Brevundimonas* and *Sphingomonadaceae*, prevalent in clean soils, exhibit extensive metabolic diversity, it is stated that species with more specialized degradation genes are favored in the toxic conditions of contaminated environments to maintain an advantage in competition (Galitskaya et al., 2021). Moreover, the activity of HGT pathways escalates in contaminated soils, facilitating the swift dissemination of degrading genes and the adaptability of the microbial population (Ma et al., 2006).

In conclusion, these species-level differences suggest that the microbial community in polluted soils is experiencing evolutionary selection and adaptation for the biodegradation of PHCs. This adaptation is essential for the advancement of bioremediation technologies and specifically facilitates the possible application of efficient degrading bacteria such as *Nocardioides* and *Acinetobacter* as biological agents. To comprehensively comprehend the functional capacity of the microbial community, it is essential to conduct deep gene-level investigations and systematically evaluate the impacts of environmental conditions.

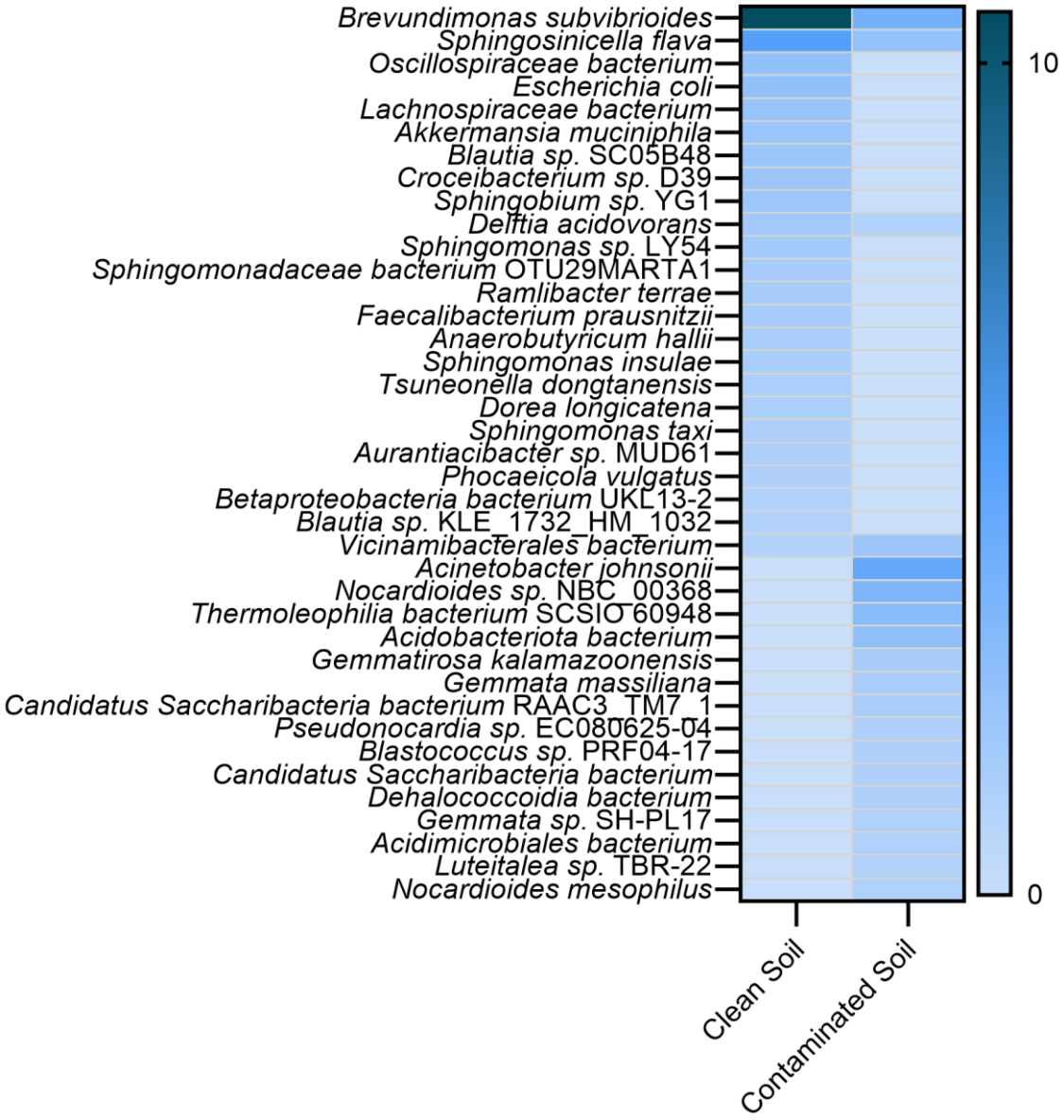


Figure 4.2. The relative abundance of microbial communities at the species level in clean and polluted soils.

4.2. Outcomes of Microbial Enrichment in PHC-Contaminated Soil: Growth, Community Shifts and Biodegradation

4.2.1. Microbial Growth Patterns During Enrichment

Crude oil served as the primary carbon source for microbes to grow on agar plates during the enrichment process. Figure 4.3 illustrates that dense colonies had developed in the edges of the crude oil droplets, signifying active hydrocarbon consumption by the microorganisms.

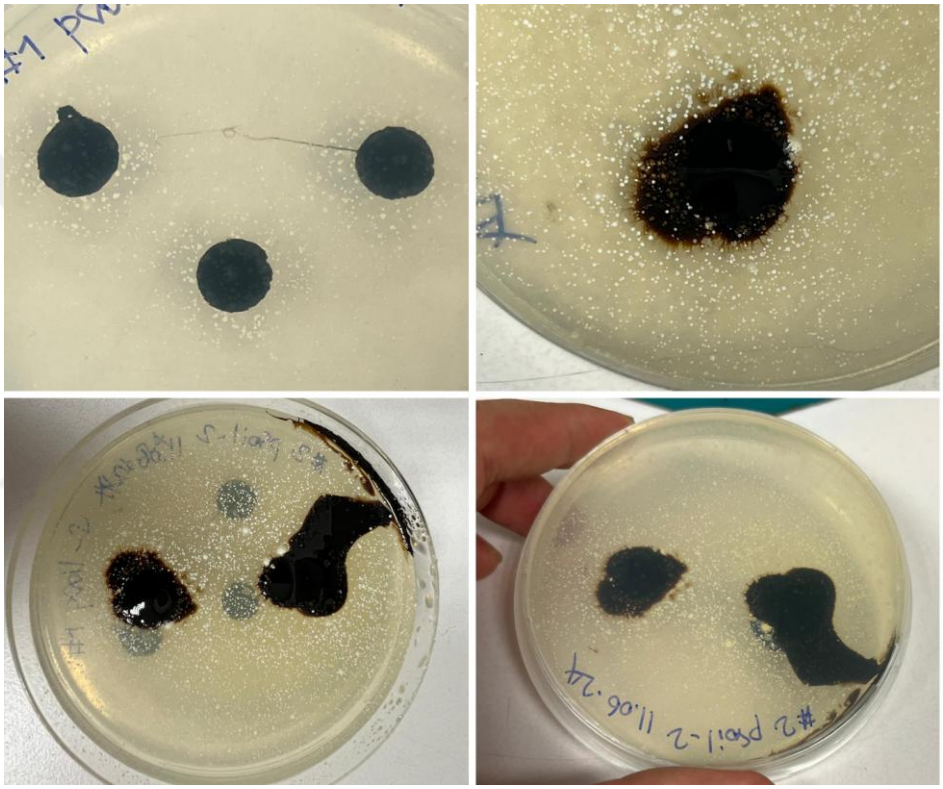


Figure 4.3. Visible colonies on and around the crude oil droplets.

Following the initial agar-based enrichment, flask incubation was initiated and the cultures were subsequently subjected to periodic transfers. During this phase, the flask containing the microbial consortia displayed significant turbidity, indicative of active bacterial growth, whereas the negative control flask lacking any bacterial inoculum remained clear (Figure 4.4). Moreover, this comparison verified the metabolic capability of the microbial consortium to utilize the crude oil substrate.



Figure 4.4. Visual comparison of microbial growth: turbidity in experimental flask vs. clarity in negative control flask.

As an example, course of incubation on the 4th transfer was given. The incubation period lasted 8 days (Figure 4.5). On day 0, microbial densities were similar at around 10^5 CFU/mL across the biological replicates of the PEC and culture controls without crude oil, Throughout the 8-day incubation period, significant microbial growth was observed in all replicates compared to their respective controls. By Day 8, the PEC-1 reached a final density of approximately 3.1 x 10^7 CFU/mL, while the C(+)-1 plateaued at 1 x 10^7 CFU/mL. Similarly, the PEC-2 achieved a density of 3.8 x 10^7 CFU/mL, whereas the C(+)-2 stabilized at 6.3 x 10^6 CFU/mL. Finally, the PEC-3 showed a final microbial density of 2.4 x 10^7 CFU/mL, while the C(+)-3 remained significantly lower, at 5.3 x 10^6 CFU/mL.

The 5th incubation period lasted 4 days for all PECs and control replicates (Figure 4.5). Initial microbial densities at Day 0 were similar across the test and control groups as same as the initiation of Incubation Period 4. During the 4-day incubation period, microbial growth was rapidly increased in all experimental groups compared to their respective controls. At Day 4, the PEC-1 group approached a final density of approximately 2.6 x 10^7 CFU/mL, while C(+)-1 group stabilized at 4.3 x 10^6 CFU/mL. Similarly, the PEC-3 group reached a final density of 2.3 x 10^7 CFU/mL, whereas the C(+)-3 control group plateaued at 4.3 x 10^6 CFU/mL.

The data, collected in triplicates, exhibited consistent trends, as indicated by the error bars, highlighting the efficiency of the experimental conditions in promoting microbial growth. These results demonstrate the enhanced microbial proliferation in the experimental groups (PEC-1, PEC-2, PEC-3) under the applied conditions compared to their respective controls during this 4^{th} and 5^{th} incubation period. The 10-fold increase observed in the experimental group compared to the control group during enrichment demonstrates the consumption of the crude oil substrate provided in the environment and indicates active microbial growth.

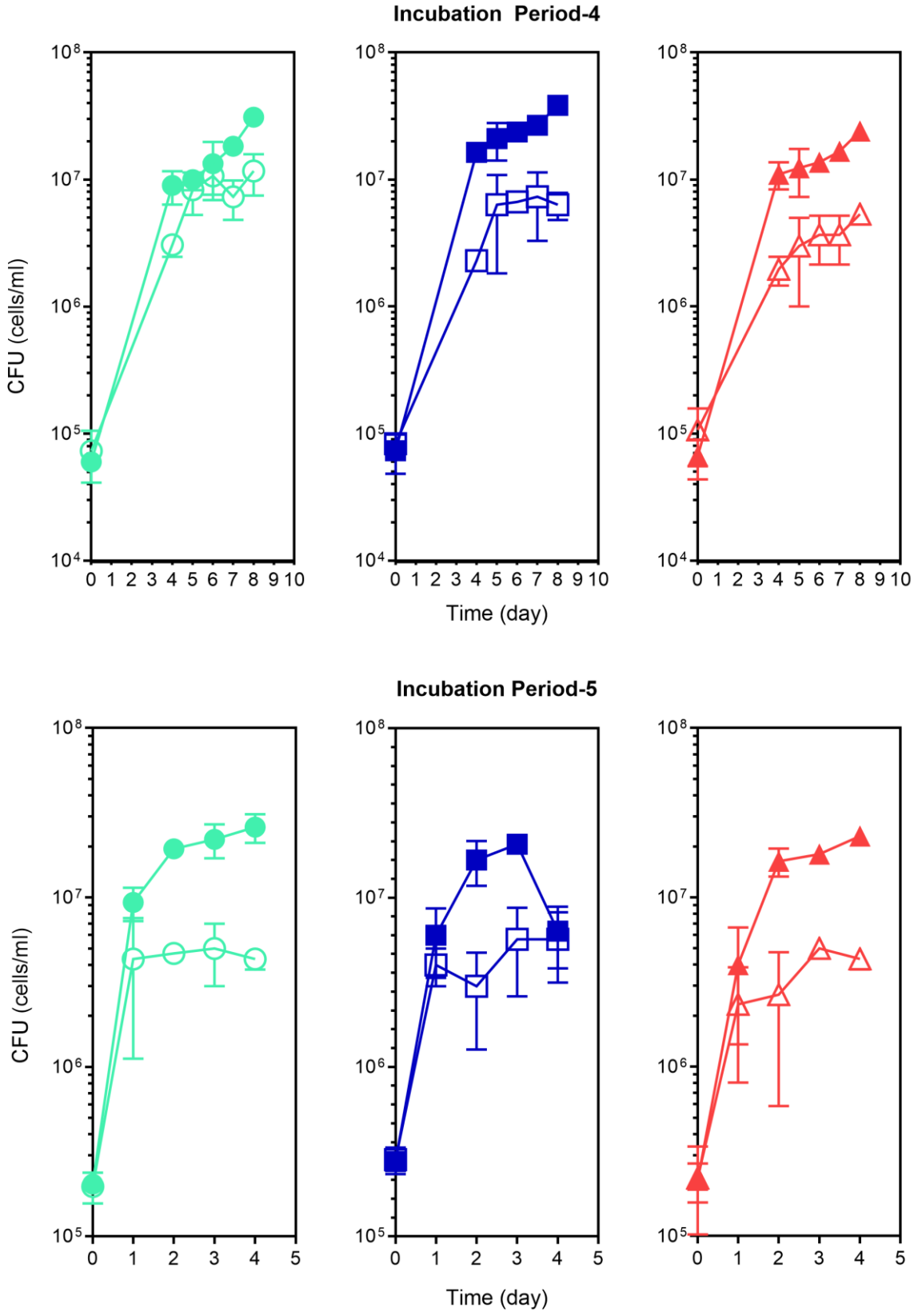


Figure 4.5. Microbial growth curve in 4th and 5th incubation period (filled represents flasks with crude oil labeled as PEC; blank represents flasks without crude oil labeled as control group C(+)).

4.2.2. 16S rRNA Based Microbial Profiling of Microbial Communities During Enrichment

During the step-wise enrichment, marked shifts in community composition were observed between the first incubation (Period 1) to the fourth transfer (Period 4). Comparative 16S-rRNA profiles for each period are presented as bar chart in Figure 4.6 and heat map in Figure 4.7.

A relative-abundance analysis normalized to the initial inoculum revealed pronounced changes in several taxa. *Pseudomonas frederiksbergensis* showed the steepest rise, increasing by 82.82% in the first transfer, 336.08% after the second, 166.41% after the third, and 196.12% after the fourth. *Achromobacter spanius* followed a similar but delayed trajectory ultimately climbing by 11.53% in Period 4 after an initial decline. These findings highlight the adaptability of both species to the selective pressures imposed by PHCs.

In contrast, several taxa declined sharply. *Stutzerimonas stutzeri* decreased by 84.25%, 90.41%, 90.26%, and 85.52% over successive periods, while *Pseudomonas sp.* FeN3W fell by more than 89% in every transfer. Such trends suggest the sensitivity of these taxa to environmental or experimental conditions.

A subset of taxa including *Bradyrhizobium barranii* and *Bradyrhizobium japonicum* remained relatively stable, exhibiting only minor fluctuations Their persistence indicates a degree of resilience irrespective of enrichment step as well as their symbiosis with the dominant taxa.

In summary, the enrichment regime strongly favoured hydrocarbon-tolerant and -degrading bacteria. *Achromobacter spanius* and *P. frederiksbergensis* consistently increased, whereas *S. stutzeri* and *Pseudomonas sp. FeN3W* were progressively eliminated. The quantitative and functional dominance of *A. spanius* and *P. frederiksbergensis* identifies them as key players capable of converting complex petroleum fractions into bioavailable intermediates, underlining their central role in hydrocarbon biodegradation (Ruiz et al., 2021). Genomic evidence shows that *A. spanius* carries a broad repertoire of aromatic-catabolic genes; although it cannot mineralize crude oil alone, its access to hydrocarbons is markedly enhanced in biosurfactant-mediated consortia, highlighting the importance of cooperative interactions for effective bioremediation (Ruiz et al., 2021).

Pseudomonas frederiksbergensis, particularly the psychrotrophic strain SI8, efficiently degrades toluene and ethylbenzene even at low temperatures (Ruiz et al., 2021; Korshunova et al., 2024). This characteristic suggests that *P. frederiksbergensis* may serve as a significant biological

agent for mitigating petroleum pollution in cold climates (Ruiz et al., 2021). The extensive metabolic plasticity of the *Pseudomonas* genus, characterized by its capacity to metabolize a variety of hydrocarbons and phenolic compounds, along with its diverse oxidase enzymes, is well-documented in the literature as essential for the activation and degradation of aromatic rings (Medić & Karadžić, 2022). These enzymes are essential for the biodegradation of aromatic hydrocarbons and represent the core mechanism of environmental bioremediation processes.

The rise of *Achromobacter* and *Pseudomonas* species in petroleum-contaminated soils indicates the resilience of these bacteria to environmental stress and their capacity to metabolize petroleum components effectively. The phytostimulant properties of *Pseudomonas frederiksbergensis*, along with its resistance to pollutants like herbicides, augment the potential of this species in microbial-plant cooperation-based bioremediation systems aimed at restoring contaminated soils (Korshunova et al., 2024). The metabolic pathways and biosurfactant production genes identified in the genome of *Achromobacter* contribute to the species' efficacy in biofilms and consortia, enhancing hydrocarbon bioavailability and improving degradation rates (Li, 2020).

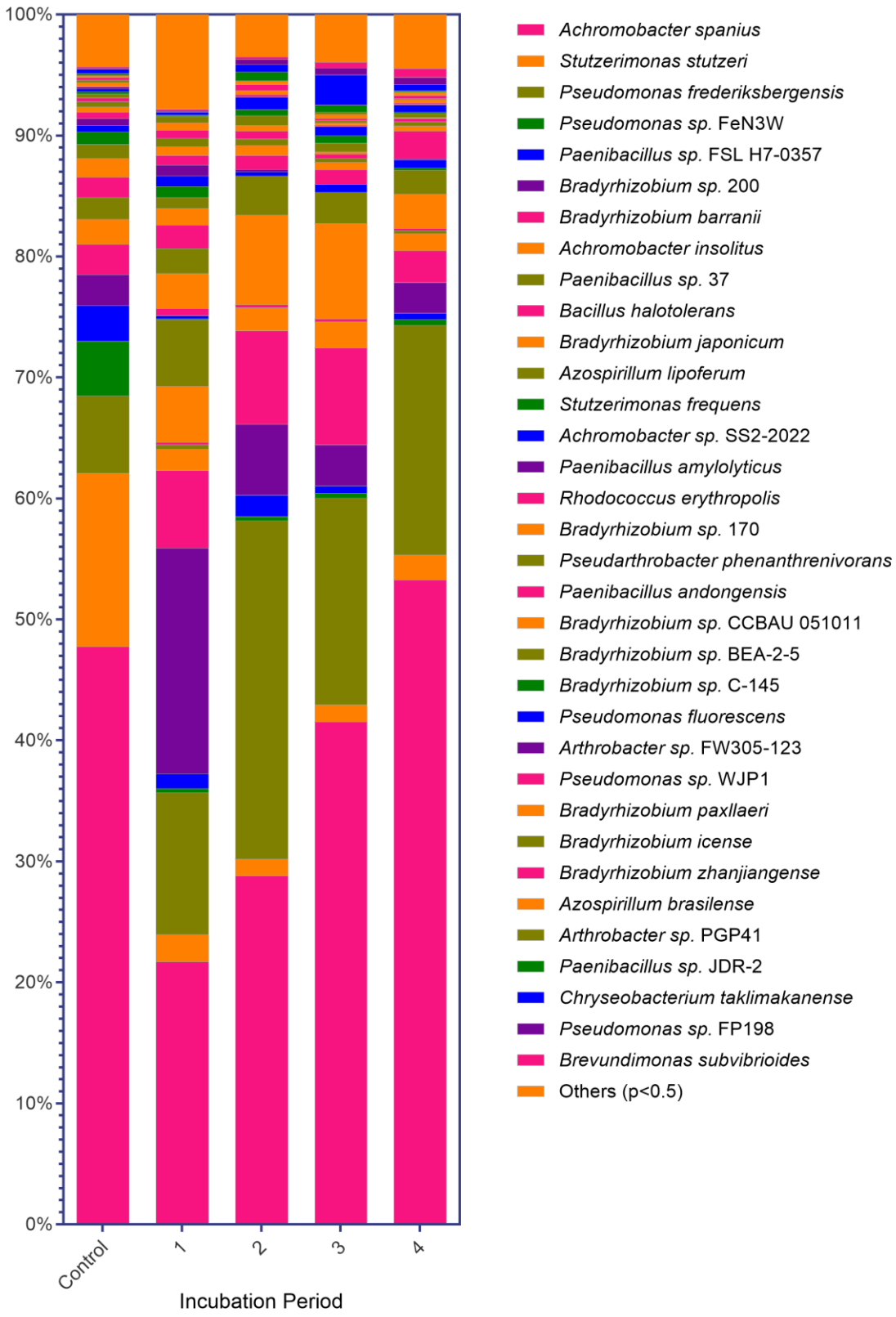


Figure 4.6. Relative abundances of dominant bacterial taxa throughout successive enrichment transfers (Incubation Period 1 – 4). Stacked bars show the mean proportion (%) of each taxon across pooled three replicate flasks per period.

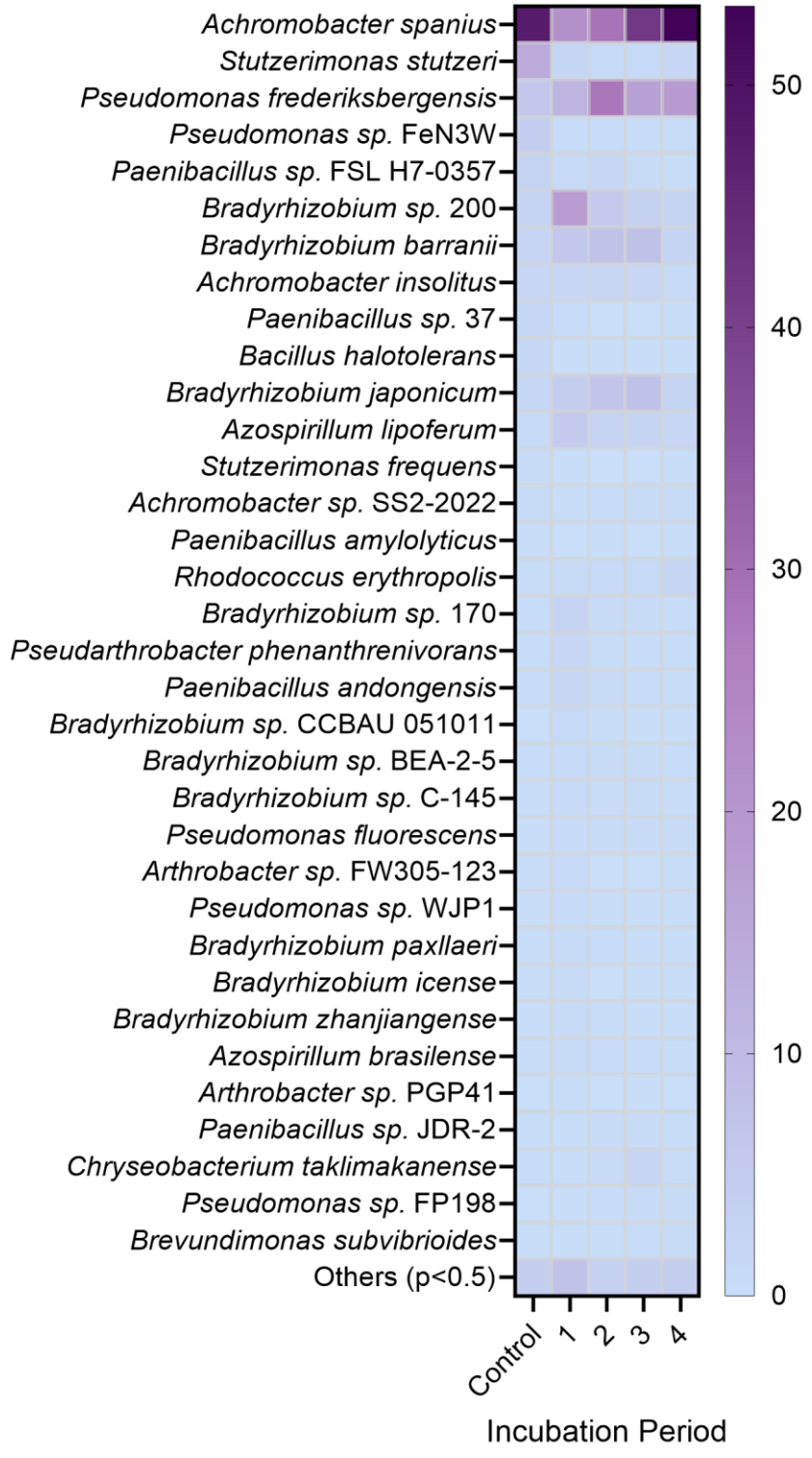


Figure 4.7. Heat map showing the relative abundance (% of total 16S-rRNA reads) of the 30 most dominant bacterial taxa in the control inoculum and after four consecutive enrichment transfers (Incubation Periods 1–4). Columns represent period averages (n = 3 flasks), while rows are ordered by decreasing abundance in the control. The blue-to-purple gradient (0–55 %) highlights the progressive enrichment of hydrocarbon-adapted taxa.

4.2.3. Petroleum Degradation Activity of the Starter Culture during Enrichment Process

Figure 4.8 compares TPH in eight sequential incubation cycles, each re-spiked with petroleum to its original concentration, against an unamended control that received the same single dose of substrate. TPH levels fell significantly in every incubation cycle relative to the control ($p < 0.05$), indicating progressively enhanced degradation over successive transfers.

The control flask set without a starter culture maintained a mean TPH concentration of 3.572 mg g^{-1} across five replicates and thus set the baseline for comparison. At the end of incubation period after first transfer of the starter culture, average residual TPH in three replicate flasks dropped was 0.922 ± 0.169 mg g-1 which is about a 74 % less than the control. Each successive transfer sustained this trend, and by the eighth incubation the cultures contained only 0.646 ± 0.112 mg g-1 TPH, representing an overall reduction of 81 %. These progressive declines were statistically significant at every step ($p < 0.05$).

Combined with the stabilized microbial community structure, effective degradation of TPH in the cultures after the fifth transfer verified the maturation of the enrichment community.

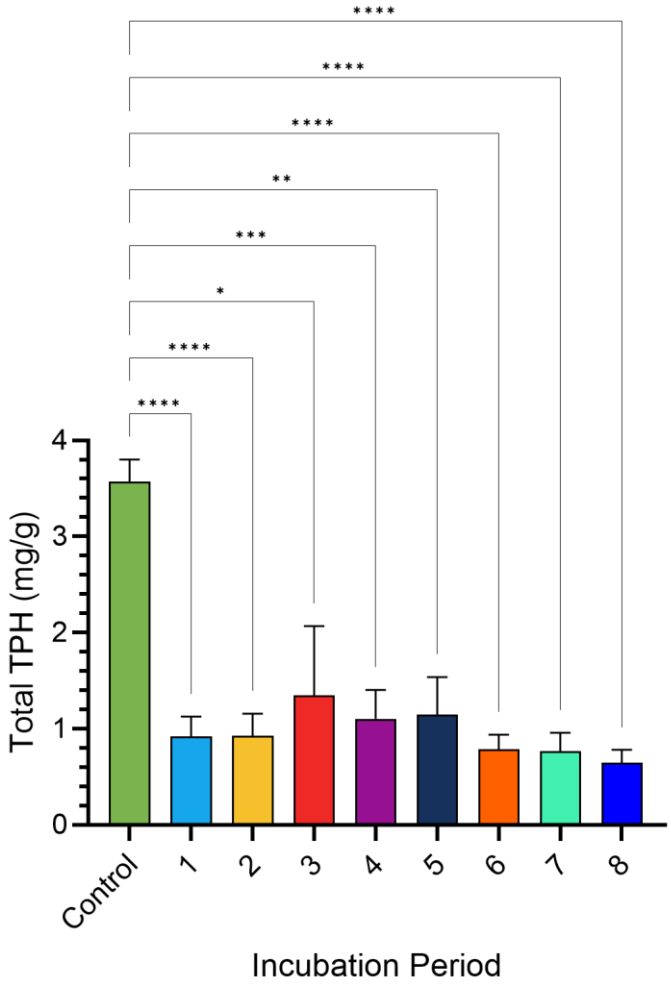


Figure 4.8. Statistical comparison of residual TPH at the end of each successive incubation periods with the control missing the PEC.

In addition, the carbon chain distributions (C_8 to C_{40}) were analyzed for each incubation period using the control as a reference. The control represents the direct measurement of the substrate prior to microbial activity. The results indicate significant variations in carbon concentrations across incubation periods given in Figure 4.9.

Short-chain hydrocarbons, such as C_8 and C_{10}, showed consistent reductions across all incubation periods, with the most significant decreases observed during the early stages. For example, C_8 exhibited an average reduction of 64%, while C_{10} showed a reduction of 27% by the 8th incubation period. These results confirm that short-chain hydrocarbons were preferentially utilized by the microbial consortia.

Medium-chain hydrocarbons, such as C_{12}, C_{16}, and C_{24}, displayed a mix of reductions and increases across periods. C_{16} showed substantial increases, averaging 371%, with the highest increase

observed during the Period 4 (511%). This pattern suggests that microbial activity shifted towards the degradation of medium-chain hydrocarbons as short-chain hydrocarbons were depleted. Similarly, C_{24} exhibited an increase of 343% during Period 2, reflecting a similar adaptive trend.

Long-chain hydrocarbons (C_{28} to C_{40}) demonstrated resistance to biodegradation, with varying degrees of change. While some long-chain hydrocarbons, such as C_{28} and C_{30}, showed consistent increases (average increases of 600% and 556%, respectively), others, like C_{40}, exhibited minimal changes. On average, C_{40} showed an 11% increase, with occasional decreases in certain periods (e.g., -14% during the 7th incubation period). This suggests that longer chains were less accessible or degradable by the microbial consortia, and their fluctuations could be attributed to intermediate accumulation or limited microbial activity.

By the 8th incubation period, the overall trend showed reduced activity for short-chain hydrocarbons, such as C_8 (76% reduction), and increased stabilization for medium and long-chain hydrocarbons. Medium-chain hydrocarbons like C_{16} and C_{30} increased by 332% and 470%, respectively, while long-chain hydrocarbons, such as C_{40}, showed a minor reduction of 8%. This final stage highlights the gradual adaptation of the microbial community and the increasing challenge posed by recalcitrant hydrocarbons.

Overall, the results demonstrate a progressive shift in microbial activity from short-chain to medium-chain hydrocarbons, while long-chain hydrocarbons exhibit the greatest resistance to degradation. These findings underscore the importance of tailoring remediation strategies to the specific composition of hydrocarbon mixtures and the need for extended incubation or enhanced conditions to address recalcitrant components effectively.

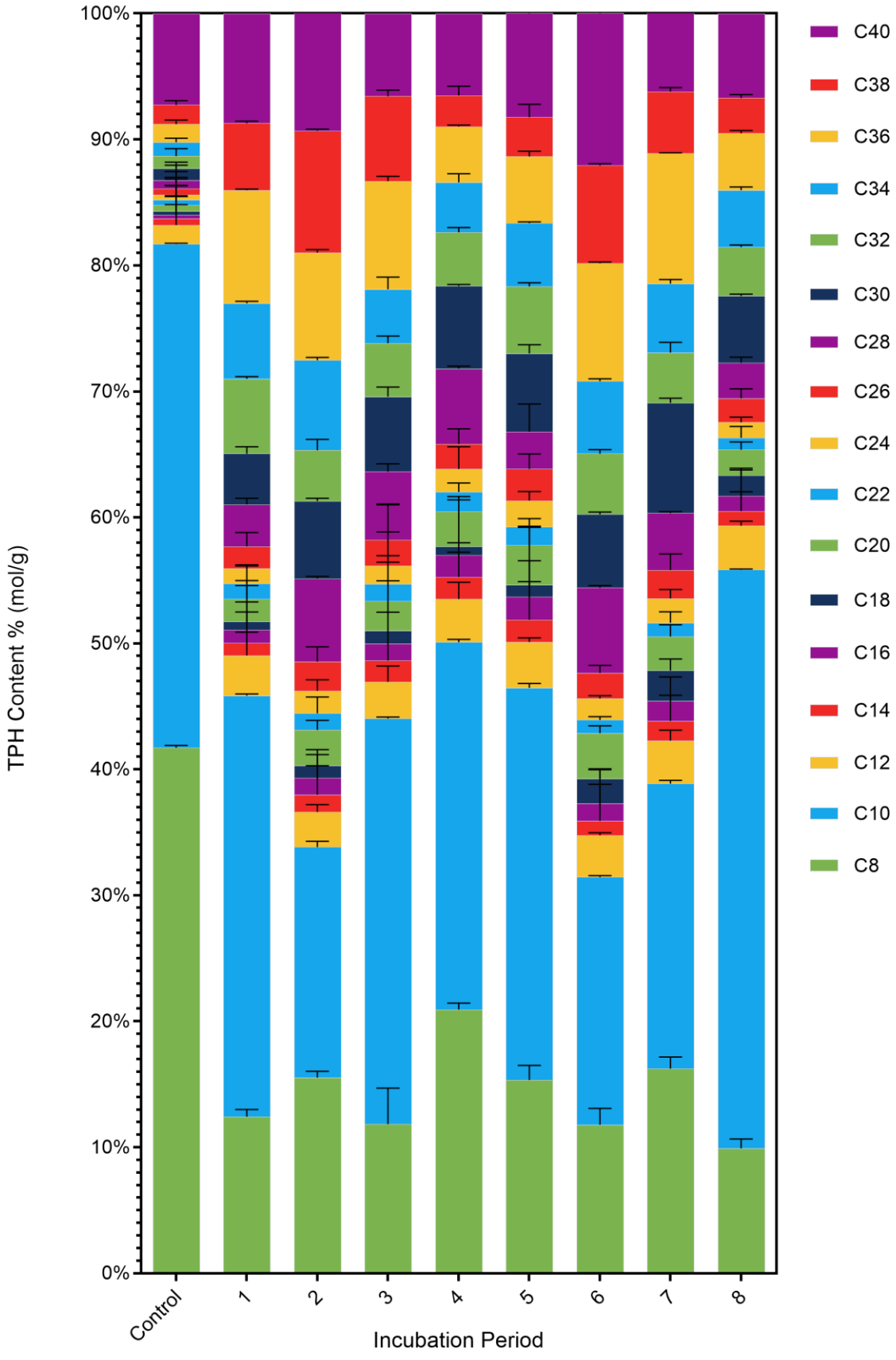


Figure 4.9. Comparison of TPH chain-length distribution (C_8-C_{40}) across eight enrichment cycles.

4.2.4. Overall Results of Enrichment of PHC-Degrading Microbial Community

The degradation of crude oil remained consistently elevated over the eight sequential enrichment transfers as indicated in Table 4.1. Removal efficiencies varied between 62.29% and 81.91%, with a mean of 73.24 ± 6.47% (n = 8, CV = 8.83%). The maximum efficiency of 81.91% was reached after approximately seven days of incubation, signifying that the petroleum-hydrocarbon-degrading consortium approaches near-steady-state within the initial week. Beyond this, there was minimal benefit to extending contact; for instance, the initial 39-day incubation eliminated 74.18%, which was nearly equal to the 7- to 8-day transfers. Pearson correlation analysis indicated no significant linear relationship between incubation time and degradation efficiency ($r = 0.07$, $p = 0.87$), suggesting that community composition and metabolic activity, rather than exposure duration, influence the observed kinetics.

Results from microbial-profiling studies support this finding. Successive transfers gradually enriched specialist hydrocarbonoclastic taxa: *Pseudomonas frederiksbergensis* increased by almost 300% compared to the inoculum, while *Achromobacter spanius* reversed its initial decrease, achieving an overall increase in abundance by the fourth transfer. In contrast, microorganisms like *Stutzerimonas stutzeri* and *Pseudomonas sp.* FeN3W had a reduction of approximately 85–90%, whilst *Bradyrhizobium* species exhibited relative stability. The taxonomic convergence towards specialists most probably increased the collective copy numbers of crucial catabolic genes such as *alkB, cyp153,* reducing lag phases and enhancing specifically degradation rates. Therefore, after the consortium has experienced a few enrichment cycles, seven-day incubations are adequate, and performance gains are primarily driven by microbial specialization rather than longer exposure periods, as evidenced by the statistical independence of efficiency from incubation time and the community-succession pattern.

4.3. Identification of PHC Degraders and Evaluation of Their Genetics

4.3.1. 16S rRNA based Identification of Dominant Bacteria in PEC

Twenty-five colonies obtained from the PEC flasks underwent comprehensive 16S rRNA sequencing. Sequence clustering at ≥99% identity resulted in four OTUs (Table 4.1). Three OTUs, specifically OTU001, OTU002, and OTU003, comprised 21 out of 25 isolates (84%) and were classified within the genus *Pseudomonas*. In contrast, OTU004, representing 4 out of 25 isolates (16%), was associated with *Achromobacter spp*. Notably, OTU002, which exhibited 100% identity

with *Pseudomonas frederiksbergensis* YE17, dominated the library, accounting for 48% of the isolates. OTU003 exhibited 100% identity with *Pseudomonas sp.* FP198, while OTU001 demonstrated 99.87% similarity to *Pseudomonas sp.* MYb327. OTU004 exhibited a 99.93% similarity to *Achromobacter sp.* SS2-2022.

Table 4.1. Taxonomic classification and distribution of OTUs derived from 16S rRNA sequencing of soil-isolate library colonies.

OTU number	**Number of replicates**	**Closest neighborhood**	**Similarity**
OTU001	2	*Pseudomonas sp.* MYb327 (CP159258.1)	%99.87
OTU002	12	*Pseudomonas frederiksbergensis* YE17 (CP142104.1)	%100
OTU003	7	*Pseudomonas sp.* FP198 (CP117452.1)	%100
OTU004	4	*Achromobacter sp.* SS2-2022 (CP107244.1)	%99.93

The maximum-likelihood analysis of the 25 colony sequences yielded a well-resolved phylogenetic tree (Figure 4.10), with all isolates categorized into two bootstrap-supported clades (≥ 100%). One clade included the four *Achromobacter* isolates (OTU004), situated between A. *marplatensis* R-46660 and *A. mucicolens* R-46658, whereas the second clade included the 21 *Pseudomonas* isolates. Three sub-clusters were identified within *Pseudomonas*: a dominant *P. frederiksbergensis* lineage that unified OTU002 (12 replicates) and OTU003 (7 replicates) with the type strain DSM 13022 (node support 91 %); a minor OTU003 lineage (2 replicates) associated with *P. baetica* a390 / *P. jessenii* CIP 105274 (65–79 %); and a basal branch formed by *P. silesiensis* A3. *Pseudomonas putida* IAM 1236, included as an out-group, rooted the *Pseudomonas* diversification and underscored the deep split from *Achromobacter*.

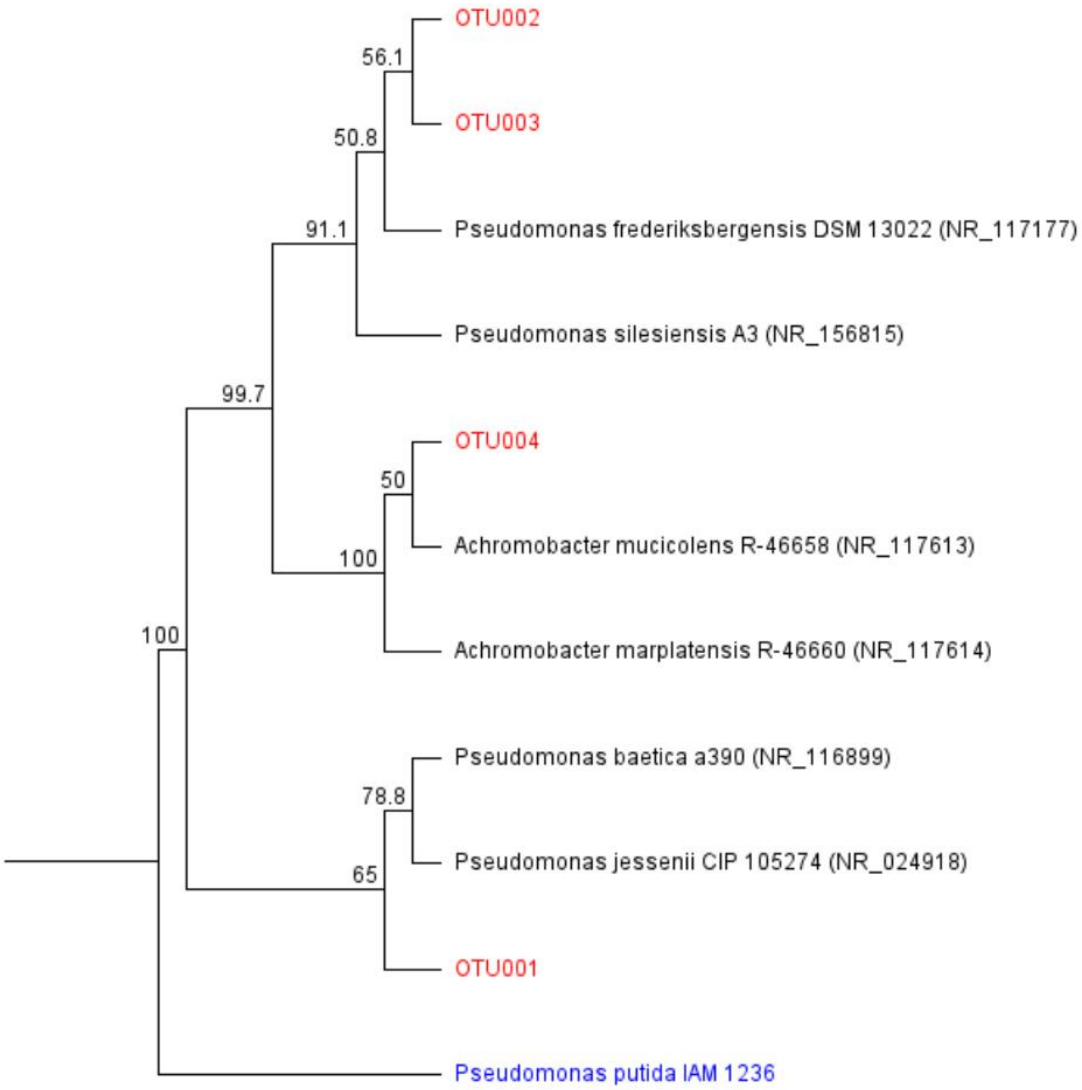


Figure 4.10. Maximum-Likelihood phylogenetic tree of soil isolates based on 16S rRNA sequences showing bootstrap-supported clades and subclusters.

4.3.2. Biodegradation of Crude Oil by Individual PEC Isolates

Serial-dilution plating and colony counts (Figure 4.11 and 4.12) revealed significant growth differences between petroleum-amended and control cultures for all four OTUs. In crude-oil tubes, OUT 002 reached from 2×10^7 to 1.2×10^8 CFU/mL, highest among the isolates, indicating a robust affinity to PHCs. OTU001 also grew markedly from 1×10^7 to 7×10^7 CFU/mL. Although their response was not as noticeable as that of OTU001 and OTU002, OTU003 and OTU004 showed considerable growth in crude oil, with CFU levels ranging from 1×10^7 to 6×10^7 CFU/mL and 2×10^7 to 5×10^7 CFU/mL, respectively, both above the control tube values. The findings demonstrate

that all four OTUs can grow on PHC individually. The enrichment method was effective in selecting for microbes capable of consuming hydrocarbons, as further evidenced by the considerable difference in growth between the control and petroleum-containing tubes. OTU002 has the most adaptability to crude oil, while the other OTUs, while still able to grow, showed less noticeable reactions. The variations in CFU values across the OTUs indicate variable levels of hydrocarbon degradation capacity. This demonstrates the microbial community's functional diversity and the continuous selection for effective hydrocarbon degraders via enrichment.

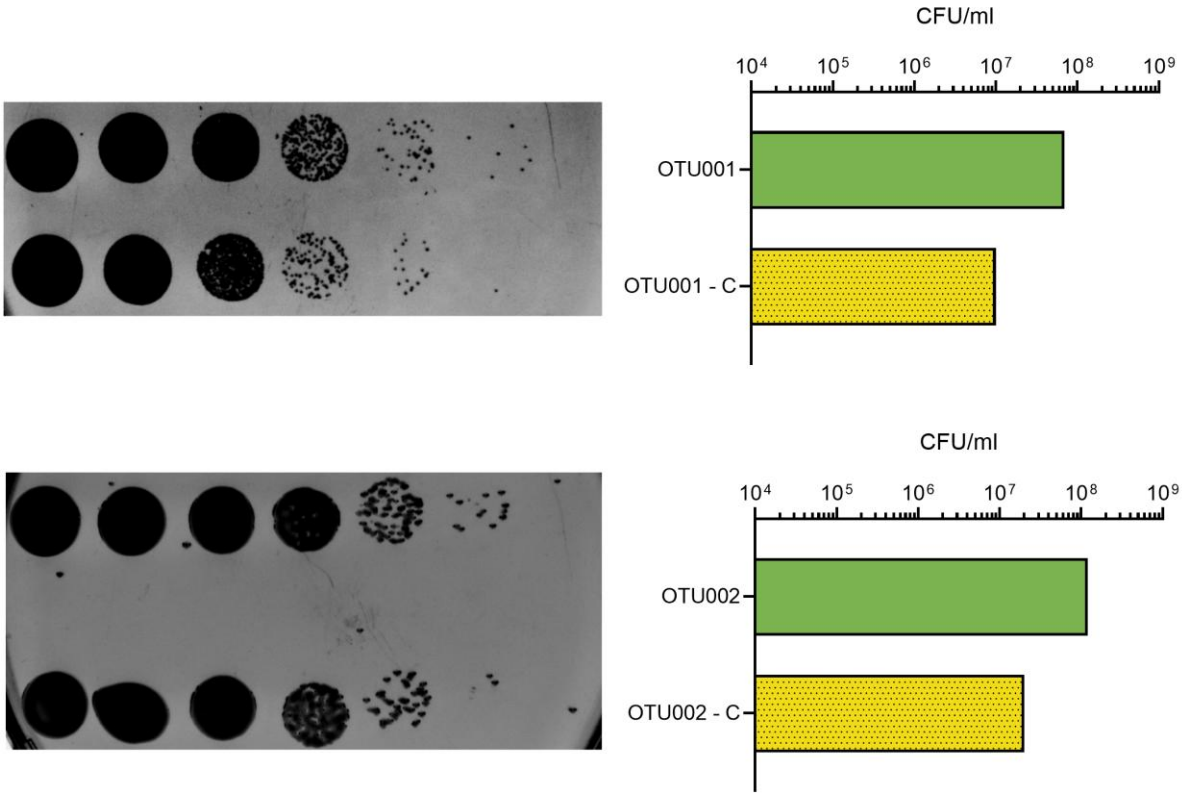


Figure 4.11. CFU counts demonstrating growth of OTU001 and OTU002 in petroleum-containing medium.

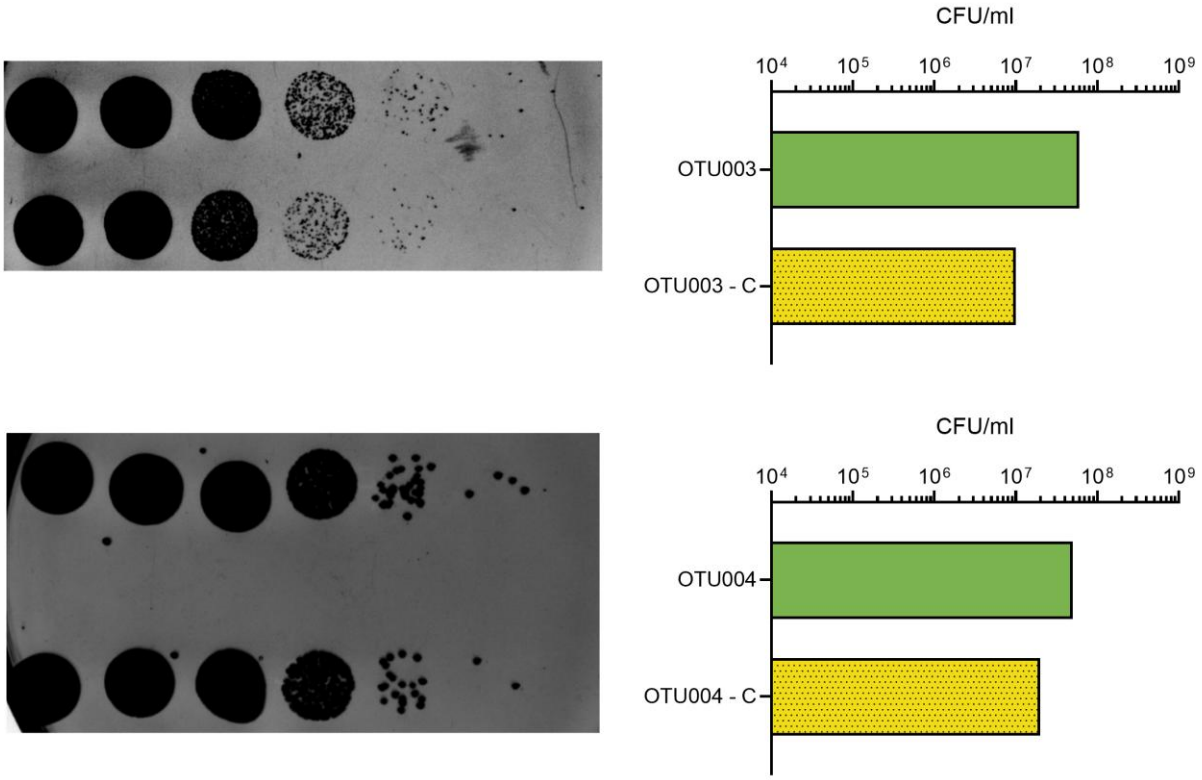


Figure 4.12. CFU counts demonstrating growth of OTU003 and OTU004 in petroleum-containing medium.

4.3.3. Whole Genome Sequencing Analysis

We obtained the complete genome sequences of four OTUs using shot-gun long-read sequencing on one of the Oxford Nanopore platforms. Total reads obtained during the sequencing event indicated that that we obtained the highest base count for OTU004 (2190.51 Mb) followed by OTU001 (1898.18 Mb), OTU002 (1602.12 Mb), and OTU003 (1219.26 Mb) (Figure 4.13). Complete genome of OTU001 aligned closely with *Pseudomonas sp.* P5_109, OTU002 with *Pseudomonas frederiksbergensis* strain YE17, OTU003 with *Pseudomonas sp.* FP198, and OTU004 with *Achromobacter sp.* SS2-2022 which verified their genetic potential for hydrocarbon degradation (Table 4.2). Phylogenetic analysis indicated that OTU001, OTU002, and OTU003 indicate close relationships with several Pseudomonas species. Specifically, OTU001 reveals 86.2% similarity to *Pseudomonas sp.* P5_109, OTU002 demonstrates 96.3% similarity to *Pseudomonas frederiksbergensis strain* YE17, and OTU003 presents 89.7% similarity to *Pseudomonas sp.* FP198. OTU004 showed a 90.1% similarity to *Achromobacter sp.* SS2-2022. According to these results, OTUs 1-3 are members of the *Pseudomonas* genus, which is well-known for its capability to break down a wide range of hydrocarbons, whereas OTU004 is a member of the *Achromobacter* genus, which is also known for its ability to break down complex aromatic hydrocarbons.

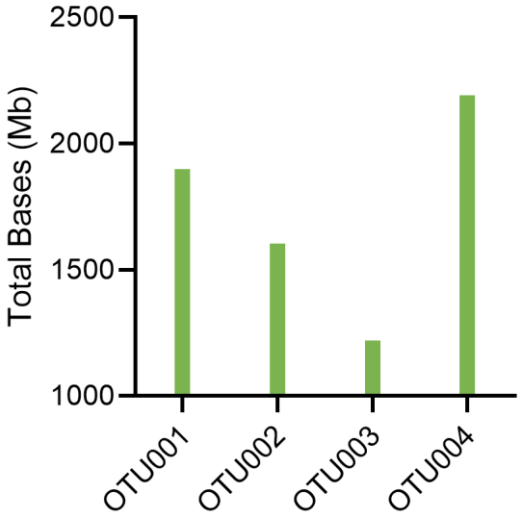


Figure 4.13. Total base counts per OTU derived from WGS analysis.

Table 4.2. Phylogenetic similarity and genetic potential for hydrocarbon degradation of OTUs based on WGS analysis.

Sample	**Read Number**	**Coverage (X)**	**Closest species**	**% Refseq alignment to closest species**	**Genome length (bp)**
OTU001	255.870	236X	*Pseudomonas sp. P5_109*	86.2%	6,246,338
OTU002	223.617	198X	*Pseudomonas frederiksbergensis* strain YE17	96.3%	6,481,867
OTU003	179.302	165X	*Pseudomonas sp.* FP198	89.7%	6,014,988
OTU004	281.127	279X	*Achromobacter sp.* SS2-2022	90.1%	6,448,060

The ability of *Pseudomonas* species to degrade hydrocarbons has been extensively reported in the literature. For instance, *Pseudomonas aeruginosa* AQNU-1, isolated from an oil-contaminated wetland, efficiently degraded 87–100% of n-alkanes (C_{13}–C_{35}), a significant component of crude oil, according to a study by Liu et al. (2022). The *alkB* genes, which code for the aliphatic hydrocarbon-degrading enzymes, were found to be crucial for this breakdown (Liu et al., 2022). Furthermore, it has been demonstrated that *Pseudomonas* species, including those that are closely related to OTU001,

OTU002, and OTU003, include alkane hydroxylase enzymes such *alkB1* and *alkB2*, which are essential for the biodegradation of n-alkanes (Zhao et al., 2018).

In relation to OTU004, it is well-known that certain species of *Achromobacter* are capable of degrading aromatic hydrocarbons. Mohammed et al. (2023) found that *Achromobacter sp.*, specifically *Achromobacter sp.* SS2-2022, exhibited substantial capabilities for crude oil degradation, as indicated by a significant decrease in the DCPIP (2,6-dichlorophenol indophenol) colorimetric assay, which provides a common indicator for hydrocarbon degradation. This further supports the potential of OTU004 in the breakdown of more complex, aromatic hydrocarbons commonly found in crude oil (Mohammed et al., 2023).

Two unique contigs were found during the WGS study of OTU001 (*Pseudomonas sp*. P5_109) and OTU003 (*Pseudomonas sp.* FP198), which did not align with the nearest reference strains. The OTU001 dataset contained the first unaligned contig with length of 349,094 bp This contig includes specific degradation genes like *dmp*, *xyl*, *ben*, *alk* and also gene clusters as T4SS, T4CP and Relaxase which is vital for bacterial conjugation for ICEs (Figure 4.14). The second contig, consisting of 68,773 base pairs, was found in the OTU003 dataset and contains gene clusters such as T4SS, T4CP, and Relaxase (Figure 4.15).

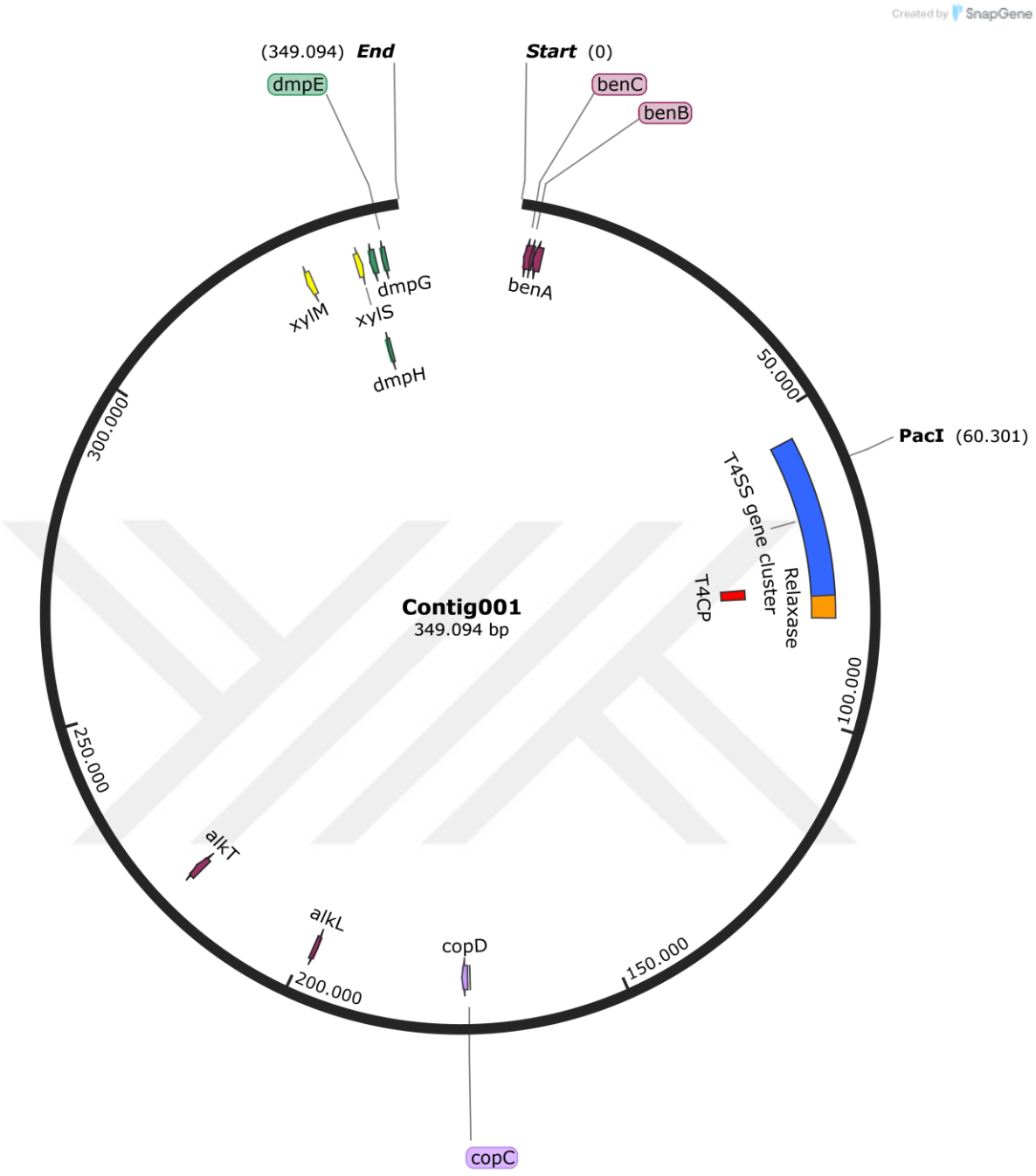


Figure 4.14. Unaligned contig of 349,094 bp identified in OTU001 whole genome sequence.

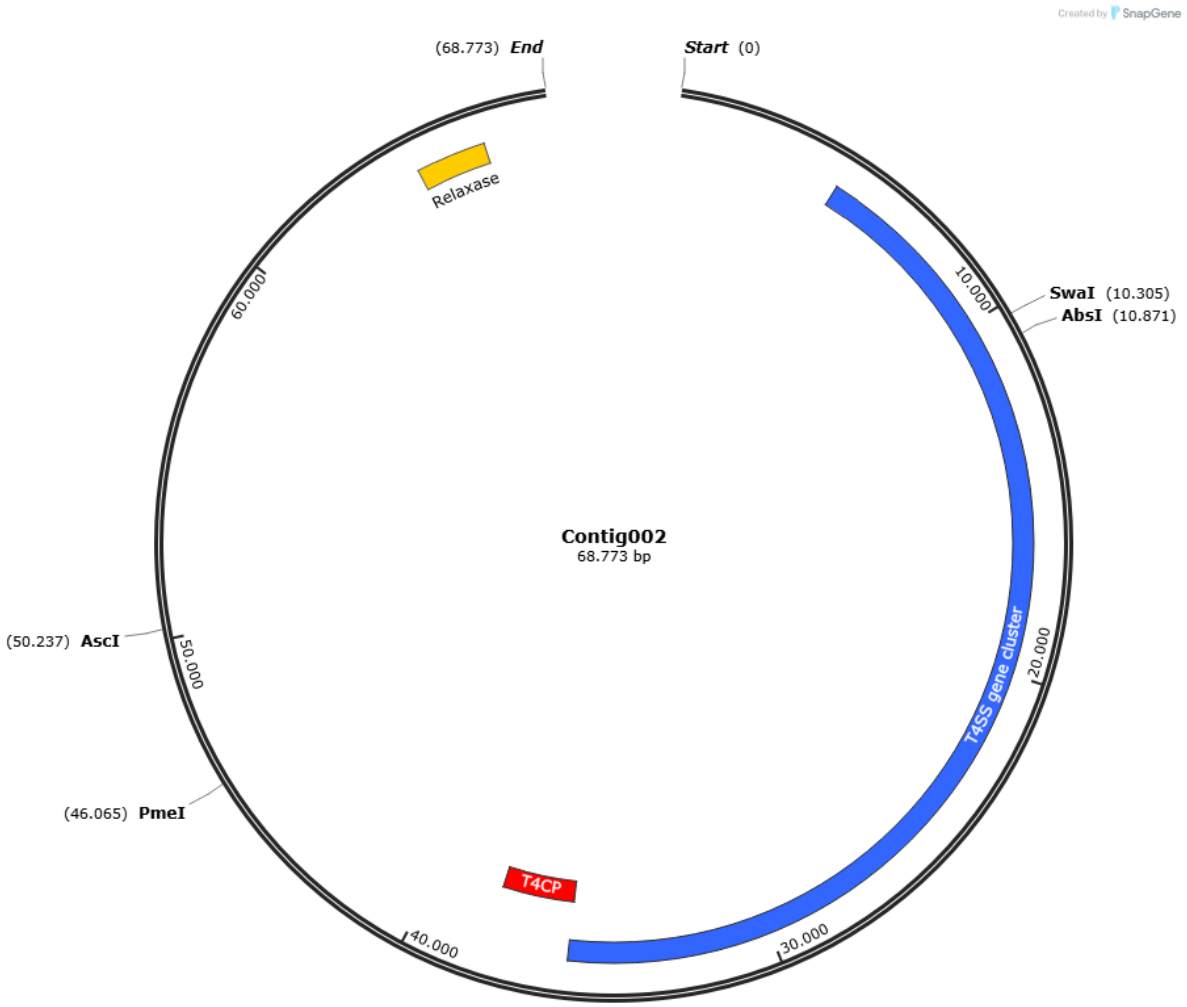


Figure 4.15. Unaligned contig of 68,773 bp identified in OTU003 whole genome sequence.

These unaligned contigs are particularly interesting since they might be distinct genomic regions not found in the mapping reference strains. Such contigs imply that OTU001 and OTU003 might have genes or genomic characteristics that are not present in the nearest known strains, which could point to new metabolic or functional capacities. These misaligned areas might contain distinct genes related to antibiotic resistance, hydrocarbon breakdown, or other environmental adaptations.

4.3.4. Subsystem-Based Functional Analysis of the Isolates' Complete Genomes

Subsystem-level functional profiling was performed for each of the four OTUs, with the analysis confined to (i) metabolic modules implicated in hydrocarbon catabolism and (ii) gene sets that may facilitate HGT.

Subsystem-level functional profiling of OTU001, visualized in the accompanying chord diagram (Figure 4.16), reveals a substantial genetic potential for aromatic-compound catabolism. Notably, the

benzoate major facilitator transporter *benK*, the *benABC*-operon transcriptional activator *benR*, and both α- and β-subunits of benzoate 1,2-dioxygenase are all present. Together, these determinants form a complete benzoate-degradation module, suggesting OTU001's capacity to funnel benzoate, other related aromatic hydrocarbons into central metabolism.

Key enzymes of the homogentisate route i.e. 4-hydroxyphenylpyruvate dioxygenase and aromatic-amino-acid aminotransferase, co-occur with catalytic nodes of the protocatechuate (β-ketoadipate) branch, especially β-ketoadipate enol-lactone hydrolase. Their combined presence confirms that OTU001 possesses an integrated aromatic-ring-cleavage system. In addition, p-hydroxybenzoate hydroxylase, which channels p-hydroxybenzoate into protocatechuate, provides an auxiliary entry point into this network (Figure 4.16).

In summary, SEED annotation of the OTU001 genome reveals a comprehensive suite of hydrocarbon-degrading enzymes that collectively suggest both alkane and aromatics catabolism. In particular, genes encoding alkane monooxygenase and associated rubredoxin/reductase components indicate the initial hydroxylation of straight-chain alkanes, while downstream ring-cleavage enzymes—such as catechol 1,2-dioxygenase and protocatechuate 3,4-dioxygenase—support further breakdown of aromatic moieties into central metabolic intermediates. Additional gene clusters for α-phenylalkanoic acid degradation, benzoate 1,2-dioxygenase, and naphthalene 1,2-dioxygenase further supports OTU001's capacity to mineralize complex hydrocarbons under aerobic conditions.

Moreover, the presence of multiple putative HGT elements suggests genomic plasticity that may facilitate rapid adaptation to hydrocarbon-contaminated environments. A complete type IV secretion system, together with several conjugative transfer proteins, implies potential for plasmid-mediated gene exchange. In parallel, phage packaging machinery and toxin–antitoxin replicon stabilization modules, along with transposase and integrase genes, point to active mobile genetic elements that could mobilize catabolic islands or resistance determinants. Taken together, these features indicate that OTU001 not only harbors the enzymatic toolkit for hydrocarbon degradation but also possesses HGT-associated loci that may accelerate the acquisition and dissemination of catabolic pathways in polluted habitats.

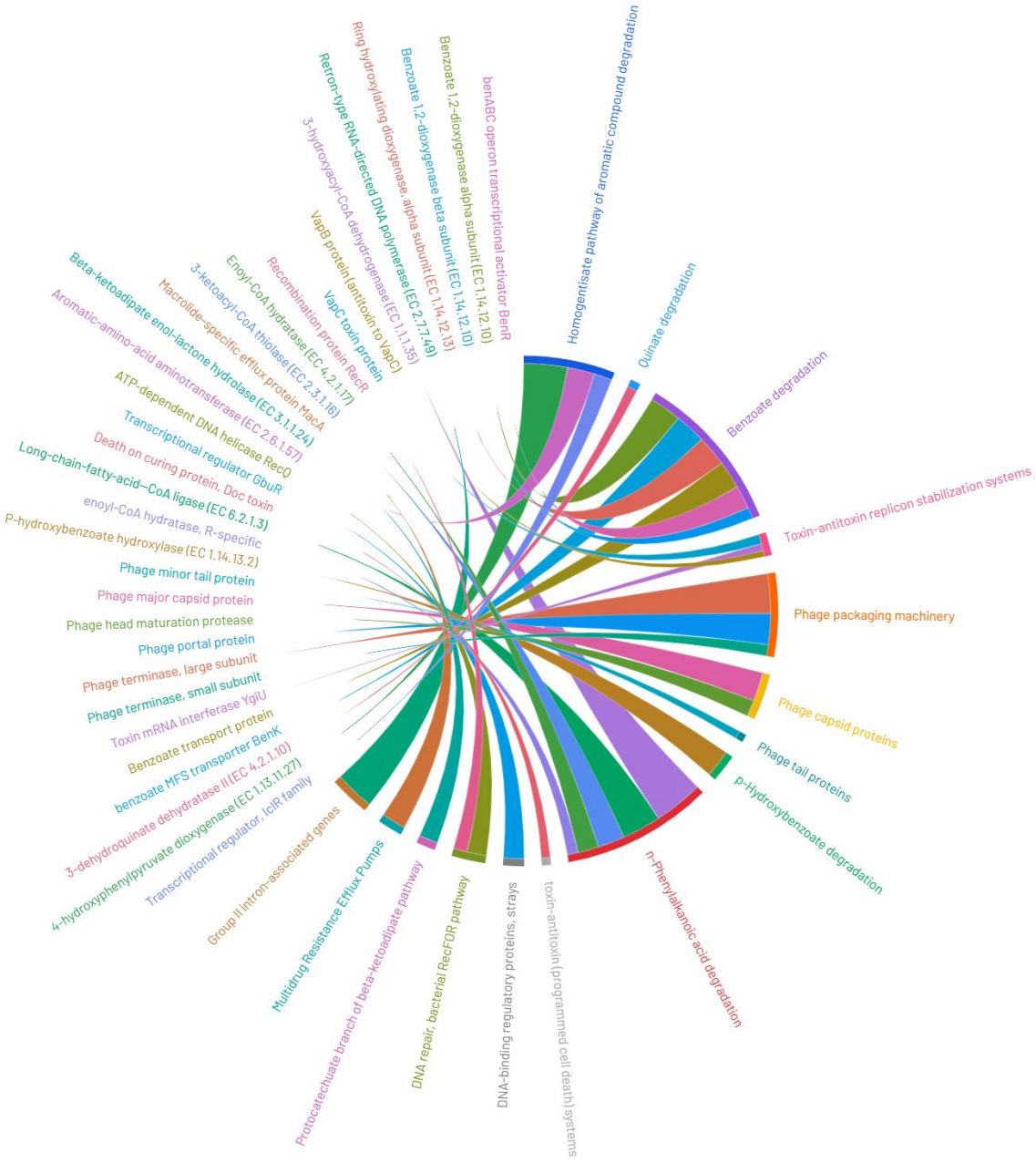


Figure 4.16. Circular SEED map of the OTU001 genome highlighting hydrocarbon degradation gene clusters and HGT elements.

The SEED annotation of the OTU002 genome reveals an array of enzymes dedicated to both aliphatic and aromatic hydrocarbon catabolism alongside several mobile genetic elements indicative of HGT potential (Figure 4.17). Key catabolic genes include naphthalene 1,2-dioxygenase (α-subunit) and 4-hydroxybenzoate 3-monooxygenase, which initiate the oxidation of PAHs; catechol 1,2-dioxygenase and protocatechuate 3,4-dioxygenase, which carry out ring-cleavage of aromatic intermediates; and omega-hydroxy fatty acid dehydrogenase combined with aryl-alcohol dehydrogenase, suggesting the oxidation of long-chain hydrocarbons and related alcohols. Additional enzymes—such as glutathione S-transferase and acetyl-CoA synthetase—support downstream

detoxification and central metabolism of hydrocarbon breakdown products. In parallel, multiple HGT-associated loci are interspersed throughout the genome: a phage integrase family protein signals prophage remnants, while conjugative transfer proteins (TraG), relaxases, and type IV pilus assembly components point to plasmid-mediated gene exchange. Together, these features indicate OTU002's robust capacity for hydrocarbon degradation in polluted environments and its genomic plasticity through HGT-mediated acquisition of adaptive traits.

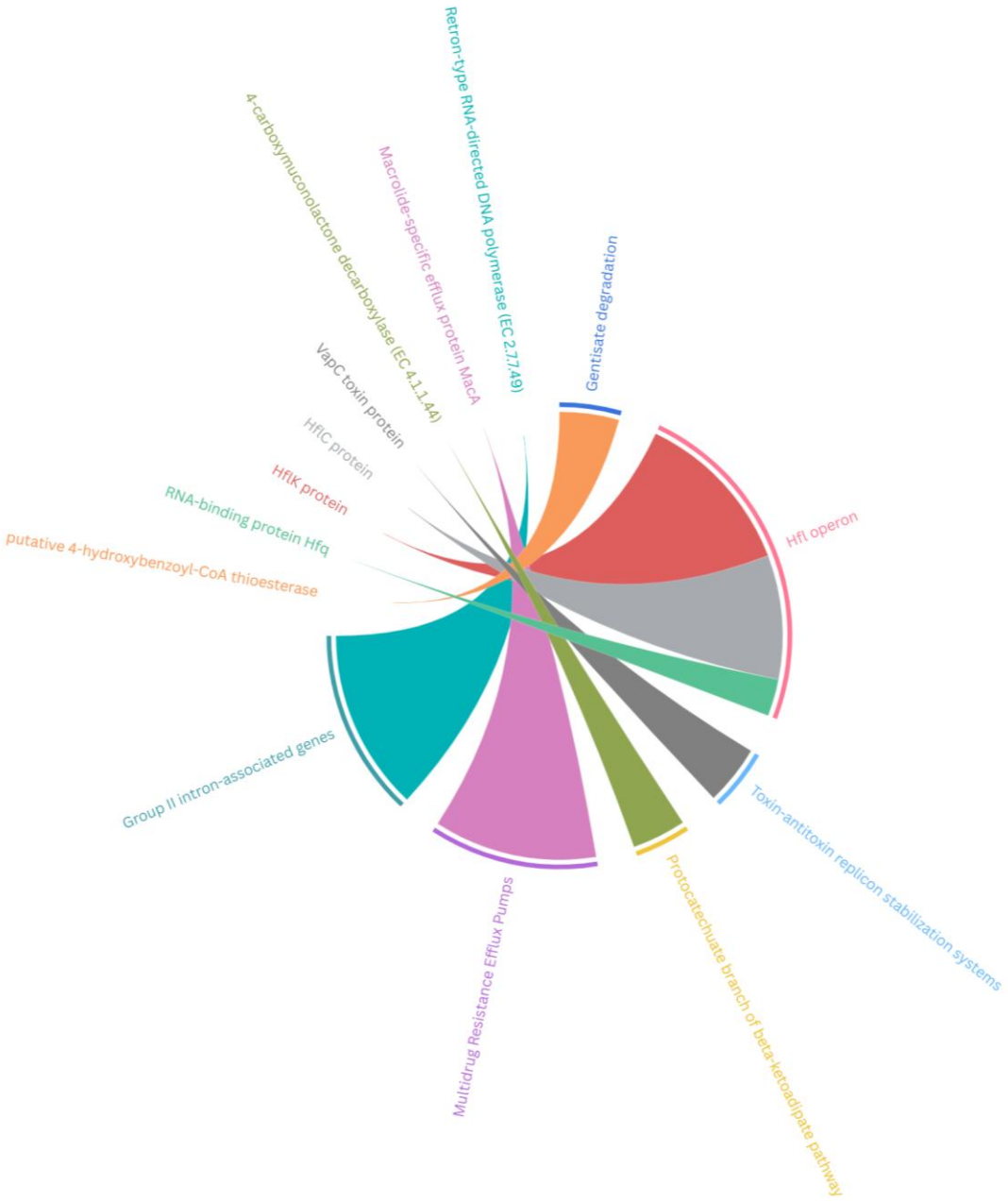


Figure 4.17. Circular SEED map of the OTU002 genome highlighting hydrocarbon degradation gene clusters and HGT elements.

The analysis of OTU003 (Figure 4.18) revealed the presence of a significant enzyme, 3-ketoacyl-CoA thiolase, which plays a crucial role in the degradation of n-phenylalkanoic acid. This enzyme is essential in fatty acid β-oxidation and significantly contributes to the integration of aromatic compounds into energy metabolism. Furthermore, the enzyme 3-dehydroquinate dehydratase II, which plays a role in the quinate degradation pathway, has been identified; this enzyme aids in the conversion of intermediate metabolites during the degradation of aromatic compounds. HGTs and the Retron-type RNA-guided DNA polymerase enzyme, which contributes to genetic diversity, along with the phage-associated DNA adenine methyltransferase, have also been identified. These enzymes contribute to maintaining genome stability and regulating MGEs. The data suggest that the OTU003 may have capable of degrading aromatic compounds and has genetic mechanisms for adaptation and defense. Furthermore, the possibility of HGT and the ability to adjust to environmental changes are highlighted.

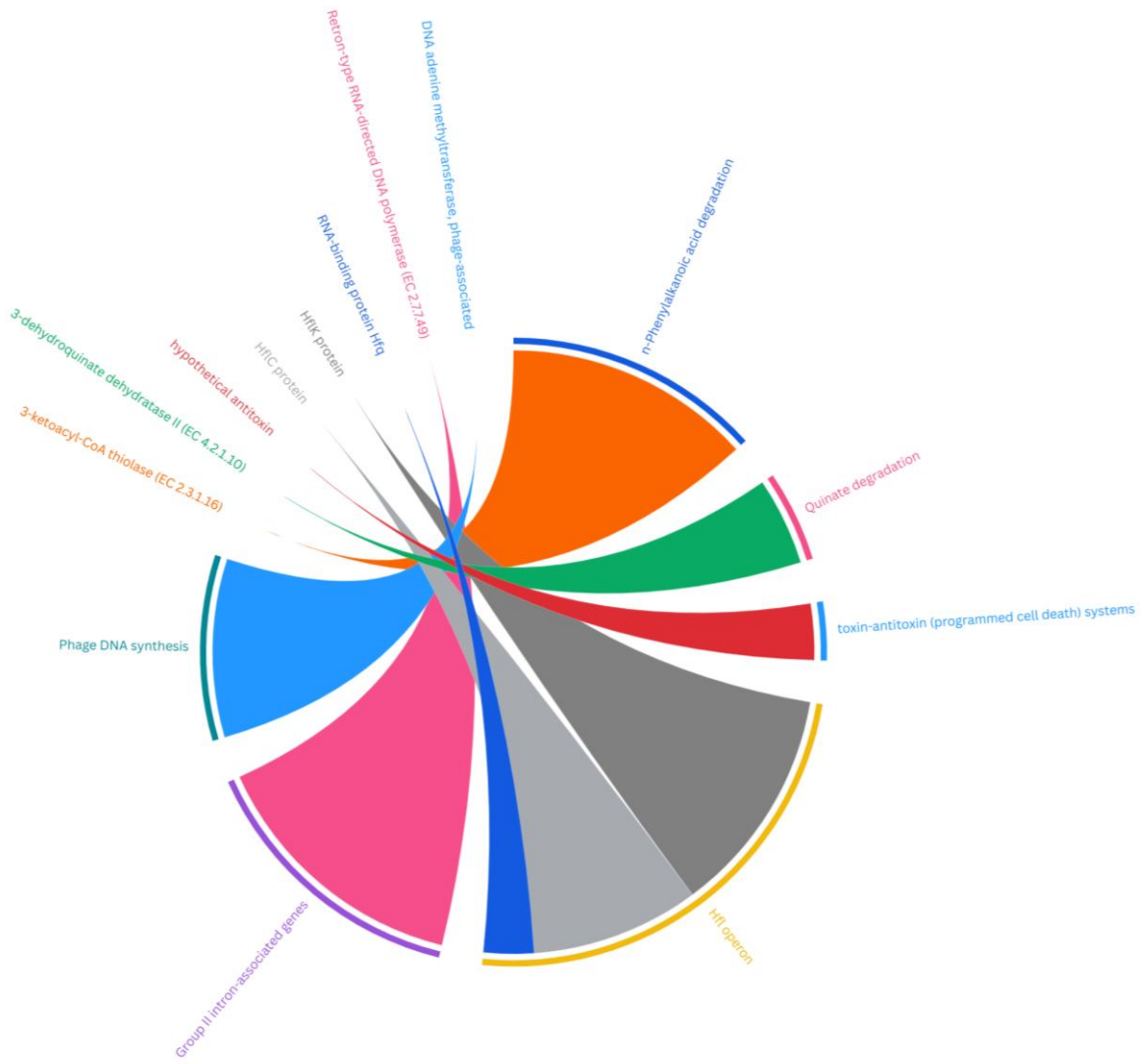


Figure 4.18. Circular SEED map of the OTU003 genome highlighting hydrocarbon degradation gene clusters and HGT elements.

The analysis of the OTU004 subsystem offers detailed insights into the metabolic and genetic adaptability of the microorganism (Figure 4.19). OTU004 possesses a gene set that is specifically centered on DNA repair mechanisms. The presence of RecFOR pathway proteins (*recO*, *recQ*, *recN*), the UvrABC excinuclease complex, MutL-MutS systems, and DNA topoisomerase III, along with numerous other DNA repair and recombination elements, highlights the essential role these components play in maintaining genetic stability and enhancing environmental stress resistance in this bacterium. The metabolism of aromatic compounds involves the IclR family transcriptional regulator, which governs the homogentisate pathway, as well as catechol branch enzymes such as muconate cycloisomerase and 3-oxoadipate CoA-transferase subunits. This suggests that OTU004 has a robust metabolic framework for the degradation of aromatic compounds. Key enzymes involved in benzoate degradation, especially ortho-halobenzoate 1,2-dioxygenase and the dioxygenase

subunits responsible for ring hydroxylation, indicate that OTU004 is capable of metabolizing a diverse array of aromatic compounds. The enzymes associated with the succinate module from propionate-CoA, including methylisocitrate lyase, 2-methylcitrate synthase, 2-methylcitrate dehydratase, and propionate-CoA ligase, play a crucial role in energy metabolism and carbon flow, thereby enhancing the metabolic flexibility of OTU004, alongside their functions in DNA repair and metabolism.

This detailed subsystem and role distribution illustrate that OTU004 has advanced abilities in the degradation of aromatic hydrocarbons, the preservation of genetic material, and adaptation to environmental stresses. The results obtained demonstrate the functional role of OTU004 within the ecosystem and its significance for potential biotechnological applications (Figure 4.19).

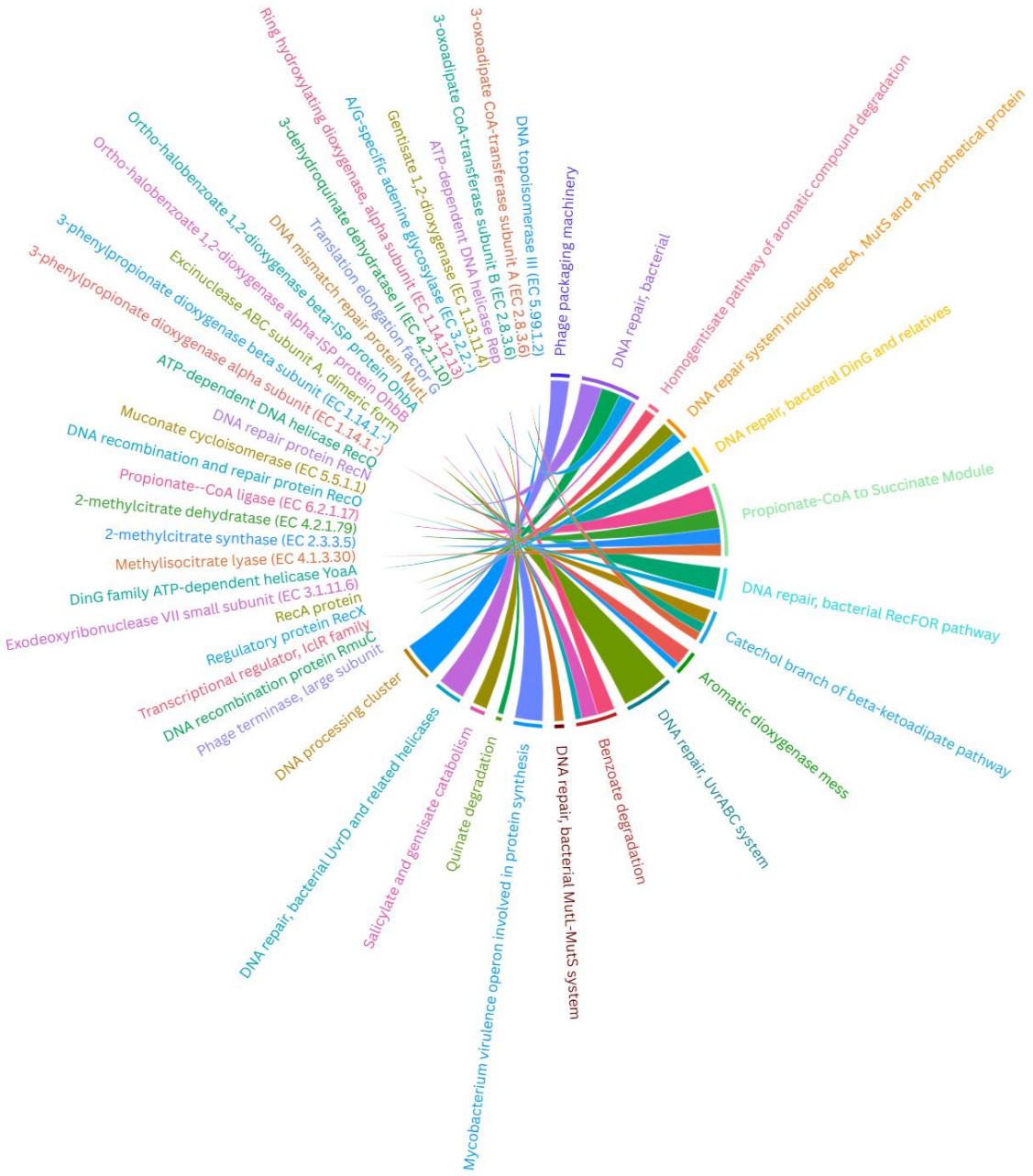


Figure 4.19. Circular SEED map of the OTU004 genome highlighting hydrocarbon degradation gene clusters and HGT elements.

4.3.5. Evaluating Functional Genes Related to Hydrocarbon Degradation in PEC Isolates

The results from the gene annotation using the HADEG database (Rojas-Vargas et al., 2023) provide insights into the potential for hydrocarbon degradation in four OTUs. Several genes known for their involvement in alkane and aromatic degradation were identified, highlighted with green, with their presence varying across the OTUs (Figure 4.20).

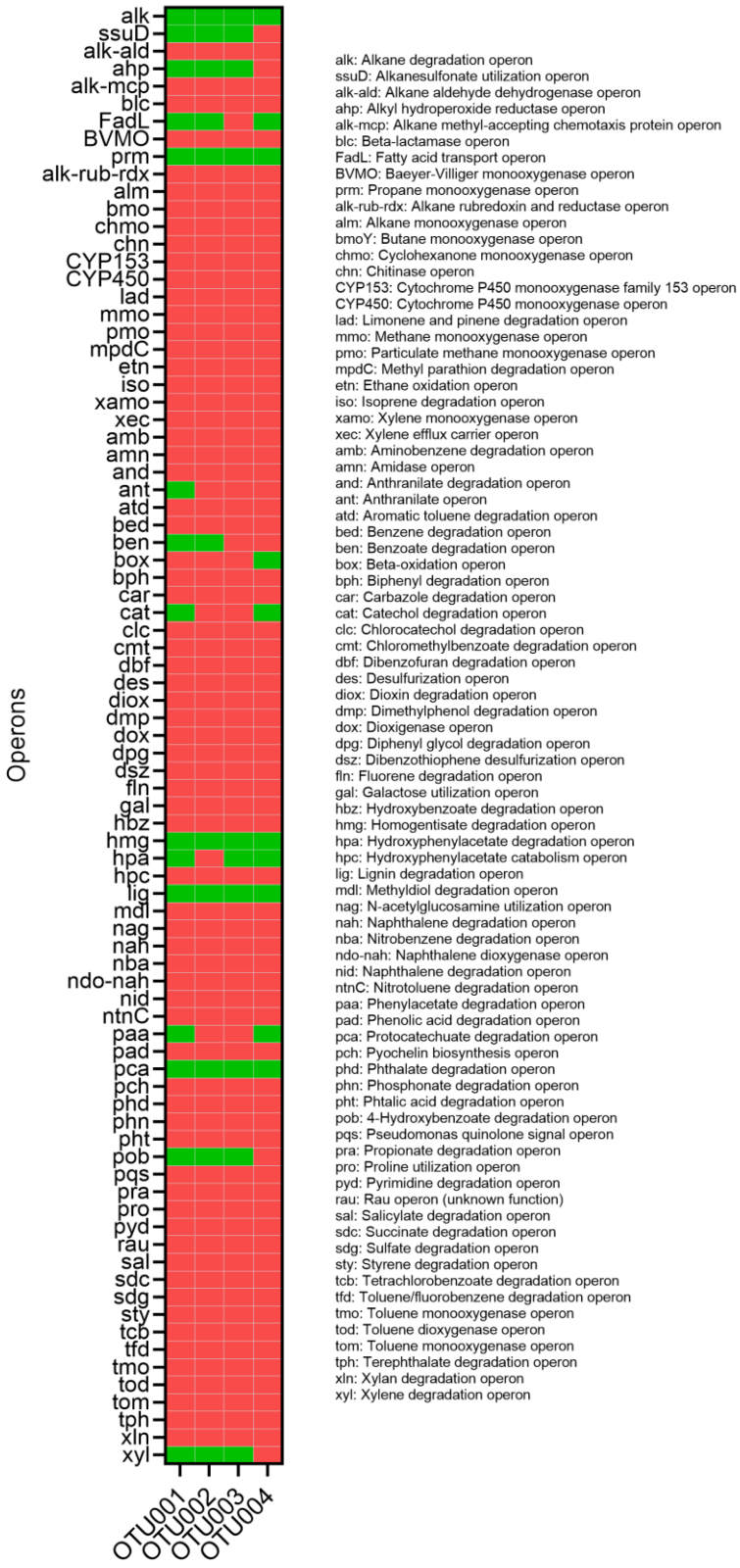


Figure 4.20. Heatmap of alkane and aromatic hydrocarbon degradation operons across OTU001–OTU004 genomes, annotated using the HADEG database.

The *fadL* gene, which encodes a transporter protein involved in the uptake of long-chain alkanes, was identified in OTU001, OTU002, and OTU004. This gene plays a key role in the early stages of the alkane degradation pathway by enabling the passage of hydrophobic alkanes across the outer membrane. Previous work by Somee et al. (2022) highlighted the importance of *fadL* in hydrocarbon uptake, which is essential for downstream degradation by enzymes such as alkane hydroxylases. The detection of *fadL* in these OTUs suggests that they possess the metabolic potential to utilize aliphatic hydrocarbons as a carbon and energy source.

The *alkB* gene, encoding alkane hydroxylase, plays a central role in the initial step of alkane degradation by catalyzing the conversion of alkanes to alcohols, thereby enabling further biodegradation. It is considered a key genetic determinant in the bioremediation of PHC-contaminated environments, as it mediates the oxidative breakdown of long-chain alkanes. Shahi et al. (2017) reported that *alkB* is widely distributed across bacterial populations in oil-contaminated soils, with some strains carrying multiple copies, potentially enhancing their capacity for alkane degradation. Similarly, Somee et al. (2022) showed that *alkB* is broadly present among members of Gammaproteobacteria and other taxonomic groups, further supporting its central role in aliphatic hydrocarbon metabolism. The degradation of *n*-alkanes, a major fraction of crude oil, has been closely linked to *alkB*-harboring bacteria, including genera such as *Pseudomonas*, *Burkholderia*, and *Acinetobacter*. The widespread occurrence of this gene across diverse taxa highlights its ecological relevance in microbial crude oil degradation and natural attenuation processes in polluted environments.

The *prmA*, *prmB*, and *prmC* gene cluster, detected in all four OTUs, is involved in the degradation of aliphatic hydrocarbons through the oxidation of alkyl chains. Their consistent presence indicates a shared metabolic capacity among these OTUs for utilizing saturated hydrocarbons under aerobic conditions. These genes are commonly found in hydrocarbon-degrading microbial communities, particularly in oxygen-rich environments. The functional relevance of this cluster extends beyond alkane metabolism; for instance, *Mycobacterium vaccae* JOB5 employs the *prmABCD* operon, which encodes a propane monooxygenase, in the breakdown of methyl tert-butyl ether (MTBE), a synthetic contaminant (Chen et al., 2023). The broad substrate range of PRM enzymes underscores the ecological importance of the *prm* genes in both natural and anthropogenic hydrocarbon degradation pathways, reinforcing their role in microbial bioremediation.

The *antA*, *antB*, and *antC* gene cluster found in OTU001 plays a role in the degradation of aromatic hydrocarbons, particularly through the catabolism of anthranilate. The genes involved in

this pathway initiate the degradation of anthranilate by catalyzing its conversion to catechol, which is subsequently further degraded via the β-ketoadipate pathway. The *antA*, *antB*, and *antC* gene cluster exhibits functional similarities to the benzoate degradation pathway found in *Acinetobacter sp.* strain ADP1. Bundy et al. (1998) illustrated that the conversion of anthranilate to catechol in *Acinetobacter* represents a critical step in the catabolism of aromatic compounds. This process is a component of the broader category of multicomponent dioxygenases that facilitate the hydroxylation of aromatic compounds. The *antA*, *antB*, and *antC* genes, encoding enzymes involved in the meta-cleavage of aromatic rings, are central to the aerobic degradation of recalcitrant aromatic hydrocarbons such as naphthalene. These compounds, commonly found in crude oil, require specialized pathways for effective breakdown. The detection of the *ant* gene cluster in OTU001 suggests that this taxon is equipped to degrade aromatic substrates including anthranilate and naphthalene. This capability points to a broader metabolic potential for processing complex petroleum-derived hydrocarbons, reinforcing the ecological role of OTU001 in hydrocarbon-contaminated environments.

The aerobic breakdown of benzoate, a significant aromatic chemical frequently derived from petroleum, is facilitated by the *benA*, *benB*, and *benC* genes found in OTU001 and OTU002. The genes encode enzymes essential for the initial stages of benzoate degradation, a significant intermediate in the breakdown of aromatic hydrocarbons. Notably, studies on the micro aerobic enriched strain *Rhodococcus qingshengii* GOMB7 demonstrate the functional significance of the *benA*, *benB*, and *benC* genes in the *catABC-benABCDE* clusters, which are involved in the breakdown of benzoate (Juarez et al., 2023). This strain's genome contains the *benABCDE* operon, which is highly versatile in aromatic chemical catabolism; it can breakdown long-chain alkanes. Similar to the findings of Ezezika et al. (2006), who revealed how regulatory processes involving transcriptional regulators like *benM* and *catM* govern the expression of the *benA* gene in *Acinetobacter baylyi* ADP1, the study likewise emphasizes the importance of *benA* in initiating benzoate catabolism. The identification of these genes in OTU001 and OTU002 indicates their potential role in the microbial degradation of petroleum-derived aromatic hydrocarbons, thereby improving the prospects for bioremediation in hydrocarbon-contaminated settings. Furthermore, from OTU001's dataset, the *benA* and *benA* genes were found in a contig known as Contig001 (Figure 4.14). Within the analyzed contig, genes critical for the degradation of aromatic hydrocarbons and aliphatic compounds have been identified. Especially, the *xylM* and *xylS* genes are known as important regulatory and enzyme-coding genes involved in xylene metabolism. Additionally, the *alkL* and *alkT* genes code for proteins involved in alkane oxidation and are functionally important in the biotransformation of hydrocarbons. The *dmpH*, *dmpG* and *dmpE* genes found in the contig belong to the dmp (dimethylphenol) operon,

which is responsible for the degradation of phenolic compounds and plays critical roles in the mineralization of complex aromatic compounds.

The *boxA*, *boxB*, and *boxC* gene cluster, identified in OTU004, is involved in the aerobic degradation of aromatic hydrocarbons, particularly benzoate and its derivatives. This cluster mediates the initial dioxygenation and ring-cleavage steps of the benzoate degradation pathway, ultimately leading to the mineralization of petroleum-derived aromatics. The detection of *box* genes in OTU004 suggests a specialized catabolic route for aromatic compounds, which is particularly relevant in marine environments frequently impacted by oil contamination. Rojas-Vargas et al. (2024) highlighted the *box* cluster as a key genetic marker for aromatic hydrocarbon degradation in such ecosystems. Additionally, the presence of *catB* and *catC* genes across multiple OTUs indicates the capacity for meta-cleavage of catecholic intermediates, further supporting the potential of these microbial groups in the oxidative breakdown of complex aromatic pollutants. The combined presence of these functional genes underscores the ecological relevance of the studied OTUs in the bioremediation of aromatic hydrocarbons in oil-impacted environments.

In conclusion, the analysis of the gene content of the four OTUs provides strong evidence that these microbes harbor a diverse set of genes involved in the degradation of both aliphatic and aromatic hydrocarbons. This ability positions them as potential candidates for bioremediation in environments contaminated with petroleum-based hydrocarbons. The presence of key genes such as *fadL*, *alkB*, *prmA*, *prmB*, *prmC*, *antA*, *benA*, *benB*, and *boxA* supports the hypothesis that these OTUs can efficiently degrade a wide range of hydrocarbons, making them highly valuable for environmental applications. Future studies should aim to further explore the metabolic pathways and the regulation of these genes to better understand their ecological roles in hydrocarbon-degrading communities.

4.4. Determination of Surfactant Tolerance Levels: MIC Analysis of Selected Strains

The growth-inhibition profiles of six surfactants as CTAB, DDAC, BDAC, SDS, Tween-20, and Triton X-100 are presented. For each compound, OD_predicted curves (blue lines) and OD_measured points (red markers) are displayed, and surfactant effects have been classified as either inhibitory or non-inhibitory toward the PEC culture. Graphical depictions for each surfactant are provided in Figure 4.21, with accompanying annotations denoting the absence or presence of microbial growth suppression. For each result, the strong correlation between measured and predicted values validates the dose–response model.

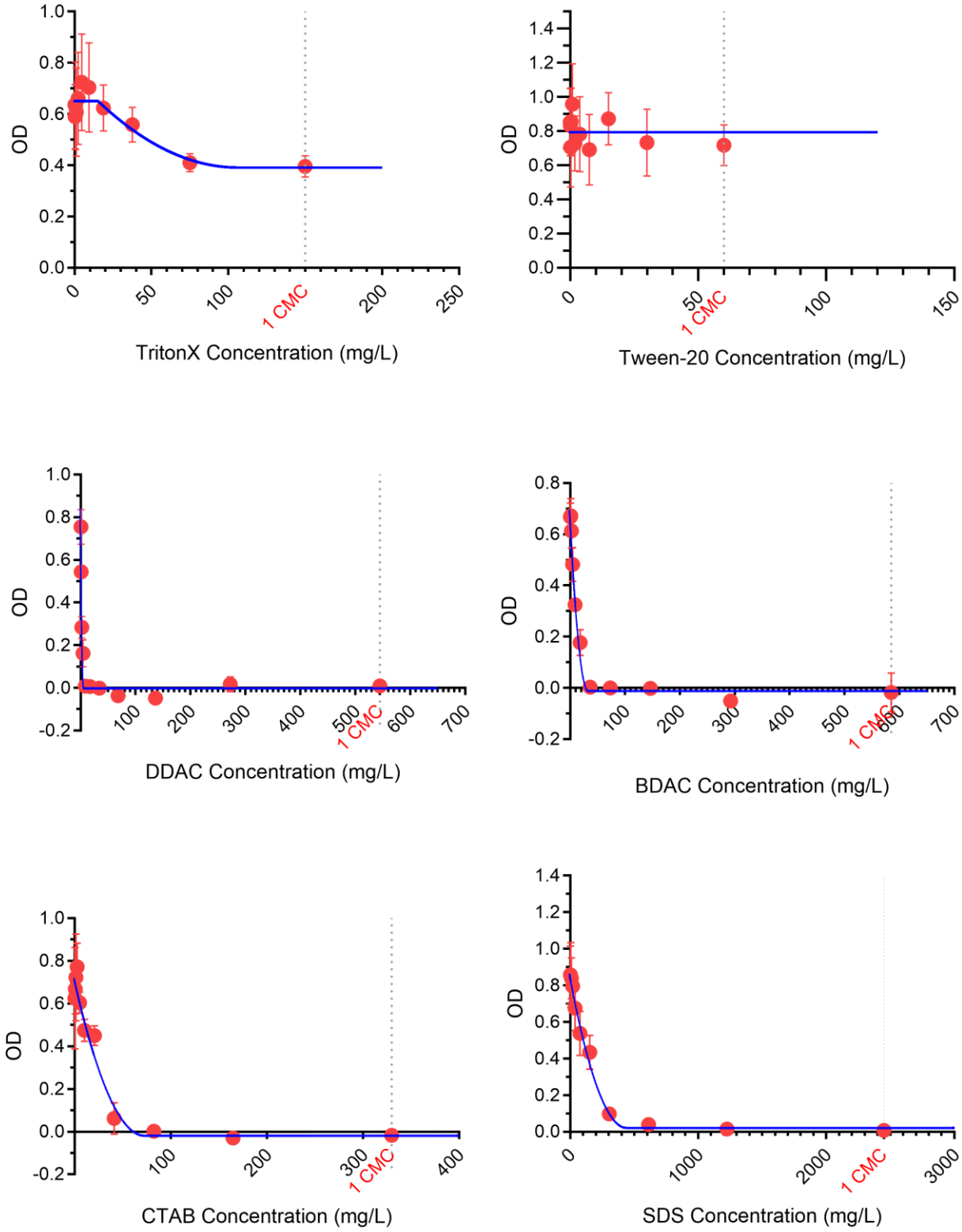


Figure 4.21. Growth-inhibition profiles of six surfactants (CTAB, DDAC, BDAC, SDS, Tween-20, and Triton X-100) on PEC culture. Predicted optical density (OD_predicted, blue lines) and measured optical density (OD_measured, red markers) are shown with annotations indicating presence or absence of microbial growth suppression.

For Triton X-100, microbial growth appeared unaffected across the tested concentration range. At the initial concentration of 0.146 mg/L, the OD was 0.637, which decreased to 0.396 ± 0.041 at 1 CMC (150 mg/L) and remained stable at higher concentrations. The observed plateau in both measured and predicted OD values suggests that TritonX-100 did not inhibit microbial growth. In the case of Tween-20, the lowest concentration tested (0.059 mg/L) yielded a mean OD of 0.852 ± 0.197, decreasing slightly to 0.718 ± 0.119 at 1 CMC (60 mg/L). The predicted OD curve remained nearly flat across concentrations, indicating minimal to no inhibitory effect by Tween-20.

In contrast, SDS demonstrated strong inhibitory activity. At 2.393 mg/L, the mean OD was 0.858 ± 0.197, which dropped sharply to 0.007 ± 0.157 at 1 CMC (2450 mg/L), suggesting near-complete suppression of microbial growth. Similarly, BDAC caused a substantial decline in OD, from 0.668 ± 0.054 at 0.571 mg/L to -0.018 ± 0.076 at 1 CMC (585 mg/L). Complete growth inhibition was observed at 36.563 mg/L, well below its CMC.

For DDAC, the OD decreased from 0.755 ± 0.081 at 0.532 mg/L to 0.009 ± 0.016 at 1 CMC (545 mg/L). A pronounced drop in OD occurred between 4.258 mg/L and 8.516 mg/L, indicating significant inhibitory effects at sub-CMC levels. CTAB also exhibited strong antimicrobial activity, with OD values falling from 0.625 ± 0.237 at 0.322 mg/L to -0.017 ± 0.022 at 1 CMC (330 mg/L). These results indicate that CTAB effectively suppresses microbial growth at concentrations well below its CMC.

In summary, Triton X-100 and Tween-20 exhibited no measurable MIC within the tested range, whereas the MICs of SDS, BDAC, DDAC, and CTAB were determined to be 446 mg/L, 33.9 mg/L, 6.24 mg/L, and 73.5 mg/L, respectively. These correspond to CMC values of 0.182 mg/L, 0.581 mg/L, 0.0114 mg/L, and 0.223 mg/L, as shown in Table 4.3. Based on these results, further studies will focus on Tween-20 and Triton X-100, which did not inhibit microbial growth, for potential applications in subsequent stages of research.

Table 4.3. MICs and CMCs of six surfactants tested against PEC culture

Surfactant	MIC	CMC
TX	-	-
TW	-	-
SDS	446.19	0.18
BDAC	33.97	0.58
DDAC	6.24	0,01
CTAB	73.49	0,22

4.5. Petroleum Biodegradation in the Presence of Surfactants

The crude oil degradation assay was conducted to assess the performance of the PEC in the presence of surfactants, focusing on the impact of surfactants on the efficiency of oil biodegradation. Four experimental conditions were established: crude oil alone, surfactant alone, a combination of crude oil and surfactant, and a PEC control. These systems were incubated under identical conditions, with microbial activity monitored daily through total plate counting to track growth and degradation dynamics. At the end of the experiment, TPH concentrations in the crude oil–sand mixtures were quantified to evaluate the extent of oil degradation. This assay aimed to determine whether surfactants enhance or inhibit the crude oil biodegradation capacity of the PEC culture, thereby contributing to the understanding of their role in bioremediation strategies.

4.5.1. Growth of PEC Cultures on Crude Oil in the Presence of Surfactants

Throughout the incubation period, no significant microbial growth was observed in the Tween-20 only group, which lacked both the PEC culture and crude oil, confirming the absence of contamination and the necessity of the inoculum for microbial proliferation. Among all conditions, the PEC + Crude Oil + TW group exhibited the highest microbial growth, starting from 1.2×10^5 CFU/mL on day 0 and rapidly increasing to 1.1×10^8 CFU/mL by day 4 (Figure 4.22). This marked increase is attributed to the biodegradation of crude oil, with Tween-20 enhancing microbial access to hydrophobic substrates and thereby facilitating the process. The PEC + Crude Oil group, which did not contain any surfactant, showed moderate growth, reaching 5.0×10^7 CFU/mL by day 4, indicating that crude oil alone supports microbial proliferation, albeit less efficiently (Figure 4.24). The PEC-only group, serving as a negative control without crude oil or surfactant, exhibited minimal growth, underscoring the importance of complex carbon sources and surfactant-mediated substrate availability. In the PEC + TW group, where Tween-20 was present in the absence of crude oil,

microbial growth was observed but at a lower rate, increasing from 1.1 × 10^5 to 4.7 × 10^7 CFU/mL by day 4 (Figure 4.24). While not as robust as in the presence of crude oil, this growth indicates that Tween-20 alone supports microbial proliferation, possibly by serving as a co-substrate or enhancing nutrient solubilization. Overall, these findings highlight the synergistic effect of crude oil and surfactants in promoting microbial activity, with the PEC + Crude Oil + TW condition demonstrating the highest biodegradation potential due to improved hydrocarbon accessibility and metabolic stimulation.

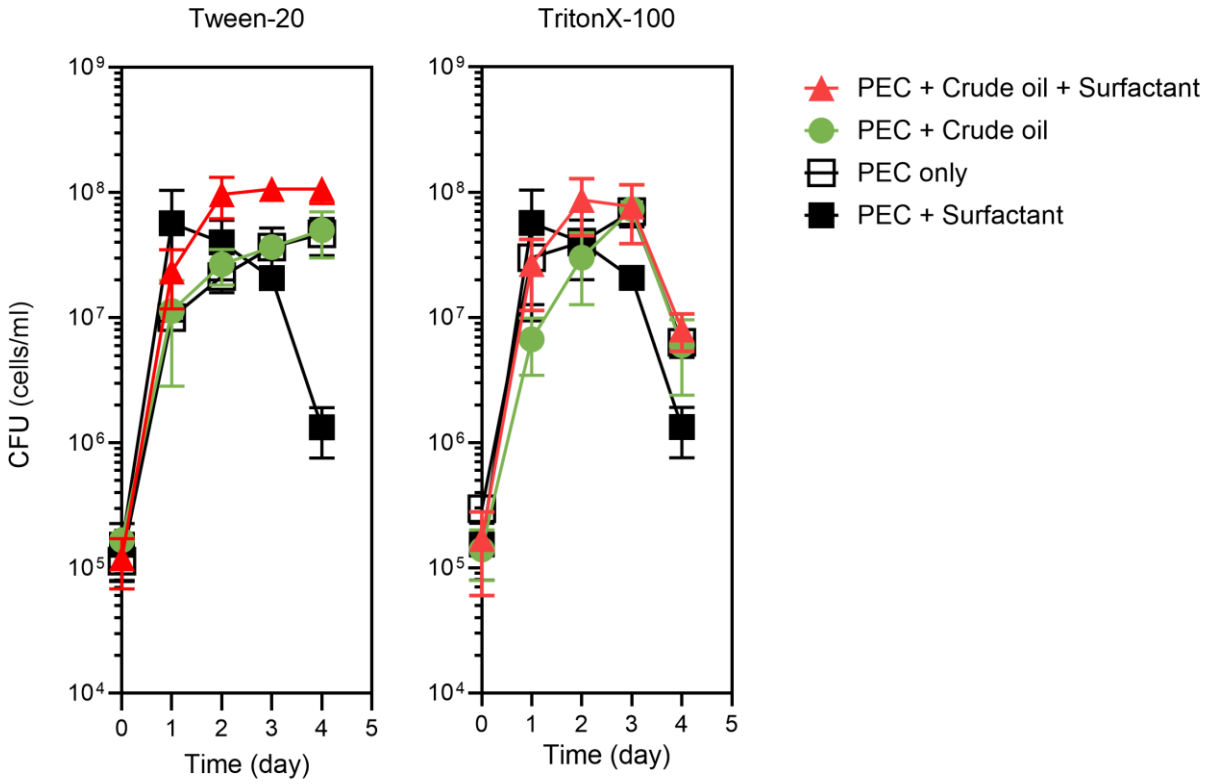


Figure 4.22. CFU counts demonstrating microbial growth in the presence of Tween-20 and TritonX-100 respectively.

The PEC + Crude Oil + TX group exhibited the most pronounced microbial growth among all tested conditions (Figure 4.22). Starting at 1.7 × 10^7 CFU/mL on day 0, the population increased rapidly to 7.7 × 10^7 CFU/mL by day 3, before declining to 8.0 × 10^6 CFU/mL on day 4. The PEC + Crude Oil group showed moderate growth, reaching a maximum of 5.0 × 10^7 CFU/mL on day 4 (Figure 4.24). In contrast, the PEC-only group demonstrated minimal growth, increasing from 1.5 × 10^5 to 5.7 × 10^7 CFU/mL by day 1, followed by a notable decline to 2.0 × 10^7 CFU/mL by day 4. The PEC + TX group, which contained Triton X-100 but no crude oil, showed slower growth, rising from 2.9 × 10^5 to 6.3 × 10^6 CFU/mL over four days (Figure 4.24). The TX-only group, lacking both PEC

and crude oil, displayed no microbial growth throughout the incubation period, confirming the necessity of inoculum and ruling out contamination. The sharp contrast in growth between the PEC + Crude Oil + TX and PEC + TX groups highlights the role of Triton X-100 in enhancing microbial access to hydrocarbons, thereby facilitating crude oil degradation without exhibiting toxic effects. Furthermore, the similar growth trends observed in the PEC-only and PEC + TX groups suggest that the surfactant does not inhibit microbial proliferation. Instead, its presence in the PEC + TX condition supports a modest increase in cell numbers, implying that Triton X-100 is bio-compatible and potentially involved in improving substrate availability during the biodegradation process.

4.5.2. Evaluation of TPH Degradation in the Presence of Surfactants

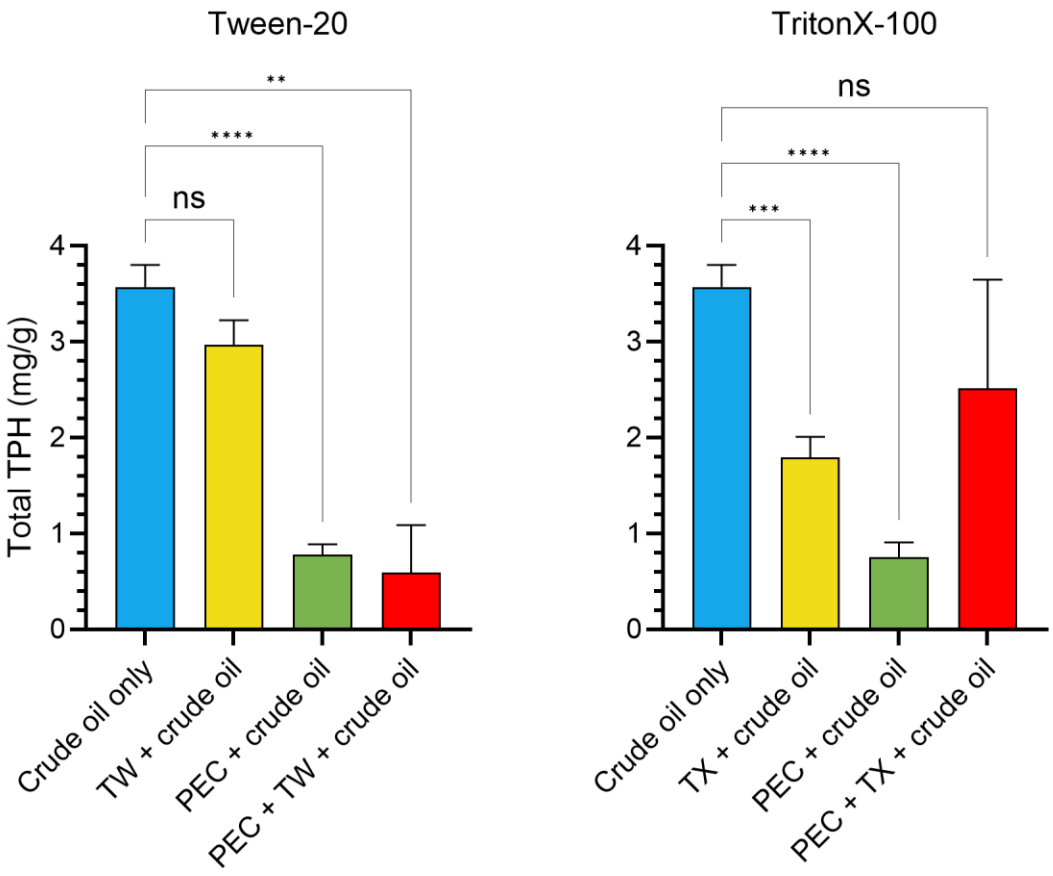


Figure 4.23. TPH biodegradation efficiency for Tween-20 and Triton X-100 amended PEC.

The residual TPH in the control group including crude oil only (blue column) during the surfactant biodegradation experiment for Tween-20 was measured at 3.66 ± 0.18 mg/g. The addition of TW alone (yellow column) resulted in a TPH reduction to 2.97 ± 0.25 mg/g; however, this reduction was not statistically significant (ns). Treatment with the PEC alone (green column) resulted

in a decline of TPH to 0.78 ± 0.11 mg/g, indicating a statistically significant decrease compared to the control ($p < 0.0001$, ****). The combined PEC + TW treatment (red column) resulted in the lowest residual TPH of 0.59 ± 0.50 mg/g, which was significantly lower than the control ($p < 0.01$, **). The results suggest that PEC is the primary factor in hydrocarbon removal, while Tween-20 alone does not significantly enhance biodegradation and provides only a minor advantage when used in combined with PEC (Figure 4.23).

The control group (blue column) that only had crude oil in the surfactant biodegradation experiment for TritonX-100 had residual TPH measured at 3.65 ± 0.17 mg/g. TPH was considerably reduced to 1.79 ± 0.22 mg/g when TX alone (yellow column) was used ($p < 0.001$, ***). A further decrease to 0.75 ± 0.16 mg/g was observed with PEC alone (green column) ($p < 0.0001$, ****). The PEC + TX combination (red column) produced a yield of 2.52 ± 1.13 mg/g, which did not show a significant difference compared to the crude-oil control (ns) (Figure 4.23). It can be proposed that while Triton X-100 alone may enhance biodegradation by increasing hydrocarbon solubilization, its simultaneous application with PEC may diminish the degradation effectiveness of PEC.

These findings suggest that the microbial consortium is crucial for effective TPH remediation, and that the selection of surfactant and its compatibility with PEC may significantly affect overall treatment performance.

4.6. Comprehensive Analysis of Crude Oil Degradation: Microbial Growth, TPH Degradation, and Gene Expression Response to Surfactants

4.6.1. Effect of Surfactants on Microbial Growth on Crude Oil

The PEC-only group, containing the enrichment culture in M9 mineral medium without surfactants or crude oil-sand mixture, began with an initial population of approximately 3.0×10^6 CFU/mL on day 0 and reached 1.7×10^7 CFU/mL by day 4. This modest increase indicates that the PEC culture can support limited microbial growth in minimal medium; however, in the absence of complex carbon sources such as crude oil or surfactants, growth remains constrained. Among all tested conditions, the PEC-only group exhibited the lowest level of microbial proliferation, underscoring the necessity of additional substrates or surfactants to enhance biodegradation activity (Figure 4.24).

The PEC + Crude Oil group, composed of the PEC culture and a crude oil–sand mixture without added surfactant, exhibited greater microbial growth compared to the PEC-only group. The population increased from 5.3×10^6 CFU/mL on day 0 to a peak of 6.0×10^7 CFU/mL by day 3. This result suggests that the presence of crude oil significantly enhances microbial proliferation, indicating its role as an effective carbon source when utilized by the PEC culture under the given experimental conditions (Figure 4.24).

The PEC + Crude Oil + TX group, incorporating Triton X-100 as the surfactant, displayed the most rapid initial microbial growth among all tested conditions. The population increased from 1.0×10^7 CFU/mL on day 0 to 4.3×10^7 CFU/mL by day 2, and then stabilized at 4.0×10^7 CFU/mL by day 4. This growth pattern indicates that Triton X-100 enhances the bioavailability of hydrocarbons in the crude oil–sand mixture, facilitating accelerated microbial proliferation and crude oil degradation. The observed plateau after day 2 suggests that while Triton X-100 promotes early-stage growth, microbial activity levels off as accessible hydrocarbons become partially depleted (Figure 4.24).

The PEC + Crude Oil + TW group, using Tween-20 as the surfactant, demonstrated a more gradual increase in microbial growth compared to the Triton X-100 condition. Starting at 2.7×10^6 CFU/mL on day 0, the population steadily increased to 8.0×10^7 CFU/mL by day 4. While the growth rate was slower than that observed with Triton X-100, the PEC + Crude Oil + TW group ultimately reached the highest cell density among all groups by the end of the experiment. These results suggest that Tween-20 effectively supports microbial proliferation over a longer period, potentially by sustaining substrate accessibility throughout the incubation period (Figure 4.24).

The data indicate that surfactants markedly improve microbial growth and the degradation of crude oil. TritonX-100 enhances microbial growth in the initial stages, whereas Tween-20 facilitates more stable growth over time, achieving the highest CFU count by day 4. This indicates that TritonX-100 is more effective in facilitating initial biodegradation, whereas Tween-20 stimulates more sustainable microbial growth throughout the experiment.

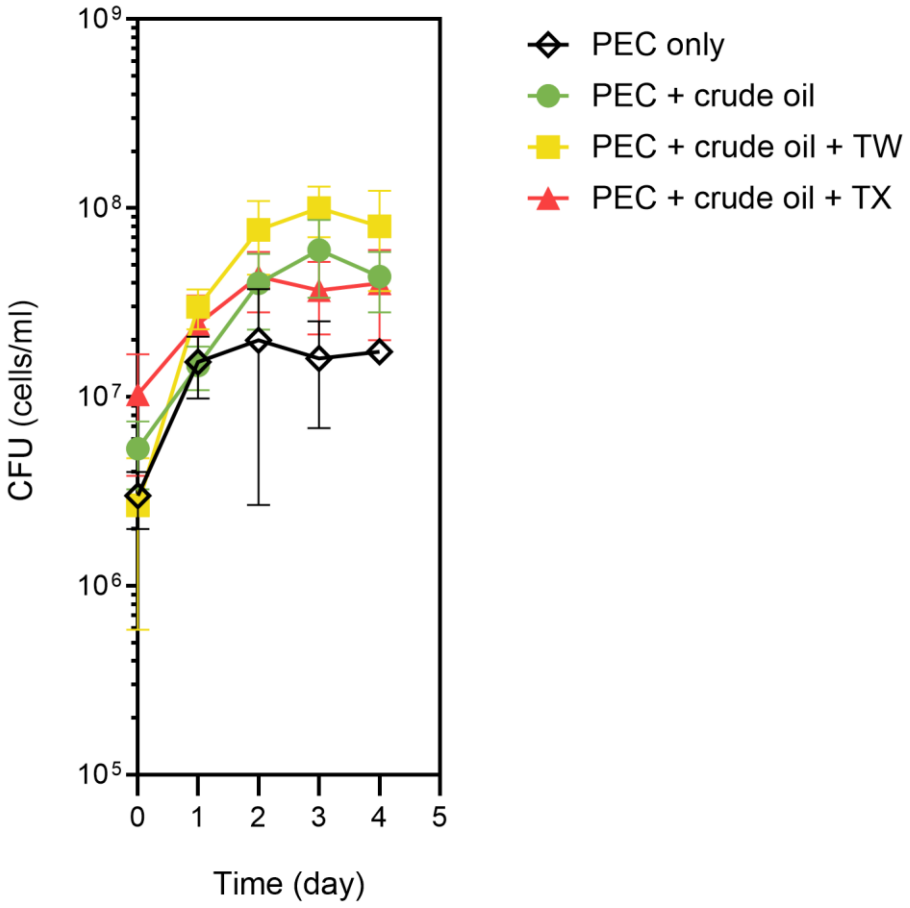


Figure 4.24. Impact of surfactants on microbial growth on crude oil.

3.6.2. Effect of TW and TX on TPH Degradation

Following five days of incubation, the residual TPH concentrations (mg/g) in soil samples were obtained as three replicates from each flask (Figure 4.25). TPH was 3.82 mg/g in the crude oil-only control group (blue column) and dropped to 1.12 mg/g in the microbial culture-added group (green column). The difference between the two groups was shown to be significant ($p = 0.0001$). According to a very significant difference with a p-value of less than 0.0001, the concentration of TPH dropped to 1.19 mg/g in the group that had Tween-20 added group (yellow column). In the TritonX-100 group (red column), TPH were measured at 3.39 mg/g, revealing a statistically significant difference at $p = 0.0189$ compared to the crude oil only control. The findings demonstrate that Tween-20 markedly improves the degradation capacity of microorganisms by efficiently dispersing oil droplets into the aqueous phase, whereas TritonX-100 partially restricts culture performance through dispersion.

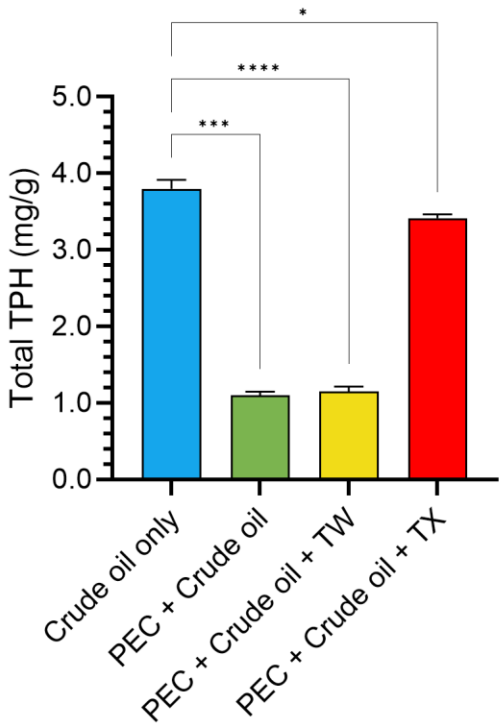


Figure 4.25. Residual TPH concentrations (mg/g) in soil samples after 5-day incubation.

3.6.3. Effect Gene Expression Profile in Crude Oil-Degrading Cultures

This study evaluated gene expression profiles across four experimental conditions using target genes selected from the HADEG database (Rojas-Vargas et al., 2023). The experimental sets were defined as follows: SET-1 included only the PEC; SET-2 included PEC with crude oil; SET-3 included PEC, crude oil, and Triton X-100; and SET-4 included PEC, crude oil, and Tween-20. Each experimental set was assessed at two time points, designated as D2 and D4, corresponding to the second and fourth days of incubation, respectively. For each condition, three biological replicates (R1, R2, R3) were analyzed. Gene expression levels in SET-2 (PEC + Crude oil) were used as the baseline for comparative analysis with the other sets at each time point. This approach enabled a focused evaluation of the influence of surfactants and crude oil on gene expression dynamics and provided a clearer understanding of how hydrocarbon exposure shapes microbial transcriptional responses over time.

The increased gene expression observed in SET-2 (PEC + Crude oil), where crude oil was present as the sole complex substrate, indicates that crude oil stimulates a broad genetic response in the PEC culture (Figure 4.26). Genes involved in the metabolism of aromatic hydrocarbons, including the *ben*, *paa*, *pca*, *prm*, and *xyl* gene clusters, exhibited marked upregulation, reflecting the activation

of multiple catabolic pathways that target structurally diverse aromatic compounds found in crude oil. In parallel, genes associated with oxidative stress response, particularly *ahpC* and *ahpF*, also showed elevated expression levels, suggesting that the microbial community experiences oxidative stress under crude oil exposure and activates defense mechanisms accordingly. Furthermore, the increased expression of *lipA* and *lipB*, which are associated with lipid and fatty acid metabolism, points to the active utilization of aliphatic hydrocarbons as an energy and carbon source. The primary factor contributing to these expression differences is the presence of crude oil in SET-2 compared to its absence in SET-1. The chemically complex nature of crude oil, containing a range of aliphatic and aromatic hydrocarbons, appears to induce both metabolic and stress-related gene expression, indicating that the PEC culture responds dynamically to the presence of hydrocarbons by engaging multiple functional pathways.

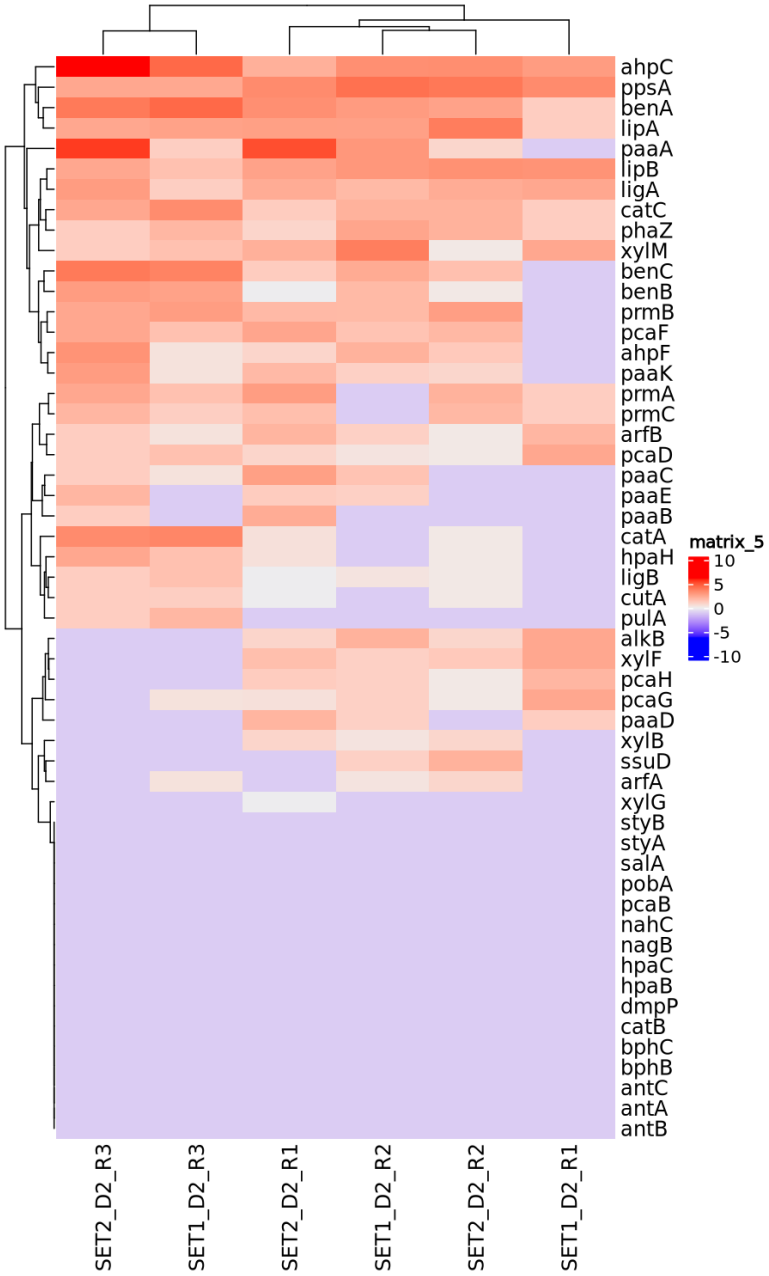


Figure 4.26. Comparison of gene expression profiles in SET-1 and SET-2 at the second day of incubation (SET-1: Only PEC; SET-2: PEC + Crude oil).

The comparison between SET-1 (only PEC) and SET-2 (PEC + Crude oil) on the fourth day of incubation reveals a clear increase in the expression of multiple gene families associated with aromatic hydrocarbon degradation (Figure 4.27). The *paa* gene family (*paaA*, *paaB*, *paaC*, *paaD*, *paaE*, *paaK*), involved in the phenylacetate pathway, showed markedly elevated expression in SET-2. Similarly, *benA* and *benC*, which are linked to the degradation of benzene derivatives, exhibited increased transcriptional activity. Genes from the *pca* cluster (*pcaD*, *pcaF*, *pcaG*, *pcaH*), responsible for protocatechuate metabolism, and members of the *xyl* gene family, associated with xylene and toluene degradation, also showed notable upregulation. These expression patterns reflect the

metabolic adaptation of the microbial community to the chemically complex aromatic fraction of crude oil. Additionally, the rise in *ligA* expression, a gene involved in DNA repair, suggests the activation of cellular defense mechanisms in response to hydrocarbon-induced stress. Overall, the results indicate that the presence of crude oil in the SET-2 medium promotes both catabolic and protective gene expression responses, enabling the efficient microbial transformation of aromatic hydrocarbons.

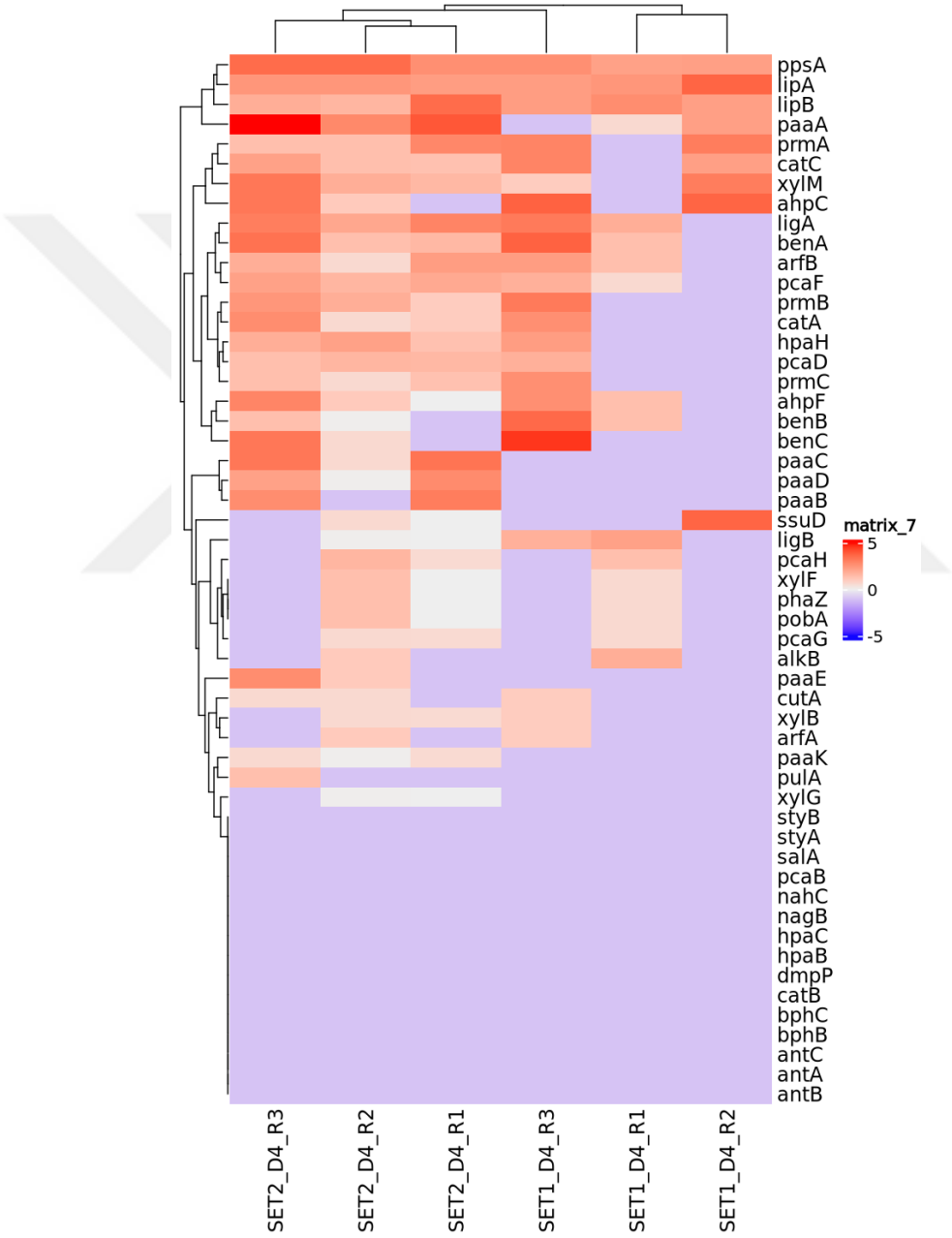


Figure 4.27. Comparison of gene expression profiles in SET-1 and SET-2 at the fourth day of incubation (SET-1: Only PEC; SET-2: PEC + Crude oil).

An increase in the expression of *xylB*, *xylF*, and *xylM* genes, which are involved in xylene degradation, was observed in the SET-3 (PEC + crude oil + TritonX-100) experimental set (Figure 4.28). This was accompanied by elevated expression of *benB*, *benC*, and *paaE*, genes linked to the degradation of benzene and phenylacetate derivatives. The presence of Triton X-100 appears to facilitate the microbial metabolism of these aromatic compounds by enhancing their bioavailability. Additionally, the oxidative stress-related gene *ahpF* and the lipid metabolism-associated genes *lipA* and *lipB* showed increased expression in SET-3 (PEC + crude oil + TritonX-100), indicating both stress adaptation and active utilization of hydrophobic substrates. In comparison, SET-2 (PEC + crude oil) exhibited upregulation of *paaA* and *benA*, further supporting the activation of the phenylacetate and benzene degradation pathways in response to crude oil exposure. The increased expression of *ligA*, a key gene involved in DNA repair, in SET-2 suggests an enhanced cellular defense mechanism against hydrocarbon-induced oxidative stress. In conclusion, while SET-3 reflects the role of Triton X-100 in promoting the metabolism of aromatic hydrocarbons, SET-2 highlights a broader metabolic adaptation to crude oil components, including the induction of stress response and DNA repair pathways.

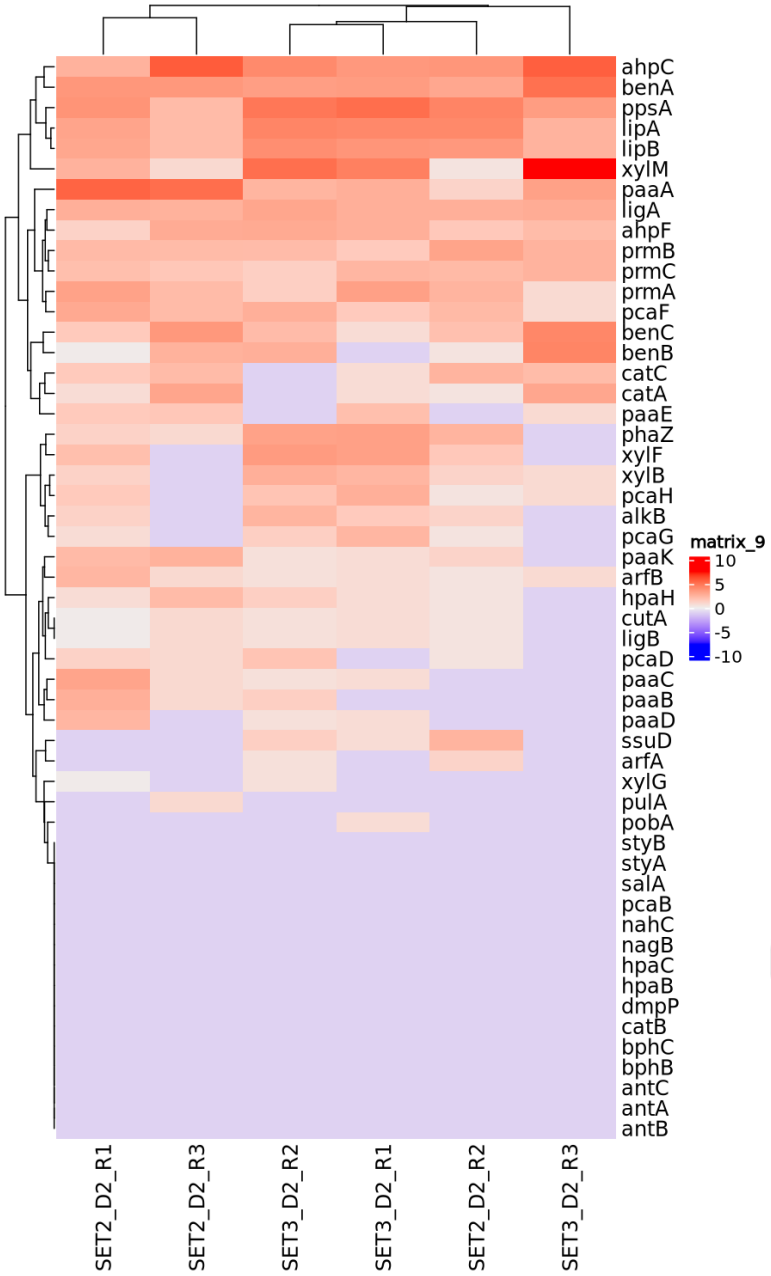


Figure 4.28. Comparison of gene expression profiles in SET-2 and SET-3 at the second day of incubation (SET-2: PEC + crude oil; SET-3: PEC + crude oil + TritonX-100).

At the fourth day of incubation, SET-3 (PEC + crude oil + TritonX-100) showed increased expression of the *xyl* gene family involved in xylene degradation, alongside *lipA* and *lipB*, which are associated with lipid metabolism, and *ahpC* and *ahpF*, linked to oxidative stress response (Figure 4.29). The upregulation of the *alkB* gene indicates elevated alkane monooxygenase activity, suggesting that Triton X-100 enhances the aerobic oxidation of aliphatic hydrocarbons. These findings imply that the surfactant present in SET-3 supports more efficient microbial metabolism of both aromatic and aliphatic hydrocarbons by improving substrate accessibility and stimulating relevant catabolic pathways. In contrast, SET-2 (PEC + crude oil) demonstrated a pronounced

increase in the expression of *ben*, *paa*, and *pca* gene clusters, which are involved in aromatic hydrocarbon degradation, along with the *ligA* gene associated with DNA repair. This gene expression profile suggests that the microbial community in SET-2 responds to crude oil exposure through activation of both metabolic and cellular defense mechanisms. Overall, the data indicate that while SET-2 reflects adaptation to the complex composition of crude oil, SET-3 benefits from the presence of Triton X-100, which enhances the biodegradation of specific aromatic compounds and promotes the utilization of aliphatic hydrocarbons.

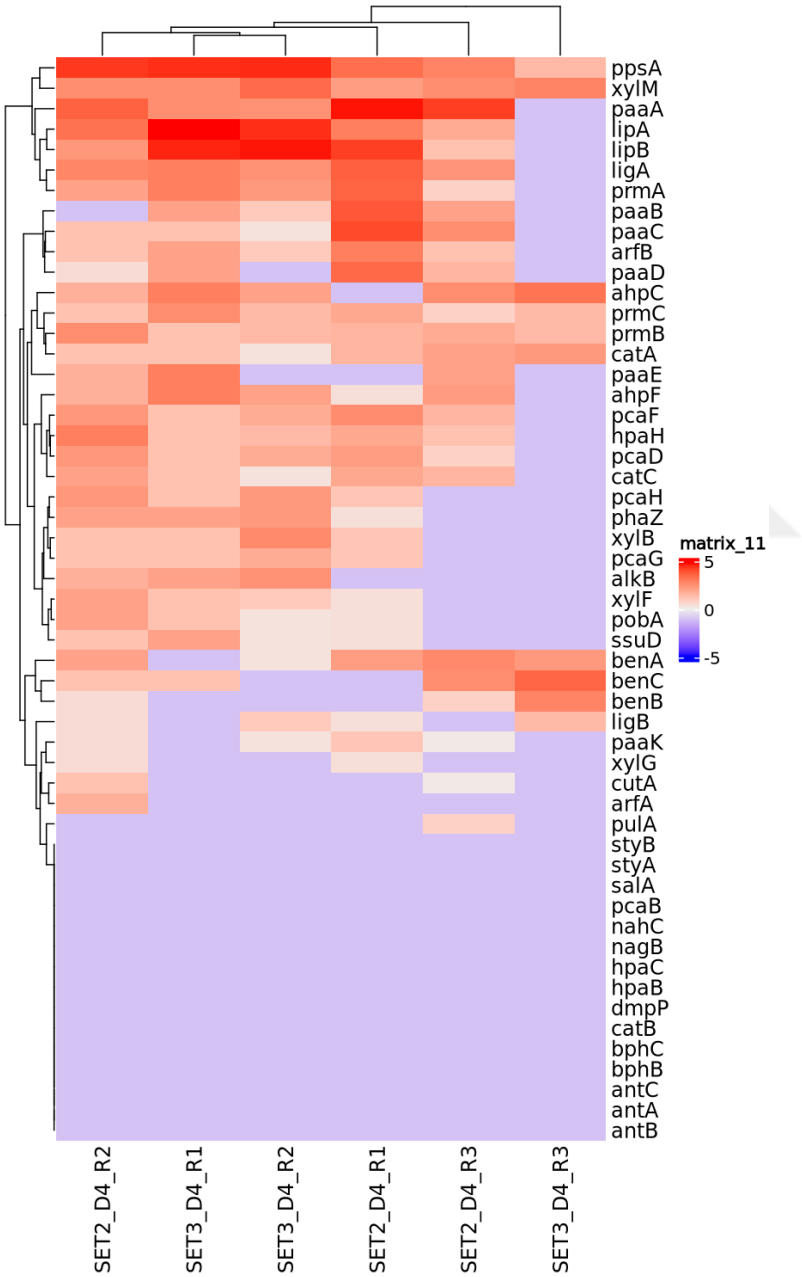


Figure 4.29. Comparison of gene expression profiles in SET-2 and SET-3 at the fourth day of incubation (SET-2: PEC + crude oil; SET-3: PEC + crude oil + TritonX-100).

Gene expression data on the second day of incubation reveal that SET-2 (PEC + crude oil) and SET-4 (PEC + crude oil + Tween-20), both involving Tween-20, trigger distinct metabolic responses in the microbial community (Figure 4.30). In SET-2, elevated expression of oxidative stress-related genes *ahpC* and *ahpF*, along with the DNA repair gene *ligA*, suggests an active stress response. Simultaneously, upregulation of *benA*, *paaA*, and *pcaF* indicates enhanced degradation of aromatic hydrocarbons. Genes involved in lipid and energy metabolism, including *lipA*, *lipB*, and *ppsA*, were also transcriptionally active, reflecting broad metabolic engagement. In SET-4, the microbial response shifts toward the phenylacetate pathway and xylene degradation. Genes such as *paaB*, *paaC*, and *paaK*, associated with phenylacetate catabolism, and *benB* and *benC*, related to benzene degradation, showed increased expression. In addition, *ligB*, implicated in DNA repair, and *xylG* and *xylM*, involved in xylene metabolism, were prominently expressed. Notably, the expression of *prmB* and *prmC*, genes associated with aromatic compound degradation, was specific to SET-4. These patterns suggest that the presence of Tween-20 in SET-4 facilitates the selective activation of aromatic degradation pathways, enabling microorganisms to target distinct hydrocarbon fractions through diverse metabolic mechanisms.

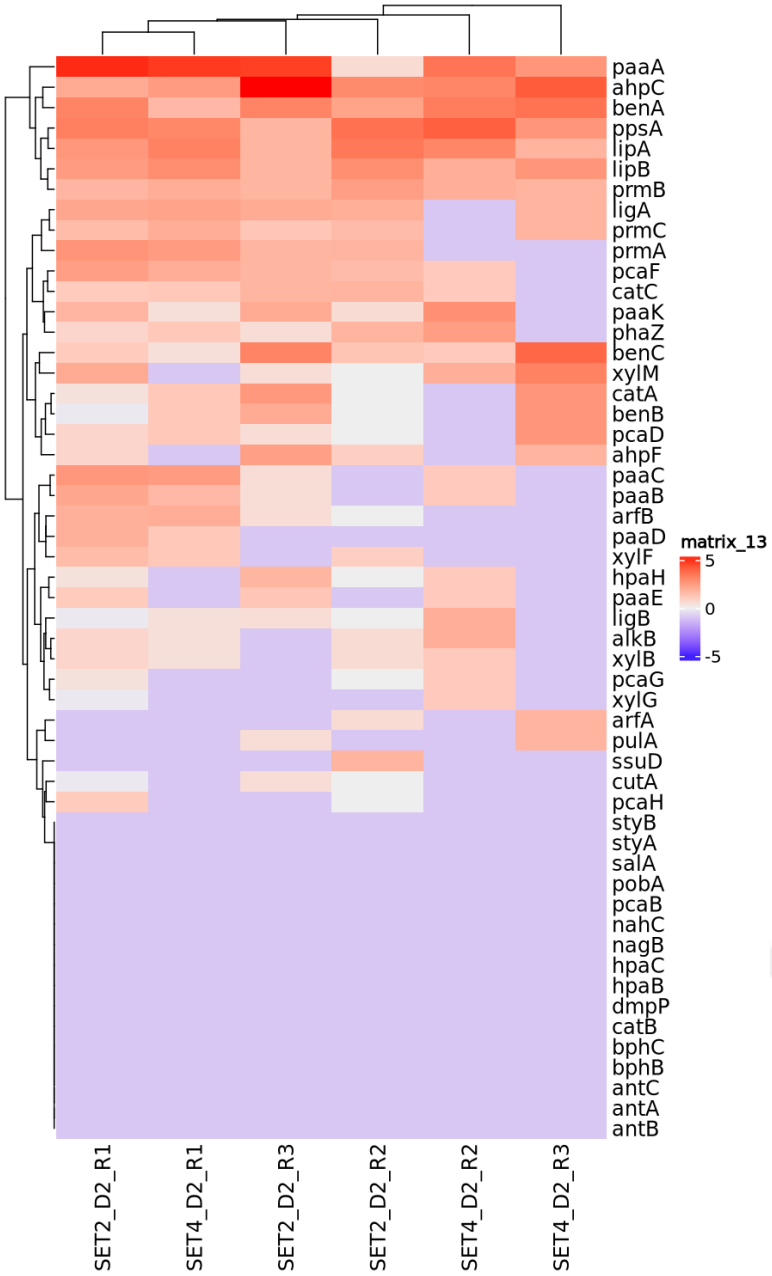


Figure 4.30. Comparison of gene expression profiles in SET-2 and SET-4 at the second day of incubation (SET-2: PEC + crude oil; SET-4: PEC + crude oil + Tween-20).

A comparison between gene expression profiles from the fourth day of incubation in SET-2 (PEC + crude oil) and SET-4 (PEC + crude oil + Tween-20) reveals notable differences in transcriptional activity across key metabolic and stress-related genes (Figure 4.31). In SET-2, elevated expression of *ahpC* and *ahpF*, involved in oxidative stress response, *ligA*, associated with DNA repair, *lipA* and *lipB*, linked to lipid metabolism, and *paaA*, a gene critical for aromatic hydrocarbon degradation, indicates a coordinated metabolic and protective response to crude oil. In contrast, SET-4 generally shows lower expression levels across these genes. However, increased transcription of *benA* and *benC*, which are involved in benzene ring degradation, is observed in

certain replicates, along with prominent expression of *lipB* and *ligA*. Notably, *alkB*, which encodes an alkane monooxygenase, shows reduced expression in SET-4, suggesting a diminished capacity for aliphatic hydrocarbon degradation. These relative expression patterns imply that the microbial community in SET-2 responds to crude oil with a broader activation of catabolic and defense mechanisms, while SET-4 elicits a more limited and selective metabolic response.

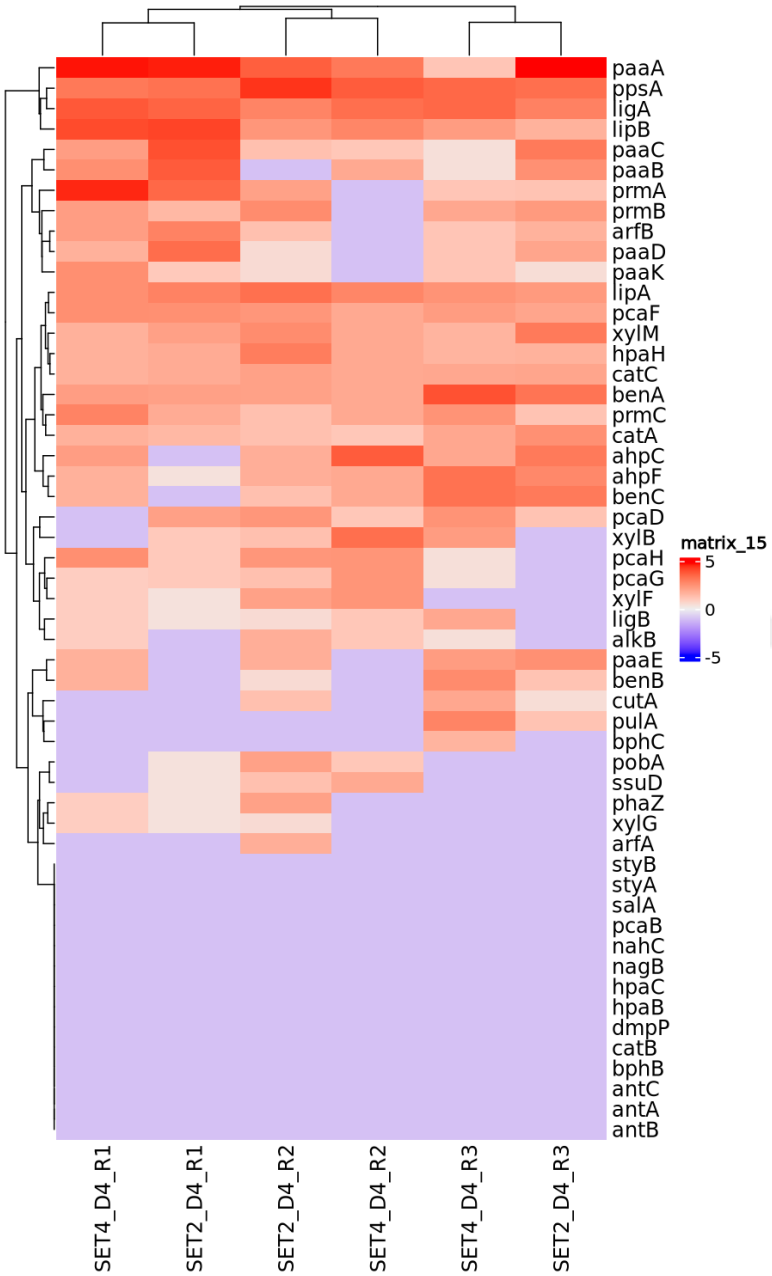


Figure 4.31. Heatmap of Gene Expression Profiles in SET-2 and SET-4 at the fourth day of incubation (SET-2: PEC + crude oil; SET-4: PEC + crude oil + Tween-20).

In accordance with these findings, gene expression profiles of microorganisms associated with hydrocarbon degradation have been investigated in various environmental conditions. The *benA*,

benB, and *benC* genes are essential for hydrocarbon metabolism, as they encode the enzymes responsible for catalyzing the initial step of benzoate catabolism (Kasahara et al., 2012). The elevated expression levels of these genes in SET-2 (PEC + crude oil) and SET-3 (PEC + crude oil + TritonX-100) environments suggest that these conditions are conducive for microorganisms to degrade benzoate and similar aromatic compounds. The *paaA*, *paaE* and *paaK* genes participate in the phenylacetate pathway, enabling the transformation of phenylacetate into phenylacetyl-CoA, thereby directing aromatic degradation intermediates into the β-ketoadipate pathway (A Luu et al., 2013). The significant expression of these genes, especially in SET-2 (PEC + crude oil), suggests that crude oil and complex aromatic compounds activate these metabolic pathways. The *pcaF* gene encodes the protocatechuate 3,4-dioxygenase subunit, which is involved in the degradation of the protocatechuate ring and promotes the flow of carbon into the tricarboxylic acid cycle (Cao and Loh, 2008). The elevated expression of the *pcaF* gene in SET-2 and SET-3 environments suggests the efficient use of these pathways in carbon metabolism. The *ligA* gene is significantly expressed in SET-2 and plays a crucial role in the repair of DNA breaks resulting from the oxidative degradation of aromatic compounds. The capacity of microorganisms to adapt to environmental stresses is thereby affirmed. The *xylB*, *xylF*, and *xylM* genes, involved in the degradation of xylene and toluene, exhibited the highest expression levels in the SET-3 medium. The genes encode essential enzymes involved in the conversion of xylene and toluene into intermediate products such as methyl catechol (Marqués and Ramos, 1993). In SET-3, TritonX-100 may have improved the degradation capacity of microorganisms by facilitating the metabolism of aromatic hydrocarbons. The *prmABC* gene cluster is implicated in the aerobic degradation of aliphatic hydrocarbons, facilitating the initial oxidation of saturated alkanes (Chen et al., 2013). Significant expression levels of these genes have been observed in SET-2 (PEC + crude oil) and SET-4 (PEC + crude oil + Tween-20), suggesting that these environments are conducive to the degradation of aliphatic hydrocarbons. The *ahpC* and *ahpF* genes constitute the alkyl hydro peroxide reductase complex that mitigates oxidative stress and contributes to the detoxification of peroxides, which are byproducts of hydrocarbon metabolism (Kothari et al., 2016). The elevated expression of these genes, especially in SET-2 and SET-3, facilitates the adaptation of microorganisms to stress conditions. The *lipA* and *lipB* genes encode lipase and its associated cofactor protein, which facilitate the degradation and emulsification of hydrophobic petroleum components (Yusoff et al., 2020). In SET-2 and SET-3, the elevated expression of these genes enhances the biological availability of hydrocarbons and facilitates their degradation.

Our results indicate that SET-3 conditions, which include crude oil and Triton X-100, more effectively activate hydrocarbon degradation pathways, whereas the SET-4 condition, containing Tween-20, facilitates these activities at comparatively lower levels. Biological replicates displayed

greater variability than technical replicates, reflecting the inherent complexity of microbial systems and the physiological diversity within the enrichment culture. This variation has been emphasized in previous studies and highlights the importance of including biological replicates to ensure the reliability and generalizability of experimental outcomes, as noted by Blainey et al. (2014). The gene expression profiles observed in this study demonstrate the adaptive responses of microorganisms to distinct chemical conditions, revealing how specific inputs influence the regulation of metabolic pathways involved in the biodegradation of aromatic and aliphatic hydrocarbons.

4.7. Identification of Mobile Gene Clusters in Crude Oil Degraders When Exposed to Surfactants

Hereafter, soil library isolates transformed with the pMAT1 plasmid will be referred to as "isolates with pMAT1" for purpose of clarity. *Pseudomonas frederiksbergensis* YE17 (CP142104.1), *Pseudomonas sp.* MYb327 (CP159258.1), *Pseudomonas sp. FP198* (CP117452.1), and *Achromobacter sp.* SS2-2022 (CP107244.1) strains, isolated from the soil isolates library and identified through whole-genome sequencing, were transformed with the pMAT1 plasmid. Four distinct experimental sets were carried out for the purpose of monitoring gene mobilization. The first set includes only isolates with pMAT1, the second set comprises isolates with pMAT1 and crude oil, the third set includes isolates with pMAT1, crude oil, and TritonX-100, while the fourth set contains isolates with pMAT1, crude oil, and Tween-20 components. Additionally, another set containing only crude oil without any culture was created and used as a negative control, and no contamination was observed during the incubation period.

4.7.1. Microbial Proliferation Analysis

The control group (black line) exhibited an initial inoculation value of 4.33×10^6 CFU/mL, which rose to 1.13×10^7 on day 2, 1.40×10^7 on day 3, and 2.85×10^7 CFU/mL on day 4, indicating a consistent growth pattern. In the group augmented with crude oil (green line), the initial concentration was 2.67×10^6 CFU/mL. Following the adaptation period, this value rose to 4.67×10^6 on the second day, 1.00×10^7 on the third day, and 2.67×10^7 CFU/mL on the fourth day, indicating that the microorganisms successfully utilized the oil as a carbon source. In flasks with Tween-20 (yellow line), the initial cell count at inoculation was 7.00×10^6 CFU/mL. This count increased to 1.27×10^7 on the second day, 4.67×10^7 CFU/mL on the third day, and 3.67×10^7 CFU/mL on the fourth day. This increase is likely relating to Tween-20's ability to finely disperse oil droplets, thus enhancing the availability of carbon for the cells. The presence of TritonX-100 (red line) exhibited a

consistent level on the second day, starting at 7.00 × 10^6 CFU/mL, increasing to 1.40 × 10^7 on the third day, and attaining 2.00 × 10^7 CFU/mL on the fourth day (Figure 4.32). This suggests that while TritonX-100's dispersive effect facilitated growth, it was not as noticeable as that of Tween-20.

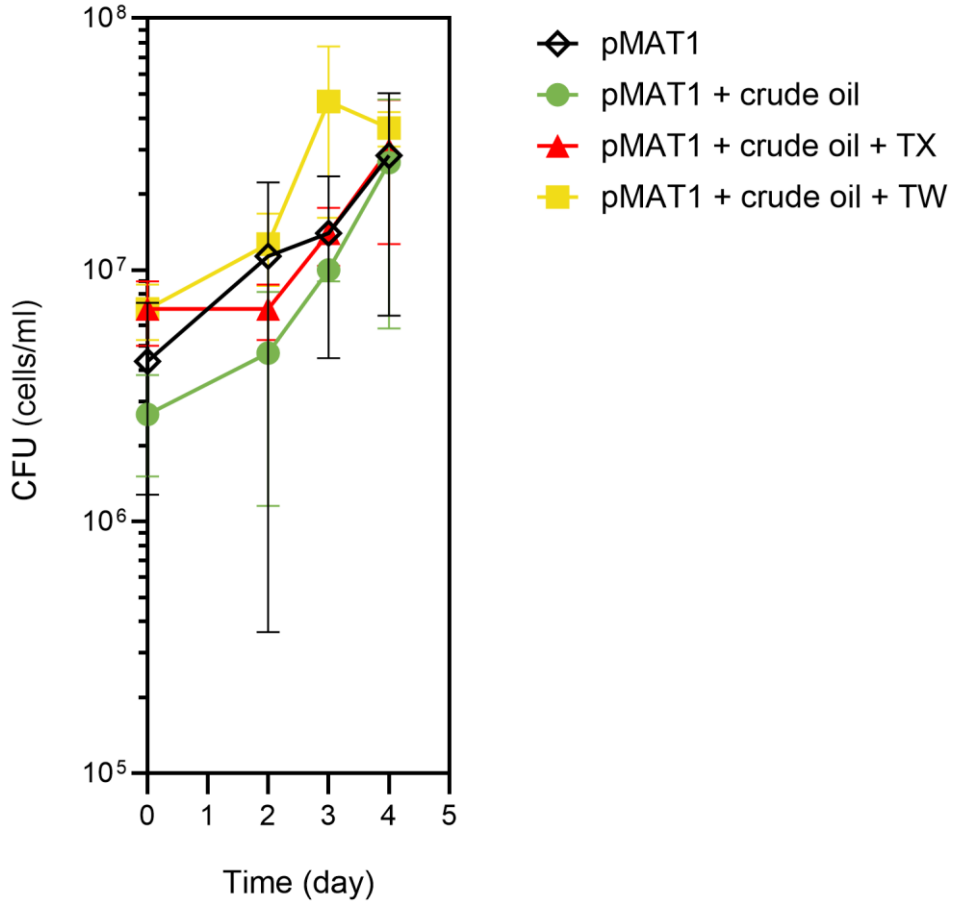


Figure 4.32. Microbial growth of different experimental sets with isolates with pMAT1 plasmid.

4.7.2. TPH Degradation During Biodegradation Assay

The efficiency of gene mobilization assay on the biodegradation of total petroleum hydrocarbons (TPH) was evaluated under kanamycin-induced antibiotic stress conditions. As shown in Figure X, the highest TPH concentration was observed in the crude oil-only condition (3.63 ± 0.90 mg/g), indicating limited natural attenuation in the absence of any microbial or surfactant intervention.

The application of the trap plasmid-bearing microbial consortium (pMAT1 + crude oil) resulted in a clear reduction in TPH levels (2.86 ± 0.08 mg/g), supporting the role of genetically enhanced isolates in promoting hydrocarbon degradation.

The addition of non-ionic surfactants led to further decreases in TPH concentrations. Among these, Tween-20 (pMAT1 + crude oil + TW) showed the most pronounced effect, with an average TPH level of 2.05 ± 0.16 mg/g. This suggests that Tween-20 improved the bioavailability of hydrocarbons for microbial uptake, thereby enhancing the degradation process even under antibiotic stress. Triton X-100 (pMAT1 + crude oil + TX), while also effective (2.54 ± 0.14 mg/g), showed a relatively milder impact compared to Tween-20.

The superior performance of Tween-20 may be attributed to its lower cytotoxicity and higher biocompatibility compared to Triton X-100, which is known to exert harsher effects on microbial membranes. Given that the kanamycin-supplemented environment already imposes a considerable physiological burden on the microbial community, the additional membrane-disruptive potential of Triton X-100 could have limited its biodegradation efficacy.

Taken together, these findings suggest that Tween-20 supplementation in trap plasmid-enhanced microbial systems may represent a promising strategy for accelerating hydrocarbon bioremediation, particularly in chemically or pharmaceutically stressed environments.

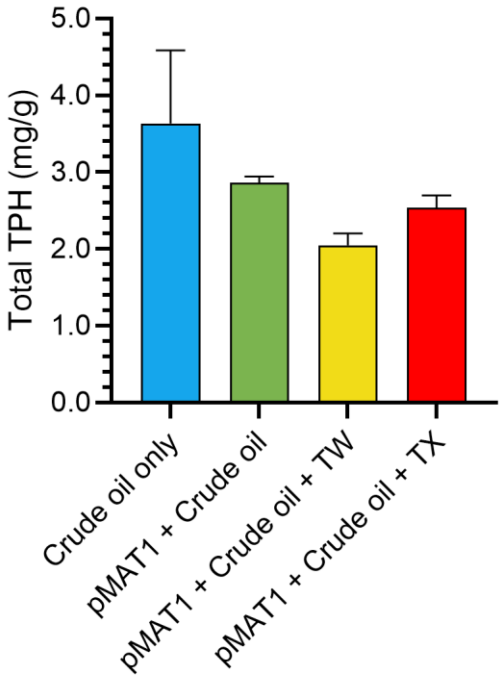


Figure 4.33. TPH Degradation Efficiency

4.7.3. Determination of Transposition Rate

To assess gene mobilization activity, *sacB* loss-of-function rates were quantified in bacterial consortia harboring the pMAT1 plasmid under various substrate and surfactant conditions. These rates were determined by comparing colony counts on sucrose-selective versus non-selective plates. In SET-1 (pMAT1 alone) and SET-2 (pMAT1 + crude oil), no detectable *sacB* inactivation was observed, and transposition rates remained at baseline levels (0 CFU/mL), as illustrated in Figure 4.34. These results indicate that, in the absence of additional chemical stimuli, the *sacB* gene remains intact and the overall transposon activity is minimal.

In contrast, SET-3 (pMAT1 + crude oil + Triton X-100) and SET-4 (pMAT1 + crude oil + Tween-20) exhibited markedly elevated *sacB* loss-of-function rates. The highest mean transposition rate was observed in SET-4 ($3.64 \times 10^{-5} \pm 2.5 \times 10^{-5}$ CFU/mL), followed by SET-3 ($2.04 \times 10^{-5} \pm 0.91 \times 10^{-5}$ CFU/mL). These findings suggest that non-ionic surfactants, particularly Tween-20, significantly promote gene mobilization under hydrocarbon-rich, antibiotic-stressed conditions. The greater variance observed in the Tween-20 group may reflect differential effects on individual isolates or variable integration dynamics of mobile elements.

Overall, these results support the hypothesis that surfactant exposure not only enhances substrate bioavailability but also stimulates transposition activity and genomic plasticity. The induction of mobile genetic elements under surfactant-amended conditions may represent a key mechanism by which bacterial populations adapt to stressful or PHC contaminated environments. Accordingly, the incorporation of biocompatible surfactants such as Tween-20 may play a dual role in both enhancing biodegradation and accelerating the evolution of functional genetic traits in bioremediation-relevant consortia.

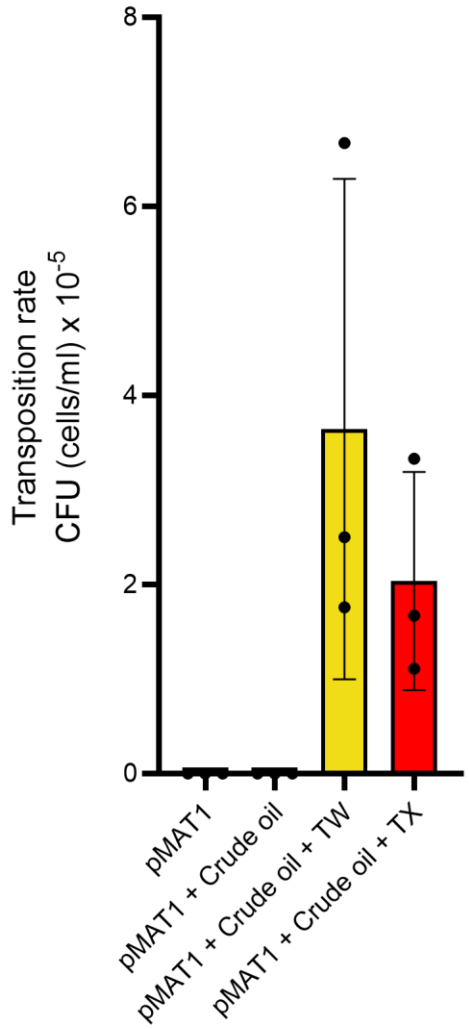


Figure 4.34. Transposition rate in gene mobilization assay.

4.7.4. Monitoring of Gene Mobilization

The quantities of IS elements and transposase in the genomes of four distinct OTUs have been shown to differ significantly as shown in Figure 4.34. OTU001 contains the highest diversity and quantity of IS elements and transposase genes relative to the others. The amounts of the IS10, IS256, and *tnpB* genes are notably elevated in OTU001. OTU002 and OTU003 contain similar IS elements; however, their amounts are comparatively restricted, with a notably greater number of transposases in OTU003. In contrast, the number of IS and transposase elements is lowest in OTU004.

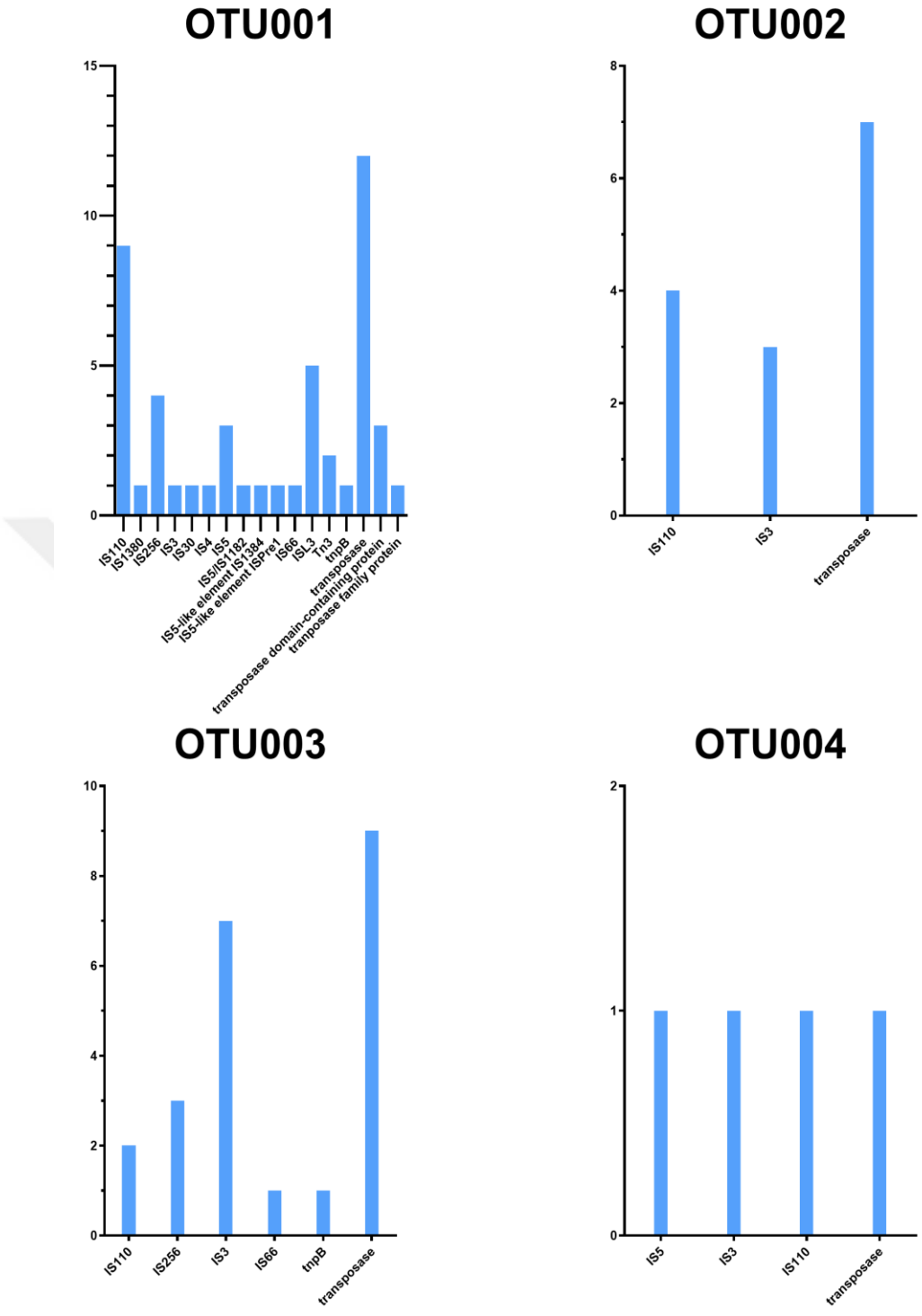


Figure 4.35. Comparative analysis of IS elements and transposase abundance across genomes of four distinct OTUs.

The findings demonstrate significant variation in the diversity and abundance of MGEs across the genomes of different OTUs. The increased IS and transposase content of OTU001 indicates that the genome of this unit exhibits more genetic dynamism and susceptibility to change. IS elements and transposons significantly contributing to adaptation and evolutionary processes by enhancing genetic diversity within the genome. Genomes with a high abundance of mobile elements, like

OTU001, exhibit enhanced adaptability to environmental stresses. The low number of IS and transposase in OTU004 may suggest greater genomic stability or a more conservative life strategy for this operational taxonomic unit. The presence of mobile elements at moderate levels in OTU002 and OTU003 suggests that the genetic structures of these OTUs exhibit a moderate capacity for change.

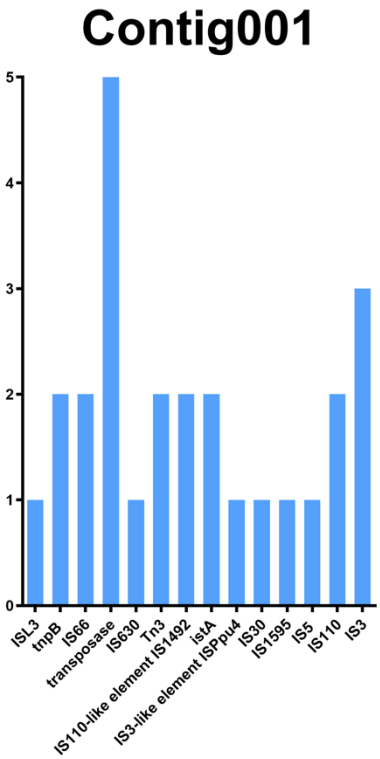


Figure 4.36. Distribution of transposon genes and IS elements within Contig001.

Contig001, a non-aligned and roughly 350 kb long segment of DNA, has an abundance of transposon genes and IS elements (Figure 4.35). The presence of transposase genes from various transposon families, including ISL3, IS66, IS630, Tn3, and IS3, suggests that this genomic region is abundant in MGEs and may act as an important reservoir for the horizontal transfer of genetic material. Mobile elements significantly influence the evolution of bacterial genomes, improving their adaptability and possibly aiding in the dissemination of antibiotic resistance genes or other functional genes.

Mobile genetic elements are essential for HGT of antibiotic resistance genes and for the transfer of various functional genes that facilitate environmental adaptation, including hydrocarbon degradation, thereby enhancing survival. This situation underscores the significance of mobile

elements in the adaptation of microorganisms to fluctuating and challenging environmental conditions.

Sequencing data were analyzed to determine whether the transposons integrated into the pMAT1 plasmid are targeted to a specific region. In the pMAT1 plasmid, the *sacB* gene and promoter region are located between 3266-5133 bp. Additionally, the cutting site of the XbaI restriction enzyme is located at 3239 bp on the plasmid (Figure 4.36). As a result of sequence analyses, it has been determined that a transposon frequently inserts into this target region, particularly within the *sacB* gene and promoter region.



Figure 4.37. Position of the XBaI as restriction enzyme for pMAT1 plasmid.

Four different transposons have been identified, and among them, the one with the highest frequency is the ISPre2 transposon as seen in Figure 4.37. The other transposons, IS110, IS3d, and ISL3b, have been found at low frequencies. These three low-frequency transposons are located at approximately 3240 bp in the pMAT1 plasmid. This region overlaps with the cutting site of the XbaI enzyme. The reason for the low number of reads from transposons may be that the plasmid has not linearized due to the XbaI enzyme not cutting in this region.

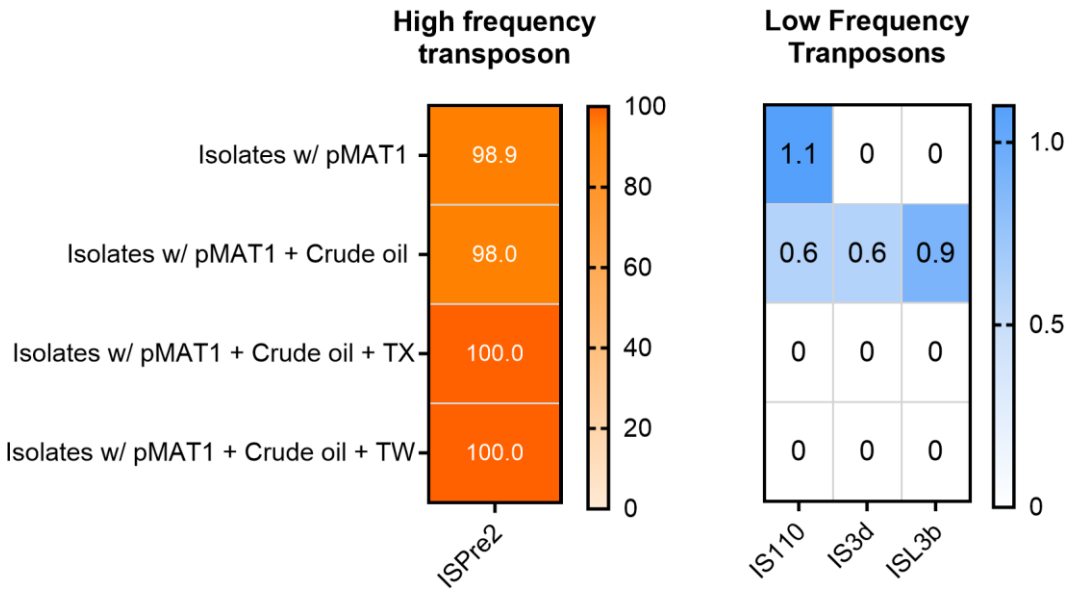


Figure 4.38. Distribution of high and low frequency transposons.

The ISPre2 transposon, found in one of the four different bacterial species, *Pseudomonas frederiksbergensis* (Figure 4.38), has been identified in the pMAT1 plasmid sequence data. In the genome of *Pseudomonas frederiksbergensis*, the pheC, pheD, and pheE gene cassettes are located between the ISPrep1 and ISPrep2 transposons. These genes encode enzymes that facilitate the breakdown of phenolic chemicals in bacteria. The pheC, pheD, and pheE genes encode oxidase and hydroxylase enzymes that enable the metabolism of phenol and other aromatic chemicals. In this manner, bacteria can utilize ambient phenolic chemicals as a source of energy and carbon, so mitigating their harmful effects.

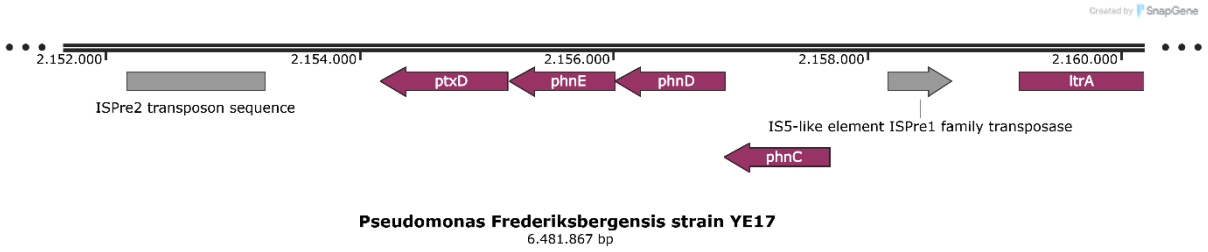


Figure 4.39. ISPre2 transposase in *Pseudomonas frederiksbergensis* genome.

The insertion positions and related repeat sequences targeting the *sacB* gene region have been identified, and these findings are shown in Figure 4.39. It has been determined that the ISPre2 transposon integrates into two different positions in the pMAT1 plasmid at the CTAA sequence at

4664 bp and the TTAA sequence at 4140 bp. In ISFinder, it is observed that a direct repeat sequence of 4 bp as CTAA is formed. It can be seen from the sequence logo that the frequency of the first nucleotide in the sequence being C or T is approximately equal.

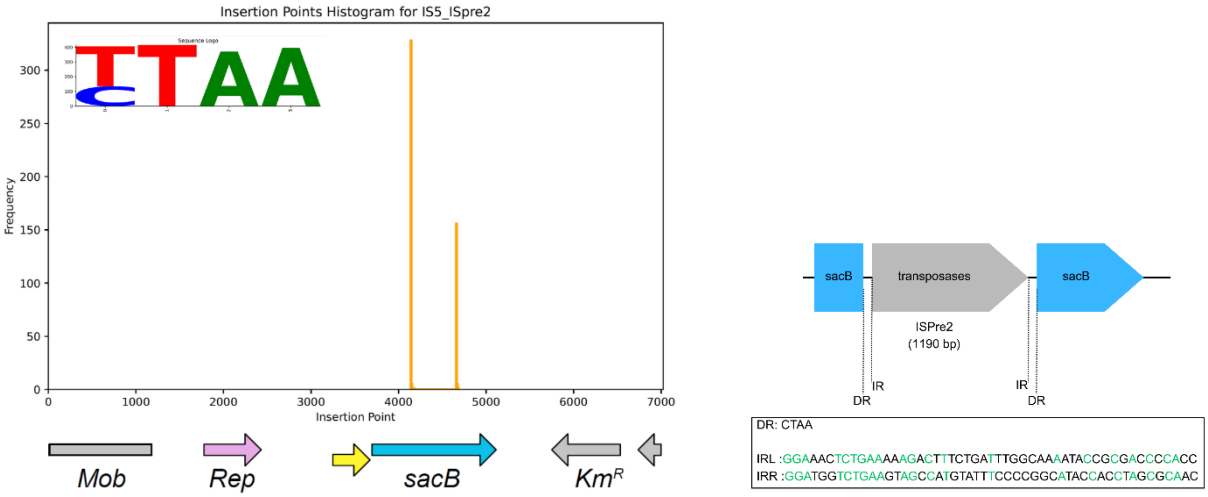


Figure 4.40. The regions preferred by the ISPre2 transposon on the plasmid, the number of transpositions it perform in those regions, and the repeat sequences.

Similar to our findings, Szuplewska and Bartosik (2014) identified an isoform of the ISPre2 transposon in Pseudomonas sp. LM8 through its transposition into the entrapment vector pMAT1, which carries the *sacB* cassette. This isoform shares 99% amino acid similarity with IS1384 and is present in approximately 10 copies within the genome of *Pseudomonas sp.* LM8, as revealed by DNA hybridization analysis. Moreover, homologous sequences were detected in multiple Pseudomonas strains, indicating a widespread distribution of this transposon family among environmental isolates. These findings support the prevalence and mobility of ISPre2-like elements, consistent with our observation of frequent ISPre2 insertions within the *sacB* region of pMAT1. Together, these studies highlight the significant role of ISPre2 transposons in gene mobilization and genome plasticity within Pseudomonas species.

In our study, it was observed that the ISPre2 transposon frequently inserted into the *sacB* gene region of the pMAT1 plasmid. This situation has been similarly reported in the Tn4676 transposon on the pCAR1 plasmid, which carries important degradation and resistance genes. It is thought that ISPre2 preferentially inserts into specific regions on the plasmid, which could affect gene function and plasmid stability (Figure 4.39).

Previous studies on pCAR1 have shown that the compatibility of plasmids and host bacteria, as well as gene expression, are important for plasmid stability and bacterial adaptation. It is suggested that transposons like ISPre2 can affect these processes by altering gene activity or plasmid behavior.

A gene cassette containing the *antA*, *antB*, and *antC* genes is located between the ISPre1 and ISPre2 transposons on the pCAR1 plasmid (Figure 4.40). These genes encode enzymes involved in the bacterial degradation of aromatic compounds, particularly xenobiotics such as carbazole. Therefore, this region represents a functional module of the plasmid critical for the metabolism of environmental xenobiotics.

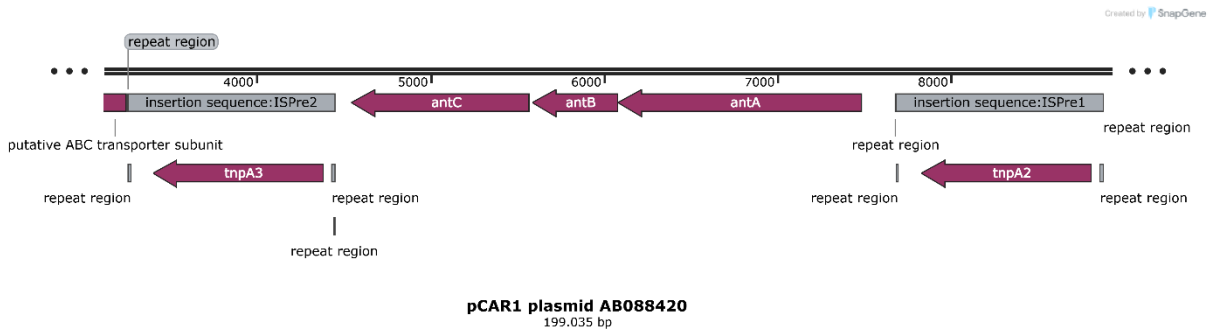


Figure 4.41. ISPre1 and ISPre2 transposons on pCAR1 plasmid.

5. CONCLUSIONS AND RECOMMENDATIONS

This study was designed to test the hypothesis that surfactants not only enhance the bioavailability of PHCs but also promote gene mobilization events that improve the metabolic versatility and degradation efficiency of indigenous microbial consortia. Specifically, the research aimed to elucidate how surfactant exposure influences HGT, transcriptional regulation of hydrocarbon catabolic pathways, and overall petroleum biodegradation efficiency. Using a comprehensive experimental framework, the study systematically investigated the enrichment, identification, genetic characterization, surfactant tolerance, transcriptional response, and mobile element dynamics of PHC-degrading microbial communities isolated from contaminated soils.

Initial enrichment of crude oil-degrading microbial communities demonstrated robust growth and metabolic adaptation to petroleum substrates. Across eight sequential transfers, microbial populations in PEC cultures increased by up to ten-fold relative to controls, reaching as high as 3.8×10^7 CFU/mL. The application of crude oil as a selective pressure drove the succession of the microbial community, enriching hydrocarbonoclastic species such as *Pseudomonas frederiksbergensis* and *Achromobacter spanius*, which increased by up to 336% and 11.53%, respectively. Meanwhile, non-adapted species such as *Stutzerimonas stutzeri* and *Pseudomonas sp.* FeN3W declined by over 85%. Corresponding TPH reduction rates across transfers ranged from 62.29% to 81.91%, with a mean degradation efficiency of $73.24 \pm 6.47\%$ (CV = 8.83%). These outcomes were achieved within 7–8 days of incubation and did not correlate with longer exposure durations ($r = 0.07$, $p = 0.87$), emphasizing that microbial specialization, rather than time, drives effective hydrocarbon removal. It is recommended that future studies focus on microbial specialization and metabolic profiling instead of extending incubation time to improve degradation efficiency.

Genomic and functional analysis of 25 dominant isolates further supported these observations. Whole-genome sequencing of four key OTUs (three *Pseudomonas*, one *Achromobacter*) confirmed the presence of extensive hydrocarbon degradation gene inventories. OTU001 (*P. frederiksbergensis*) and OTU002 exhibited the highest alkane and aromatic degradation gene content, including *alkB*, *fadL*, *ben*, *paa*, *xyl*, *prm*, and *ant* clusters. Unaligned contigs within OTU001 and OTU003 harbored unique gene arrangements and mobile elements (e.g., T4SS, integrases, *dmp*, *xyl*, and *alk* operons), pointing to potential novel catabolic capabilities and plasmid-mediated HGT. Subsystem-level annotations reinforced this, with OTU001 and OTU002 demonstrating full operons for benzoate and phenyl acetate degradation, lipid metabolism, and oxidative stress response, while OTU004's genome

was enriched in DNA repair systems and the box gene cluster, indicating environmental resilience and robust aromatic compound catabolism. Based on these results, selecting microorganisms according to their genomic potential is recommended when forming microbial consortia for bioremediation.

Surfactant tolerance testing revealed that non-ionic surfactants (Tween-20 and Triton X-100) did not inhibit PEC growth across tested concentrations, with measured OD values (e.g., 0.396 ± 0.041 for Triton X-100 at 1 CMC) confirming biocompatibility. In contrast, ionic surfactants such as SDS, BDAC, DDAC, and CTAB displayed strong antimicrobial activity, with MIC values of 446 mg/L, 33.97 mg/L, 6.24 mg/L, and 73.49 mg/L, respectively. These findings delineate surfactants into inhibitory and non-inhibitory classes and guided the selection of Tween-20 and Triton X-100 for subsequent biodegradation assays. It is recommended to test the compatibility of surfactants with microbial cultures before their use in field-scale applications to prevent inhibition.

Petroleum biodegradation assays in the presence of surfactants showed that Tween-20 enhanced both microbial growth and TPH removal. PEC + Crude Oil + Tween-20 yielded the highest CFU (1.1×10^8 CFU/mL) and lowest residual TPH (0.59 ± 0.50 mg/g, $p < 0.01$). In contrast, Triton X-100, despite reducing TPH alone (1.79 ± 0.22 mg/g, $p < 0.001$), underperformed when combined with PEC (2.52 ± 1.13 mg/g), suggesting an antagonistic interaction that potentially hampers microbial degradation efficiency. These results confirm the need for compatibility screening between microbial consortia and surfactant types in applied bioremediation strategies. Tween-20 is recommended for future biodegradation applications, while Triton X-100 should be used with caution and only after compatibility testing.

A more detailed, integrative analysis of microbial growth, TPH reduction, and gene expression under surfactant-modified conditions further elucidated these dynamics. Tween-20 supported gradual and sustained microbial proliferation, achieving the highest biomass levels, while Triton X-100 enhanced early-stage growth but plateaued quickly. Gene expression profiling demonstrated strong upregulation of hydrocarbon-degradation pathways in the PEC + crude oil condition (SET-2), including the *ben*, *paa*, *xyl*, *prm*, and *pca* clusters. Stress response genes (*ahpC*, *ahpF*) and DNA repair genes (*ligA*, *ligB*) were also activated, indicating a combined metabolic and protective adaptation to hydrocarbon exposure. In Triton X-100-amended cultures (SET-3), enhanced expression of *xyl*, *alkB*, *lipA/B*, and oxidative stress markers suggested improved hydrocarbon access and metabolic activity. SET-4 (Tween-20) induced a more selective transcriptional response, with expression focused on phenyl acetate and xylene degradation pathways. Collectively, these profiles

highlight distinct modes of surfactant interaction: Triton X-100 promotes immediate catabolic activation, whereas Tween-20 enables extended and stable transcriptional engagement. Future transcriptomic studies should evaluate gene expression at different time points to better understand surfactant–microbe interactions during biodegradation.

Crucially, surfactant exposure was linked to increased genetic mobility within the microbial consortium. Mobilization assays using pMAT1-transformed isolates revealed that *P. frederiksbergensis* (OTU001) carried the highest diversity of mobile elements, including IS10, IS256, and *tnpB*. The unaligned Contig001 contained multiple IS families (e.g., ISL3, IS630, Tn3), identifying it as a potential HGT hotspot. The ISPre2 transposon was the most active, preferentially integrating into the sacB gene region of pMAT1 and frequently targeting CTAA and TTAA motifs. Integration events were associated with catabolic gene cassettes (*pheC/D/E*, *antA/B/C*), highlighting the potential for surfactants to promote functional gene dissemination under selective pressure.

To further validate this observation, *sacB* loss-of-function assays were performed to directly quantify transposition activity under different surfactant conditions. In pMAT1-only and pMAT1 + crude oil treatments (SET-1 and SET-2), no detectable *sacB* inactivation occurred, indicating that baseline mobility was negligible. However, in surfactant-amended conditions—particularly SET-4 (Tween-20)—transposition rates significantly increased ($3.64 \times 10^{-5} \pm 2.5 \times 10^{-5}$ CFU/mL), followed by SET-3 (Triton X-100; $2.04 \times 10^{-5} \pm 0.91 \times 10^{-5}$ CFU/mL). These findings support the idea that surfactants, especially Tween-20, induce genomic plasticity by activating transposable elements in bacterial populations. The higher variability observed in the Tween-20 condition may reflect differential responses among isolates or heterogeneous insertional activity.

Taken together, these results suggest that non-toxic surfactants not only facilitate microbial access to hydrophobic substrates but also modulate genomic architecture by enhancing horizontal gene transfer through transposition. This dual function—enhancing both substrate availability and gene dissemination—positions biocompatible surfactants like Tween-20 as valuable tools in bioremediation strategies aiming to improve both efficiency and adaptability.

In conclusion, this study validates the hypothesis that surfactants can act as dual-function enhancers in PHC biodegradation—improving substrate bioavailability and concurrently stimulating gene mobilization pathways that promote adaptive metabolic capacity. By integrating physiological, genomic, and transcriptional data, the findings provide a mechanistic basis for leveraging surfactant-compatible microbial consortia in bioremediation strategies targeting complex petroleum-

contaminated environments. It is recommended to apply the findings of this study in small-scale field experiments, especially in areas contaminated with complex petroleum mixtures.

REFERENCES

Abbasian, F., Lockington, R., Mallavarapu, M., & Naidu, R. (2015). A comprehensive review of aliphatic hydrocarbon biodegradation by bacteria. *Biotechnology and Applied Biochemistry*, 176, 670–699.

Abed, R. M. M., Al-Sabahi, J., Al-Maqrashi, F., Al-Habsi, A., & Al-Hinai, M. (2014). Characterization of hydrocarbon-degrading bacteria isolated from oil-contaminated sediments in the Sultanate of Oman and evaluation of bioaugmentation and biostimulation approaches in microcosm experiments. *International Biodeterioration & Biodegradation*, 89, 58–66.

Agency for Toxic Substances and Disease Registry. (1999). Toxicological profile for total petroleum hydrocarbons (TPH). U.S. Department of Health and Human Services, Public Health Service.

Alexander, M. (1999). Biodegradation and bioremediation. Academic Press.

Alexander, M. (2000). Aging, bioavailability, and overestimation of risk from environmental pollutants. *Environmental Science & Technology*, 34(20), 4259–4265.

Alidoosti, F., Giyahchi, M., Moien, S., & Moghimi, H. (2024). Unlocking the potential of soil microbial communities for bioremediation of emerging organic contaminants: Omics-based approaches. *Microbial Cell Factories*, 23, 210.

Al-Kindi, S., & Abed, R. M. M. (2016). Comparing oil degradation efficiency and bacterial communities in contaminated soils subjected to biostimulation using different organic wastes. *Water, Air, & Soil Pollution*, 227, 36.

Alori, E. T., Gabasawa, A. I., Elenwo, C. E., & Agbeyegbe, O. O. (2022). Bioremediation techniques as affected by limiting factors in soil environment. *Frontiers in Soil Science*, 2, 937186.

Alvarez, P. J. J., & Illman, W. A. (2006). Bioremediation and natural attenuation: Process fundamentals and mathematical models. John Wiley & Sons.

Andreolli, M., Lampis, S., Brignoli, P., & Vallini, G. (2015). Bioaugmentation and biostimulation as strategies for the bioremediation of a burned woodland soil contaminated by toxic hydrocarbons: A comparative study. *Journal of Environmental Management*, 153, 121–131.

Andrews, S. (2010). FastQC: A quality control tool for high throughput sequence data. Babraham Bioinformatics, Babraham Institute. https://www.bioinformatics.babraham.ac.uk/projects/fastqc/

Ayilara, M. S., & Babalola, O. O. (2023). Bioremediation of environmental wastes: The role of microorganisms. *Frontiers in Agronomy*, 5, 1183691.

Babuji, P., Thirumalaisamy, S., Duraisam, K., & Periyasamy, G. (2023). Human health risks due to exposure to water pollution: A review. *Water*, 15(14), 2532.

Behera, I. D., Nayak, M., Biswas, S., Meikap, B. C., & Sen, R. (2021). Enhanced biodegradation of total petroleum hydrocarbons by implementing a novel two-step bioaugmentation strategy using indigenous bacterial consortium. *Journal of Environmental Management*, 292, 112746.

Bento, F. M., Camargo, F. A., Okeke, B. C., & Frankenberger, W. T. (2005). Comparative bioremediation of soils contaminated with diesel oil by natural attenuation, biostimulation and bioaugmentation. *Bioresource Technology*, 96(9), 1049–1055.

Berkeley Madonna. (2020). User's guide (Version 10.1.2). Berkeley Madonna, Inc. http://www.berkeleymadonna.com

Blainey, P., Krzywinski, M., & Altman, N. (2014). Replication. *Nature Methods*, 11, 879–880.

Bolger, A. M., Lohse, M., & Usadel, B. (2014). Trimmomatic: A flexible trimmer for Illumina sequence data. *Bioinformatics*, 30(15), 2114–2120.

Boopathy, R. (2000). Factors limiting bioremediation technologies. *Bioresource Technology*, 74(1), 63–67.

Boronin, A. M., & Kosheleva, I. A. (2014). The role of catabolic plasmids in biodegradation of petroleum hydrocarbons. In G. Cao & R. Orrù (Eds.), Current environmental issues and challenges, 159-168, Springer.

Brzeszcz, J., & Kaszycki, P. (2018). Aerobic bacteria degrading both n-alkanes and aromatic hydrocarbons: An undervalued strategy for metabolic diversity and flexibility. *Biodegradation*, 29, 359–407.

Brzeszcz, J., Steliga, T., Ryszka, P., Kaszycki, P., & Kapusta, P. (2024). Bacteria degrading both n-alkanes and aromatic hydrocarbons are prevalent in soils. *Environmental Science and Pollution Research*, 31, 5668–5683.

Bundy, B. M., Campbell, A. L., & Neidle, E. L. (1998). Similarities between the antABC-encoded anthranilate dioxygenase and the benABC-encoded benzoate dioxygenase of Acinetobacter sp. strain ADP1. *Journal of Bacteriology*, 180, 17.

Bykova, M. V., Alekseenko, A. V., Pashkevich, M. A., & Drebenstedt, C. (2021). Thermal desorption treatment of petroleum hydrocarbon-contaminated soils of tundra, taiga, and forest steppe landscapes. *Environmental Geochemistry and Health*, 43, 2331–2346.

Cameotra, S. S., & Makkar, R. S. (2004). Recent applications of biosurfactants as biological and immunological molecules. *Current Opinion in Microbiology*, 7(3), 262–266.

Cao, B., & Loh, K.-C. (2008). Catabolic pathways and cellular responses of Pseudomonas putida P8 during growth on benzoate with a proteomics approach. *Biotechnology and Bioengineering*, 101(6), 1297–1312.

Cases, I., & de Lorenzo, V. (2005). Genetically modified organisms for the environment: Stories of success and failure and what we have learned from them. *International Microbiology*, 8, 213–222.

Cecotti, M., Coppotelli, B. M., Mora, V. C., Viera, M., & Morelli, I. S. (2018). Efficiency of surfactant-enhanced bioremediation of aged polycyclic aromatic hydrocarbon-contaminated soil: Link with bioavailability and the dynamics of the bacterial community. *Science of the Total Environment*, 634, 224–234.

Chaineau, C. H., Rougeux, G., Yepremian, C., & Oudot, J. (2005). Effects of nutrient concentration on the biodegradation of crude oil and associated microbial populations in the soil. *Soil Biology and Biochemistry*, 37(8), 1490–1497.

Chen, C. H., Liu, P. W. G., & Whang, L. M. (2019). Effects of natural organic matters on bioavailability of petroleum hydrocarbons in soil-water environments. *Chemosphere*, 233, 843–851.

Chen, Y., Ren, H., Kong, X., Wu, H., & Lu, Z. (2023). A multicomponent propane monooxygenase catalyzes the initial degradation of methyl tert-butyl ether in Mycobacterium vaccae JOB5. *Applied and Environmental Microbiology*, 89(10).

Chettri, D., Verma, A. K., & Verma, A. K. (2023). Bioaugmentation: An approach to biological treatment of pollutants. *Biodegradation*, 35, 117–135.

Cui, J. Q., Li, Y. Q., He, Q. S., Li, B. Z., Yuan, Y. J., & Wen, J. P. (2021). Effects of different surfactants on the degradation of petroleum hydrocarbons by mixed-bacteria. *Journal of Chemical Technology & Biotechnology*, 97, 208–217.

Das, N., & Chandran, P. (2011). Microbial degradation of petroleum hydrocarbon contaminants: An overview. *Biotechnology Research International*, Article ID 941810.

Davis, J. W., & Madsen, S. (1996). Factors affecting the biodegradation of toluene in soil. *Environmental Science & Technology*, 33(1), 107–130.

Deborah Gnana Selvam, A., & Thatheyus, A. J. (2018). Microbial degradation of petroleum hydrocarbons: An overview. In V. Kumar, M. Kumar & R. Prasad (Eds.), Microbial action on hydrocarbons (pp. 485-503). Springer, Singapore.

Deng, Y., Sun, W., Li, Y., Wei, J., Rao, R., Cao, Q., Wang, S., Zhang, Q., & Ke, C. (2025). Innovative microbial activators for enhanced bioremediation of oil-contaminated soils: Mechanistic insights. *World Journal of Microbiology and Biotechnology*, 41, 47.

Ezezika, O. C., Collier-Hyams, L. S., Dale, H. A., Burk, A. C., & Neidle, E. L. (2006). CatM regulation of the benABCDE operon: Functional divergence of two LysR-type paralogs in Acinetobacter baylyi ADP1. *Applied and Environmental Microbiology*, 72(3), 749–758.

Falih, K. T., Mohd Razali, S. F., Abdul Maulud, K. N., Abd Rahman, N., Abba, S. I., & Yaseen, Z. M. (2024). Assessment of petroleum contamination in soil, water, and atmosphere: A comprehensive review. *International Journal of Environmental Science and Technology*, 21, 8803–8832.

French, K. E., Zhou, Z., & Terry, N. (2020). Horizontal 'gene drives' harness indigenous bacteria for bioremediation. *Scientific Reports*, 10(1), 15091.

Fuentes, S., Méndez, V., Aguila, P., & Seeger, M. (2014). Bioremediation of petroleum hydrocarbons: Catabolic genes, microbial communities, and applications. *Applied Microbiology and Biotechnology*, 98, 4781–4794.

Galitskaya, P., Biktasheva, L., Kuryntseva, P., & Selivanovskaya, S. (2021). Response of soil bacterial communities to high petroleum content in the absence of remediation procedures. *Environmental Science and Pollution Research*, 28, 9610–9627.

García-Alcalde, F., Okonechnikov, K., Carbonell, J., Cruz, L. M., Götz, S., Tarazona, S., Dopazo, J., Meyer, T. F., & Conesa, A. (2012). Qualimap: Evaluating next-generation sequencing alignment data. *Bioinformatics*, 28(20), 2678–2679.

Gentry, T. J., Rensing, C., & Pepper, I. L. (2004). New approaches for bioaugmentation as a remediation technology. *Critical Reviews in Environmental Science and Technology*, 34(5), 447–494.

Gerhardt, K. E., Huang, X. D., Glick, B. R., & Greenberg, B. M. (2009). Phytoremediation and rhizoremediation of organic soil contaminants: Potential and challenges. *Plant Science*, 176(1), 20–30.

Ghazali, F. M., Rahman, R. N. Z. A., Salleh, A. B., & Basri, M. (2004). Biodegradation of hydrocarbons in soil by microbial consortium. *International Biodeterioration & Biodegradation*, 54(1), 61–67.

Goronja, J. M., Janošević Ležaić, A. M., Dimitrijević, B. M., Malenović, A. M., Stanisavljev, D. R., & Pejić, N. D. (2016). Determination of critical micelle concentration of cetyltrimethyl-ammonium bromide: Different procedures for analysis of experimental data. *Hemijska Industrija*, 70(4), 485–492.

Halder, S., Yadav, K. K., Sarkar, R., Mukherjee, S., Saha, P., Haldar, S., Karmakar, S., & Sen, T. (2015). Alteration of zeta potential and membrane permeability in bacteria: A study with cationic agents. *Springer Plus*, 4, 672.

Hamoud, S. A., Adel, R. U., Adel, S. A., Yong, S. O., Abdulelah, I. A., & Mohammad, I. A. (2018). Carbon mineralization and biochemical effects of short-term wheat straw in crude oil contaminated sandy soil. *Applied Geochemistry*, 88(B), 276–287.

Haritash, A. K., & Kaushik, C. P. (2009). Biodegradation aspects of polycyclic aromatic hydrocarbons (PAHs): A review. *Journal of Hazardous Materials*, 169(1–3), 1–15.

Harms, H., & Bosma, T. N. P. (1997). Mass transfer limitation of microbial growth and pollutant degradation. *Journal of Industrial Microbiology & Biotechnology*, 18, 97–105.

Harms, H., Schlosser, D., & Wick, L. Y. (2011). Untapped potential: Exploiting fungi in bioremediation of hazardous chemicals. *Nature Reviews Microbiology*, 9(3), 177–192.

Harmsen, J., & Naidu, R. (2013). Bioavailability as a tool in site management. *Journal of Hazardous Materials*, 261, 840–846.

Hazen, T. C., Dubinsky, E. A., DeSantis, T. Z., Andersen, G. L., Piceno, Y. M., Singh, N., Jansson, J. K., Probst, A., Borglin, S. E., Fortney, J. L., Stringfellow, W. T., Bill, M., Conrad, M. E., Tom, L. M., Chavarria, K. L., Alusi, T. R., Lamendella, R., Joyner, D. C., Spier, C., ... Mason, O. U. (2010). Deep-sea oil plume enriches indigenous oil-degrading bacteria. *Science*, 330, 204–207.

Head, I. M., Jones, D. M., & Röling, W. F. (2006). Marine microorganisms make a meal of oil. *Nature Reviews Microbiology*, 4(3), 173–182.

Helenius, A., McCaslin, D. R., Fries, E., & Tanford, C. (1979). Properties of detergents. *Methods in Enzymology*, 56, 734–749.

Holmberg, K., Jönsson, B., Kronberg, B., & Lindman, B. (2002). Surfactants and polymers in aqueous solution. John Wiley & Sons.

Hosokawa, R., Nagai, M., Morikawa, M., & Okuyama, H. (2009). Autochthonous bioaugmentation and its possible application to oil spills. *World Journal of Microbiology and Biotechnology*, 25, 1519–1528.

Hylland, K. (2006). Polycyclic aromatic hydrocarbon (PAH) ecotoxicology in marine ecosystems. *Journal of Toxicology and Environmental Health*, Part A, 69(1–2), 109–123.

International Agency for Research on Cancer (IARC). (2022). Carcinogenicity of PAHs. IARC Monographs on the Evaluation of Carcinogenic Risks to Humans.

International Tanker Owners Pollution Federation (ITOPF). (2022). Oil spill statistics 2022. https://www.itopf.org/knowledge-resources/data-statistics/statistics/

Ji, Y., Mao, G., Wang, Y., & Bartlam, M. (2013). Structural insights into diversity and n-alkane biodegradation mechanisms of alkane hydroxylases. *Frontiers in Microbiology*, 4, 58.

Johnson, M., Zaretskaya, I., Raytselis, Y., Merezhuk, Y., McGinnis, S., & Madden, T. L. (2008). NCBI BLAST: A better web interface. *Nucleic Acids Research*, 36(Supplement_2), W5–W9.

Jørgensen, K. S., Puustinen, J., & Suortti, A. M. (2000). Bioremediation of petroleum hydrocarbon-contaminated soil by composting in biopiles. *Environmental Pollution*, 107(2), 245–254.

Karapanagioti, H. K., Kleineidam, S., Sabatini, D. A., Grathwohl, P., & Ligouis, B. (1999). Impacts of heterogeneous organic matter on phenanthrene sorption and desorption in aquifer material. *Environmental Science & Technology*, 34(3), 406–414.

Karthick, A., Roy, B., & Chattopadhyay, P. (2019). A review on the application of chemical surfactant and surfactant foam for remediation of petroleum oil contaminated soil. *Journal of Environmental Management*, 243, 187–205.

Kasahara, Y., Morimoto, H., Kuwano, M., & Kadoya, R. (2012). Genome-wide analytical approaches using semi-quantitative expression proteomics for aromatic hydrocarbon metabolism in Pseudomonas putida F1. *Journal of Microbiological Methods*, 91(3), 434–442.

Khot, V., Zorz, J., Gittins, D. A., Chakraborty, A., Bell, E., Bautista, M. A., Paquette, A. J., Hawley, A. K., Novotnik, B., Hubert, C., ... Bhatnagar, S. (2022). CANT-HYD: A curated database of phylogeny-derived hidden Markov models for annotation of marker genes involved in hydrocarbon degradation. *Frontiers in Microbiology*, 12, 764058.

Kim, J., & Park, W. (2018). Genome analysis of naphthalene-degrading Pseudomonas sp. AS1 harboring the megaplasmid pAS1. *Journal of Microbiology and Biotechnology*, 28(2), 330–337.

Korshunova, T. Y., Kuzina, E. V., Iskuzhina, M. G., Mukhamatdyarova, S. R., & Sharipova, Y. Y. (2024). Oil-degrading microorganisms of the genus Pseudomonas with resistance to additional pollutants and phytostimulating activity as promising agents of environmental biotechnology. *Journal of Siberian Federal University*, 17(1), 64–81.

Kothari, A., Charrier, M., Wu, Y.-W., Malfatti, S., Zhou, C. E., Singer, S. W., Dugan, L., & Mukhopadhyay, A. (2016). Transcriptomic analysis of the highly efficient oil-degrading bacterium Acinetobacter venetianus RAG-1 reveals genes important in dodecane uptake and utilization. *FEMS Microbiology Letters*, 363(20), fnw230.

Koul, B., & Taak, P. (2018). Ex situ soil remediation strategies. In B. Koul & P. Taak (Eds.), Biotechnological strategies for effective remediation of polluted soils (pp. 39-57). Springer.

Kueper, B. H., Stroo, H. F., Vogel, C. M., & Ward, C. H. (2014). Chlorinated solvent source zone remediation. Springer.

Kumar, A., Mohan, D., Paramkusam, B. R., & Singh, A. P. (2024). Efficacy of surfactants in the sustainable restoration of the geotechnical properties of diesel-contaminated soil. *International Journal of Environmental Science and Technology*, 21, 867–874.

Kumari, R., Kakati, A., Nagarajan, R., & Sangwai, J. S. (2019). Synergistic effect of mixed anionic and cationic surfactant systems on the interfacial tension of crude oil-water and enhanced oil recovery. *Journal of Dispersion Science and Technology*, 40(7), 969–981.

Kupryianchyk, D., Rakowska, M. I., Grotenhuis, J. T. C., & Koelmans, A. A. (2012). In situ sorption of hydrophobic organic compounds to sediment amended with activated carbon. *Environmental Pollution*, 161, 23–29.

Leharne, S. (2021). Risk assessment and remediation of NAPL contaminated soil and groundwater. *ChemTexts*, 8, 5.

Li, H., Handsaker, B., Wysoker, A., Fennell, T., Ruan, J., Homer, N., Marth, G., Abecasis, G., & Durbin, R. (2009). The sequence alignment/map format and SAMtools. *Bioinformatics*, 25(16), 2078–2079.

Li, Q. (2020). Mining secondary metabolism of Achromobacter and analysis of key genes of petroleum degradation. *IOP Conference Series: Earth and Environmental Science*, 692, 042032.

Ling, H., Hou, J., Du, M., Zhang, Y., Liu, W., Christie, P., & Luo, Y. (2023). Surfactant-enhanced bioremediation of petroleum-contaminated soil and microbial community response: A field study. *Chemosphere*, 322, 138225.

Liu, J. W., Wei, K. H., Xu, S. W., Cui, J., Ma, J., Xiao, X. L., Xi, B. D., & He, X. S. (2021). Surfactant-enhanced remediation of oil-contaminated soil and groundwater: A review. *Science of the Total Environment*, 756, 144142.

Liu, H., Yang, G., Jia, H., & Sun, B. (2022). Crude oil degradation by a novel strain Pseudomonas aeruginosa AQNU-1 isolated from an oil-contaminated lake wetland. *Processes*, 10(2), 307.

Ma, Y., Wang, L., & Shao, Z. (2006). Pseudomonas, the dominant polycyclic aromatic hydrocarbon-degrading bacteria isolated from Antarctic soils and the role of large plasmids in horizontal gene transfer. *Environmental Microbiology*, 8(3), 455–465.

Ma, Y., Wang, J., Liu, Y., Wang, X., Zhang, B., Zhang, W., Chen, T., Liu, G., Xue, L., & Cui, X. (2023). Nocardioides: "Specialists" for hard-to-degrade pollutants in the environment. *Molecules*, 28, 7433.

MacKay, D., Shiu, W. Y., & Ma, K. C. (1994). Illustrated handbook of physical-chemical properties and environmental fate for organic chemicals. CRC Press.

Mackay, D., & Callcott, D. (1998). Partitioning and physical chemical properties of PAHs. In PAHs and related compounds (pp. 325–346). Springer.

Mao, X., Jiang, R., Xiao, W., & Yu, J. (2015). Use of surfactants for the remediation of contaminated soils: A review. *Journal of Hazardous Materials*, 285, 419–435.

Margesin, R., & Schinner, F. (2001). Bioremediation (natural attenuation and biostimulation) of diesel-oil-contaminated soil in an Alpine glacier skiing area. *Applied and Environmental Microbiology*, 67(7), 3127–3133.

Mariano, D. C. O., Dias, G. M., Castro, M. R., Tschoeke, D. A., de Oliveira, F. J. S., Séervulo, E. F. C., & Neves, B. C. (2024). Exploring the diversity and functional profile of microbial communities of Brazilian soils with high salinity and oil contamination. *Heliyon*, e34336.

Martínková, L., Uhnáková, B., Pátek, M., Nešvera, J., & Křen, V. (2009). Biodegradation potential of the genus Rhodococcus. *Environment International*, 35, 162–177.

Marqués, S., & Ramos, J. L. (1993). Transcriptional control of the Pseudomonas putida TOL plasmid catabolic pathways. *Molecular Microbiology*, 9(5), 923–929.

Meckenstock, R. U., Boll, M., Mouttaki, H., Koelschbach, J. S., Tarouco, P. C., Weyrauch, P., Dong, X., & Himmelberg, A. M. (2016). Anaerobic degradation of benzene and polycyclic aromatic hydrocarbons. *Journal of Molecular Microbiology and Biotechnology*, 26, 92–118.

Medić, A. B., & Karadžić, I. M. (2022). Pseudomonas in environmental bioremediation of hydrocarbons and phenolic compounds: Key catabolic degradation enzymes and new analytical platforms for comprehensive investigation. *World Journal of Microbiology and Biotechnology*, 38, 165.

Mekonnen, B. A., Aragaw, T. A., & Genet, M. B. (2024). Bioremediation of petroleum hydrocarbon-contaminated soil: A review on principles, degradation mechanisms, and advancements. *Frontiers in Environmental Science*, 12, 1354422.

Miguel, A. B. R., Jetten, M. S. M., & Welte, C. U. (2020). The role of mobile genetic elements in organic micropollutant degradation during biological wastewater treatment. *Water Research X*, 9, 100065.

Mishra, P., Kiran, N. S., & Ferreira, L. F. R. (2023). New insights into the bioremediation of petroleum contaminants: A systematic review. *Chemosphere*, 326, 138391.

Mrozik, A., & Piotrowska-Seget, Z. (2010). Bioaugmentation as a strategy for cleaning up of soils contaminated with aromatic compounds. *Microbiological Research*, 165(5), 363–375.

Mohammed, S. A., Omar, T. J., & Hasan, A. H. (2023). Degradation of crude oil and pure hydrocarbon fractions by some wild bacterial and fungal species. *Biologia*, 78, 3637–3651.

Motin, Md. A., Hafiz Mia, M. A., & Nasimul Islam, A. K. M. (2015). Thermodynamic properties of sodium dodecyl sulfate aqueous solutions with methanol, ethanol, n-propanol and iso-propanol at different temperatures. *Journal of Saudi Chemical Society*, 19, 172–180.

Mukherjee, S., Das, P., & Sen, R. (2017). Towards commercial production of microbial surfactants. *Trends in Biotechnology*, 24(11), 509–515.

National Center for Biotechnology Information (NCBI). (2021). Database resources of the National Center for Biotechnology Information. *Nucleic Acids Research*, 49(D1), D10–D17.

Nong, J., Peng, P., Pan, J., Shen, T., & Xie, Q. (2023). Effect of bioaugmentation and biostimulation on hydrocarbon degradation and bacterial community composition in different petroleum-contaminated soil layers. *Water, Air, & Soil Pollution*, 234, 189.

Nzila, A. (2018). Current status of the degradation of aliphatic and aromatic petroleum hydrocarbons by thermophilic microbes and future perspectives. *International Journal of Environmental Research and Public Health*, 15(12), 2782.

Oro, C. E. D., Saorin Puton, B. M., Venquiaruto, L. D., Dallago, R. M., & Tres, M. V. (2024). Effective microbial strategies to remediate contaminated agricultural soils and conserve functions. *Agronomy*, 14(11), 2637.

Pacwa-Płociniczak, M., Płaza, G. A., Piotrowska-Seget, Z., & Cameotra, S. S. (2011). Environmental applications of biosurfactants: Recent advances. *International Journal of Molecular Sciences*, 12(1), 633–654.

Pande, V., Pandey, S. C., Sati, D., Pande, V., & Samant, M. (2020). Bioremediation: An emerging effective approach towards environment restoration. *Environmental Sustainability*, 3, 91–103.

Pankow, J. F., & Cherry, J. A. (1996). Dense chlorinated solvents and other DNAPLs in groundwater: History, behavior, and remediation. Waterloo Press.

Perez-Vazquez, A., Barciela, P., & Prieto, M. A. (2024). In situ and ex situ bioremediation of different persistent soil pollutants as agroecology tool. *Processes*, 12(10), 2223.

Rabani, M. S., Habib, A., & Gupta, M. K. (2020). Polycyclic aromatic hydrocarbons: Toxic effects and their bioremediation strategies. In R. A. Bhat & K. R. Hakeem (Eds.), Bioremediation and biotechnology (Vol. 4) (pp. 65-105). Springer.

Rabus, R., Boll, M., Heider, J., Meckenstock, R. U., Buckel, W., Einsle, O., Ermler, U., Golding, B. T., Gunsalus, R. P., Kroneck, P. M. H., Krüger, M., Lueders, T., Martins, B. M., Musat, F., Richnow, H. H., Schink, B., Seifert, J., Szaleniec, M., Treude, T., ... Wilkes, H. (2016). Anaerobic microbial degradation of hydrocarbons: From enzymatic reactions to the environment. *Journal of Molecular Microbiology and Biotechnology*, 26(5), 28.

Reddy, K. R., & Adams, J. A. (2001). Effects of soil heterogeneity on airflow patterns and hydrocarbon removal during in situ air sparging. *Journal of Geotechnical and Geoenvironmental Engineering*, 127(3), 234–242.

Rivett, M. O., & Allen-King, R. M. (2003). A controlled field experiment on groundwater contamination by a multicomponent DNAPL: Dissolved-plume retardation. *Journal of Contaminant Hydrology*, 66(1–2), 117–146.

Rojas-Vargas, J., Castelán-Sánchez, H. G., & Pardo-López, L. (2023). HADEG: A curated hydrocarbon aerobic degradation enzymes and genes database. *Computational Biology and Chemistry*, 107, 107966.

Rojas-Vargas, J., Rebollar, E. A., Sanchez-Flores, A., & Pardo-López, L. (2024). A comparative genomic study of a hydrocarbon-degrading marine bacterial consortium. *PLOS ONE*, 19(8), e0303363.

Rosell-Melé, A., Moraleda-Cibrián, N., Cartró-Sabaté, M., Colomer-Ventura, F., Mayor, P., & Orta-Martínez, M. (2018). Oil pollution in soils and sediments from the Northern Peruvian Amazon. *Science of the Total Environment*, 610–611, 1010–1019.

Rosen, M. J., & Kunjappu, J. T. (2012). Surfactants and interfacial phenomena (4th ed.). John Wiley & Sons.

Röling, W. F. M., Milner, M. G., Jones, D. M., Lee, K., Daniel, F., Swannell, R. J. P., & Head, I. M. (2002). Robust hydrocarbon degradation and dynamics of bacterial communities during nutrient-enhanced oil spill bioremediation. *Applied and Environmental Microbiology*, 68(11), 5537–5548.

Ruiz, O. N., Brown, L. M., Radwan, O., Bowen, L. L., Gunasekera, T. S., Mueller, S. S., West, Z. J., & Striebich, R. C. (2021). Metagenomic characterization reveals complex association of soil hydrocarbon-degrading bacteria. *International Biodeterioration & Biodegradation*, 157, 105161.

Ruiz, O. N., Radwan, O., & Striebich, R. C. (2021). GC–MS hydrocarbon degradation profile data of Pseudomonas frederiksbergensis SI8, a bacterium capable of degrading aromatics at low temperatures. *Data in Brief*, 35, 106864.

Schloss, P. D., Westcott, S. L., Ryabin, T., Hall, J. R., Hartmann, M., Hollister, E. B., Lesniewski, R. A., Oakley, B. B., Parks, D. H., Robinson, C. J., Sahl, J. W., Stres, B., Thallinger, G. G., Van Horn, D. J., & Weber, C. F. (2009). Introducing mothur: Open-source, platform-independent, community-supported software for describing and comparing microbial communities. *Applied and Environmental Microbiology*, 75(23), 7537–7541.

Semple, K. T., Reid, B. J., & Fermor, T. R. (2001). Impact of composting strategies on the treatment of soils contaminated with organic pollutants. *Environmental Pollution*, 112(2), 269–283.

Semple, K. T., Morriss, A. W., & Paton, G. I. (2003). Bioavailability of hydrophobic organic contaminants in soils: Fundamental concepts and techniques for analysis. *European Journal of Soil Science*, 54(4), 809–818.

Semple, K. T., Doick, K. J., Jones, K. C., Burauel, P., Craven, A., & Harms, H. (2004). Defining bioavailability and bioaccessibility of contaminated soil and sediment is complicated. *Environmental Science & Technology*, 38(12), 228A–231A.

Shahi, A., Ince, B., Aydin, S., & Ince, O. (2017). Assessment of the horizontal transfer of functional genes as a suitable approach for evaluation of the bioremediation potential of petroleum-contaminated sites: A mini-review. *Applied Microbiology and Biotechnology*, 101, 4341–4348.

Sharuddin, S. S. N., Abdullah, S. R. S., Hasan, H. A., Othman, A. R., & Ismail, N. I. (2024). Rhizobacterial-assisted phytoremediation for accelerated petroleum-hydrocarbon removal in crude-oil sludge. *Science of the Total Environment*, 954, 176189.

Shen, W., Koirala, N., Mukherjee, D., Lee, K., Zhao, M., & Li, J. (2022). Tween 20 stabilized conventional heavy crude oil-in-water emulsions formed by mechanical homogenization. *Frontiers in Environmental Science*, 10, 873730.

Shintani, M., & Nojiri, H. (2013). Mobile genetic elements (MGEs) carrying catabolic genes. In A. Malik, E. Grohmann, & M. Alves (Eds.), Management of microbial resources in the environment (pp. 167-214). Springer.

Sierra-Garcia, I. N., Belgini, D. R. B., Torres-Ballesteros, A., Paez-Espino, D., Capilla, R., Santos Neto, E. V., Gray, N., & de Oliveira, V. M. (2020). In-depth metagenomic analysis in contrasting oil wells reveals syntrophic bacterial and archaeal associations for oil biodegradation in petroleum reservoirs. *Science of the Total Environment*, 715, 136646.

Singh, S. N., Kumari, B., & Mishra, S. (2012). Microbial degradation of alkanes. In S. S. Singh (Ed.), Microbial degradation of xenobiotics (pp. 439–469). Springer.

Singha, N. A., Neihsial, R., Kipgen, L., Lyngdoh, W. J., Nongdhar, J., Chettri, B., Singh, P., & Singh, A. K. (2024). Taxonomic and predictive functional profile of hydrocarbonoclastic bacterial consortia developed at three different temperatures. *Current Microbiology*, 81, 22.

Somee, M. H., Amoozegar, M. A., Dastgheib, S. M. M., Shavandi, M., Maman, L. G., Bertilsson, S., & Mehrshad, M. (2022). Genome-resolved analyses show an extensive diversification in key aerobic hydrocarbon-degrading enzymes across bacteria and archaea. *BMC Genomics*, 23, 690.

Song, Q., Xue, Z., Wu, H., Zhai, Y., Lu, T., Du, X., Zheng, J., Chen, H., & Zuo, R. (2023). The collaborative monitored natural attenuation (CMNA) of soil and groundwater pollution in large petrochemical enterprises: A case study. *Environmental Research*, 216, 114816.

Sui, X., Li, Y., Wang, X., Yu, L., Wang, J., & Ji, H. (2023). Genomics and degradation law of Acinetobacter junii in response to petroleum pollution. *Process Biochemistry*, 126, 41–50.

Szuplewska, M., Sentkowska, D., Lasek, R., Decewicz, P., Hałucha, M., Funk, Ł., Chmielowska, C., & Bartosik, D. (2024). Genome-wide comparative analysis of clinical and environmental strains of the opportunistic pathogen Paracoccus yeei (Alphaproteobacteria). *Frontiers in Microbiology*, 15, 1483110.

Tezel, U. (2009). Fate and effect of quaternary ammonium compounds in biological systems (Doctoral dissertation, Georgia Institute of Technology).

Tiller, G. E., Mueller, T. J., Dockter, M. E., & Struve, W. G. (1984). Hydrogenation of Triton X-100 eliminates its fluorescence and ultraviolet light absorption while preserving its detergent properties. *Analytical Biochemistry*, 141, 262–266.

Top, E., & Springael, D. (2003). The role of mobile genetic elements in bacterial adaptation to xenobiotic organic compounds. *Current Opinion in Biotechnology*, 14(3), 262–269.

Tyagi, M., da Fonseca, M. M. R., & de Carvalho, C. C. C. R. (2011). Bioaugmentation and biostimulation strategies to improve the effectiveness of bioremediation processes. *Biodegradation*, 22(2), 231–241.

United Nations Environment Programme (UNEP). (2011). Environmental assessment of Ogoniland. UNEP.

United Nations Environment Programme (UNEP). (2021). Global assessment of oil spill incidents and soil pollution. Nairobi: UNEP.

United Nations Environment Programme (UNEP). (2023). Global status report on the impact of petroleum pollution. UNEP.

Urum, K., & Pekdemir, T. (2004). Evaluation of biosurfactants for crude oil contaminated soil washing. *Chemosphere*, 57(9), 1139–1150.

Vaidya, S., Jain, K., & Madamwar, D. (2017). Metabolism of pyrene through phthalic acid pathway by enriched bacterial consortium composed of Pseudomonas, Burkholderia, and Rhodococcus (PBR). *3Biotech*, 7, 29.

van Beilen, J. B., & Funhoff, E. G. (2007). Alkane hydroxylases involved in microbial alkane degradation. *Applied Microbiology and Biotechnology*, 74, 13–21.

Varjani, S. (2017). Microbial degradation of petroleum hydrocarbons. *Bioresource Technology*, 223, 277–286.

Vidali, M. (2001). Bioremediation: An overview. *Pure and Applied Chemistry*, 73(7), 1163–1172.

Villaverde, J., Láiz, L., Lara-Moreno, A., González-Pimentel, J. L., & Morillo, E. (2019). Bioaugmentation of PAH-contaminated soils with novel specific degrader strains isolated from a contaminated industrial site: Effect of hydroxypropyl-β-cyclodextrin as PAH bioavailability enhancer. *Frontiers in Microbiology*, 10, 2588.

Wang, D., Lin, J., Lin, J., & Wang, W., Li, S. (2019). Biodegradation of petroleum hydrocarbons by Bacillus subtilis BL-27, a strain with weak hydrophobicity. *Molecules*, 24, 3021.

Wang, L., Cheng, Y., Naidu, R., & Bowman, M. (2021). The key factors for the fate and transport of petroleum hydrocarbons in soil with related in/ex situ measurement methods: An overview. *Frontiers in Environmental Science*, 9, 756404.

Wang, R., Wu, B., Zheng, J., Chen, H., Rao, P., Yan, L., & Chai, F. (2020). Biodegradation of total petroleum hydrocarbons in soil: Isolation and characterization of bacterial strains from oil contaminated soil. *Applied Sciences*, 10, 4173.

World Bank. (2022). Global soil pollution analysis: Focus on petroleum hydrocarbon contamination. World Bank.

World Bank. (2023). Oil spills and environmental risk management: Policy recommendations. World Bank.

Wu, H., He, Y., Yang, J., Zhang, X., & Liu, X. (2021). Interfacial solar evaporation for heavy metal removal from contaminated soils. *Environmental Pollution*, 3(5), e12140.

Xu, R., Zhang, Z., Wang, L., Yin, N., & Zhan, X. (2018). Surfactant-enhanced biodegradation of crude oil by mixed bacterial consortium in contaminated soil. *Environmental Science and Pollution Research*, 25, 14437–14446.

Yan, G., Ma, W., Chen, C., Wang, Q., Guo, S., & Ma, J. (2016). Combinations of surfactant flushing and bioremediation for removing fuel hydrocarbons from contaminated soils. *Clean–Soil, Air, Water*, 44(8), 984–991.

Yu, C., Li, M., Cui, J., Xin, Y., Song, R., Tan, W., Hou, J., Guo, Z., Chen, W., & Xi, B. (2024). Decades-long effects of petroleum extraction on soil microbial communities and physical properties. *Environmental Research*, 231, 115678.

Yusoff, D. F., Raja Abd Rahman, R. N. Z., Masomian, M., Ali, M. S. M., & Leow, T. C. (2020). Newly isolated alkane hydroxylase and lipase producing Geobacillus and Anoxybacillus species involved in crude oil degradation. *Catalysts*, 10(8), 851.

Zhang, X., Liu, C.-G., Yang, S.-H., Wang, X., Bai, F.-W., & Wang, Z. (2022). Benchmarking of long-read sequencing, assemblers and polishers for yeast genome. *Briefings in Bioinformatics*, 23(3), bbac146.

Zhao, Q., Yue, S., Bilal, M., Hu, H., Wang, W., & Zhang, X. (2017). Comparative genomic analysis of 26 Sphingomonas and Sphingobium strains: Dissemination of bioremediation capabilities, biodegradation potential and horizontal gene transfer. *Science of the Total Environmen*t, 609, 1238–1247.

Zhao, D., Zeng, Y., & Xu, J. (2018). Biodegradation of crude oil by Pseudomonas frederiksbergensis and its potential application in bioremediation. *Science of the Total Environment*, 642, 890–896.

Zhen, M., Tang, J., Li, C., & Sun, H. (2021). Rhamnolipid-modified biochar-enhanced bioremediation of crude oil-contaminated soil and mediated regulation of greenhouse gas emission in soil. *Journal of Soils and Sediments*, 21, 123–133.

APPENDIX A: 16S rRNA SEQUENCES OF ISOLATED PHC DEGRADERS

OTU001

TAAGGAGGTGATCCAGCCGCAGGTTCCCCTACGGCTACCTTGTTACGACTTCACCCCAG
TCATGAATCACACCGTGGTAACCGTCCCCCCGAAGGTTAGACTAGCTACTTCTGGTGCA
ACCCACTCCCATGGTGTGACGGGCGGTGTGTACAAGGCCCGGGAACGTATTCACCGCG
ACATTCTGATTCGCGATTACTAGCGATTCCGACTTCACGCAGTCGAGTTGCAGACTGCG
ATCCGGACTACGATCGGTTTTGTGGGATTAGCTCCACCTCGCGGCTTGGCAACCCTCTG
TACCGACCATTGTAGCACGTGTGTAGCCCAGGCCGTAAGGGCCATGATGACTTGACGT
CATCCCCACCTTCCTCCGGTTTGTCACCGGCAGTCTCCTTAGAGTGCCCACCATAACGT
GCTGGTAACTAAGGACAAGGGTTGCGCTCGTTACGGGACTTAACCCAACATCTCACGA
CACGAGCTGACGACAGCCATGCAGCACCTGTCTCAATGTTCCCGAAGGCACCAATCCA
TCTCTGGAAAGTTCATTGGATGTCAAGGCCTGGTAAGGTTCTTCGCGTTGCTTCGAATT
AAACCACATGCTCCACCGCTTGTGCGGGCCCCCGTCAATTCATTTGAGTTTTAACCTTG
CGGCCGTACTCCCCAGGCGGTCAACTTAATGCGTTAGCTGCGCCACTAAGAGCTCAAG
GCTCCCAACGGCTAGTTGACATCGTTTACGGCGTGGACTACCAGGGTATCTAATCCTGT
TTGCTCCCCACGCTTTCGCACCTCAGTGTCAGTATCAGTCCAGGTGGTCGCCTTCGCCA
CTGGTGTTCCTTCCTATATCTACGCATTTCACCGCTACACAGGAAATTCCACCACCCTCT
ACCATACTCTAGCTCGACAGTTTTGAATGCAGTTCCCAGGTTGAGCCCGGGGATTTCAC
ATCCAACTTAACGAACCACCTACGCGCGCTTTACGCCCAGTAATTCCGATTAACGCTTG
CACCCTCTGTATTACCGCGGCTGCTGGCACAGAGTTAGCCGGTGCTTATTCTGTCGGTA
ACGTCAAAACACTAACGTATTAGGTTAATGCCCTTCCTCCCAACTTAAAGTGCTTTACA
ATCCGAAGACCTTCTTCACACACGCGGCATGGCTGGATCAGGCTTTCGCCCATTGTCCA
ATATTCCCCACTGCTGCCTCCCGTAGGAGTCTGGACCGTGTCTCAGTTCCAGTGTGACT
GATCATCCTCTCAGACCAGTTACGGATCGTCGCCTTGGTGAGCCATTACCTCACCAACT
AGCTAATCCGACCTAGGCTCATCTGATAGCGCAAGGCCCGAAGGTCCCCTGCTTTCTCC
CGTAGGACGTATGCGGTATTAGCGTCCGTTTCCGAGCGTTATCCCCCACTACCAGGCAG
ATTCCTAGGCATTACTCACCCGTCCGCCGCTCGCCACCAGGTACAAGTACCCGTGCTGC
CGCTCGACTTGCATGTGTTAGGCCTGCCGCCAGCGTTCAATCTGAGCCATGATCAAACT
CTTCAGTTCA

OTU002

TAAGGAGGTGATCCAGCCGCAGGTTCCCCTACGGCTACCTTGTTACGACTTCACCCCAG
TCATGAATCACACCGTGGTAACCGTCCTCCCGAAGGTTAGACTAGCTACTTCTGGTGCA

ACCCACTCCCATGGTGTGACGGGCGGTGTGTACAAGGCCCGGGAACGTATTCACCGCG
ACATTCTGATTCGCGATTACTAGCGATTCCGACTTCACGCAGTCGAGTTGCAGACTGCG
ATCCGGACTACGATCGGTTTTGTGGGATTAGCTCCACCTCGCGGCTTGGCAACCCTCTG
TACCGACCATTGTAGCACGTGTGTAGCCCAGGCCGTAAGGGCCATGATGACTTGACGT
CATCCCCACCTTCCTCCGGTTTGTCACCGGCAGTCTCCTTAGAGTGCCCACCATTACGT
GCTGGTAACTAAGGACAAGGGTTGCGCTCGTTACGGGACTTAACCCAACATCTCACGA
CACGAGCTGACGACAGCCATGCAGCACCTGTCTCAATGTTCCCGAAGGCACCAATCCA
TCTCTGGAAAGTTCATTGGATGTCAAGGCCTGGTAAGGTTCTTCGCGTTGCTTCGAATT
AAACCACATGCTCCACCGCTTGTGCGGGCCCCCGTCAATTCATTTGAGTTTTAACCTTG
CGGCCGTACTCCCCAGGCGGTCAACTTAATGCGTTAGCTGCGCCACTAAGAGCTCAAG
GCTCCCAACGGCTAGTTGACATCGTTTACGGCGTGGACTACCAGGGTATCTAATCCTGT
TTGCTCCCCACGCTTTCGCACCTCAGTGTCAGTATCAGTCCAGGTGGTCGCCTTCGCCA
CTGGTGTTCCTTCCTATATCTACGCATTTCACCGCTACACAGGAAATTCCACCACCCTCT
ACCATACTCTAGCTCGTCAGTTTTGAATGCAGTTCCCAGGTTGAGCCCGGGGCTTTCAC
ATCCAACTTAACGAACCACCTACGCGCGCTTTACGCCCAGTAATTCCGATTAACGCTTG
CACCCTCTGTATTACCGCGGCTGCTGGCACAGAGTTAGCCGGTGCTTATTCTGTCGGTA
ACGTCAAAACAGCAAAGTATTAATTTACTGCCCTTCCTCCCAACTTAAAGTGCTTTACA
ATCCGAAGACCTTCTTCACACACGCGGCATGGCTGGATCAGGCTTTCGCCCATTGTCCA
ATATTCCCCACTGCTGCCTCCCGTAGGAGTCTGGACCGTGTCTCAGTTCCAGTGTGACT
GATCATCCTCTCAGACCAGTTACGGATCGTCGCCTTGGTGAGCCATTACCTCACCAACT
AGCTAATCCGACCTAGGCTCATCTGATAGCGCAAGGCCCGAAGGTCCCCTGCTTTCTCC
CGTAGGACGTATGCGGTATTAGCGTTCCTTTCGAAACGTTGTCCCCCACTACCAGGCAG
ATTCCTAGGCATTACTCACCCGTCCGCCGCTGAATCAGAGAGCAAGCTCTCTTCATCCG
CTCGACTTGCATGTGTTAGGCCTGCCGCCAGCGTTCAATCTGAGCCATGATCAAACTCT
TCAGTTCA

OTU003

TAAGGAGGTGATCCAGCCGCAGGTTCCCCTACGGCTACCTTGTTACGACTTCACCCCAG
TCATGAATCACACCGTGGTAACCGTCCTCCCGAAGGTTAGACTAGCTACTTCTGGTGCA
ACCCACTCCCATGGTGTGACGGGCGGTGTGTACAAGGCCCGGGAACGTATTCACCGCG
ACATTCTGATTCGCGATTACTAGCGATTCCGACTTCACGCAGTCGAGTTGCAGACTGCG
ATCCGGACTACGATCGGTTTTGTGGGATTAGCTCCACCTCGCGGCTTGGCAACCCTCTG
TACCGACCATTGTAGCACGTGTGTAGCCCAGGCCGTAAGGGCCATGATGACTTGACGT
CATCCCCACCTTCCTCCGGTTTGTCACCGGCAGTCTCCTTAGAGTGCCCACCATAACGT
GCTGGTAACTAAGGACAAGGGTTGCGCTCGTTACGGGACTTAACCCAACATCTCACGA

CACGAGCTGACGACAGCCATGCAGCACCTGTCTCAATGTTCCCGAAGGCACCAATCCA
TCTCTGGAAAGTTCATTGGATGTCAAGGCCTGGTAAGGTTCTTCGCGTTGCTTCGAATT
AAACCACATGCTCCACCGCTTGTGCGGGCCCCCGTCAATTCATTTGAGTTTTAACCTTG
CGGCCGTACTCCCCAGGCGGTCAACTTAATGCGTTAGCTGCGCCACTAAGAGCTCAAG
GCTCCCAACGGCTAGTTGACATCGTTTACGGCGTGGACTACCAGGGTATCTAATCCTGT
TTGCTCCCCACGCTTTCGCACCTCAGTGTCAGTATCAGTCCAGGTGGTCGCCTTCGCCA
CTGGTGTTCCTTCCTATATCTACGCATTTCACCGCTACACAGGAAATTCCACCACCCTCT
ACCATACTCTAGCTCGACAGTTTTGAATGCAGTTCCCAGGTTGAGCCCGGGGATTTCAC
ATCCAACTTAACGAACCACCTACGCGCGCTTTACGCCCAGTAATTCCGATTAACGCTTG
CACCCTCTGTATTACCGCGGCTGCTGGCACAGAGTTAGCCGGTGCTTATTCTGTCGGTA
ACGTCAAAACAATTACGTATTAGGTAACTGCCCTTCCTCCCAACTTAAAGTGCTTTACA
ATCCGAAGACCTTCTTCACACACGCGGCATGGCTGGATCAGGCTTTCGCCCATTGTCCA
ATATTCCCCACTGCTGCCTCCCGTAGGAGTCTGGACCGTGTCTCAGTTCCAGTGTGACT
GATCATCCTCTCAGACCAGTTACGGATCGTCGCCTTGGTGAGCCATTACCTCACCAACT
AGCTAATCCGACCTAGGCTCATCTGATAGCGCAAGGCCCGAAGGTCCCCTGCTTTCTCC
CGTAGGACGTATGCGGTATTAGCGTCCGTTTCCGAGCGTTATCCCCCACTACCAGGCAG
ATTCCTAGGCATTACTCACCCGTCCGCCGCTCGCCACCAGGTACAAGTACCCGTGCTGC
CGCTCGACTTGCATGTGTTAGGCCTGCCGCCAGCGTTCAATCTGAGCCATGATCAAACT
CTTCAGTTCA

OTU004

AAACTGAAGAGTTTGATCCTGGCTCAGATTGAACGCTAGCGGGATGCCTTACACATGC
AAGTCGAACGGCAGCACGGACTTCGGTCTGGTGGCGAGTGGCGAACGGGTGAGTAAT
GTATCGGAACGTGCCTAGTAGCGGGGGATAACTACGCGAAAGCGTAGCTAATACCGCA
TACGCCCTACGGGGGAAAGCAGGGGATCGCAAGACCTTGCACTATTAGAGCGGCCGAT
ATCGGATTAGCTAGTTGGTGGGGTAACGGCTCACCAAGGCGACGATCCGTAGCTGGTT
TGAGAGGACGACCAGCCACACTGGGACTGAGACACGGCCCAGACTCCTACGGGAGGC
AGCAGTGGGGAATTTTGGACAATGGGGGAAACCCTGATCCAGCCATCCCGCGTGTGCG
ATGAAGGCCTTCGGGTTGTAAAGCACTTTTGGCAGGAAAGAAACGTCATGGGCTAATA
CCCCGTGAAACTGACGGTACCTGCAGAATAAGCACCGGCTAACTACGTGCCAGCAGCC
GCGGTAATACGTAGGGTGCAAGCGTTAATCGGAATTACTGGGCGTAAAGCGTGCGCAG
GCGGTTCGGAAAGAAAGATGTGAAATCCCAGAGCTTAACTTTGGAACTGCATTTTTAA
CTACCGAGCTAGAGTGTGTCAGAGGGAGGTGGAATTCCGCGTGTAGCAGTGAAATGCG
TAGATATGCGGAGGAACACCGATGGCGAAGGCAGCCTCCTGGGATAACACTGACGCTC
ATGCACGAAAGCGTGGGGAGCAAACAGGATTAGATACCCTGGTAGTCCACGCCCTAAA

CGATGTCAACTAGCTGTTGGGGCCTTCGGGCCTTGGTAGCGCAGCTAACGCGTGAAGT
TGACCGCCTGGGGAGTACGGTCGCAAGATTAAAACTCAAAGGAATTGACGGGGACCC
GCACAAGCGGTGGATGATGTGGATTAATTCGATGCAACGCGAAAAACCTTACCTACCC
TTGACATGTCTGGAATTCCGAAGAGATTTGGAAGTGCTCGCAAGAGAACYGGAACACA
GGTGCTGCATGGCTGTCGTCAGCTCGTGTCGTGAGATGTTGGGTTAAGTCCCGCAACGA
GCGCAACCCTTGTCATTAGTTGCTACGAAAGGGCACTCTAATGAGACTGCCGGTGACA
AACCGGAGGAAGGTGGGGATGACGTCAAGTCCTCATGGCCCTTATGGGTAGGGCTTCA
CACGTCATACAATGGTCGGGACAGAGGGTCGCCAACCCGCGAGGGGGAGCCAATCCC
AGAAACCCGATCGTAGTCCGGATCGCAGTCTGCAACTCGACTGCGTGAAGTCGGAATC
GCTAGTAATCGCGGATCAGCATGTCGCGGTGAATACGTTCCCGGGTCTTGTACACACC
GCCCGTCACACCATGGGAGTGGGTTTTACCAGAAGTAGTTAGCCTAACCGTAAGGGGG
GCGATTACCACGGTAGGATTCATGACTGGGGTGAAGTCGTAACAAGGTAGCCGTATCG
GAAGGTGCGGCTGGATCACCTCCTTTC